

RHEL/R 180

A. CARNE

R.1.

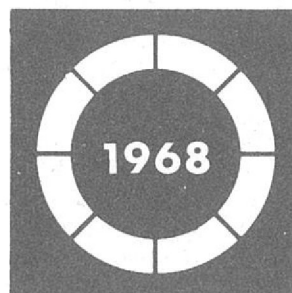
RHEL/R 180  
**Rutherford Laboratory  
Report**

---

**The Work of the Rutherford Laboratory  
in 1968**

Edited by

**A P Banford and F M Telling**



---

Science Research Council

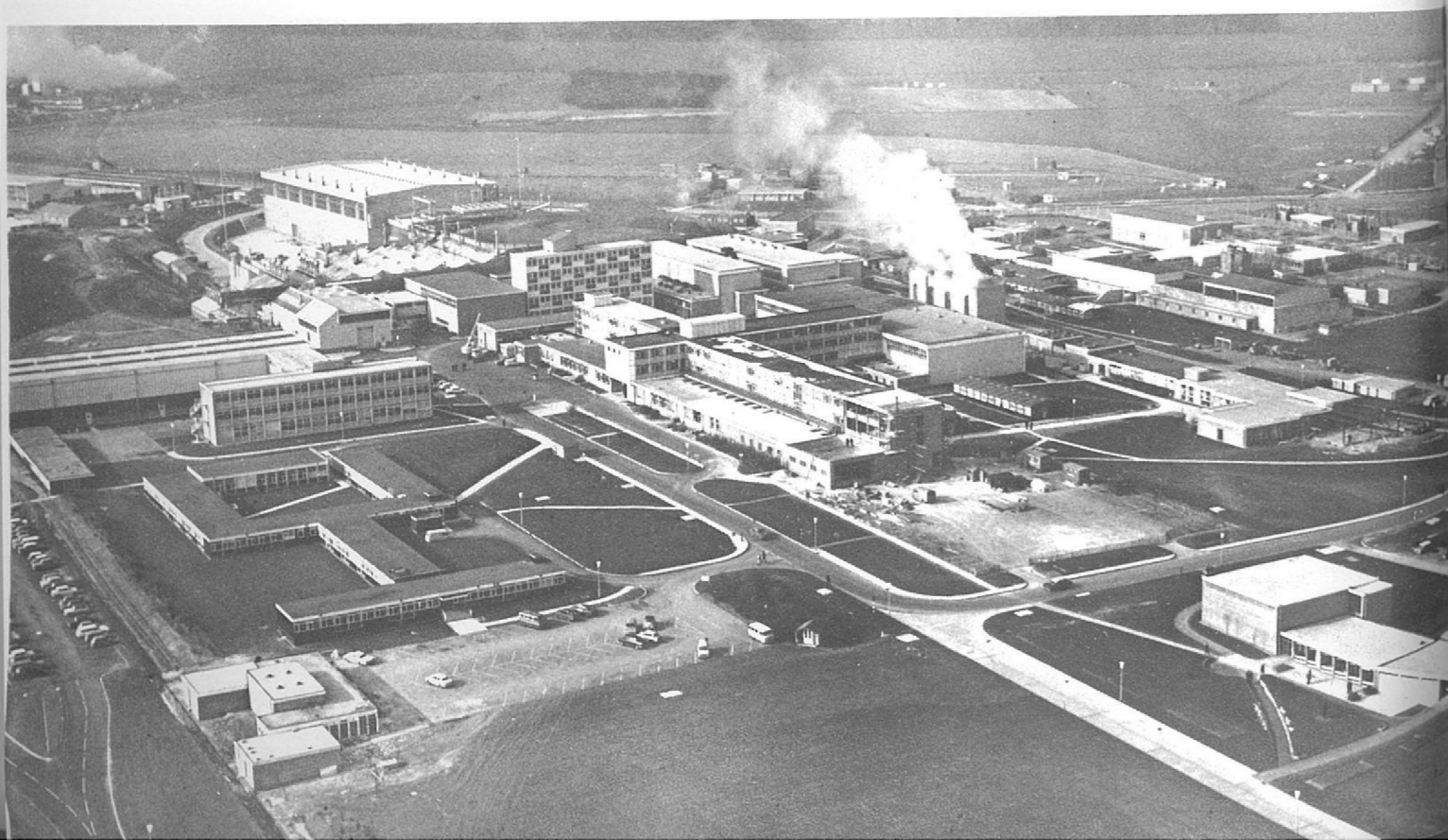
Scientific Administration Group  
Rutherford High Energy Laboratory  
Chilton Didcot Berkshire  
1969



Available from HMSO  
price 15s net



*Two recent aerial views of the Rutherford Laboratory. The upper photograph, taken from the west, shows the nearly completed Experimental Hall 3 at lower right, Nimrod itself being located under the central grassed-over shielding mound. In the lower picture the site is seen from the east.*



**Science Research Council**

**THE WORK OF THE RUTHERFORD LABORATORY  
IN 1968**

Rutherford High Energy Laboratory  
Chilton Didcot Berkshire  
April 1969

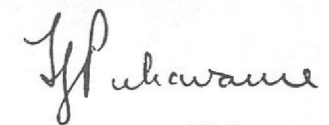
## Contents

<b>Foreword</b>	<b>7</b>
<b>High Energy Physics Division</b>	<b>10</b>
<b>Nimrod Division</b>	<b>48</b>
<b>Proton Linear Accelerator Division</b>	<b>72</b>
<b>Applied Physics Division</b>	<b>84</b>
<b>Engineering Division</b>	<b>100</b>
<b>Administration Division</b>	<b>126</b>
<b>List of Publications</b> (References to specific publications are by means of marginal numbers in the main text)	<b>132</b>

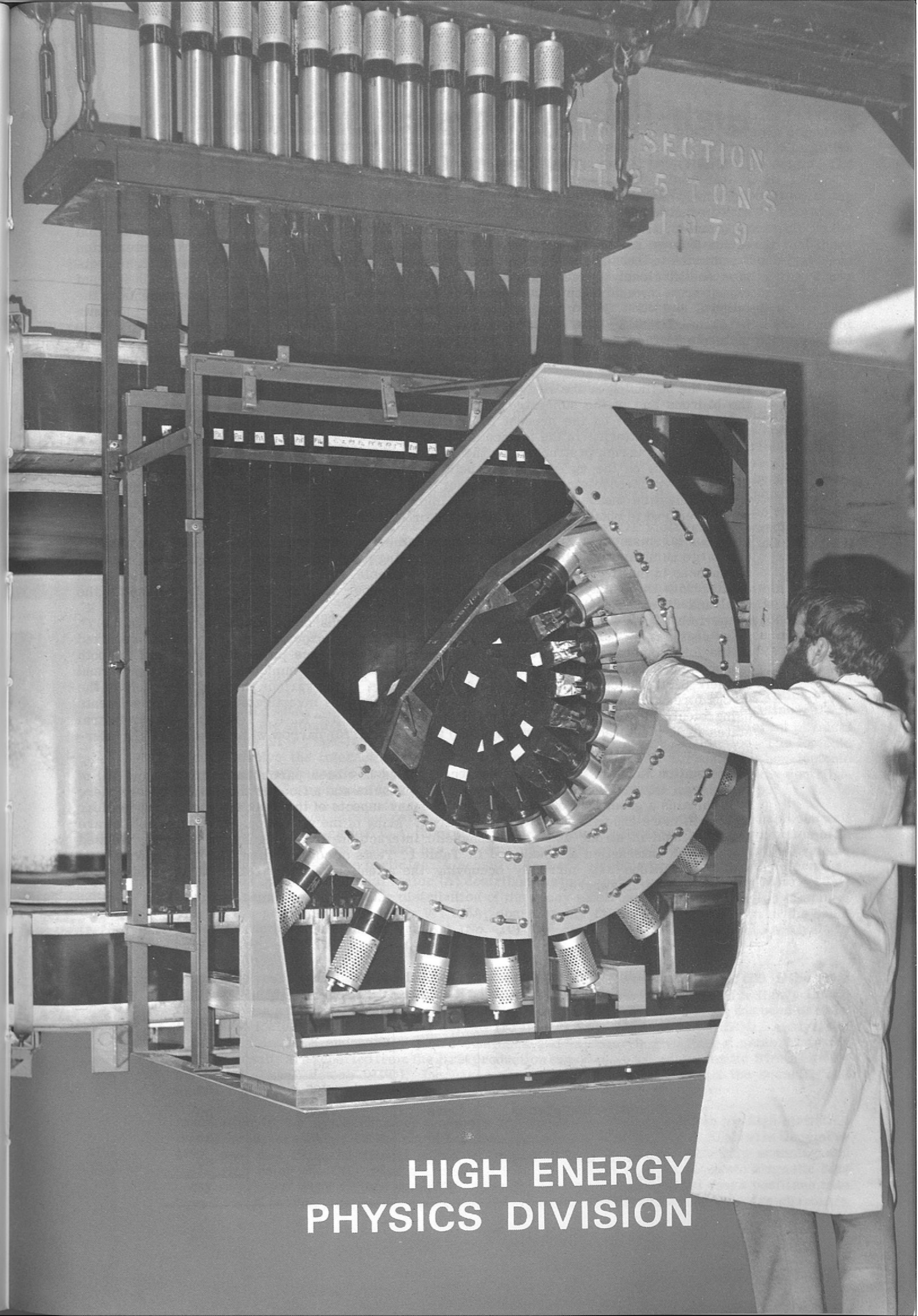
## Foreword

This Report, the fourth in the series describing the year's activities of the Rutherford Laboratory, covers the calendar year 1968 which has been as busy and productive as any in our history. The experiments making up the High Energy Physics research programme have covered a wide range of topics; in addition to continuing the work on elastic scattering cross-sections and polarizations, and the bubble chamber studies, an increasing number of investigations have been concerned with weak interactions where the validity of invariance principles remains in doubt. Several of these experiments are using the most advanced spark chamber and on-line computer techniques. Nimrod itself has operated at a very satisfactory level of intensity and reliability. Two extracted proton beams have been in use, and the ability to switch from one to the other during the pulse has resulted in greatly enhanced operational flexibility and efficiency. The new experimental area (Hall 3) is near completion, and during 1969 will provide welcome relief from the present congestion in the other areas. The PLA, in its penultimate year of operation, has broken previous records for hours of good beam, and we were particularly pleased at being able to assist our Canadian colleagues from the TRIUMF project by mounting an experiment involving the acceleration of negative hydrogen ions.

There is also good progress to report from the many other fields of work necessary to support a successful research programme in high energy physics. Detailed accounts of these will be found in the following pages; the aim has been to present a balanced portrayal of our work without undue emphasis on any particular field. As a result, most of our staff and visitors will be able to identify their individual contributions to the Laboratory's progress, though in a co-operative venture such as ours everyone is entitled to feel associated with each and every success.



T. G. Pickavance  
Director.



**HIGH ENERGY  
PHYSICS DIVISION**

# High Energy Physics Division

Division Head and Deputy Director: G. H. Stafford.

For many years much of the experimental work on Nimrod has been devoted to the study of elastic scattering reactions. The widely-acclaimed successes of the unitary symmetry scheme ( $SU_3$  octets,  $\Omega$ -minus etc.) just as Nimrod was starting up encouraged a detailed investigation of low energy scattering processes. The existence of a large number of strong interaction resonances in the  $\pi$ -N and K-N systems requires that measurements be made with high precision and at closely spaced intervals of momentum and angle. In the first series (1964-67) of experiments measurements were made on elastic  $\pi^+p$  and  $\pi^-p$  scattering at 22 momenta in the interval 0.9 - 2.8 GeV/c and charge exchange scattering,  $\pi^- + p \rightarrow \pi^0 + n$ , at 5 momenta between 1.7 and 2.5 GeV/c. Polarization data were obtained in  $\pi^-p$  elastic scattering at 50 momenta in the interval 0.6 - 2.2 GeV/c and at 8 momenta in  $K^-p$  elastic scattering. The  $\pi p$  results represent a very substantial fraction of the world data on pion-nucleon scattering and have made significant contributions to identifying and classifying baryon resonant states. This is just the beginning of the study directed towards an understanding of the internal structure of the hadrons and of the superstrong interactions which give rise to them. More extensive measurements are on the present Nimrod programme. Two experiments (Nos. 3 and 5) are studying  $Kp$  scattering in the momentum interval 0.5 - 1.4 GeV/c. It is expected that the  $K^-p$  system will be as rich in structure as the  $\pi p$  system and be a very fruitful field of investigation. Measurements on the  $\pi p$  system are being extended to very low energies (Experiment 15 - at the CERN synchrocyclotron) and to higher momenta (Experiment 11). An extensive series of  $\pi^\pm p$  polarization measurements using an improved Rutherford Laboratory polarized target is being prepared to obtain data at 70 momenta throughout the range 0.6 - 2.7 GeV/c.

In a similar momentum interval the bubble chamber groups are continuing their investigation of a large number of reaction channels concentrating particularly on the formation and decay of resonances in multi-particle final states. For example, the analysis during 1968 of film taken earlier with the Saclay 80cm hydrogen bubble chamber at Nimrod has yielded values for the total and differential cross-sections for the reactions  $K^- + p \rightarrow K^0 + \Xi^0$  and  $K^- + p \rightarrow K^+ + \Xi^-$  (Experiment 24). These results were interpreted in terms of resonance formation in the  $Y^*$  mass region from 1915 to 2168 MeV. The bubble chamber experiments (Nos. 19-30) reported in the following pages are providing information on resonance production and decay for both mesonic and hadronic states. The systematics of the quantum numbers of the resonances and of their partial decay widths provide sensitive tests of the various theoretical models of the strong forces. Selected inelastic processes are also being investigated by three experiments using electronic techniques, namely polarization in  $\pi^- + p \rightarrow K^+ + \Sigma^-$  (Experiment 2), neutral states in  $K^-p$  interactions (Experiment 5) and a search for narrow width mesons in  $\pi^-p$  interactions (Experiment 18).

The situation in weak interactions in recent years has been particularly exciting and full of surprises. In spite of many new experimental results and a flood of theoretical papers there still remains a great lack of understanding of many aspects of the weak interaction. It is clear that much more experimental work is required. Many of the strict conservation rules that are known to hold in strong and electromagnetic interactions are, for unknown reasons, violated in the weak interaction as indicated in Table 1. Tests of conservation laws and searches for further violations are currently occupying the attention of many teams at the Rutherford Laboratory and elsewhere.

**Table 1**

Validity of symmetry principles in the interactions

Type of Interaction	Strong	Electromagnetic	Weak
I, isotopic spin	yes	no	no
S, strangeness	yes	yes	no
C, charge conjugation	yes	yes	no
P, parity	yes	yes	no
CP or T, time reversal	yes	yes	no
CPT	yes	yes	yes

Following the discovery of the violation of parity and charge conjugation symmetries in 1957 it was believed that intuitive ideas of left-right symmetry could still be preserved by a combined CP symmetry. CP symmetry requires that the physical laws remain unchanged if particles are replaced by anti-particles and the co-ordinate system is reflected through the origin. The symmetry rule was supported by the then available experimental information. In 1964 CP symmetry also fell as a result of the observation at the Brookhaven National Laboratory of the CP-forbidden decay  $K_L^0 \rightarrow \pi^+ + \pi^-$ , confirmed the following year at the Rutherford Laboratory. Several types of model were proposed to explain CP violation but it was not possible on the available experimental evidence to select the most appropriate one. It was clear that there was a need to study other possible CP-violating processes and, in particular, those that were critical tests of the various models. An experiment (No. 16) aimed at measuring the decay rate  $K_L^0 \rightarrow \pi^0 + \pi^0$  was mounted at CERN by a team from the Rutherford Laboratory and AERE working with physicists from Aachen and CERN. The final result was presented at the 14th International Conference on High Energy Physics at Vienna in August. A follow-up experiment (No. 17) by members of the same team and others is currently measuring the magnitude and phase of the decay amplitude. A preliminary result confirms the previous measurement on the decay rate. The world situation is somewhat confused but the weight of data seems to come down against the so-called "super-weak" model of CP violation.

Hints of CP violation have arisen in connection with possible  $\Delta S = -\Delta Q$  contributions to the leptonic decays of  $K^0$  mesons. Published experiments suffer from low statistics and a 10,000 events experiment started data collection on Nimrod during the year. This experiment (No. 7) involves measuring the time dependence of the decays  $K^0 \rightarrow \pi e \nu$  following the associated production of neutral kaons in the reaction  $\pi^- + p \rightarrow \Lambda^0 + K^0$ . An experiment (No. 14) by a collaboration between the Rutherford Laboratory and three UK universities was installed at CERN in September 1968 to study the decay modes  $K^\pm \rightarrow \pi \pi \gamma$  and  $K^\pm \rightarrow \pi \pi \pi$ . The aims of the experiment are to test for C violation in electromagnetic interactions and CP violation in the weak interaction by measuring the charge asymmetry in the rates for  $K^\pm \rightarrow \pi^\pm \pi^0 \gamma$  and for  $\Delta I > 3/2$  CP violating terms in  $K^\pm \rightarrow \pi^\pm \pi^0 \pi^0$ .

A test of the validity of the CPT theorem, a cornerstone for local field theories, is in progress (Experiment 6). The experiment will obtain an accurate value of the mean life of the  $K^+$  meson by a delayed coincidence technique. Comparison with the lifetime of the corresponding anti-particle, the  $K^-$  meson, will check the validity of CPT invariance for the forces involved in K decay.

A high statistics study of  $K^+$  leptonic decays has been completed at Nimrod and final values of branching ratios and form factors have been reported. The values of the branching ratios of the  $K_{\mu 3}$  and  $K_{e 3}$  decay modes give strong evidence for a pure leptonic  $\Delta I = \frac{1}{2}$  selection rule in contrast to the situation previously. The leptonic  $\Delta I = \frac{1}{2}$  selection rule has a different physical basis to the  $\Delta I = \frac{1}{2}$  non-leptonic rule for which there is some evidence of violation. The leptonic decays involve the interaction of a hadronic current and a leptonic current while non-leptonic decays have two hadronic components. Experiment No. 8 is aimed at measuring the contribution of  $\Delta I \geq 3/2$  amplitudes to the non-leptonic decay of the  $\Sigma^+$  in the mode  $\Sigma^+ \rightarrow p \pi^0$ .

The beta decay of non-strange particles, as in muon decay or nuclear beta decay, has been well described by the so-called V-A theory of Feynmann and Gell-Mann. The introduction of an additional parameter by Cabibbo has proved remarkably successful in predicting the leptonic decay rates of the strange particles. A sensitive test of Cabibbo's prediction is the determination of the vector (V) and axial vector (A) contributions to  $\Sigma^-$  beta decay (branching ratio  $\sim 10^{-3}$ ) by measurement of the angular distribution of the decay electrons about the direction of spin of the  $\Sigma^-$ , the predicted form being  $V + 0.3A$ , considerably different from the V-A of the basic weak interaction. Such an experiment (No. 10) was completed in July, 1968 and analysis is progressing.

During the year nearly a million bubble chamber photographs were taken, 605,000 in the 1.5m National Bubble Chamber with hydrogen or deuterium and 343,000 in the 1.4m Heavy Liquid Chamber with a filling of propane -  $CF_3$  Br mixture. The film taken at Nimrod has been used by 16 groups including 6 groups from abroad (France, USA, Belgium and CERN). Analysis of data taken in 1968 and earlier years continues and is described in Experiments 19 to 30. Physics results are reported from the first production experiment on the automatic film measuring Hough Powell device (HPD). Increased use of the HPD will accelerate the scanning and measuring processes in the bubble chamber technique.

Automation in the spark chamber technique has enabled the teams to obtain the high statistics that are now necessary. Of the six spark chamber experiments running at Nimrod in December 1968, one uses film and manual scanning, another film followed by automatic scanning and measuring using the CRT film scanner and a third digitises immediately onto magnetic tape using an array of eight vidicon cameras. Three teams record the digitised spark positions onto tape through on-line computers, one uses sonic chambers and the remaining two wire chambers.

In 1968 Nimrod produced 5170 hours of High Energy Physics time at an average intensity of  $1.5 \times 10^{12}$  protons per pulse and an efficiency of 84%. The layout of beam lines in the experimental areas in December, 1968 is shown in figure 1. Beam switching and sharing techniques have been developed to allow a large number of teams to run simultaneously, for example, during December, one bubble chamber and six electronics experiments.

Increased use has been made during the year of CERN facilities by groups from the Laboratory and associated Universities through RHEL channels. Two complete teams comprising 20 physicists and support staff from the Laboratory and the Universities of Cambridge, Glasgow, Liverpool and Oxford arrived at CERN in the late summer to set up electronics experiments on the CERN SC and PS. 55 tons of apparatus and electronic equipment was dispatched from the laboratory for their use at CERN. A team of CERN, Orsay and Rutherford physicists is taking data at CERN in an experiment for which 90% of the scanning of the spark chamber film is done at the Rutherford Laboratory. Two of the bubble chamber experiments reported here used film taken in CERN chambers. A collaboration of physicists from RHEL and the Universities of Bristol, Cambridge, Liverpool and London (UCL and WCL) are designing an experiment to search for the intermediate vector boson (the quantum field particle of the weak interaction). This experiment will be carried out at CERN when the intersecting storage rings (ISR) become available in 1971.

**Table 2**

Composition of Teams using Nimrod in 1968

	Physicists		Research Students		Support Staff*	
	Electronic Techniques	Bubble Chambers	Electronic Techniques	Bubble Chambers	Electronic Techniques	Bubble Chambers
Visitors**	60	35	35	30	8	1
Resident RL staff†	26††	10††	-	-	21	13
TOTAL	86	45	35	30	29	14

\* Includes only technical assistance directly concerned with experiments and does not include engineering support.

\*\* Staff from Universities and other groups.

† Including RL physicists at present working at CERN, but excluding the PLA Nuclear Physics Group.

†† These numbers include 24 fixed term Research Fellows and 3 staff members with joint University appointments.

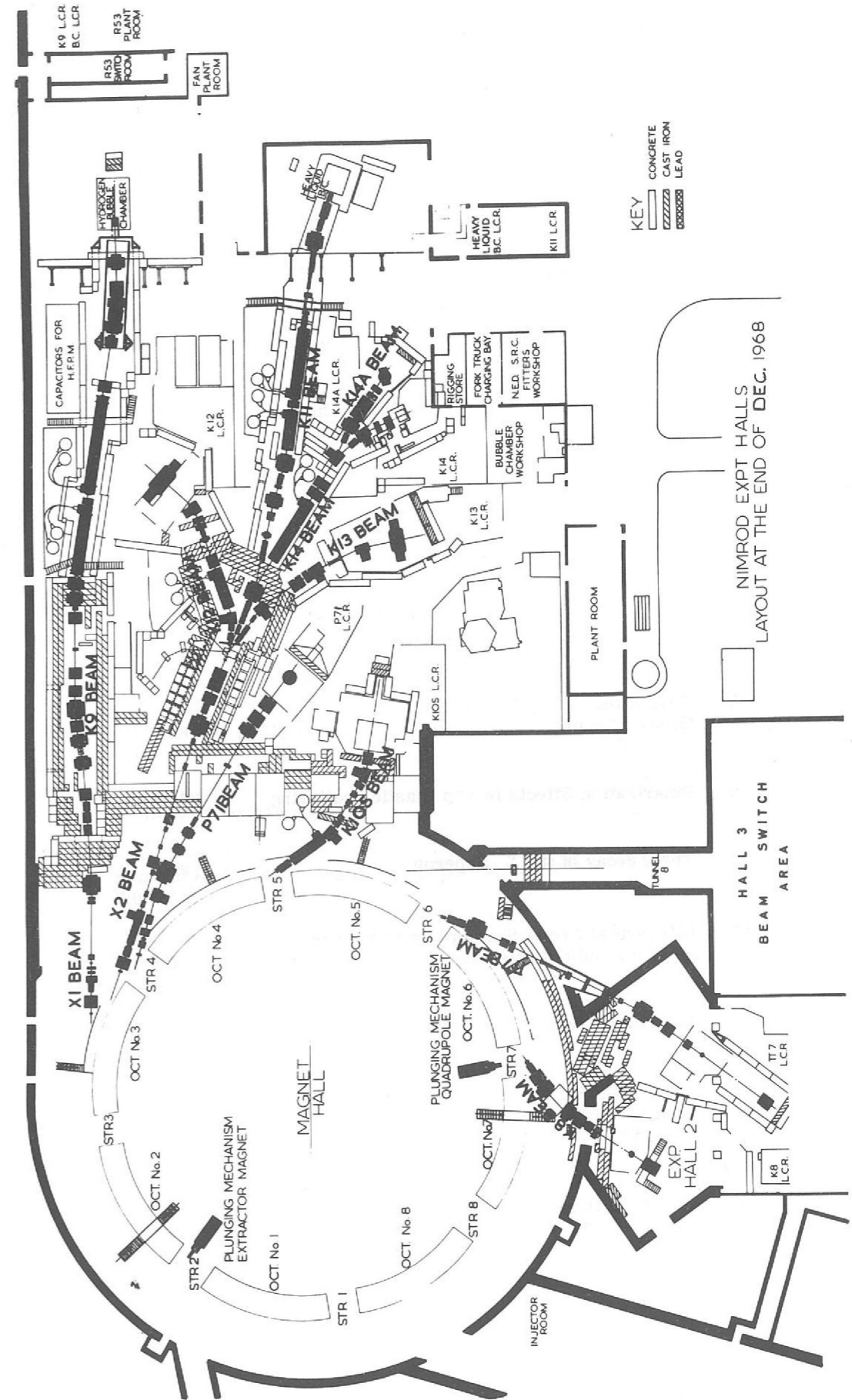


Figure 1. Nimrod Experimental Halls. Layout at 31st December 1968 (This figure is also available in pull-out form at the end of the Report).

## Experiments at Nimrod

### ELECTRONIC TECHNIQUES

Number	Experiment	Beam Line (see Fig.1 where applicable)	Status of Expt. at December 1968
1	The Leptonic Decay Modes and a Radiative Decay Mode of the $K^+$ Meson	K4	Completed
2	Polarization of $\Sigma^-$ in the Reaction $\pi^- + p \rightarrow \Sigma^- + K^+$ at 1130 MeV/c	K7'	Completed
3	$K^-p$ Differential Cross-Section Measurements	K8	Data taking
4	Neutral States produced in $K^-p$ Interactions	K10S	Data taking
5	$K^\pm p$ Differential Cross-Sections	K12	Data taking
6	$K^+$ Lifetime Measurement	K12*	Data taking
7	Test of the $\Delta S = \Delta Q$ rule for $K^0$ Leptonic Decays	K13	Data taking
8	Test of the $\Delta I = \frac{1}{2}$ Rule in the Decay $\Sigma^+ \rightarrow p\pi^0$ .	K14	Data taking
9	Polarization Effects in $\pi^\pm p$ Elastic Scattering	K14A	Setting up
10	The $\beta$ decay of the $\Sigma^-$ Hyperon	$\pi 4$	Analysis
11	Differential Cross-Section Measurements for $\pi^- p$ Elastic Scattering	$\pi 5$	Analysis
12	The Partial Width of the Decay $\phi \rightarrow e^+ e^-$ .	$\phi 1$	Analysis
13	Wide Angle Elastic Proton-Proton Scattering in the Momentum Range 1.5-4.5 GeV/c	P71	Setting up
14	A Study of the Decay Modes $K^\pm \rightarrow \pi^\pm \pi^0 \gamma$ and $K^\pm \rightarrow \pi^\pm \pi^0 \pi^0$	CERN	Setting up
15	Elastic Pion Scattering through Low Energies	CERN	Data taking
16	The Decay of Long-Lived Neutral Kaons into Two Neutral Pions	CERN	Completed

### ELECTRONIC TECHNIQUES

Number	Experiment	Beam Line (see Fig.1 where applicable)	Status of Expt. at December 1968
17	Measurement of $\phi_{00}$ , the Phase of $\eta_{00}$	CERN	Data taking
18	An Investigation of Narrow Width Mesons Produced in $\pi^- p$ Interactions	$\pi 7$	Setting up

### BUBBLE CHAMBER EXPERIMENTS

19	Decays of $\eta$ Mesons	P3X	Completed
20	2.2 GeV/c $K^-$ Exposure in the Heavy Liquid Bubble Chamber	K11	Data taking
21	A Study of $K_{s4}$ Decays	CERN	Completed
22	$\pi^+ p$ Interactions in the Range (a) 0.9 - 1.05 GeV/c (b) 1.10 - 1.17 GeV/c	K1 K9	Analysis Data taking
23	Single and Double Pion Production in pd Collisions	K1	Analysis
24	A Study of $K^- p$ Interactions in the Range 1.24 - 1.86 GeV/c	K1	Analysis
25	$K^-$ Deuterium Interactions	K1	Analysis
26	$K^+ p$ and $K^+ d$ Interactions in the Range 2.0 - 2.8 GeV/c	K9	Data taking
27	$\pi^+ p$ Interactions between 0.6 and 0.8 GeV/c	K1	Analysis
28	$\pi^- p$ Interactions between 0.4 and 0.7 GeV/c	K1	Analysis
29	$\pi^+ p$ Interactions at 2 GeV/c in Helium	K1S	Analysis
30	np and $\Delta p$ Interactions	K9	Data taking



## Experiment 1

The Leptonic Decay Modes and a Radiative Decay Mode of the  $K^+$  Meson.  
(2, 3, 4, 23, 24, 25)

This experimental study of the decay modes  $K^+ \rightarrow e^+ \pi^0 \nu$ ,  $\mu^+ \nu$  and  $\pi^+ \pi^0 \gamma$  has been described in both the 1966 Annual Report (Experiment 7) and the 1967 Annual Report (Experiment 4). The analysis of the data has continued during 1968. The experiment is concerned with the following measurements:

1. The electron momentum spectrum in the  $K_{e3}$  mode;
2. The branching ratio for the  $K_{e3}$  mode;
3. The relative branching ratio of the  $K_{\mu3}$  and  $K_{e3}$  modes;
4. The branching ratio for the  $\pi^+ \pi^0 \gamma$  mode and the  $\gamma - \pi^+$  angular correlation;
5. The  $\pi^0$  spectra in the  $K_{e3}$  and  $K_{\mu3}$  modes.

The first four sections of the analysis have been completed. The final section will be finished early in 1969.

The results obtained from the first two sections were described in last year's report.

It has since been found that the relative branching ratios of the  $K_{\mu3}$  and  $K_{e3}$  decays is

$$\Gamma(K_{\mu3}) / \Gamma(K_{e3}) = 0.667 \pm 0.017$$

assuming  $\lambda_+ = 0.023$  and  $\lambda_- = 0$ . This result corresponds to a value for the parameter  $\xi$  of  $-0.08 \pm 0.13$  in good agreement with theoretical expectations. ( $\xi$  is the ratio of the form factors for vector coupling in  $K_{\mu3}$  decay). The results for various values of  $\lambda_+$  and  $\lambda_- = 0$  are presented in figure 2.

The branching ratio for the decay  $\pi^+ \pi^0 \gamma$  has been found to be consistent with pure inner bremsstrahlung though a comparative structure amplitude with destructive interference cannot be ruled out.

## Experiment 2

Polarization of  $\Sigma^-$  in the Reaction  $\pi^- + p \rightarrow \Sigma^- + K^+$  at 1130 MeV/c  
(27, 43, 60)

This experiment, involving a  $\pi^-$  beam incident on a polarized proton target, was described in the 1967 Annual Report (Experiment 8). Analysis of the data was completed in 1968. The final values for the polarization of the  $\Sigma^-$  are listed in Table 3. These values supersede the preliminary data presented in the previous Annual Report. The polarization data are being used by the QMC/AERE/RHEL group to analyze their measurements on the asymmetry in the beta-decay mode of the  $\Sigma^-$  (Experiment 10).

We have combined our measurement with the results of other studies of the associated production reactions  $\pi p \rightarrow \Sigma K$ , and have performed an energy-dependent partial wave analysis of these processes between threshold and 1170 MeV/c. We use, for the amplitudes  $A_n$ , the momentum-dependent form

$$A_n = a_n \exp(i\psi_n) K_\Sigma (1 + \frac{1}{2})$$

where  $K_\Sigma$  is the c.m. momentum of the  $\Sigma$ , the parameters  $A_n$  and  $\psi_n$  are real, and the index  $n$  labels the isospin, total spin and parity of the amplitude. Near 1130 MeV/c, we obtained a

UNIVERSITY OF OXFORD

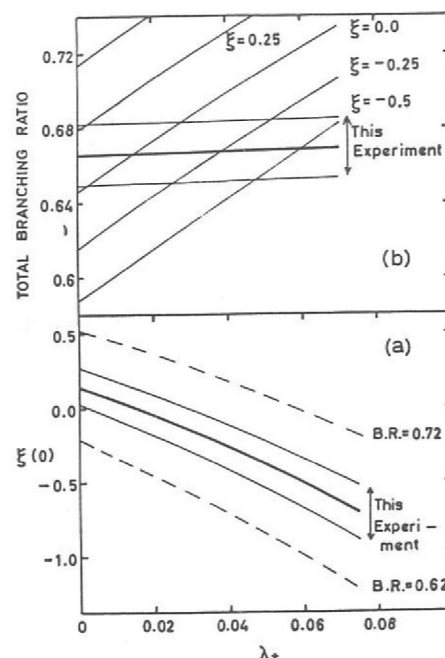


Fig. 2 Relation between experimental branching ratio and the total branching ratio.

QUEEN MARY COLLEGE, LONDON  
UNIVERSITY OF OXFORD  
RUTHERFORD LABORATORY.

good fit to the associated Legendre series expansion of  $P(\frac{d\sigma}{d\Omega})$  using S and P waves only. Consequently the set of data points (66 in number) below 1130 MeV/c was fitted with S and P waves, while we added D waves to fit the complete set of 124 data points up to 1170 MeV/c. Four solutions with acceptable values of  $\chi^2$  were found for the restricted data set, but only one (which had a probability  $\approx 5\%$ ) for the complete set. The  $I = 3/2$  amplitudes are equal, within errors, for all five solutions, and thus the data on  $\pi^+ p \rightarrow \Sigma^+ K^+$  are well fitted at all momenta. We conclude that the  $I = 3/2$  amplitudes are uniquely determined.

However the four solutions for the restricted set have distinctly different values of the  $I = \frac{1}{2}$  amplitudes, and for the single solution to the complete set the contribution of these amplitudes to the total  $\chi^2$  is disproportionately great. This suggests that our energy-dependent parametrization is inadequate, at least for the  $I = \frac{1}{2}$  amplitudes, above 1130 MeV/c.

Table 3

(absolute normalization error of  $\pm 16\%$  not included)

$\cos \theta_\Sigma^*$	Polarization of $\Sigma^-$
$-1.000 \pm 0.019$	$(3.71 \pm 5.03)$
$-0.968 \pm 0.025$	$-0.431 \pm 0.242$
$-0.903 \pm 0.046$	$-0.236 \pm 0.198$
$-0.784 \pm 0.075$	$-0.125 \pm 0.180$
$-0.639 \pm 0.096$	$-0.111 \pm 0.198$
$-0.435 \pm 0.124$	$-0.247 \pm 0.207$
$-0.184 \pm 0.159$	$-0.378 \pm 0.181$
$+0.128 \pm 0.165$	$-0.440 \pm 0.174$

## Experiment 3

$K^-p$  Differential Cross-Section Measurements

During the course of the year, the automatic wire spark chamber system used for the observation of elastic scattering events has become completely operational. During a trial run, about 1.5 million triggers of  $\pi^- p$  collisions have been recorded in the momentum range of 1.0 to 1.4 GeV/c. Some 3% of these are represented in figure 3 which shows the differential cross-section at 1.207 GeV/c. Data on  $K^- p$  interactions are at present being accumulated, and about 200,000 triggers have so far been recorded in the momentum range of 1.8 to 2.3 GeV/c. The scope of the experiment has been extended and the present intention is to collect sufficient data to yield angular distributions, each of ten thousand elastic events, at forty values of momentum between 0.85 and 2.5 GeV/c, rather than at the fifteen values originally proposed. It is estimated that some 2 million triggers will be required.

UNIVERSITY COLLEGE, LONDON  
RUTHERFORD LABORATORY

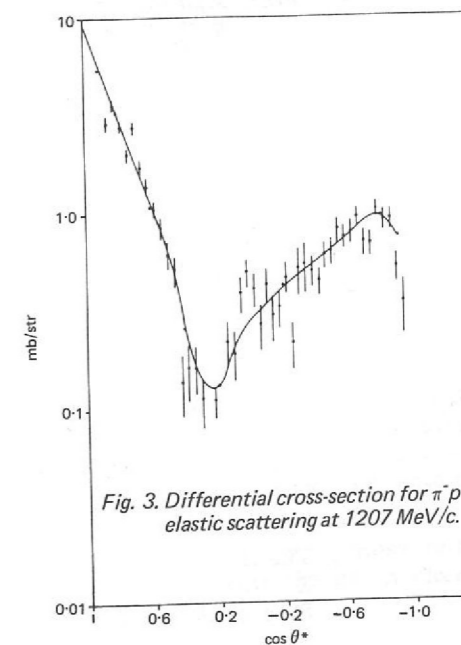


Fig. 3. Differential cross-section for  $\pi^- p$  elastic scattering at 1207 MeV/c.

## Experiment 4

### Neutral States Produced in $K^-p$ Interactions

The experiment is a study of neutral states, primarily  $\Lambda^0 \pi^0$ ,  $\Lambda^0 \eta^0$ ,  $\Sigma^0 \pi^0$  and  $\Sigma^0 \eta^0$ , produced in  $K^-p$  interactions in the range 650 to 1250 MeV/c. A partial wave analysis of these reactions will allow a separation of some of the many excited hyperon states formed in the  $K^-p$  interaction. In a first data run, 130,000 photographs have been taken and analysis of these and associated magnetic tape information is proceeding.

Figure 4 is a plan view of the apparatus, the separated  $K^-$  beam impinging from the left on the small hydrogen target at the centre. Neutral interactions are selected by the veto counter surrounding the

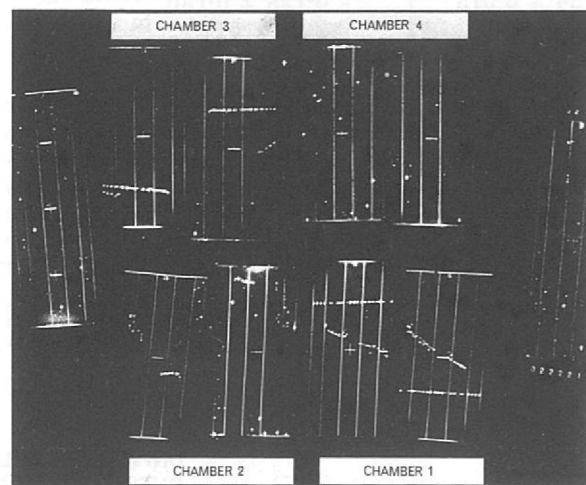


Fig. 5. A photograph showing two orthogonal views of each spark chamber. The event is an example of the reaction  $K^- + p \rightarrow \Lambda^0 + \pi^0$ ,  $\Lambda^0 \rightarrow p \pi^-$ ,  $\pi^0 \rightarrow \gamma\gamma$ . The views at the extreme left and right are of chamber 5 which is underneath the hydrogen target and not shown in figure 4.

## Experiment 5

### $K^\pm p$ Differential Cross-Sections.

Arrays of scintillation counters and sonic spark chambers in a separated K-meson beam, (derived from X2), are being used to study firstly  $K^+p$  and secondly  $K^-p$  elastic differential cross-sections from  $5^\circ$  to  $180^\circ$  at about 10 momenta between 0.45 and 0.9 GeV/c. The aim of the former experiments is to investigate the possibility of structure near 0.6 GeV/c and to improve the data, at present statistically poor, in this momentum interval.

The flux of  $K^-$ -mesons ranges from a few tens to a few hundreds per  $2 \times 10^{11}$  extracted protons.  $K^+$  fluxes are approximately six times larger. The detector subtended large solid angles at a 50 cm long hydrogen target. Forward and backward scattering are studied by measuring the

UNIVERSITY OF OXFORD

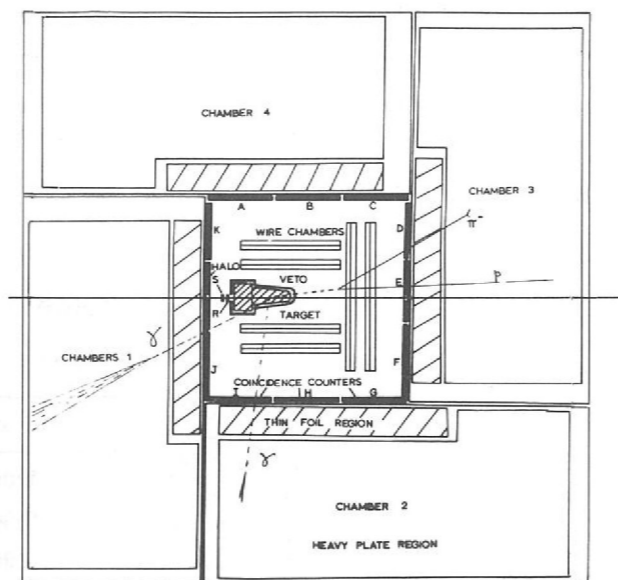


Fig. 4. Plan view of the experimental apparatus. The event shown in figure 5 has been indicated.

target, and  $\Lambda^0$  decay particles are detected by the wire spark chambers and the counters A-K. These particles are also seen in the optical spark chambers, where showers produced by  $\gamma$  rays from  $\Sigma^0$  and  $\pi^0$  decays are produced.

Figure 5 shows a typical event of the  $\Lambda^0 \pi^0$  type. Paired views (top and side) of each chamber are seen, chamber 1 at bottom right has the beam track and a backward-going shower, chamber 2 a low energy shower, and chamber 3 the proton and pion from the decay of the  $\Lambda^0$ . A drawing of this event has been superimposed on the layout figure (figure 4).

Initially, interactions are being investigated in the momentum range 720-960 MeV/c. A further run with 150,000 photographs will take place early in 1969.

UNIVERSITY OF BIRMINGHAM

momentum and angle of either the K-meson or the proton, using a large aperture spectrometer magnet. For the remainder of the angular range the scattered K-meson and the recoil proton are detected in coincidence. About 10,000 events per momentum will be obtained; the data will be fed on-line to a DDP-116 computer and thence on to a magnetic tape for eventual processing by the IBM 360/75. The on-line computer monitors the performance of the equipment and provides a CRT display of interesting quantities.

$K^+$  data taking has commenced with the detector configuration that covers the intermediate angle range. Preliminary analysis indicates that the elastic data is readily separable from the background. Test data taken over the entire momentum range in both geometries indicates that no unexpected problem will arise. Preliminary angular distributions for the  $K^+p$  data will shortly become available.

## Experiment 6

QUEEN MARY COLLEGE, LONDON

### $K^+$ Lifetime Measurement.

This is an experiment to measure the  $K^+$  meson life-time to an accuracy of 1 part in 1000. The objects of doing this are to help sort out the disagreement between the two most accurate measurements of the lifetime, a discrepancy of approximately 3-4 standard deviations, and to look for non-exponentiality in the  $K^+$  decay over a large number of lifetimes. The latter is important when considering theoretical explanations of CP violation in  $K^0$  meson decays.

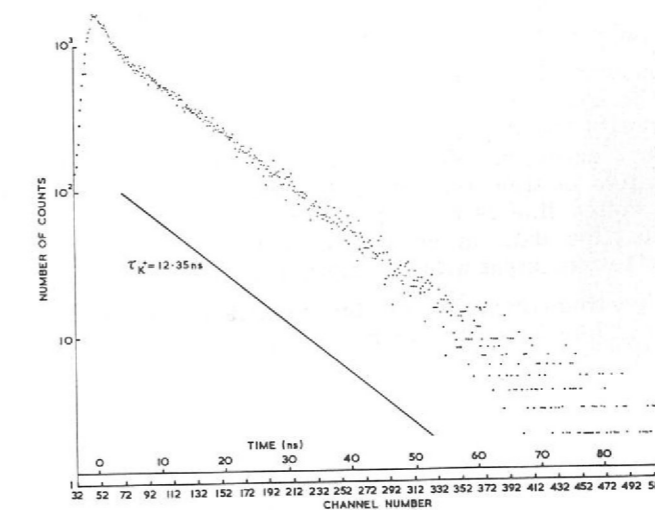


Fig. 6. Measured decay spectrum of  $K^+$  mesons.

800 MeV/c  $K^+$  mesons produced in a separated beam are selected from the  $\pi^+$  and p components by a DISC Cerenkov counter. The  $K^+$  mesons are then brought to rest in aluminium and their decay particles detected by surrounding scintillation counters. The decay spectrum is measured using a pre-calibrated, highly linear Time-to-Amplitude Converter, displayed on a LABEN pulse height analyser and stored on paper tape for subsequent analysis.

Preliminary data has been taken, as shown in figure 6, and should give an answer to an accuracy of 3 parts in 1000. From this it is estimated that the required precision of 0.1% should be readily achieved, given sufficient statistics (approximately 500,000  $K^+$  decays).

## Experiment 7

UNIVERSITY OF CAMBRIDGE  
RUTHERFORD LABORATORY

### Test of the $\Delta S = \Delta Q$ Rule for $K^0$ Leptonic Decays

The present theory of weak interactions has been built up assuming several basic selection rules. Amongst these, two fundamental ones are;

- CP conservation** (This assumes that the forces governing the weak decays are unchanged if one simultaneously changes particles into anti-particles and reflects the co-ordinate systems in a mirror).
- $\Delta S = \Delta Q$  rule** (The rule permits decays for which the change in strangeness of the strongly interacting particles ( $\Delta S$ ) is equal to the corresponding change in charge ( $\Delta Q$ )).

The current theory of weak interaction has enjoyed considerable success but violation of the two selection rules outlined above is not easily fitted into the theory. In the last few years experimental proof of CP non-conservation has been obtained for  $K^0$  decay and, while no conclusive evidence exists for violation of the  $\Delta S = \Delta Q$  rule, experiments on  $K^0 \rightarrow \pi e \nu$  decay give an indication of such effects.

This experiment aims at obtaining a large sample of  $K^0 \rightarrow \pi e \nu$  decays (10,000 events compared to 500 for typical published experiments) resulting from the decay of a pure  $K^0$  state produced in the reaction  $\pi^- + p \rightarrow \Lambda^0 + K^0$ . These events should enable a measurement of the ratio  $x = \frac{\text{Amplitude } \Delta S = -\Delta Q}{\text{Amplitude } \Delta S = \Delta Q}$  to an accuracy of a few percent or less. Should a violation be observed the analysis of the experiment will be able to say if the  $\Delta S = -\Delta Q$  amplitude is also CP violating.

The experimental equipment is shown in figure 7. A beam of  $\pi^-$  mesons of 1.035 GeV/c momentum is incident upon a polythene target and produces  $K^0$  mesons by the reaction  $\pi^- + p \rightarrow \Lambda^0 + K^0$ . A trigger system has been devised to select events corresponding to this reaction, followed by the decays  $\Lambda^0 \rightarrow \pi^- p$  and  $K^0 \rightarrow \pi e \nu$ .

This selection requires an incoming  $\pi$  meson to disappear and the produced particles to be neutral when they pass the veto counters (see figure 7). The picket fence counters are used to select events decaying into four charged particles and the Cerenkov counter selects events in which one of these four particles is an electron.

Optical spark chambers are used to record the incoming  $\pi^-$  and to observe the two V's corresponding to decay of the  $\Lambda$  ( $\Lambda \rightarrow p \pi^-$ ) and decay of K ( $K \rightarrow \pi e \nu$  with the neutral neutrino unobserved). An event is shown in figure 8.

A trigger system has been set up and 320,000 pictures, corresponding to 50% of those, scheduled, have been taken. Data collection is continuing and should be complete by March, 1969. Pictures corresponding to the more common decay  $K^0 \rightarrow \pi^+ \pi^-$  have also been taken by removing the requirement of a signal from the electron Cerenkov counter.

Data analysis of the pictures using hand measuring machines and an automatic measuring system is under way. Geometric reconstruction and kinematic fitting programmes are working and have been used to analyse events corresponding to  $K^0 \rightarrow \pi e \nu$  and to  $K^0 \rightarrow \pi^+ \pi^-$ . Clear events corresponding to the required reaction and decays are seen and figure 9 shows a plot of the number of  $\Lambda$  decays as a function of time (in units of the known  $\Lambda$  lifetime) corrected for the experimental efficiency. The dotted line is the expected result corresponding to the known  $\Lambda$  lifetime and it can be seen that the data is consistent with this value. Similar plots for  $K^0 \rightarrow \pi^+ \pi^-$  and  $K^0 \rightarrow \pi e \nu$  are also consistent with the known lifetimes of  $K_S^0$  and  $K_L^0$ .

Analysis is continuing and a preliminary value for the amplitude ratio  $x$  should be obtained early in 1969. Final analysis will take about one year.

### Experiment 8

WESTFIELD COLLEGE, LONDON  
RUTHERFORD LABORATORY

Test of the  $\Delta I = \frac{1}{2}$   
Rule in the Decay  
 $\Sigma^+ \rightarrow p \pi^0$ .

The current-current structure of the weak interaction Lagrangian contains a term of the form

$$G J_\lambda(x) J_\lambda^*(x) / \sqrt{2}$$

where  $J_\lambda(x)$  is the hadron current. This term gives rise to non-leptonic  $\Delta S=1$  transitions with both  $\Delta I = \frac{1}{2}$  and  $\Delta I = 3/2$ . There is strong experimental evidence for a  $\Delta I = \frac{1}{2}$  selection rule. The only evidence for the presence of a  $\Delta I = 3/2$  amplitude comes from  $K^+ \rightarrow \pi^+ \pi^0$  decay, which would require a  $\Delta I = 3/2$  amplitude that is ~5% of the  $\Delta I = 1/2$  amplitude observed in  $K_S^0 \rightarrow 2\pi$ . The  $\Delta I = 3/2$  may be suppressed for dynamical reasons or there may be an explicit  $\Delta I = 1/2$  selection rule in the weak interaction. The decay rates and asymmetry parameters of the non-leptonic sigma hyperon decays are sensitive tests of the  $\Delta I = 1/2$  rule. Angular momentum conservation in the decay  $\Sigma \rightarrow N \pi$  requires that the decay nucleon and pion be in an S or P state; parity violation in the weak interaction allows a linear combination of these two states. The decays  $\Sigma^- \rightarrow n \pi^-$  denoted by  $\Sigma^-$  and  $\Sigma^+ \rightarrow p \pi^+$  ( $\Sigma^+$ ) have been determined to be almost pure S and P wave respectively. The decay  $\Sigma^+ \rightarrow p \pi^0$  ( $\Sigma^+$ ) has approximately equal S and P waves; the exact ratio of S/P can be determined by measuring the asymmetry parameters  $\alpha$ ,  $\beta$  and  $\gamma$  in the decay of polarized sigmas.

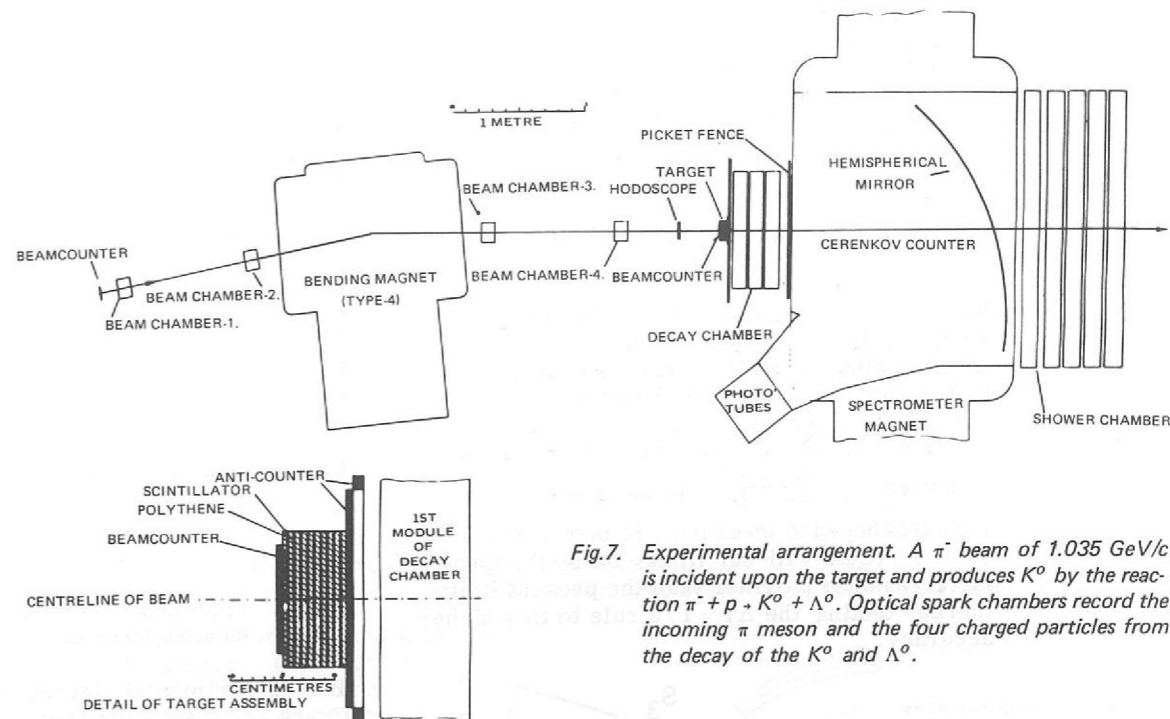


Fig. 7. Experimental arrangement. A  $\pi^-$  beam of 1.035 GeV/c is incident upon the target and produces  $K^0$  by the reaction  $\pi^- + p \rightarrow K^0 + \Lambda^0$ . Optical spark chambers record the incoming  $\pi$  meson and the four charged particles from the decay of the  $K^0$  and  $\Lambda^0$ .

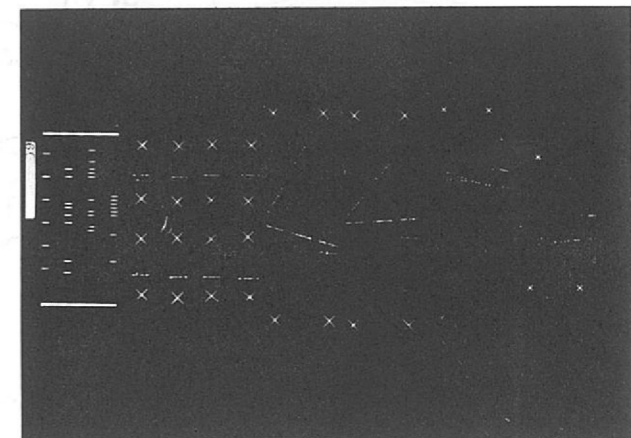
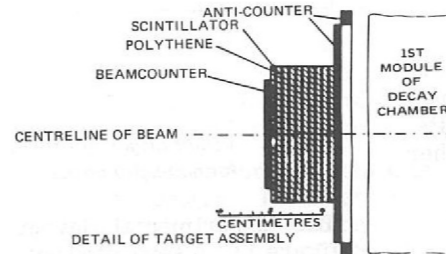


Fig. 8. An event showing the incoming pion and two V's corresponding to the decay of the  $K^0$  ( $K^0 \rightarrow \pi e \nu$  with the neutral  $\nu$  unseen) and the  $\Lambda^0$  ( $\Lambda^0 \rightarrow p \pi^-$ ). All spark chambers are photographed in two views at  $90^\circ$ .

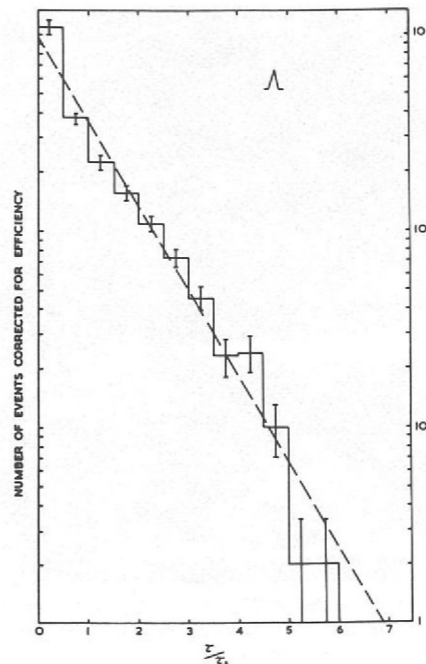


Fig. 9 Number of  $\Lambda$  decays as a function of time (in units of the  $\Lambda$  lifetime) corrected for the experimental efficiency. The dotted line corresponds to the known  $\Lambda$  lifetime.

The empirical selection rule  $\Delta I = 1/2$ , requires that, treated as vectors in the S-P plane, the three transition amplitudes

$$\Sigma^- = \Sigma^- \rightarrow n\pi^-$$

$$\Sigma_0^- = \Sigma^+ \rightarrow p\pi^0$$

$$\Sigma_0^+ = \Sigma^+ \rightarrow n\pi^+$$

form a triangle satisfying the relation

$$\sqrt{2} \Sigma_0^- = \Sigma^- - \Sigma_0^+$$

The current status of the vector diagram is shown in figure 10. Within the errors the triangle is closed, but the large uncertainty in the S/P ratio for  $\Sigma_0^-$  reduces the usefulness of this test. The region where  $S \approx P$  happens to be the very point where the parameter  $\gamma$  is particularly sensitive. ( $\gamma = \frac{S^2 - P^2}{S^2 + P^2}$ ). In the present experiment it is hoped to measure  $\gamma$  to better than 10%. Such a result will put limits on S/P approximately a factor 5 tighter than the present limits, thereby testing the  $\Delta I = 1/2$  rule to this higher accuracy.

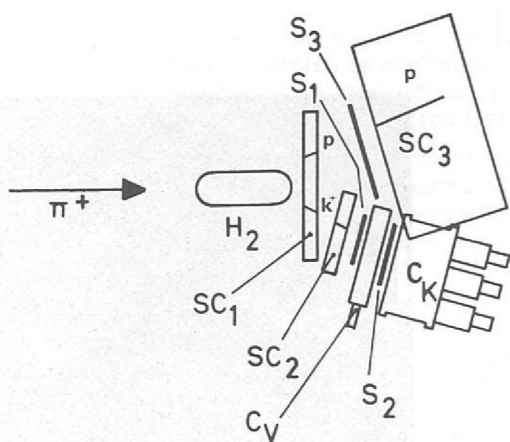


Fig. 11. Schematic view of the experimental apparatus. The event shown in fig. 12 has been indicated.

spark chambers are triggered by an electronically identified  $K^+$  plus an associated charged particle in  $S_3$  and viewed by an array of eight vidicon cameras. The spark positions are immediately digitized and recorded directly on magnetic tape.

Data taking is in progress. The performance of the apparatus and the quality of the data is checked on an IBM 1130 computer by reconstructing the events on an oscilloscope. Figure 12 shows a selected event reconstructed from the four plan view cameras. A drawing of this event has been superimposed on the layout diagram (figure 11). The spark chambers have been triggered 250,000 times (30% of total required) and a preliminary analysis of identified  $\Sigma^+ \rightarrow p\pi^0$  decays is in agreement with Monte Carlo predictions. Data collection is expected to be completed by March, 1969.

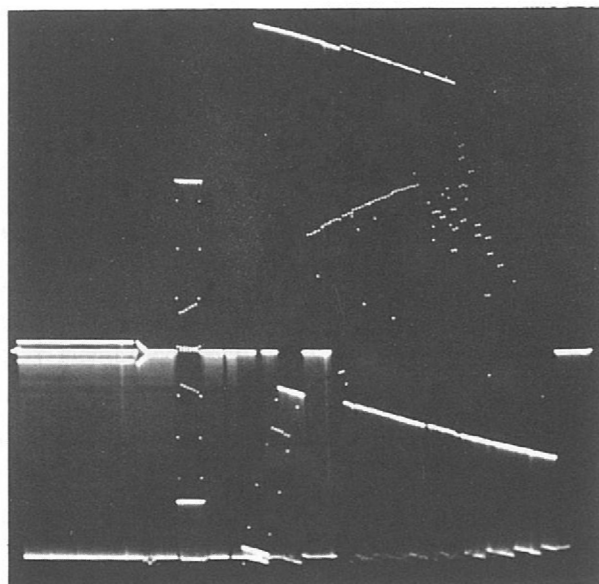


Fig. 12. A view of a decay  $\Sigma^+ \rightarrow p + \pi^0$  together with the outline of the hydrogen target and spark chambers. Reconstructed by computer from the four plan view vidicon chambers.

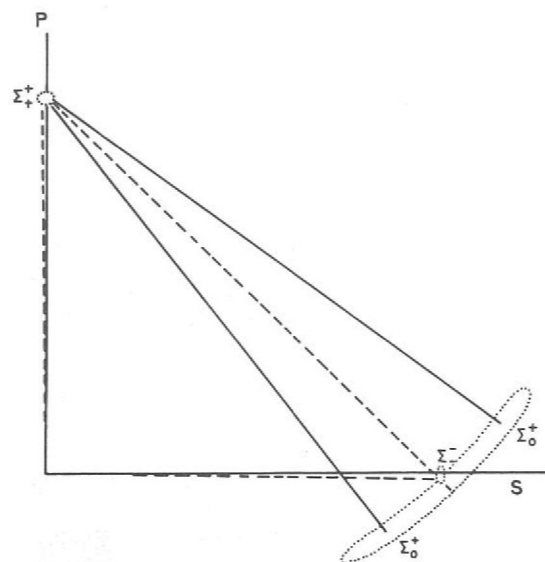


Fig. 10. Vector diagram of transition amplitudes for non-leptonic decays of  $\Sigma^\pm$ .

The experimental layout is shown in figure 11. A separated beam of  $\pi^+$  mesons of momentum 1111 MeV/c incident upon a liquid hydrogen target produces polarized sigmas by the reaction  $\pi^+ + p \rightarrow \Sigma^+ + K^+$ . The experiment involves measuring the decay proton polarization with respect to the  $\Sigma$  polarization direction. The  $K^+$  detector consists of two scintillators  $S_1$  and  $S_2$ , a thin water Cerenkov counter  $C_V$  to veto fast particles and a  $80 \times 40 \times 30$  cm<sup>3</sup> water Cerenkov tank,  $C_K$ , to detect the fast muon from the decay of a  $K^+$  stopping in the tank. Thin foil spark chambers  $SC_1$  and  $SC_2$  measure the direction of the  $K^+$  and decay proton. The polarization and range of the proton are measured in a 60 gap, 1½ ton, aluminium plate spark chamber  $SC_3$  ( $140 \times 140 \times 60$  cm<sup>3</sup>). The

## Experiment 9

UNIVERSITY OF OXFORD  
RUTHERFORD LABORATORY

Polarization  
Effects in  $\pi^+ p$   
Elastic  
Scattering  
(12, 42, 50, 56)

The present experiment is a continuation of the work on  $\pi p$  scattering described in the Annual Reports of 1966 (Experiment 10) and 1967 (Experiment 7). The asymmetry in the scattering of  $\pi^-$  mesons by polarized protons was measured at 50 different momenta from 0.643 to 2.14 GeV/c. Data was obtained at values of  $\cos \theta$  ranging from approximately +0.9 to -0.95 in the c.m. system at each incident pion momentum. The results have been expressed in the form of an expansion in terms of first associated Legendre polynomial series and compared with the predictions of recent phase shift solutions. It is concluded that although these analyses give satisfactory predictions of the general features of the results, no one solution gives complete agreement with the data above about 1.0 GeV/c.

It is planned to continue the investigation of the pion-nucleon system by a series of measurements on  $\pi^+ p$  elastic scattering from a polarized target.

The  $\pi^- p$  system is a combination of  $I = 1/2$  and  $I = 3/2$  states. The acquisitions of polarization data on  $\pi^+ p$  elastic scattering, which is a pure  $I = 3/2$  system, will facilitate a full I-spin phase shift analysis. Data will be taken at approximately 70 momenta between 600 MeV/c and 2700 MeV/c incident  $\pi^+$  momentum. The experimental layout is shown in Figure 13.

Electrons in the beam are vetoed by a gas Cerenkov counter. Pions are separated from protons at low momenta by a separator, and by time of flight. At higher momenta a DISC Cerenkov counter is required. The new LMN polarized target has achieved a polarization of approximately 70%, which can be measured by an NMR system to an accuracy of  $\pm 4\%$ . The counter hodoscope consists of vertical counters to determine scattering angle, horizontal counters to enable elastic (coplanar) events to be separated from inelastic background, and Cerenkov counters to separate pions from protons in those regions where they are not clearly distinguishable by kinematics. It is hoped to extract differential cross-sections from the data if the background is not too high.

Setting up has commenced and data taking is expected to start during 1969.

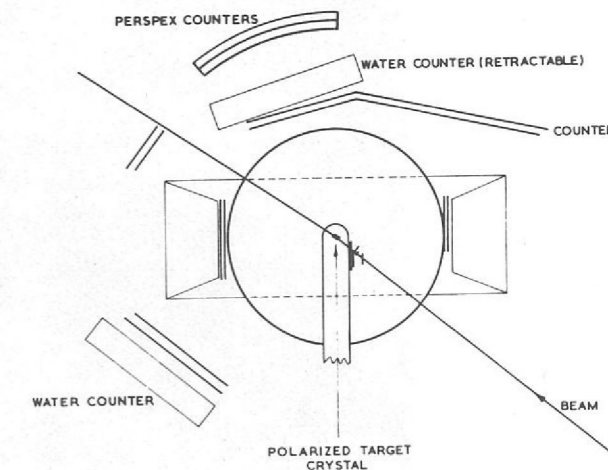


Figure 13. Plan view of the experimental apparatus.

## Experiment 10

QUEEN MARY COLLEGE, LONDON,  
AERE, RUTHERFORD LABORATORY

The  $\beta$ -Decay of  
the  $\Sigma^-$  Hyperon.

The experiment involves the study of the decay  $\Sigma^- \rightarrow ne\bar{\nu}$  which occurs with a branching ratio of  $\sim 10^{-3}$  with respect to the normal decay  $\Sigma^- \rightarrow n\pi^-$ . The angular distribution of the electrons about the direction of the spin of the  $\Sigma^-$  is given by the expression

$$I(\theta) = 1 + \alpha \bar{P}_\Sigma \cos \theta_{\Sigma e},$$

where  $\bar{P}_\Sigma$  is the average polarization of the  $\Sigma^-$  hyperons and  $\theta_{\Sigma e}$  the angle between the electron momentum and the direction of the  $\Sigma$  spin. The quantity  $\alpha$  is given by

$$\alpha \approx 2(-G_A/G_V) \left( \frac{1 - (-G_A/G_V)}{1 + 3(-G_A/G_V)^2} \right)$$

where  $G_V$  and  $G_A$  are the coupling constants of the vector and axial vector currents present in the weak interaction responsible for the decay. A determination of  $\alpha$  will yield the ratio of  $G_A/G_V$ . The form of the weak interaction in this decay is predicted to be  $V + 0.3A$  from an  $SU_3$  analysis of hyperon leptonic decays.

The  $\Sigma^-$  hyperons produced in the reaction  $\pi^- + p \rightarrow K^+ + \Sigma^-$  are polarized along the direction  $\vec{K}_+ \times \vec{K}_-$ . The mean polarization of the hyperons used in the decay is  $-0.24 \pm 0.09$ . This value is derived from the result of experiment 2, where the polarization in the above production process was measured directly using a polarized target.

The momentum of the pion beam, incident on the liquid hydrogen target, was  $1.13 \text{ GeV}/c$  in order to work below the threshold for producing an extra pion in addition to the  $\Sigma^-$  and  $K^+$ . In this situation the identification of a  $K^+$  meson could be used to indicate the production of a  $\Sigma^-$  hyperon. The  $K^+$  was identified by selecting particles with  $v/c < 0.75$  (i.e. with velocity below that required to produce Cerenkov radiation in water) which were stopped in a large water tank where the relativistic decay products produced delayed counts through Cerenkov radiation emitted in the water. The decay electrons were detected in a Cerenkov counter filled with freon-12 at a pressure of one atmosphere. For particles with momentum  $\sim 200 \text{ MeV}/c$ , this detector had a measured efficiency of about 0.9 for electrons and not more than  $10^{-5}$  for pions, thus making it possible to select the  $\beta$ -decay events from the large potential background of normal decays.

The  $K^+$  detectors were placed above and below the beam with electron detectors to the left and right in order to maximise the possible asymmetry by measuring the rate with  $\theta_{\Sigma e} \approx 0$  or  $\pi$ . The electronic trigger fired a system of wire spark chambers with a ferrite core read-out, which were used to determine the directions of the incident pion, the kaon, and the decay particle (either an electron or a pion depending on the trigger requirements).

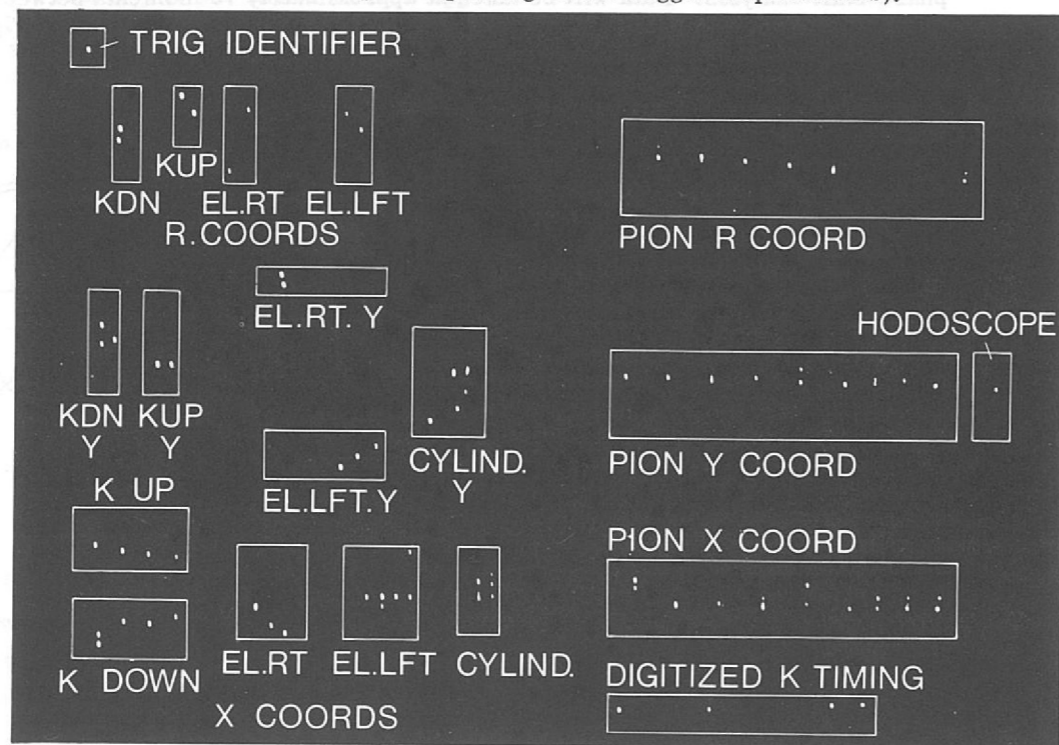


Figure 14 shows display from the wire chambers produced by the PDP8. The 'boxes' have been superimposed to aid interpretation — they were not present on the display. The chambers measured X-coordinates (vertical) Y-coordinates (horizontal) and R-coordinates (at  $45^\circ$ ). The trigger shown is identified by dot in top left hand corner as UP LEFT i.e.  $K^+$ -UP; decay product-LEFT

A PDP8 computer was used to write the information from the wire chambers on to a 7-track magnetic tape, to display the spark chamber co-ordinates of an event on a CRT (figure 14), and to histogram relevant quantities from the spark chambers and the electronic trigger so that the performance of the apparatus could be monitored. During data collection, at intervals of  $\sim 8$  hours, the information on the 7-track tape was read back into the PDP8 and transmitted via an on-line link to the IBM360/75 where a 9-track tape was written. After each transmission a program which constructed  $(\pi-K)$  vertices and decay particle vectors was run in the 360/75, in order to keep a check on the chamber efficiencies.

Before its conclusion at the end of July the experiment collected 110,000  $\beta$ -decay triggers, with an incident pion intensity of  $3-5 \times 10^5$  pions per pulse, and at an average rate of one trigger per 6 pulses. In addition 45,000 normal decay triggers were taken.

The pattern of the normal decay in the spark chambers is the same as that for the  $\beta$ -decay so these events have been used to refine the software designed to find the  $\beta$ -decay events. Basically the analysis program selects sparks to form the pion, kaon, and decay product vectors, associates the pion and kaon and performs a  $(\pi-K)$  vertex fit, predicts a  $\Sigma^-$  direction and

attempts to associate the decay track with it. A geometrical fit is performed to the event and the separation of the  $(\pi-K)$  and  $(\Sigma-e)$  vertices determined along with its estimated error. If the separation of the two vertices is taken as the length of the  $\Sigma^-$  track, and the momentum determined from the kinematics of the production process, then the time for which the  $\Sigma^-$  lived may be calculated. Figure 15 shows a plot obtained from a small sample of normal decay events analysed during the data collection, where the length of the  $\Sigma^-$  was required to be  $\geq 6$  times the error. The line drawn is not a fit but corresponds to a lifetime of  $1.66 \times 10^{-10}$  seconds. Events are lost at short times since the production and decay vertices are not clearly separated and the event is rejected.

Work is in progress on a final determination of the parameters to be used in the track reconstruction and a thorough checking of the co-ordinate system before a large sample of data is computed.

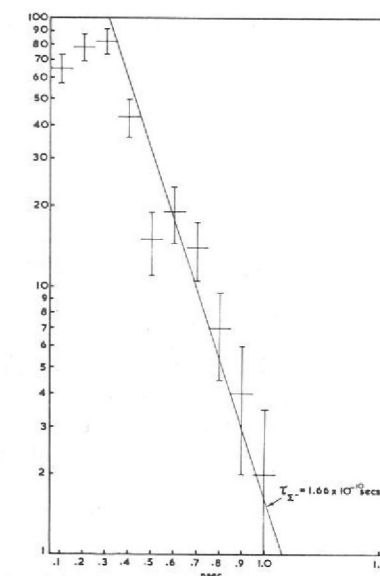


Figure 15. Measurement of the  $\Sigma^-$  life time obtained from 329 events of the decay  $\Sigma^- \rightarrow n\pi$

## Experiment 11

Differential  
Cross-Section  
Measurements for  
 $\pi^-p$  Elastic  
Scattering  
(163)

In the experiment carried out on Nimrod during 1967, differential cross-sections were measured for  $\pi^-p$  elastic scattering at momenta from 1.2 to 2.5  $\text{GeV}/c$ , and at 3.03  $\text{GeV}/c$ . Details of the experimental method were given in the 1967 Annual Report (Experiment 11).

Analysis of these measurements continued into 1968, and experimental results covering 40 laboratory-system angles in the interval  $20^\circ$  to  $170^\circ$ , at each of 25 momenta (1.34 to 2.49  $\text{GeV}/c$ ) have now been circulated to other groups and laboratories.

Beyond the purely experimental analysis comes the further analysis of the experimental results in terms of partial wave amplitudes, and the interpretation of these amplitudes in terms of resonances with definite quantum numbers. Techniques for this further analysis have been developed in recent years by several specialised theoretical research groups. These groups are now incorporating the new experimental results into their data.

## Experiment 12

The Partial  
Width of the  
Decay  $\phi^0 \rightarrow e^+e^-$   
(1, 57)

The main interest in the leptonic decays of vector mesons lies in the relative magnitudes of the transition rates, as these give information on the form of the observed meson in terms of the  $SU_3$  or  $SU_6$  eigenstates. Recent theoretical advances have turned this from a rather rough concept into a precise tool, and accurate measurements would be invaluable.

The analysis of the data collected in the autumn of 1966 has been completed; experimental details were given in the 1967 Annual Report (Experiment 6). It has been shown that

- (i) there was good evidence for the existence of the decay mode  $\phi \rightarrow e^+e^-$
- (ii) using the value for the  $\phi$  production cross-section measured under the same conditions ( $\pi^- + p \rightarrow \phi^0 + n$  at 1.58  $\text{GeV}/c$ ) and the standard values for the  $\phi^0$  width and for the branching ratio of  $\phi^0 \rightarrow K^+K^- / \phi^0 \rightarrow \text{total}$ , the partial width for  $\phi^0 \rightarrow e^+e^-$  was  $2.4 \pm 1.5 \text{ keV}/c^2$ . While this result was consistent with expectations and with other experiments, it was also concluded that there was only limited scope for development in the technique used, especially in comparison with the achievements and potentialities of the colliding beam technique, and it was decided not to pursue these investigations further at the present time.

IMPERIAL COLLEGE, LONDON  
RUTHERFORD LABORATORY

## Experiment 13

Wide Angle Elastic  
Proton-Proton  
Scattering in the  
Momentum Range  
1.5-4.5 GeV/c.

The aim of the experiment is to measure the differential cross-section for proton-proton scattering at incident proton momenta in the range 1.5-4.5 GeV/c and at scattering angles from 40°-90° in the centre of mass. These cross-sections are not well known at present. The data should also allow a careful study of the behaviour of the plot of  $d\sigma/dt$  (90°) against  $s$  - the square of the total energy in the centre of mass. Figure 16 shows the existing data which suggest a discontinuity at 2.4 GeV/c incident momentum.

Recent experiments<sup>1,2</sup> show that in the range 5-21 GeV/c,  $d\sigma/dt$  can be fitted by the function  $d\sigma/dt = a \exp\left(\frac{-s \sin\theta}{b}\right)$  where the parameters  $a$  and  $b$  have two discrete values

$$5 \leq p \leq 8 \text{ GeV/c} \quad a = 134.6 \text{ mb GeV}^{-2} \quad b = 1.24 \text{ GeV}^2$$

$$11 \leq p \leq 21 \text{ GeV/c} \quad a = 56.4 \text{ mb GeV}^{-2} \quad b = 2.77 \text{ GeV}^2$$

The low energy data show that a discontinuity exists at 0.52 GeV/c. The aim is to make measurements at intervals of ~300 MeV/c around the region of 2.4 GeV/c in order to establish the shape of the curve there.

The experiment will use a low intensity (~10<sup>4</sup> protons per burst) proton beam scattered out of Nimrod at 19°. Figure 17 shows a schematic diagram of the apparatus. The detection system is made symmetrical in order to nullify any difficulties that may arise from the incident beam being partially polarized. Two scintillation counter hodoscopes, one on the left, and one on the right are the main components of the trigger. They are combined logically to define roughly the geometry of a p-p elastic scatter. It is estimated that the signal to noise ratio will be 1:5 at worst. The electronic trigger fires a system of wire spark chambers with a ferrite core read-out, on-line to a PDP8 computer which writes the information on to a 7-track magnetic tape. Final analysis will be done off-line on the 360/75 computer.

The experiment commenced setting up in December 1968 and should collect a sample of data before the March 1969 shutdown.

<sup>1</sup> Akerlof C.W. et al., Phys. Rev., 159 (5) 1138 (July 1967)

<sup>2</sup> Allaby J.V. et al., Phys. Lett., 25B (2) 156 (August 1967)

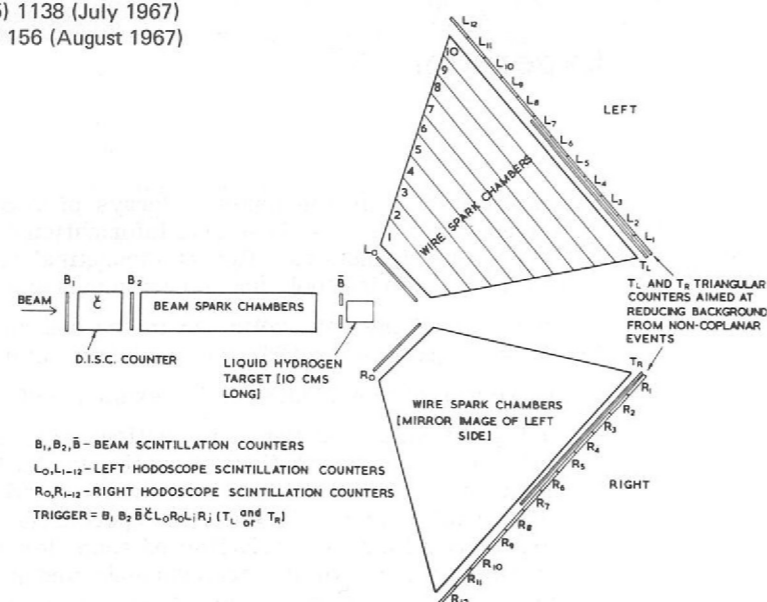


Figure 17. Schematic diagram of the experimental apparatus.

AERE, UNIVERSITY OF BERGEN  
QUEEN MARY COLLEGE, LONDON  
RUTHERFORD LABORATORY.

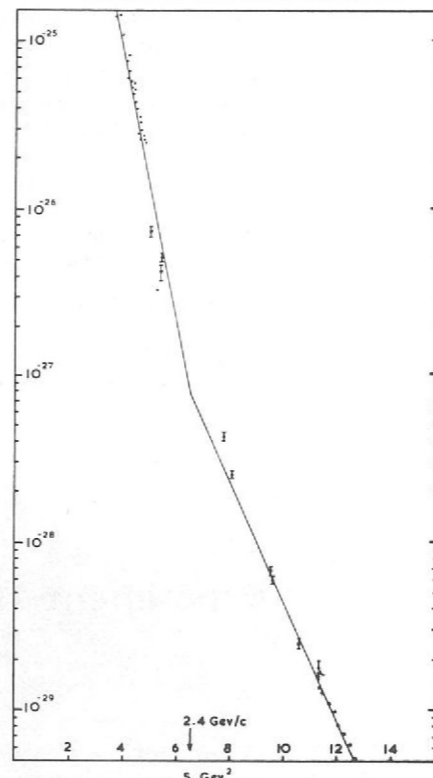


Figure 16. Existing measurements of  $d\sigma/dt$  (90° cm) for elastic p-p scattering as a function of  $s$ .

## Experiment 14

UNIVERSITY OF GLASGOW  
UNIVERSITY OF LIVERPOOL  
UNIVERSITY OF OXFORD  
RUTHERFORD LABORATORY

A Study of the  
Decay Modes  
 $K^\pm \rightarrow \pi^\pm \pi^0 \gamma$   
and  $K^\pm \rightarrow \pi^\pm \pi^0 \pi^0$

The aims in this experiment are;

- To measure the charge asymmetry in the rates for  $K^\pm \rightarrow \pi^\pm \pi^0 \gamma$  in order to test for C non-invariance in electromagnetic interactions and CP non-invariance in the weak interaction and to measure for this mode the electric and magnetic dipole structure amplitudes and the interference between the electric dipole amplitude and the inner bremsstrahlung.
- To measure the charge asymmetry in the rates for  $K^\pm \rightarrow \pi^\pm \pi^0 \pi^0$  in order to test for  $\Delta I = 5/2, 7/2$  CP non-invariant terms in the non-leptonic interaction.

The experiment is being carried out in a 5 GeV/c unseparated kaon beam at the CERN PS. A differential Cerenkov counter identifies the kaons in the beam and a system of counter hodoscopes and wire spark chambers defines their momenta and directions. The vector momentum of the charged pion produced when a kaon decays into either of the two desired final states is measured by sonic spark chambers in conjunction with a large spectrometer magnet. A counter hodoscope detects the final state  $\gamma$ -rays (including those from the neutral pion) and defines their outgoing directions.

The experiment was installed at CERN in September 1968. It is scheduled for data taking in the first half of 1969. It is hoped to measure the charge asymmetry in the  $\pi^\pm \pi^0 \gamma$  mode (branching ratio  $2.2 \times 10^{-4}$ ) to a precision of  $\pm 1\frac{1}{2}\%$  and in the  $\pi^\pm \pi^0 \pi^0$  mode (branching ratio  $1.69 \times 10^{-2}$ ) to  $\pm 0.015\%$ .

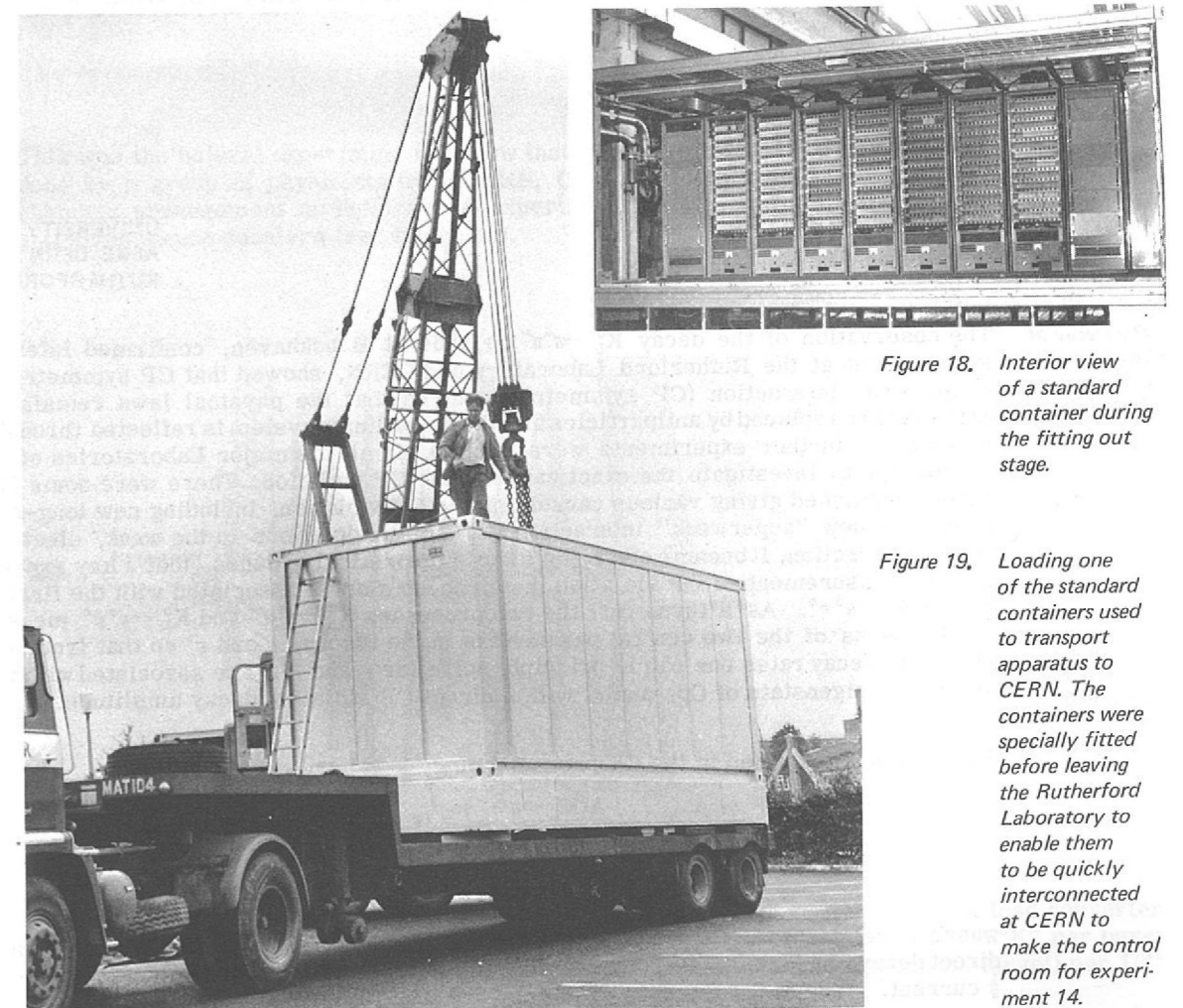


Figure 18. Interior view of a standard container during the fitting out stage.



Figure 19. Loading one of the standard containers used to transport apparatus to CERN. The containers were specially fitted before leaving the Rutherford Laboratory to enable them to be quickly interconnected at CERN to make the control room for experiment 14.

## Experiment 15

UNIVERSITY OF CAMBRIDGE  
RUTHERFORD LABORATORY

*EPISTLE (Elastic  
Pion Scattering  
Through Low  
Energies)  
(28, 44, 62)*

The aims of this experiment are as follows:

- (i) to measure the total cross-sections for scattering of  $\pi^+$  and  $\pi^-$  from hydrogen between 80 and 310 MeV with an accuracy of about  $\pm 0.3\%$ .
- (ii) to measure the differential cross-sections in the same energy range and over the angular range  $\cos\theta = +0.8$  to  $-0.8$  with an accuracy of about  $\pm 1\%$ .
- (iii) to measure the total charge exchange cross-section with an accuracy of about  $\pm 1\%$ .

The experiment is being done at the CERN 600 MeV synchrocyclotron. The  $\pi^+$  and  $\pi^-$  measurements have to be done in two separate beams. Equipment for measuring total cross-sections has been set up in the variable energy  $\pi^-$  beam. Total cross-sections have so far been measured successfully in the range 120 to 310 MeV. At the bottom end of the energy range there were problems with the beam optics, caused by the non-uniform fringing field of the cyclotron. It is believed that these problems have now been understood, and it is hoped to complete the  $\pi^-$  measurements and measurements of  $\pi^+$  total cross-sections from 80 to 150 MeV shortly, after some small modifications to the beam.

In this energy region, where the  $N^*$  (1238) resonance dominates the scattering, cross-sections vary very rapidly with energy. A feature of the experiment is the accurate measurement of the beam energy ( $\pm 0.1\%$ ) by means of a magnet and four spark chambers at the end of the beam-line.

At these very low energies, pions penetrate only the long range nuclear forces. The ultimate objective of the experiment is the precise measurement of these long range forces. Putting it more precisely, the aim is to measure the  $\pi$ -N and  $\rho$ -N coupling constants precisely, and to provide quantitative information on the elusive S-wave  $\pi$ - $\pi$  interaction. Once this has been achieved higher energy data can be used with vastly increased accuracy to probe the short range forces.

## Experiment 16

UNIVERSITY OF AACHEN  
AERE, CERN  
RUTHERFORD LABORATORY

*The Decay of  
Long-Lived Neutral  
Kaons into Two  
Neutral Pions.  
(28, 44, 62)*

The observation of the decay  $K_L^0 \rightarrow \pi^+\pi^-$  in 1964 at Brookhaven, confirmed later that year by experiments at the Rutherford Laboratory and CERN, showed that CP symmetry was violated in the weak interaction (CP symmetry requires that the physical laws remain unchanged if particles are replaced by antiparticles and the co-ordinate system is reflected through the origin). A series of further experiments were started, in all the major Laboratories of the world, in an attempt to investigate the exact cause of the CP violation. There were some 50 theoretical papers published giving various causes for the CP violation, including new long-range galactic forces, a new "superweak" interaction, or small violations in the weak, electromagnetic or strong interaction. It became clear, on simple theoretical grounds, that a key experiment would be the measurement of CP violation in a process closely associated with the first, namely the decay  $K_L^0 \rightarrow \pi^0\pi^0$ . As it turns out, the two processes  $K_L^0 \rightarrow \pi^+\pi^-$  and  $K_L^0 \rightarrow \pi^0\pi^0$  measure different combinations of the two central parameters in the theory,  $\epsilon$  and  $\epsilon'$  so that from measurement of the two decay rates one can in principle solve for  $\epsilon$  and  $\epsilon'$ .  $\epsilon$  is associated with the  $K_L^0$  being an impure eigenstate of Cp, and  $\epsilon'$  with a direct CP violating decay amplitude.

Two ratios are defined in the CP phenomenology

$$\eta_{+-} = \frac{A(K_L^0 \rightarrow \pi^+\pi^-)}{A(K_S^0 \rightarrow \pi^+\pi^-)} = (\epsilon + \epsilon') = |\eta_{+-}| \exp(i\phi_{+-})$$

$$\eta_{00} = \frac{A(K_L^0 \rightarrow \pi^0\pi^0)}{A(K_S^0 \rightarrow \pi^0\pi^0)} = (\epsilon - 2\epsilon') = |\eta_{00}| \exp(i\phi_{00})$$

where  $\epsilon$  relates to a CP violation in the mass matrix, and  $\epsilon'$  relates to a CP violation in the direct decay channel, arising from a  $\Delta I = 3/2$  or  $5/2$  current out of phase with the normal  $\Delta I = 1/2$  current. Many of the theories require  $\epsilon' = 0$  i. e.  $|\eta_{+-}| = |\eta_{00}|$ .

A collaboration was formed between RHEL, CERN and the University of Aachen to perform the difficult  $K_L^0 \rightarrow 2\pi^0$  experiment. What makes this experiment difficult is that the decay leads to four neutral particles, namely the four  $\gamma$  rays from the decay of the two  $\pi^0$ s,  $\gamma$  rays being difficult particles to detect and measure. Two banks of thick plate spark chambers, placed on either side of the  $K_L^0$  beam, were used to detect the 4  $\gamma$  rays from the showers they produced.

The  $K_L^0$  decay region was surrounded by some 100 scintillation counters sandwiched with iron plates, in the form of a truncated cone. This system was used to veto  $\gamma$  rays coming out sideways, in order to reduce triggers from the very intense background process  $K_L^0 \rightarrow 3\pi^0 \rightarrow 6\gamma$ . The veto cone and the heavy plate spark chambers are seen in figure 20.

170,000 events were recorded on film. The films were scanned for 4  $\gamma$  events (a typical one is shown in figure 21) and some 60,000 4  $\gamma$  events were found and measured. Gamma ray directions were measured to  $\pm 2^\circ$  using the early part of the showers and the energies were obtained to an accuracy of  $\pm 25\%$  by counting total sparks in a shower. For each event the 4  $\gamma$  rays were reconstructed kinematically into two  $\pi^0$ s which were in turn reconstructed into a particle X; the mass ( $M_x$ ) direction ( $\theta_x$ ) and momentum ( $P_x$ ) of this "particle X" were calculated. The peak at a mass of 500 MeV (the mass of the  $K_L^0$ ), in the  $M_x$  plot (figure 22) was evidence that  $K_L^0 \rightarrow \pi^0\pi^0$  does occur.

The final result of the experiment reported at the International Conference on High Energy Physics, Vienna (August 1968) was

$$|\eta_{00}| = (3.6 \pm 0.6) \times 10^{-3}$$

This should be compared with the parameter  $|\eta_{+-}|$  which has a value of  $(1.90 \pm 0.05) \times 10^{-3}$ . Therefore, with a confidence corresponding to about 3 standard deviations, those theories requiring  $\epsilon' = 0$  (e.g. the superweak theory and all those assuming the validity of a  $|\Delta I| = \frac{1}{2}$  rule) are contradicted by the present experiment.

## Experiment 17

CERN, ORSAY  
RUTHERFORD LABORATORY

*Measurement of  $\phi_{00}$ ,  
the phase of  $\eta_{00}$*

This was the natural experiment to follow that which measured  $|\eta_{00}|$  as described above. It was done by a group of physicists from CERN, Orsay and RHEL using essentially the same spark chamber arrangement as the previous experiment but with a slightly different arrangement of anti-coincidence counters (see figure 23).

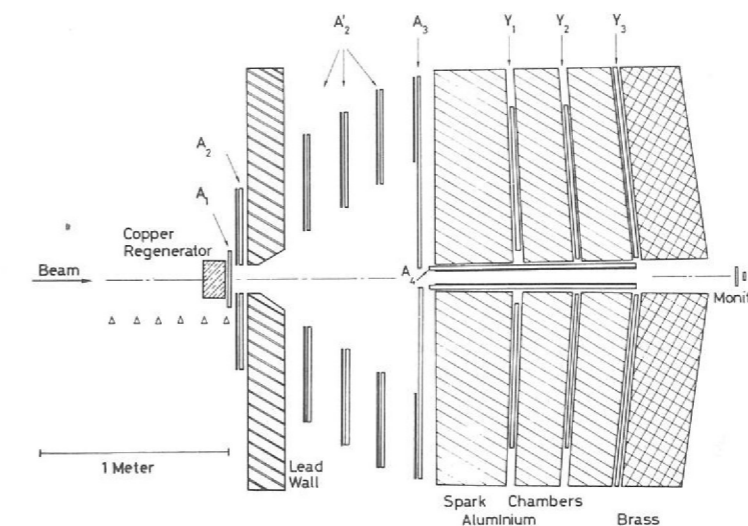


Figure 23. Plan view of the experimental apparatus.  $A_{1-4}$  are anti-coincidence counters,  $Y_{1-3}$  are trigger counters.

A neutral beam was taken at  $17^\circ$  from an external target at the CERN PS with a lead converter and a bending magnet to remove gamma rays and charged particles. Some  $5 \times 10^3 K_L^0$  per burst were obtained in the region of the detection equipment (situated 18m from the target) per  $10^{11}$  protons incident on the target.

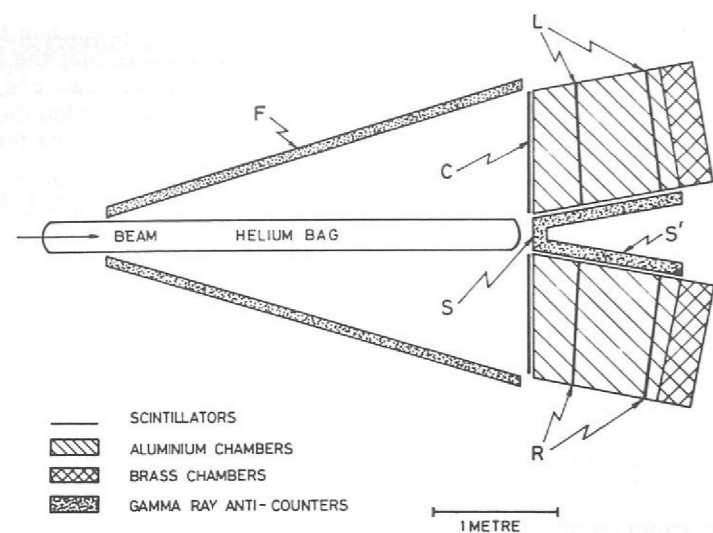


Figure 20. Schematic diagram of the experimental apparatus. L and R are trigger counters, C, S, S' and F are anti-coincidence counters.

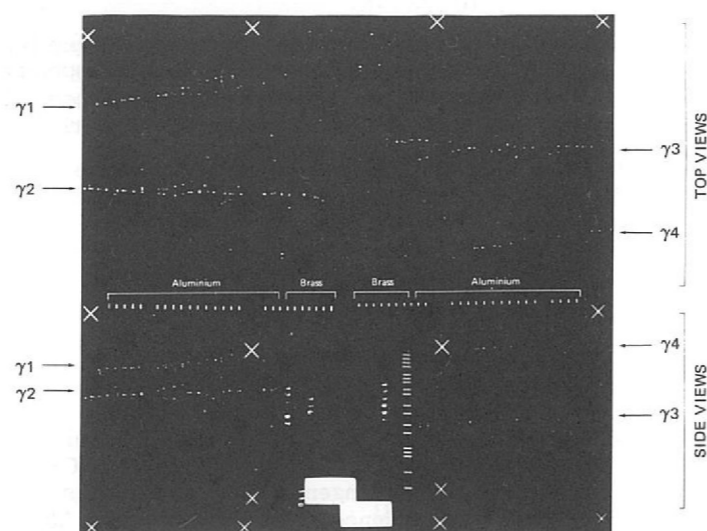


Figure 21. Photograph of a four shower event. (Experiment 16)

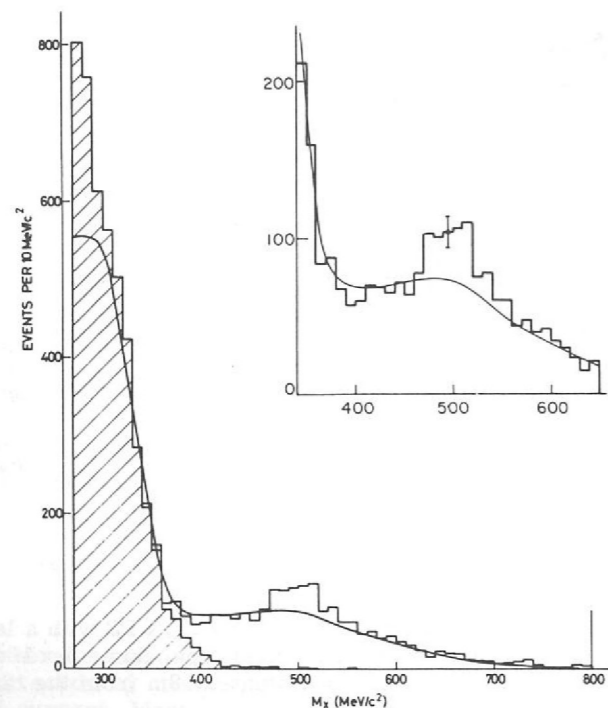


Figure 22. Mass plot for free decay (all pairings), showing a peak at the  $K_L^0$  mass of  $500 \text{ MeV}/c^2$ .

A copper regenerator 12 cm thick was in one of six fixed positions in front of a 20 cm thick lead wall which defined the beginning of the decay region of interest (the first spark chamber defined the end of the region). The trigger requirement favoured at least one gamma ray in each of four counter-defined quadrants.

A total of 240,000 photographs were taken and all the film was reverse processed by the film processing laboratory at RHEL. Approximately 90% of the scanning was carried out at the RHEL and all the four shower events were then measured at CERN or at Orsay. The events which consisted of just four showers were reconstructed to give the mass of the decaying object (assuming a decay into two neutral pions), its direction with respect to the incident beam direction and its decay point. Events were selected to satisfy certain criteria and the number of events observed was then plotted as a function of the real time (expressed in  $K_S^0$  lifetimes) between the exit of the regenerator and the decay point.

There were three contributions to the events observed in the decay region:-

- (i) Regeneration of  $K_S^0$  (which can be calculated) which then decay to two neutral pions,
- (ii) Decay of  $K_L^0$  to two neutral pions,
- (iii) The term arising from the interference between (i) and (ii).

The decay region used covered fifteen  $K_S^0$  lifetimes and the final plot is shown in figure 24. At early lifetimes one observes the exponential decay of the regeneration term, at long lifetimes, when all the  $K_S^0$  have decayed away, only the  $K_L^0 \rightarrow 2\pi^0$  term is present and in the central region (7 to 10  $K_S^0$  lifetimes) the destructive interference between the two terms is seen. The solid curve represents the 'best fit' to the data allowing  $\phi_{00}$  and  $|\eta_{00}|$  to be free parameters.

The results from the fit are:-

$$\phi_{00} = 27^\circ \pm 30^\circ$$

$$|\eta_{00}| = (3.2 \pm 0.7) \times 10^{-3}$$

This result is in excellent agreement with that of the CERN/RHEL/Aachen experiment to measure  $|\eta_{00}|$ .

The apparatus has now been modified to make a new measurement of  $|\eta_{00}|$  to  $\pm 10\%$  and  $\phi_{00}$  to  $\pm 15^\circ$ . Data collection is already in progress and will be complete at the end of February 1969.

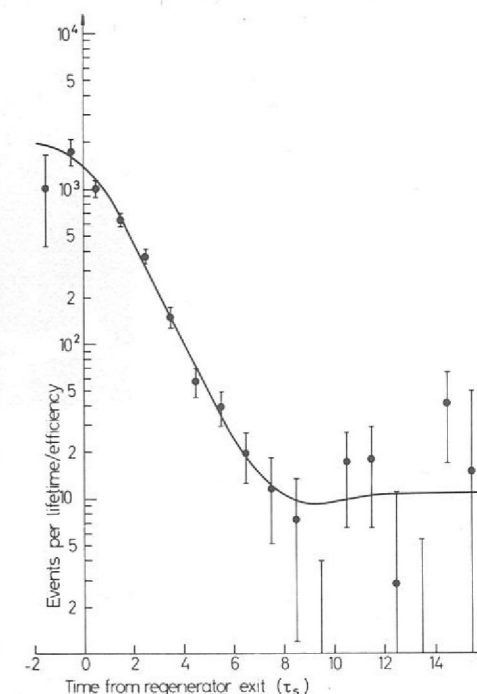


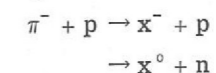
Figure 24. Plot of the number of observed events against  $K_S^0$  lifetime. The solid curve representing the 'best fit' to the data allowing  $\phi_{00}$  and  $|\eta_{00}|$  to be free parameters.

## Experiment 18

IMPERIAL COLLEGE, LONDON  
UNIVERSITY OF SOUTHAMPTON

An Investigation  
of Narrow Mesons  
produced in  $\pi^- p$   
Interactions

This experiment is designed to study in some detail narrow mesons produced in the reactions



up to a mass of about  $2 \text{ GeV}/c^2$ . It exploits the technique developed in earlier studies of  $\eta$  and  $\phi^0$  production near threshold but, in addition, incorporates an arrangement of  $\gamma$  and charged particle detectors surrounding the hydrogen target with which it is hoped to identify some major decay channels.

The detailed performance of the  $\gamma$  detectors has been determined over an energy range from 30 to 1500 MeV in a photon beam made by a simple 'tagging' technique in which the secondary electron was required to have very low energy. At the present time, setting up of the main experiment is almost completed and it is hoped to collect data in the first months of 1969.



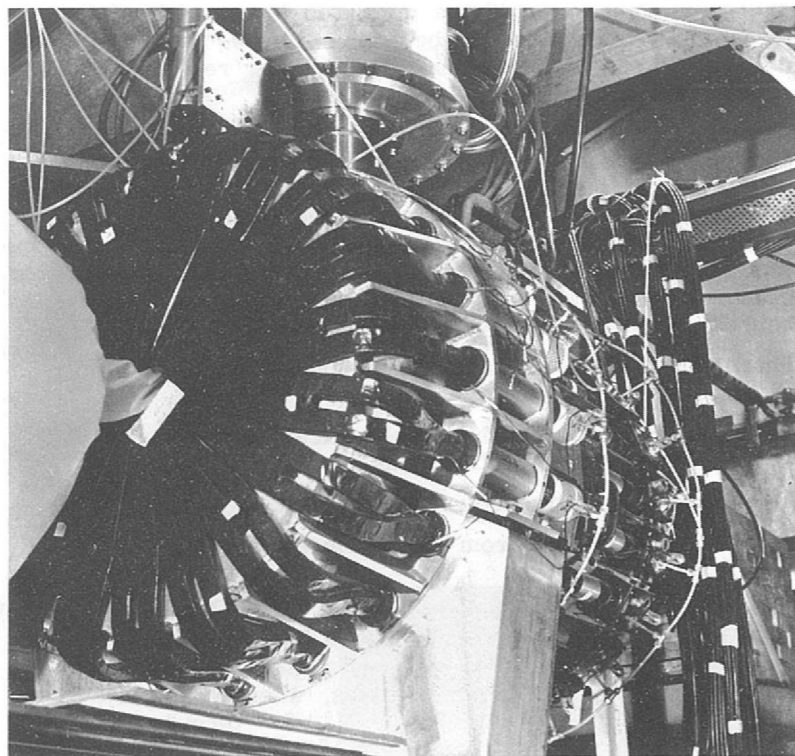


Figure 25. The array of charged particle detectors and  $\gamma$  counters surrounding the hydrogen target in experiment 18.

## Experiment 19

UNIVERSITY COLLEGE, LONDON

Decays of  
 $\eta$ -Mesons  
(7, 26, 61)

A third investigation has now been completed with an exposure of the UCL/RHEL Heavy Liquid Bubble Chamber to a 930 MeV/c  $\pi^+$  beam at Nimrod.

Previously this film has been used to search for the C violating decay  $\eta^0 \rightarrow \pi^0 e^+ e^-$ , and it has also yielded the first examples of inverse electro-production via intermediate vector mesons, i.e.  $\pi^+ + n \rightarrow p + \rho^0$ ;  $\rho^0 \rightarrow e^+ e^-$ . These studies were made in collaboration with the University of Oxford.

The examination of a proportion of the films in order to establish the ratio

$$R = \frac{\eta^0 \rightarrow 3\pi^0}{\eta^0 \rightarrow \pi^+ \pi^- \pi^0}$$

has now been completed.

In recent years experimental values have ranged from 0.35 to 1.5, with results coming mainly from hydrogen and spark chamber groups. The uncertainties have arisen from difficulties associated with the separation of the various neutral decay modes of the  $\eta$ , viz.  $\eta \rightarrow \pi^0 \gamma \gamma$ ,  $\eta \rightarrow \gamma \gamma$  and  $\eta \rightarrow 3\pi^0$ . The detection of as many  $\gamma$ -rays as possible represents a decided advantage; in this chamber filled with  $\text{CF}_3\text{Br}$ , the average conversion probability was very high viz. 73%.

The experiment consisted of looking for  $\pi^+$  interactions yielding 5 or 6  $\gamma$ -rays converted to  $e^- e^+$  pairs. 260 5  $\gamma$  events and 69 6  $\gamma$  events were found.

Several novel features were incorporated in the analysis which distinguished this experiment from previous ones. For example, a special template was devised which allowed objective corrections to be made for  $\gamma$ -rays mistaken for bremsstrahlung from other electron pairs. Only the 5  $\gamma$  events were used to obtain the value of R because the number of events with 5  $\gamma$ -rays converted was particularly insensitive to uncertainties in the radiation length, and a new statistical method was employed for estimating the background from non-resonant  $3\pi^0$  emission.

Normalising to the number of  $\eta \rightarrow \pi^+ \pi^- \pi^0$  decays found in a separate scan, the result is

$$R = 1.47 \pm 0.20 \\ - 0.17$$

This agrees with the theoretical ratio of 1.7 obtained by neglecting  $|\Delta I| = 3$  transition and the effects of final state interactions. Furthermore, the result provides additional evidence that the  $\pi^0 \gamma \gamma$  mode does not contribute appreciably to the neutral decays of the  $\eta$  meson.

## Experiment 20

UNIVERSITY COLLEGE, LONDON  
TUFTS UNIVERSITY, USA  
UNIVERSITY OF BRUSSELS  
CERN.

2.2 GeV/c  $K^-$   
Exposure in the  
1.4m Heavy  
Liquid Bubble  
Chamber

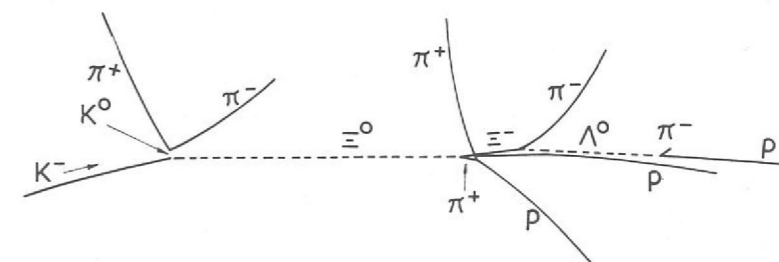
The object of the experiment is first to study the properties of the  $\Xi^0$  hyperon. Later it is intended to investigate the neutral decays of the  $X^0$  and  $\phi^0$  mesons. The main aims are:-

- (i) To look at  $X^0$  and  $\phi^0$  neutral decays, especially  $X^0 \rightarrow \eta^0 \pi^0 \pi^0$  and the processes  $X^0 \rightarrow \gamma \gamma$  and  $\phi^0 \rightarrow \gamma \gamma$  which provide a check of the electromagnetic predictions of symmetry schemes.
- (ii) To measure the  $\alpha$ ,  $\beta$  and  $\gamma$ -parameters of the  $\Xi^-$  which are at present in dispute.
- (iii) To find the lifetime of the  $\Xi^0$  by a method which uses the  $\gamma$ -rays from the  $\Xi^0$ -decay  $\pi^0$  to fix the decay point. This method cannot be used in a hydrogen chamber.

It is planned to take 600,000 pictures at 6 kaons per picture in a chamber mixture of propane and  $\text{CF}_3\text{Br}$  which an incident momentum of 2.2 GeV/c. 343,000 pictures have been obtained so far.



Figure 26. An example of a  $\Xi^0$  interaction photographed in the UCL - RHEL heavy liquid chamber. The  $\Xi^0$  is produced in the reaction  $K^- + p \rightarrow \Xi^0 + K^0$ ,  $K^0 \rightarrow \pi^+ \pi^-$ . The  $\Xi^0$  charge exchanges in the reaction  $\Xi^0 + p \rightarrow \Xi^- + \pi^+ + p$ ,  $\Xi^- \rightarrow \Lambda^0 + \pi^-$ ,  $\Lambda^0 \rightarrow p + \pi^-$ . The  $\pi^+$  from the  $\Xi^0$  interaction scatters on a proton.



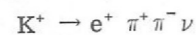
## Experiment 21

UNIVERSITY COLLEGE, LONDON  
UNIVERSITY OF WISCONSIN  
LAWRENCE RADIATION LABORATORY

A Study of  
 $K_{e4}$  Decays  
(17, 65)

This experiment was originally proposed at RHEL, but was transferred to CERN following the alternator break-down at Nimrod in 1965.

The CERN enlarged 1.1 metre heavy liquid bubble chamber was filled with  $C_2F_5Cl$  and exposed to a stopping  $K^+$  beam. 551,000 pictures yielded a total of  $13.3 \times 10^6$   $K^+$  decays. The film was scanned for examples of the rare  $K_{e4}$  decay mode:



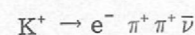
The events could readily be identified since the electrons radiate their energy and spiral to rest.

269 events were found, and when these are added to 69 events obtained in a previous investigation, the world total now stands at 338.

The particular significance of  $K_{e4}$  decays is their unique property of allowing one to investigate the S-wave  $\pi$ - $\pi$  interaction at low energy in the absence of any strongly interacting particles. This experiment yielded two acceptable solutions for the phase shift, which differ in sign but have the same magnitude,  $25^\circ \pm 9^\circ$ .

Values for the form factors were obtained which demonstrated that the vector form factor,  $h$ , was significantly non-zero, as was also  $f_p$ , an additional form factor omitted in certain theoretical treatments of the decay.

The branching ratio for the decay is  $(3.25 \pm 0.35) \times 10^{-5}$  which agrees well with current algebra predictions. No example was found of the decay



and this adds further confirmation to the  $\Delta Q = \Delta S$  rule. An upper limit for the violation parameter, defined as the ratio of the amplitudes of the  $\Delta Q = -\Delta S$  current to the  $\Delta Q = \Delta S$  current, is  $X < 0.3$  at the 95% confidence level.

No evidence of a  $\sigma$  resonance was seen. The angular distribution between the secondary particles was consistent with time reversal invariance and the locality of lepton production.

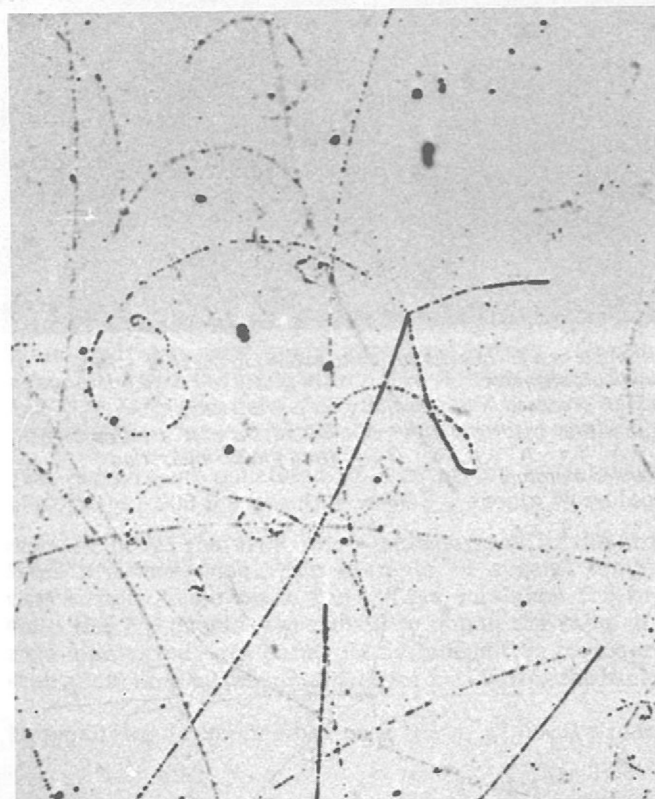
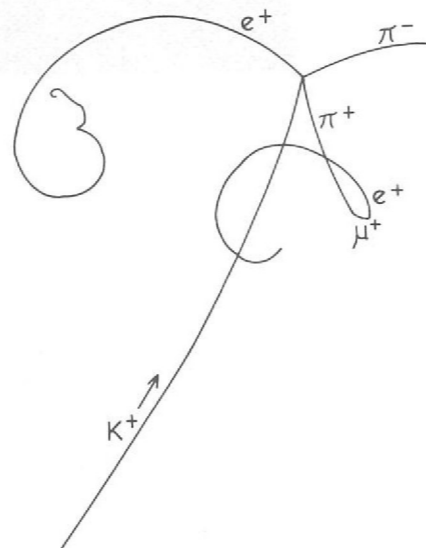


Figure 27. An example of  $K_{e4}$  decay ( $K^+ \rightarrow \pi^+ \pi^- e^+ \nu$ ) taken in the 1.1 m CERN heavy liquid bubble chamber, and analysed at University College, London.



## Experiment 22

IMPERIAL COLLEGE, LONDON  
WESTFIELD COLLEGE, LONDON

$\pi^+p$  Interactions  
(a) 0.90-1.05 GeV/c

The objectives of the study are:

- (i) the determination of the behaviour of the  $N^{*++}\pi^0$ ,  $N^{*+}\pi^0$  and  $N^{*+}\pi^+$  cross-sections as a function of momentum
- (ii) the study of the  $N^{*++} - N^{*+}$  interference in the  $p\pi^+\pi^0$  channel
- (iii) the partial wave analysis of the  $N^{*++}\pi^0$  channel.

Out of a total of 44,000 events obtained in the Saclay 80 cm chamber, the percentage completely analysed at each of the four incident  $\pi^+$  momenta is as follows:

(GeV/c)	%
0.90	100
0.95	40
1.00	50
1.05	10

Analysis is continuing.

(b) 1.10-1.70 GeV/c

Scanning has begun on 200,000 frames exposed in the British National Chamber in the K9 beam. Pictures were obtained at eight momenta in the momentum range 1.10 to 1.70 GeV/c. The aim of this exposure is to study the inelastic decay modes of the  $N^*$  resonances observed in the elastic channel at higher momenta.

## Experiment 23

UNIVERSITY OF CAMBRIDGE

Single and Double  
Pion Production  
in  $pd$  Collisions  
(52)

This year has seen the completion of the analysis of 65,000 pictures taken in the 80 cm Saclay chamber filled with deuterium. The K1 beam was used at proton momenta of 1.825 and 2.110 GeV/c, the latter being the maximum available with that beam line. The film was completely scanned for three and four-prong events corresponding to the reactions



and

where  $p_s$  is a 'spectator' proton. The scanning produced some 6,000 events which were measured on conventional machines and processed by the CRAB system of programs on the Cambridge Titan computer.

The number of events of types (1) and (2) are as follows:

Channel	1.825 GeV/c	2.110 GeV/c
$p_s pp\pi^-$	1369	1372
$p_s pp\pi^-\pi^0$	48	97
$p_s pn\pi^+\pi^-$	300	564

The laboratory distributions for the spectator nucleon show considerable deviations from the predictions of the impulse model. In particular the angular distribution shows strong departure from isotropy and an increasing tendency to peak along the beam direction at higher spectator momenta. Fairly good agreement with the experimental results can be obtained by adding a double scattering background to the impulse model predictions; the proportion of background is appreciably higher for double pion production (30-40%) than for single pion production (15-17%) but does not vary significantly with energy. Calculations have shown that nucleon-nucleon final state interactions may account for part of the deviation from isotropy in the angular distribution, but have very little effect on the spectator momentum distribution.

Some 650 4-prong events of the type  $pd \rightarrow n_s pp\pi^+\pi^-$  (where  $n_s$  is a spectator neutron) were measured and the results compared with those for the reaction  $pp \rightarrow pp\pi^+\pi^-$  at slightly higher energies<sup>1,2</sup>. From this comparison it was concluded that deviations from the impulse model were not appreciable, providing that only events with spectator laboratory momentum  $< 150$  MeV/c were selected.

After allowing for the double-scattering background and the Glauber shadowing correction the following cross-sections were obtained:

Reaction	Cross-section (mb)	
	1.825 GeV/c	2.110 GeV/c
$pn \rightarrow pp\pi^-$	$2.57 \pm 0.14$	$2.68 \pm 0.19$
$pn \rightarrow pp\pi^-\pi^0$	$0.16 \pm 0.03$	$0.35 \pm 0.04$
$pn \rightarrow pn\pi^+\pi^-$	$0.77 \pm 0.07$	$1.75 \pm 0.20$
$pp \rightarrow pp\pi^+\pi^-$	$0.30 \pm 0.03$	$0.66 \pm 0.10$
$pn \rightarrow d\pi^+\pi^-$	$0.13 \pm 0.03$	$0.17 \pm 0.03$
$pd \rightarrow pd\pi^+\pi^-$ <sup>a</sup>	$0.18 \pm 0.02$	$0.17 \pm 0.02$

<sup>a</sup> Events with no spectator nucleon.

The analysis of the reaction  $pn \rightarrow pp\pi^-$  has shown that  $(50 \pm 5)\%$  of the events contain a  $\Delta^0$  (1236) isobar. The experimental distributions are in good agreement with one-pion exchange calculations, and show no clear evidence for the existence of any  $T = 0$  amplitude in the reaction.

The reaction  $pn \rightarrow pn\pi^+\pi^-$  takes place mostly from the  $T = 0$  state. The energies of this experiment are too close to threshold for the events to be very peripheral but fair agreement with one-pion exchange calculations has been found. No evidence for  $N^*(1470)$  production has been found. Thus, although the  $T = 0$  part of the  $pn \rightarrow pn\pi^+\pi^-$  cross-section rises by  $0.92 \pm 0.22$  mb between 1.825 and 2.110 GeV/c (compared with a rise of 3 mb in the total  $T = 0$  nucleon-nucleon cross-section in the same momentum range<sup>3</sup>), this rise is not due to the threshold for the reaction  $pp \rightarrow NN^*$  (1470).

In the course of the experiment 281 events with deuterons in the final state were observed. Most were examples of the reaction  $pd \rightarrow pd\pi^+\pi^-$  and separated cleanly, on the basis of laboratory momentum, into 'fast proton' and 'fast deuteron' events, the latter proceeding by baryon exchange. In these events evidence has been found for a  $d\pi$  resonance of mass 2130 and width 50 MeV.

<sup>1</sup> Pickup E. et al., Phys. Rev., 125 (6) 2091 (March 1962).

<sup>2</sup> Hart E.L. et al., Phys. Rev., 126 (2) 747 (April 1962).

<sup>3</sup> Bugg D.V. et al., Phys. Rev., 146 (4) 980 (June 1966).

## Experiment 24

A Study of  $K^-p$  Interactions in the Range 1.25 to 1.85 GeV/c (8, 33, 34)

$K^-p$  interactions, at 13 incident  $K^-$  laboratory momenta approximately evenly spaced in the interval 1.25 to 1.85 GeV/c are being studied. The pictures were taken at Nimrod using the Saclay Hydrogen Bubble Chamber.

The  $K^-p$  system can form baryon resonances of strangeness -1 and isotopic spin 0 or 1. The properties of these resonances e.g. mass, width, spin, parity, isotopic spin, are obtained from analysing their decay into two-body final states. Experimentally, total cross-sections, differential cross-sections and polarization are measured, and the data are then analysed in terms of partial wave amplitudes, of different spin and parity.

The various final state topologies in this experiment are at different stages of analysis. The common topologies are:-

- Two-prong events with a charged decay. These yield, for example, the two-body final states  $\Xi^- K^+$  and  $\Sigma^\pm \pi^\mp$
- Zero-prong events with one or two visible neutral decays. These yield states  $\Xi^0 K^0$ ,  $\Lambda^0 \pi^0$ ,  $\Lambda^0 \eta$ ,  $\bar{K}^0 n$
- Two-prong events with a visible neutral decay. These yield intermediate two-body states such as  $Y^* \pi$ ,  $K^* p$  (which decay into  $\Lambda^0 \pi^+ \pi^-$ ,  $\Sigma^0 \pi^+ \pi^-$ ,  $K^0 p \pi^-$  etc.)
- Two-prong events. These yield for example, the two-body states  $K^- p$  (elastic),  $Y^* \pi$ ,  $K^* p$ ,  $K^* n$ .

CEN, SACLAY  
COLLEGE DE FRANCE  
UNIVERSITY OF STRASBOURG  
RUTHERFORD LABORATORY

The measurement and selection of topologies (i) and (ii) is now complete and analysis is well advanced. Approximately 60,000 events have been measured in this part of the experiment.

It is to be noted that for final states not far above threshold, only partial waves with low spin tend to be excited. This situation is open to relatively simple analysis and in this way it has been possible to obtain results for the final states  $\Xi^- K^+$  and  $\Xi^0 K^0$  (see below) even though the numbers of events are much fewer than for  $\Sigma^\pm \pi^\mp$ ,  $\Lambda^0 \pi^0$ ,  $K^0 n$  final states, where the situation is more complicated.

The measurement of topology (iii) is almost complete and about three quarters of the events have been written onto a Data Summary Tape for final analysis.

Topology (iv) is being measured as the first production experiment on the automatic film measuring Hough Powell device (HPD).

### The Reactions $K^- + p \rightarrow K^+ + \Xi^-$ and $K^- + p \rightarrow K^0 + \Xi^0$ .

The reaction channels (a)  $K^- + p \rightarrow \Xi^- + K^+$ , (b)  $K^- + p \rightarrow \Xi^0 + K^0$  have been studied throughout the range of the survey. A total of 1100  $\Xi^- K^+$  and 110  $\Xi^0 K^0$  events were observed. The mean lifetime of the  $\Xi^-$  particle was found to be  $(1.67 \pm 0.07) \times 10^{-10}$  seconds and of the  $\Xi^0$  particle  $(2.44 \pm 0.6) \times 10^{-10}$  seconds, both values being in good agreement with the previous world averages.

The differential cross-sections and polarization distributions for the  $\Xi^-$  channel have been fitted according to the usual expansions in terms of the Legendre polynomial and first order Legendre polynomial functions:

$$\frac{d\sigma}{d\Omega} = \lambda^2 \sum_l A_l P_l(\cos \theta^*)$$

$$\vec{P} \frac{d\sigma}{d\Omega} = \hat{n} \lambda^2 \sum_l B_l P_l^1(\cos \theta^*)$$

where  $\theta^*$  is the  $K^+$  production angle in the centre of mass system;  $\hat{n}$  the normal to the production plane and  $\vec{P}$  the polarization vector of the  $\Xi^-$ . Due to the lack of statistics in reaction (b) only the coefficient  $A_0 = \sigma/4\pi\lambda^2$  where  $\sigma$  is the cross section, is meaningful. Figure 28 shows the variation of  $A_0$  for both (a) and (b) and Figure 29 shows the variation of the  $A_l$ 's up to  $l=7$  for reaction (a). Clearly both reactions show a resonant behaviour in  $A_0$ , peaking at  $\sim 2080$  MeV. The coefficients  $A_1, A_2, A_3$  for reaction (a) also show a resonant behaviour whereas  $A_4$  to  $A_7$  are compatible with zero.

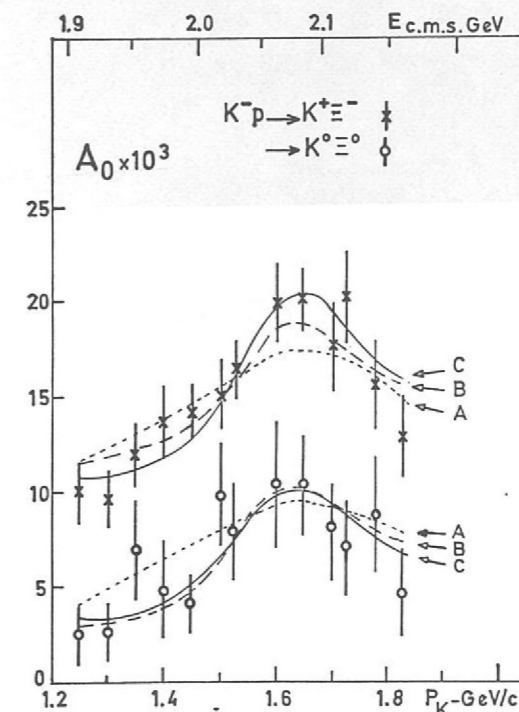


Figure 28.  $A_0 (= \sigma/4\pi\lambda^2)$  vs. incident  $K^-$  lab. momentum for the reactions  $K^- + p \rightarrow K^+ + \Xi^-$  and  $K^- + p \rightarrow K^0 + \Xi^0$ . The top scale indicates the total energy available in the  $K^-p$  centre of mass system. The curves shown correspond to the solutions (1), (2) and (3) discussed in the text.

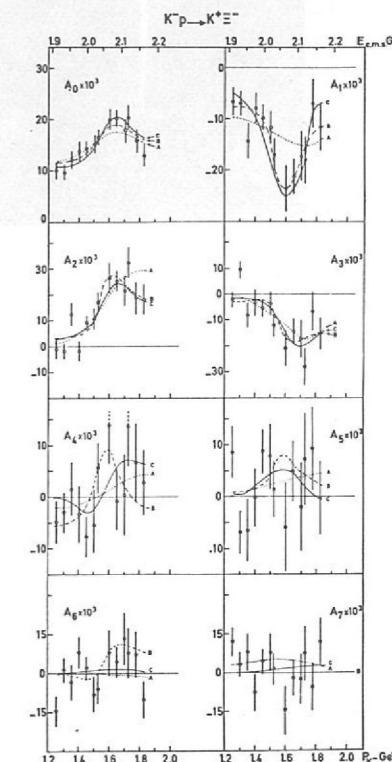


Figure 29.  $A_l$  coefficients vs. the incident  $K^-$  momentum for the reaction  $K^- + p \rightarrow K^+ + \Xi^-$ . The curves shown correspond to the solutions (1), (2) and (3) discussed in the text.

These results have been fitted under the assumptions (1) all partial waves up to  $J = 5/2$  contribute a constant background and  $F_{17}$  and  $G_{07}$  are resonant with masses and widths fixed (the  $\Sigma(2030)$  and  $\Lambda(2100)$ ), (2) with the  $G_{07}$  ( $\Lambda(2100)$ ) resonant but allowing the mass and width to vary in the fitting procedure, and (3) with a new resonance of lower spin dominating the  $\Xi K$  interaction.

Assumption (1) does not give an acceptable fit. Assumption (2) gives a much improved fit if the mass of the  $G_{07}$  resonance is shifted to  $M \approx 2080 \pm 10$  MeV and the width to  $\Gamma \approx 80 \pm 10$  MeV.

The best fit however is obtained from hypothesis (3) with a new  $J^P = 3/2^+$ , or  $5/2^+$  resonance of I-spin 0 or 1, mass approximately 2070 MeV, width  $\sim 120$  MeV and  $(J + \frac{1}{2}) x_{e1} \cdot x_{\Xi K} \approx 0.030 \pm 0.005$ , where  $x_{e1}$  and  $x_{\Xi K}$  are the elastic and  $\Xi K$  branching fractions. The analysis, therefore, strongly suggests the existence of this new resonance. However, the statistics are such that fit (2) cannot be ruled out and confirmation is required.

### 2-prong events

This part of the experiment is a collaboration of the Rutherford Laboratory with the Centre de Recherches Nucleaires, Strasbourg. The analysis will be based on approximately 40,000 events measured on the Rutherford Laboratory HPD and conventional machines at the two laboratories.

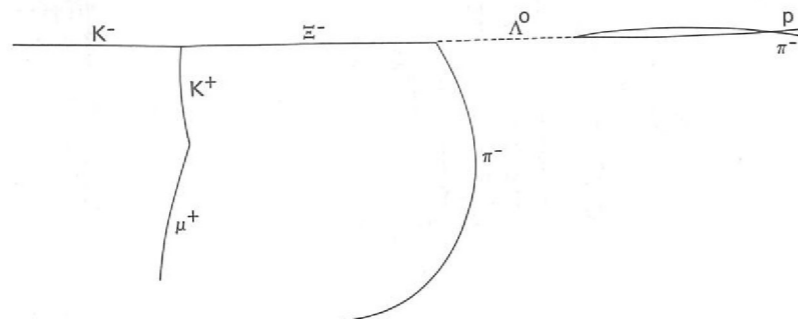
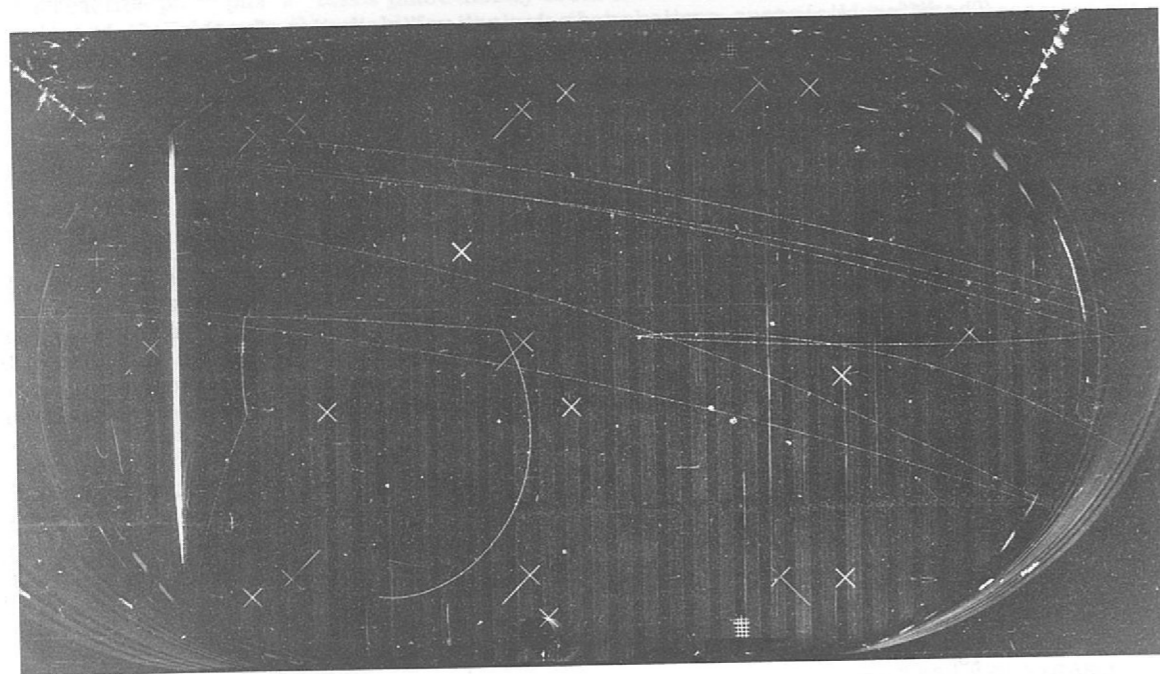


Figure 30. An example of the reaction  $K^- p \rightarrow \Xi^- K^+$ , from the  $K^- p$  survey experiment. The  $\Xi^-$  subsequently decays to  $\Lambda^0 + \pi^-$ , followed by  $\Lambda^0$  decay to  $p + \pi^-$ ; the  $K^+$  decays to  $\mu^+ + \nu$ .

The following final states are being analysed.

- (i)  $K^- p$  elastic scattering.
- (ii)  $K^- + p \rightarrow K^- + p + \pi^0$  or  
 $K^0 + p + \pi^-$  or  
 $K^- + n + \pi^+$

In these channels involving final state kaons the production of the charged and neutral  $K^*$  (890) appears especially interesting. Some two-body  $Y^* \pi$  production is also observed.

- (iii)  $K^- + p \rightarrow \Lambda + \pi^+ + \pi^-$  or  
 $\Sigma^0 + \pi^+ + \pi^-$

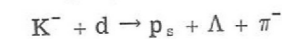
Events in these channels in which the  $\Lambda$  decays in the neutral mode will supplement the data obtained from the measurement of topology (iii). The higher resolution provided by the HPD may assist in the resolution of the  $\Sigma^0$  from the  $\Lambda$ .

## Experiment 25

UNIVERSITY OF BIRMINGHAM  
UNIVERSITY OF EDINBURGH  
UNIVERSITY OF GLASGOW  
IMPERIAL COLLEGE, LONDON

$K^-$ -Deuterium  
Interactions  
(19, 20)

Film taken during 1966 and 1967 using  $K^-$  mesons at 1.45 and 1.65 GeV/c incident momentum in the Saclay bubble chamber has now been completely processed. In all approximately 80,000 events have been measured and work is progressing on the results obtained. The channel



where  $p_s$  is a spectator proton, is being studied in detail and a partial wave analysis is now being performed. In addition, there is abundant production of  $Y^*$  resonances at 1385, 1405, 1520 and in the region 1650 - 1720 MeV/c<sup>2</sup>; the analysis of production and decay characteristics of these resonances is proceeding.

## Experiment 26

IMPERIAL COLLEGE, LONDON  
WESTFIELD COLLEGE, LONDON  
CEN, SACLAY

$K^+ p$  and  $K^+ d$   
Interactions  
in the Range  
2.0-2.8 GeV/c

In this survey experiment, approximately 40,000 photographs have been taken at each of the momenta 2.1, 2.3, 2.5, 2.7, 2.9 GeV/c, in the British National Hydrogen Bubble Chamber. Further exposures at intermediate energies and with deuterium are required to complete the planned series. In the meantime work is proceeding on the analysis of the film already obtained. The film for each energy has been shared between the three collaborating groups for analysis; the Saclay part is being measured independently and is well advanced, but the Imperial College and Westfield College film is being measured on the FSD at Imperial College. Since this is the first experiment measured on this device, the progress of the experiment is closely tied to the progress of the FSD.

At each laboratory the scanning and predigitizing of the film is complete, and measurements are complete on the film at 2.7 GeV/c and on the Imperial College part of the film at 2.5 GeV/c. The early rolls had a rather low success rate of about 50%, and a second pass is being prepared. It is believed that improvements in the system have substantially increased the success rate in more recent measurements.

## Experiment 27

$\pi^+p$  Interactions  
between 0.6 and  
0.8 GeV/c

Measurement of all 100,000 pictures, taken at 0.6, 0.65, 0.7, 0.75 and 0.8 GeV/c in the Saclay 80 cm. hydrogen bubble chamber, is now almost complete and analysis of the data at 0.6, 0.7, and 0.8 GeV/c has commenced. The experiment was designed to study primarily the inelastic reactions  $\pi^+p \rightarrow \pi^+\pi^0p$  and  $\pi^+p \rightarrow \pi^+\pi^+n$  but, as a byproduct of the analysis, excellent data on the elastic scattering have been amassed. As an example of this, the distribution of the centre of mass scattering angle at 600 MeV/c is shown in Figure 31: it contains some 13,000 events. Preliminary phase shift analyses have been performed on the elastic scattering data at these three momenta, but these data are expected to be of most value when combined with world data in an energy dependent phase shift analysis.

In this experiment it has been found that the ratio of inelastic cross section to total cross section is about 20% lower than the value predicted from the CERN phase shift analysis, and an attempt to perform a partial wave analysis of the inelastic channel, thus providing valuable additional information on the  $\pi^+p$  interaction, is at present in progress.

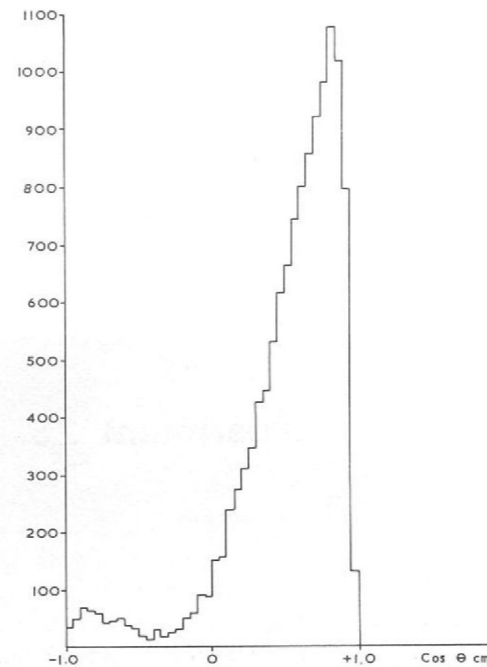


Figure 31. Centre of mass angular distribution for  $\pi^+p$  elastic scattering at 600 MeV/c.

## Experiment 28

$\pi^-p$  Interactions  
between  
400 MeV/c and  
700 MeV/c

250,000 pictures were taken in the Saclay Chamber at Nimrod during 1967 and a further 250,000 at Saturne (Saclay) in late 1968.

About 3,000 examples of the reaction  $\pi^-p \rightarrow \pi^+\pi^-n$  will be obtained at each of six momenta in this region, and will be used to study the  $\pi^+\pi^-$  interaction well below the  $\rho$  threshold.

First reports on elastic scattering and analysis of the inelastic processes will become available early in 1969.

## Experiment 29

$\pi^+$  and  $p$   
Interactions  
at 2 GeV/c  
in Helium

Scanning and measuring of the 300,000  $\pi^+$  pictures taken in the Helium Bubble Chamber is now complete. In these pictures only 90 events making a unique form constraint fit to the final state  $\pi^+\pi^-\pi^+He^4$  have been identified. There is no indication of the A1 meson in the data.

A study of events with 3 prongs but no visible recoil is now in progress with a view to obtaining a better understanding of the reliability of the 90 events with a visible recoil.

UNIVERSITY OF  
OXFORD

UNIVERSITY OF OXFORD  
UNIVERSITY OF CALIFORNIA,  
BERKELEY.

UNIVERSITY OF  
OXFORD

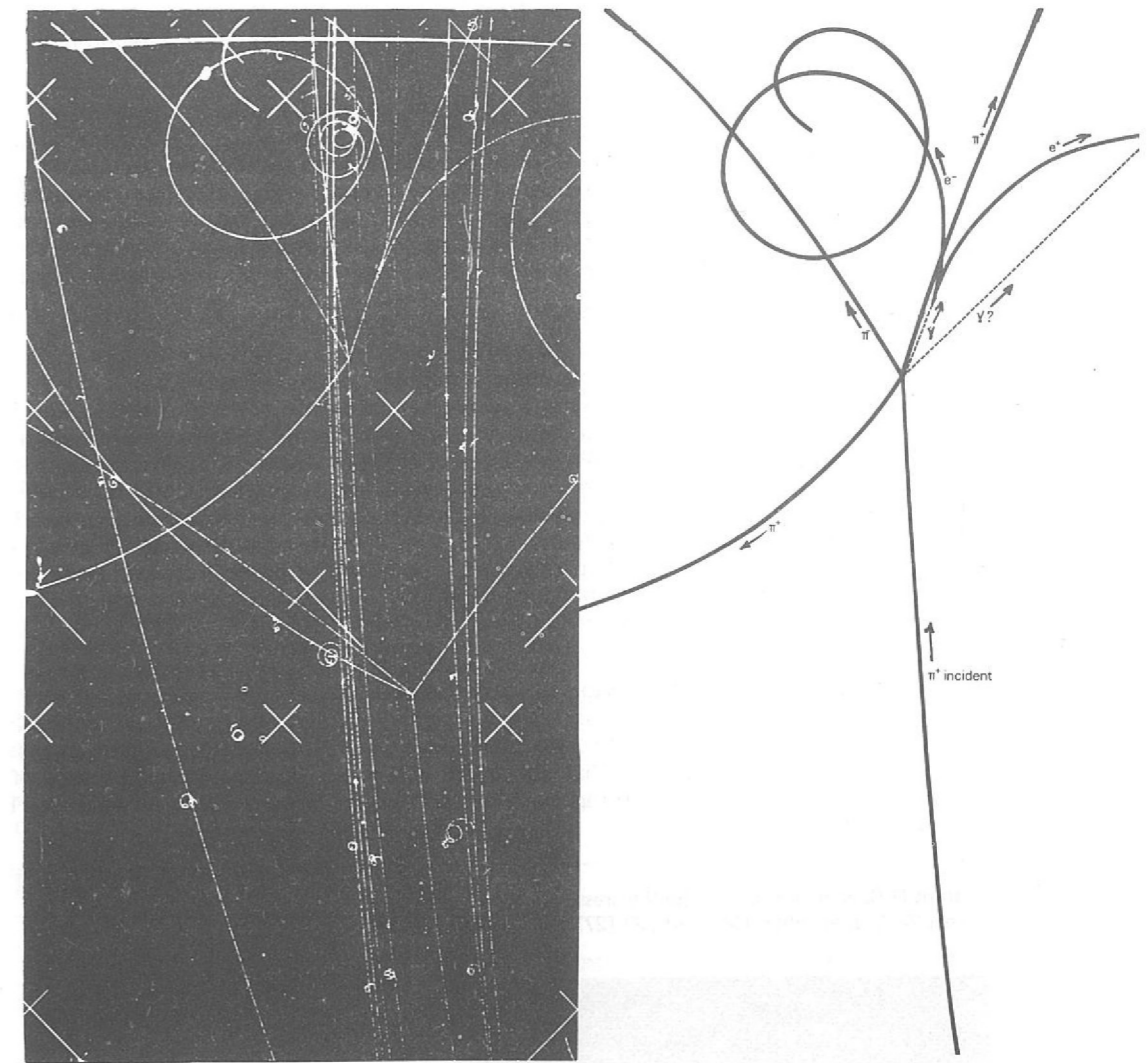


Figure 32.  $\pi^+ + He^4 \rightarrow \pi^+ + \pi^+ + \pi^- + \pi^0 + He^4$

$\gamma + \gamma$   
 $e^+ + e^-$

Note: (1)  $He^4$  recoil momentum is too low to give a visible track  
(2) one of the photons from the  $\pi^0$ -decay is converted into an electron-positron pair, the other photon escaped without visible trace.

## Experiment 30

$np$  and  $\Lambda p$   
Interactions

Due to limited statistics the hyperon-nucleon interaction has so far only been studied on a small scale in bubble chambers, using hyperons produced in the chamber liquid by the interactions of longer-lived particles. Conventional beam-handling equipment is totally inadequate for the task of separating and transporting hyperon beams because of the very short lifetimes of these particles. For this reason the development of high-field pulsed magnets has been undertaken at the Laboratory with a view to producing the necessary focussing and dispersing properties over short distances. It is believed that useful hyperon beams can be produced for a bubble chamber exposure.

In January 1968, using a scattered out proton beam at a momentum of about 7.5 GeV/c, a neutron beam was set up at the end of the K9 beam line and about 40,000 test pictures taken.

UNIVERSITY OF CAMBRIDGE

The aim of these test pictures was to gain experience in the scanning and analysis of neutral beam events and to determine how many neutrons and how much charged background could be tolerated in the chamber.

Work has continued throughout the year at the Rutherford Laboratory on the development of suitable high field pulsed magnets. 8.3 GeV/c protons have been transported the whole length of the K9 beam-line and a spot-size of less than 1 mm diameter produced at the high field magnet position with the required intensity of about  $2 \times 10^5$  protons per pulse. As it will be some time before a sufficient degree of magnet reliability can be achieved to enable a lambda-beam exposure to take place, it is proposed to take more neutron-beam pictures in January 1969 with a view to studying interactions of secondary lambdas produced in liquid hydrogen.

Meanwhile a study of the processes  $n+p \rightarrow p+p+\pi^-$  and  $n+p \rightarrow$  strange particles is continuing as follows:

(a) The reaction  $n+p \rightarrow p+p+\pi^-$  in the momentum range 1-7 GeV/c

The spectrum of neutrons giving 3 prong events is almost uniform between 1 and 7 GeV/c. Any events with obvious  $\pi^+$  secondaries were rejected at the scanning stage. About 25% of the remaining 3 prongs (13-14% of all 3 prongs) give rise to 3C fits to the process  $n+p \rightarrow p+p+\pi^-$ . About 8,000 events have been measured to date giving about 2,000 fitted events. It is proposed to study resonance production as a function of momentum, in particular  $N^*(1470)$  production, which was not found at 2.11 GeV/c in pd collisions by Brunt et al.<sup>1</sup> but has since been observed by Shapira et al.<sup>2</sup> in 7 GeV/c pd collisions. Brunt et al. had 1,372 events corresponding to the process  $pd \rightarrow p, pp\pi^-$  compared with the 276 of Shapira et al. The initial intention is to measure a sufficient number of events to give about 1,000  $pp\pi^-$  events per GeV/c interval.

(b) Strange particle production in np collisions

About 20,000 of the test pictures were scanned for strange events. About 1,400 such events have been found including two definite cases of  $\Xi^-$  production. These events have all been measured. It is expected that about 400 will yield 3C fits. Several cases of  $\Lambda^0$  scattering have been observed involving secondary  $\Lambda^0$ 's from np events, an example being shown in figure 33.

<sup>1</sup> Brunt D.C. et al., Phys. Rev., (in the press).

<sup>2</sup> Shapira A. et al., Phys. Rev. Lett., 27 (27) 1835 (December 1968).

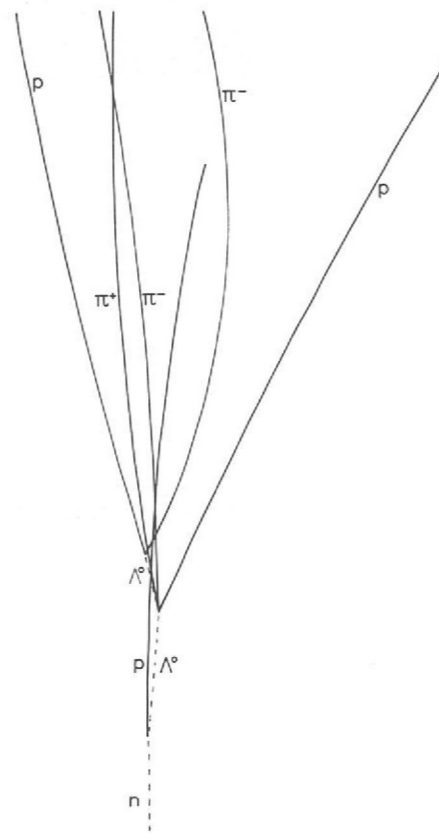
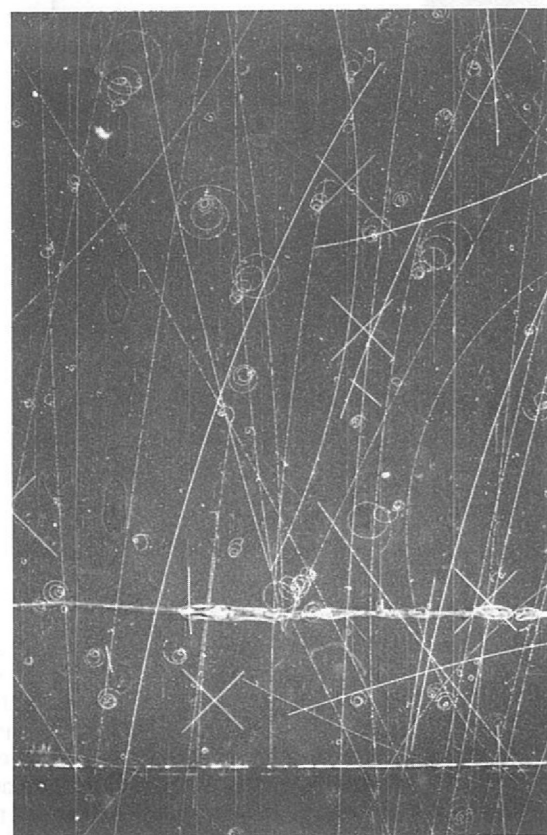


Figure 33.  $\Lambda^0$  production, interaction and decay. The reactions involved are  $n+p \rightarrow p+\Lambda^0$ ;  $\Lambda^0+p \rightarrow \pi^+\pi^-\Lambda^0+p$   
 $\Lambda^0 \rightarrow p\pi^-$ .

## Electronics Group

Counter  
Electronics  
(39, 48)

A paper on the Miniature Logic System (MLS) was given at the International Symposium on Nuclear Electronics, Versailles (September 1968). A description of MLS was given in last year's progress report. The poor delivery rate of certain tunnel diodes has caused manufacturing delays. The gradual, and continuous, improvement of the 'S' (transistor and integrated circuit) modules has increased their speed so that they can now perform some of the more demanding requirements previously performed exclusively by 'T' (tunnel) modules. Three new 'S' cards are in the early development stage

153/S 4 I. P. 'OR' gate  
303/S Discriminator  
472/S Fast 3 I. P. 'AND' gate with logic store after gate

Data Acquisition  
from  
Spark Chambers  
(35, 37, 38, 47)

This system, primarily designed for magnetostrictive chamber applications, was described in last year's report. During the current year five additional systems were made and further work was done to apply them to sonic chambers. Two of these are in use at CERN. Work is in progress to update the sonic and magnetostrictive discriminators and gating circuits into CAMAC modules.

Computer  
Interfacing  
and  
Tape Systems

Two units were built to interface DDP 516 computers to COMUS and other data systems. One of these is in use on the S70 experiment at CERN (Experiment No. 14) and the other will be used next year at RHEL for the second K13 experiment. Another unit for interfacing CAMAC and COMUS modules to an Argus 400 is in the early design stage. A controller for reading out COMUS modules and driving a CERN tape deck was built and is in use at CERN on the 'EPISTLE' (Experiment No. 15)

An interface between a Sigma Two computer and a large magnetic disc store was built and commissioned for the ATLAS laboratory.

Table 4

	Location	Sonic/ Magneto- strictive Data Handling	'COMUS' Registers and Scalers and Numerical Display	COMUS Print/ Type/Punch Equipment	MLS	Computer Interface & Tape System	On-Line Link to IBM 360
Commissioned and Operational during 1968							
Oxford/RHEL/Glasgow/ Liverpool	CERN	✓	✓	✓	✓	Interface to DDP 516	
Cambridge/RHEI 'EPISTLE'	CERN	✓	✓	✓	✓	Interface to CERN Tape Deck	
AERE/QMC	AERE				✓		
AERE/QMC	$\pi 4$	NIMROD					✓
RHEL/Cambridge	K13	NIMROD			✓		
Birmingham	K12	NIMROD	✓		✓	2nd Tape Deck	✓
RHEL	K14a	NIMROD			✓		✓
Imperial College	$\pi 7$	NIMROD	✓		✓		
UCL	K8	NIMROD					✓
	ATLAS					Interface between S2 Computer and Disc File	
Equipment Partially or Wholly Delivered but Experiment not Scheduled to run yet							
Bristol	K15	NIMROD	✓	✓	✓	Interface to Argus 400 being designed	
RHEL/Cambridge (proposal 71)	K13	NIMROD	✓	✓	✓	Interface to DDP 516	

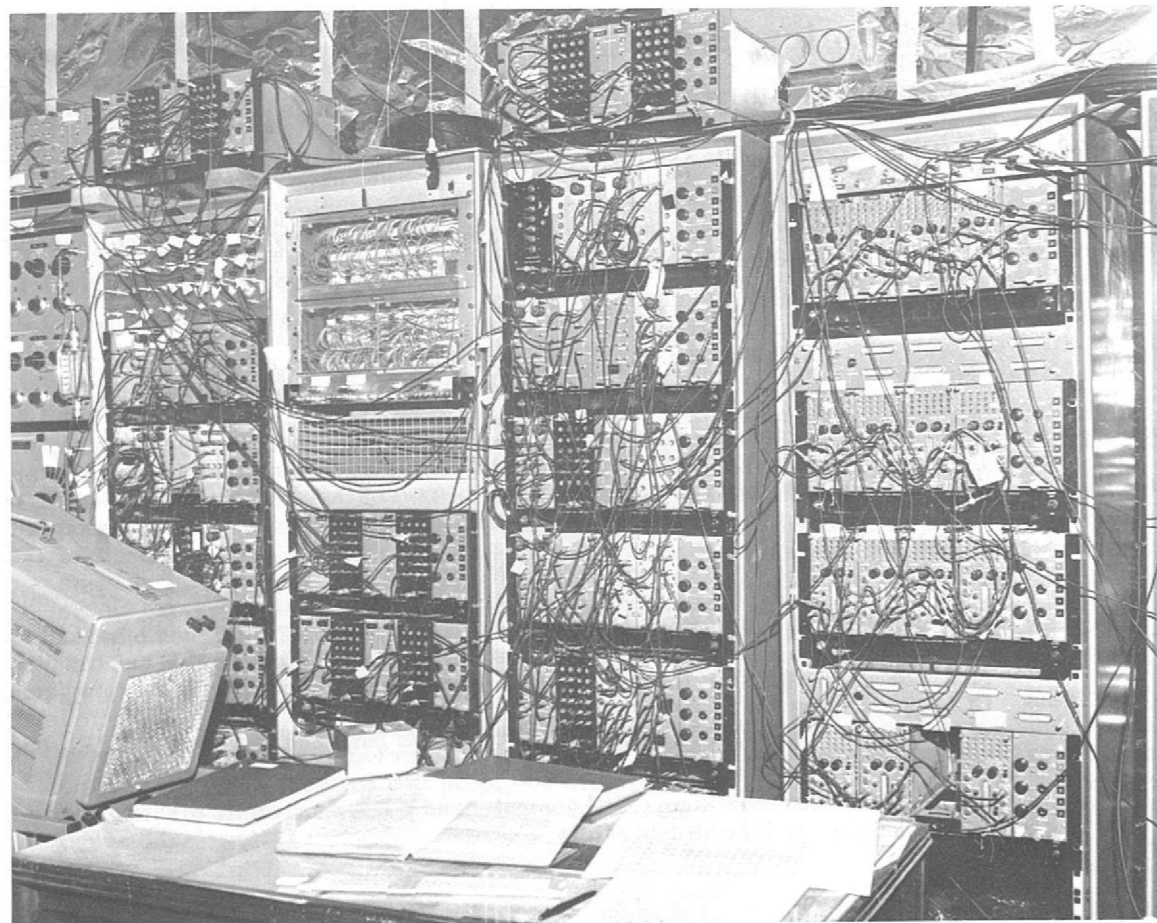


Figure 34. General view of a local control room.

*COMUS Scalers  
Registers and  
Display Systems  
(36)*

COMUS modular equipment (described last year) was supplied to three experimental teams, two of them at CERN. These modules, in association with decimal display units and drive units for typewriter, punch or line printer have provided a good grounding for the future exploitation of the CAMAC system. Liaison with other European laboratories and UK industry regarding CAMAC took place throughout the year.

*Data Link*

A multiplexed data link enabling up to six 'on-line' Nimrod users to use a single channel into the IBM 360/75 computer was completed during 1968 and four teams are using it.

*Manufacture*

Much of the work this year revolved around manufacture, testing and commissioning of equipment designed in the previous year. Table 4 indicates the range of equipment involved.

*Maintenance*

The group maintains existing equipment that has been manufactured in previous years together with various types of film scanning equipment and several magnetic tape transport units.

## Film Processing

The Film Processing Laboratory, the installation of which was reported in the 1967 Annual Report, is now fully commissioned. It is capable of processing all gauges of film from 16 mm to 70 mm, negative or reversal, perforated or unperforated, to the standards required by the various automatic film measuring machines. Experiments have continued on the processing parameters for the range of film stocks from various manufacturers to maintain these standards.

During the year the sources from which film is being processed has widened significantly, since RHEL is the only laboratory in Europe able to process such a wide range of scientific film. Processing has been undertaken not only for the users of the bubble chambers and spark chambers at Nimrod but also for the Atlas and Daresbury Laboratories, Oxford University (film from Saclay), Yale University USA, and a variety of spark chamber groups working at CERN. After collating, reeling and boxing, the film is despatched to a large number of universities in the UK, Europe and USA.

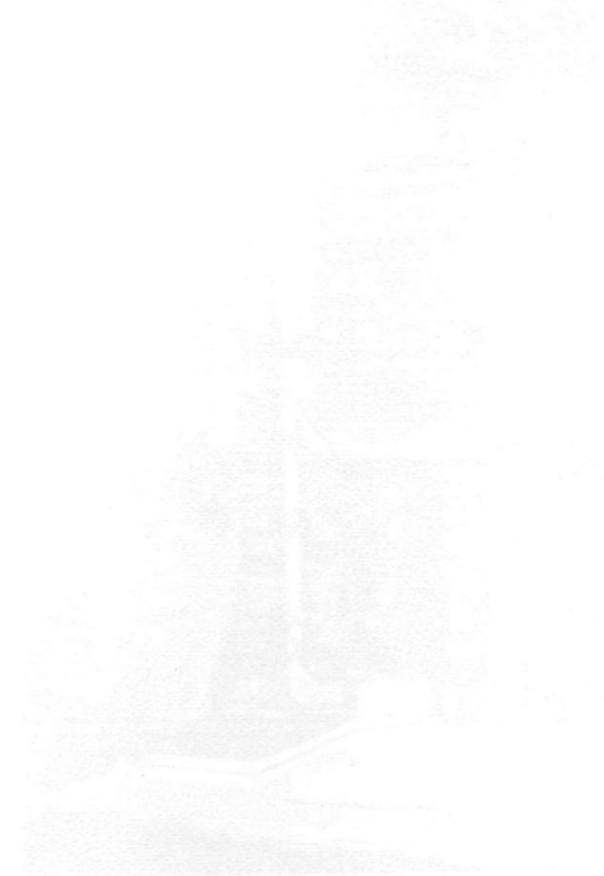
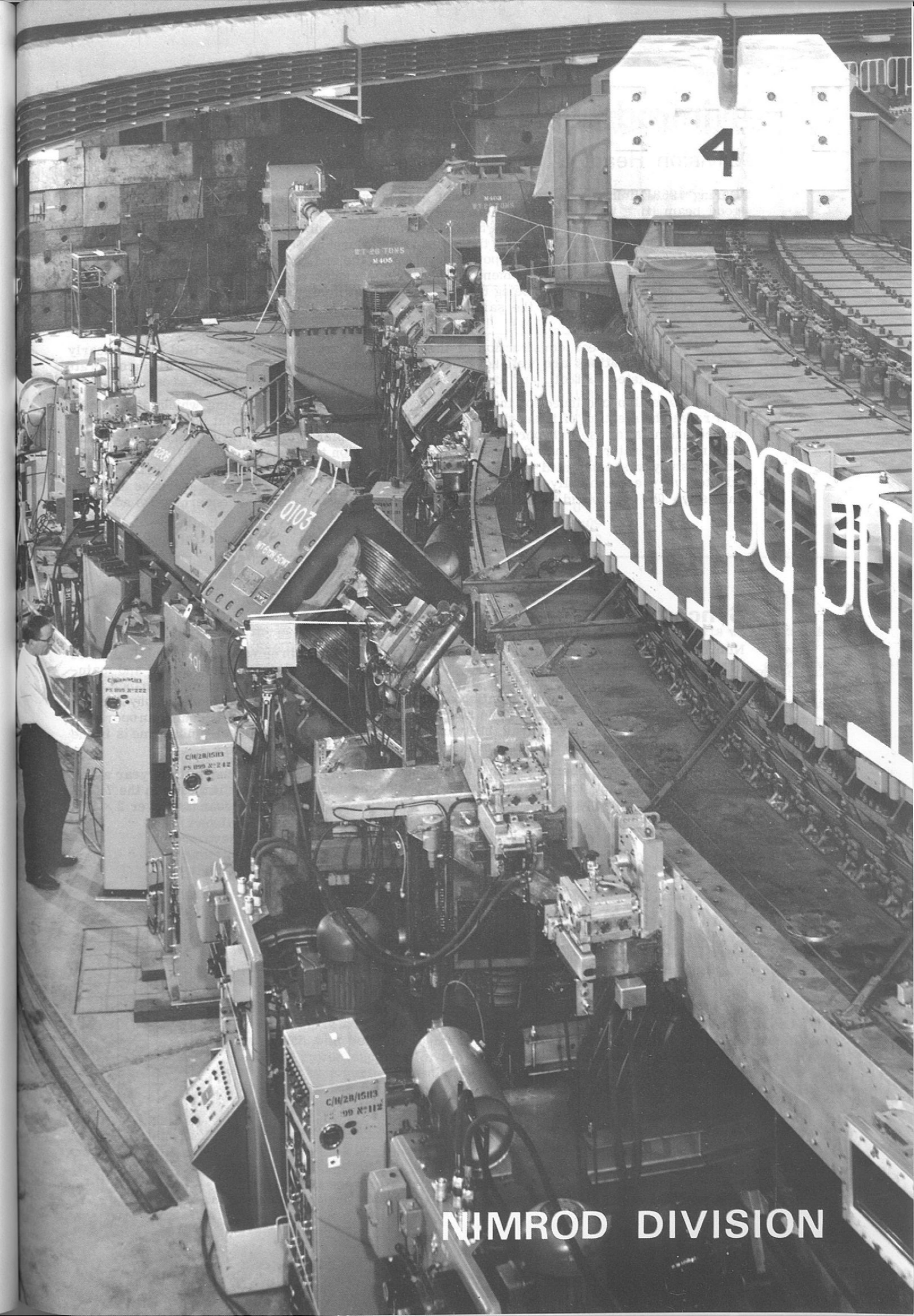


Figure 1. The NIMROD Division at CERN. These machines, built in 1960, such as the proton beam transport system. Liaison with other divisions throughout the year.

The NIMROD Division at CERN was completed during the year covered by this report. Table 1 shows the major equipment that is being replaced.

The NIMROD Division at CERN is the result of the merger of the NIMROD and the NIMROD Division. The NIMROD Division at CERN is the result of the merger of the NIMROD and the NIMROD Division.



NIMROD DIVISION



# Nimrod Division

Division Head: L. C. W. Hobbs

During 1968 Nimrod was scheduled to run 6152 hours for High Energy Physics; 5170 hours of good beam time was actually available representing an overall operational efficiency of 84%. The average beam intensity was  $1.52 \times 10^{12}$  protons per pulse. Extracted beams were run for almost the whole year. Following the alternator failure in September 1967, 7 GeV operation was continued with half the magnet power supply until the end of July; the full system was in use again from September. Development of the various modes of beam utilization continued, the most important achievements being the realization of switching between the two extracted beam channels, X1 and X2, within the same machine pulse and improvement to the effective duty cycle of slow spill.

By the end of the year construction of the large new experimental area, Hall 3, was nearly finished. Preparations are well advanced for its ejection channel, X3 (which will incorporate computer-assisted control), and for the first two secondary beams in the new area.

Studies have also continued for the new types of beam extraction systems which, it is hoped, will raise the ejection efficiency to about 60%. Other projects of special note are: high field pulsed magnets for use in hyperon beams, safer and simpler hydrogen targets based on a small helium refrigerator, the new designs for polarized proton targets, and PLANIM. The PLANIM design study was completed towards the end of 1968; it showed that the 50 MeV PLA could be adapted very economically as a new injector for Nimrod to give a 3.5-fold increase in beam intensity. The cost would be £570,000. No decision has yet been taken concerning its adoption.

## Synchrotron Operation

Overall  
Performance

Nimrod has continued to operate, as in previous years, on a three week cycle, nominally 404 hours for high energy physics experiments and 100 hours accelerator development and maintenance. Of the 100 hours machine time 12 hours is allocated to routine maintenance. The 5170 hours for which beam was available for HEP is 59% of clock time. Machine physics and development were scheduled for 1254 hours and beam was available for 913 hours, an operating efficiency of 73%. The lower availability of beam during accelerator development time is in the main accounted for by the inclusion of start-up time and by special repairs.

The 15 MeV injector operated with 20 mA, 350  $\mu$ s beam pulse and for most of the year a new device, the debuncher phase ramper, was in service making a significant increase in the 7 GeV beam intensity (see page 53). The maximum intensity seen during the year was over  $2 \times 10^{12}$  protons per pulse.

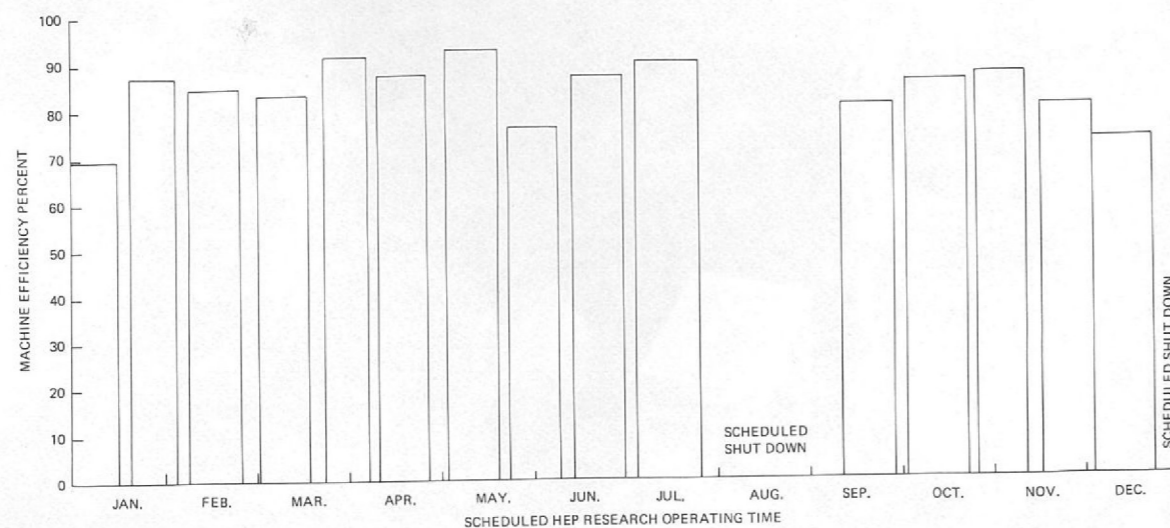


Figure 35. Nimrod efficiency during HEP research scheduled operating time January to December 1968

Equipment  
Reliability  
(76, 77, 78)

Nimrod efficiency during HEP scheduled operating time from 1 January to 31 December, 1968 is shown in figure 35. There was one shut down during the year, from August to September.

The main causes of lost beam time are summarised in Table I.

Table 1

System	Beam time lost as a percentage of total scheduled time
Plunging mechanisms	7.39 (including inspection time)
Injector	2.55
Nimrod power supply	1.33
Synchrotron r. f.	1.14
Vacuum	0.82
Coolants	0.67
Targets and target mechanisms	0.58
Nimrod magnet	0.55
Pole face winding systems	0.16
Diagnostics	0.10
Inflector	0.09
Beam control	0.08

Details of the performance and development of Nimrod are given in reports which are issued quarterly. (See list of Publications, Page 132).

The down time caused by the Mk I plunging mechanism was due to fatigue failure of the silicon bronze swash plates in the oil pumps which are a major component of these mechanisms. The duty required of the pumps is extremely severe and improvement can only be made by major modification. The maximum running hours are therefore limited to 4000 and it is planned to change the pumps after 2000 hours.

Major design changes, to improve reliability, have been incorporated into the Mk II plunging mechanism, now nearing the end of its commissioning trials, which will be used for the X3 external proton beam serving Hall 3. The whole mechanism is now mounted on rails and fixed to them by spring loaded clamps which are unloaded hydraulically when movement of the mechanism is required. The minimum stroke time is now limited to 0.35 seconds, allowing the use of an improved design of swash pump and a smaller drive motor. The system provides an accurate magnet position control and enables a magnet to be withdrawn and disconnected from the mechanism in the much shorter time of 15 minutes. Quick disconnects are used for both power and water.

During the shut down a great deal of work was carried out on the Nimrod equipment, some of which is briefly described below:

- A 750 kV power supply, of the open Cockroft-Walton type, for the Nimrod pre-injector was installed and commissioned. (See figure 36). It has replaced the 600 kV electrostatic generator (though one of these has been retained as an emergency supply) and proved satisfactory in service.
- A separate EHT platform housing a 50Hz alternator has been fitted. The object of this development is to remove from the main EHT platform a major source of heat and vibration which was believed to have been reducing the reliability of the electronic equipment and power supplies for the ion source and focussing electrodes. The alternator is driven by a vertical insulating shaft made from 1 inch diameter fibre glass. The device itself has been very reliable and there have been fewer malfunctions of the main platform units.
- A new infra-red light guide signalling system was installed on the EHT platform.
- A capacitor bank was installed as an alternative to the battery used on the Mk. 2 Bias Supply (which provides the bias current for the ferrite cores in the synchrotron r.f. cavity). This has now been in operation for some months and has proved satisfactory. Some further work on the system frequency response remains to be done.

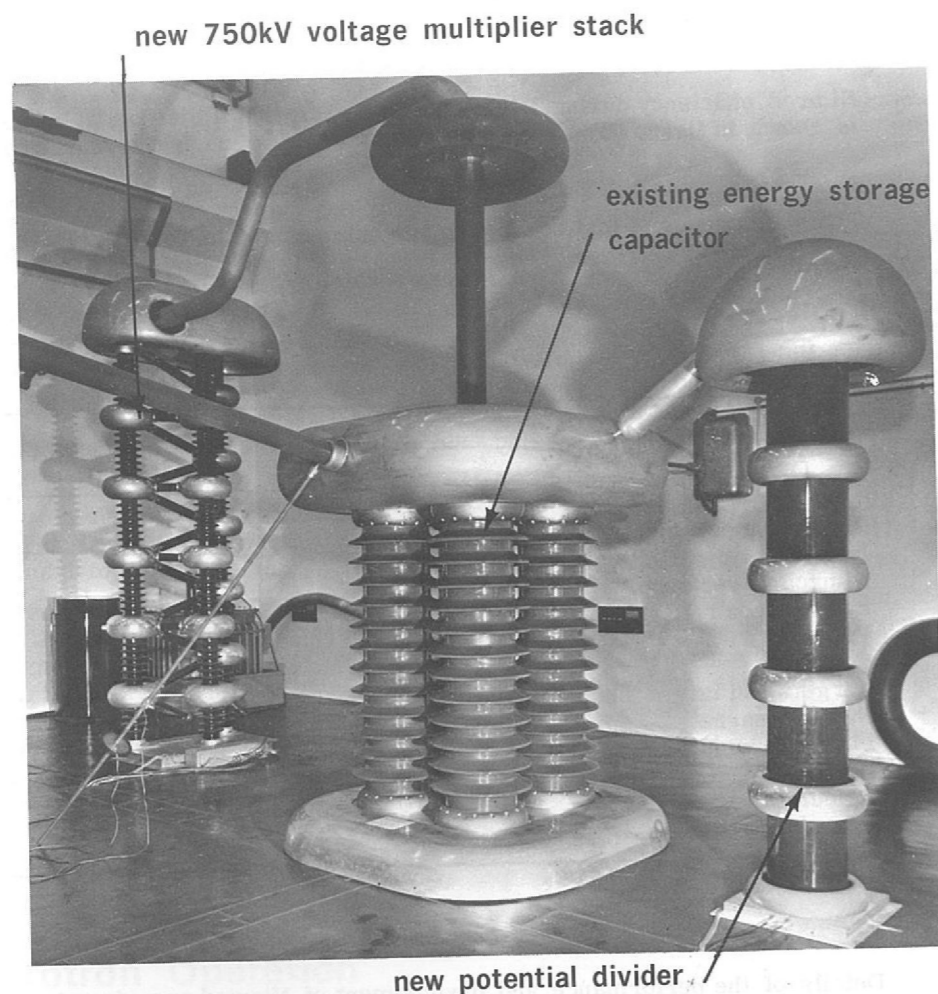


Figure 36. New arrangement of pre-injector HT supply.

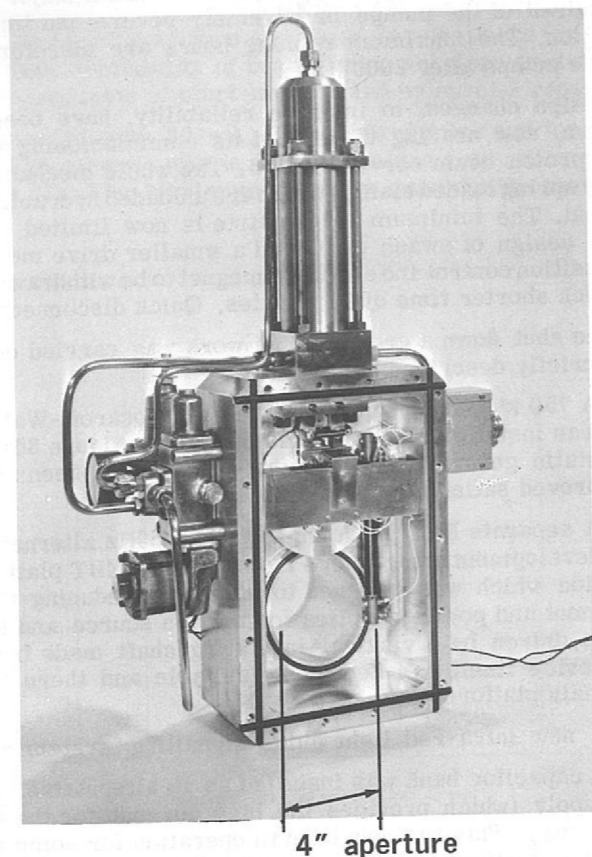


Figure 37. Fast shut off valve for the Nimrod injector.

- (e) The main control room monitor and control facilities were improved, particularly in regard to the primary frequency generator, beam control, targetting systems and extracted proton beam. Alarm annunciation system displays on the control desk were re-engineered to facilitate operation. The beam safety interlock system, has been improved in the light of experience gained when operating with two simultaneous extracted proton beams.
- (f) An extensive series of tests was carried out on the coil clamping arrangements on the main Nimrod magnet. These were to investigate the possibility of running without throat conductor pressure bags, because, if these were to leak (e.g. due to radiation damage) replacing them would involve a major strip down of the magnet. It was concluded that the magnet windings can be energised safely with zero pressure in these bags.
- (g) Two new fast shut off valves were installed in the injector high energy drift space. These valves, shown in figure 37, have a closure time of 16 ms and operate with a complete absence of bounce.

*Magnet Power Supply*

The magnet has been pulsed for the greater part of the present year using the No.1 motor alternator set with both flywheels. During the August shut down, rebuilding and re-commissioning of No.2 motor alternator took place. Subsequent operation has been with both alternators electrically paralleled, but, for the first time, without interpolar links. Operational statistics are as follows: -

	<i>Pulsing Hours</i>	<i>Total Pulses</i>
Pulsing from No.1 alternator and A1 convertors	4,341	2,570,390
Pulsing from both alternators and the complete convertor plant	2,320*	2,887,427*
Total for 1968	6,661	5,457,817

\*(Based on Estimates for December, 1968)

During the August shut down, No.1 rotor was fitted with V coil support bolts of a new design having the shank region relieved and the threads formed by cold rolling in order to give better fatigue life. (All other bolts and studs on the rotor except those which anchor the connections between the field spools, were also changed for new ones with cold rolled threads).

The V coil support blocks were modified, to allow limited axial movement of the bakelised cloth packing onto which they bed, and so prevent the cracking which had been observed on some packing pieces (see figure 38).

When this rotor was removed from its stator for the above modifications to be carried out it was found that axial movement of part of the end of the top turn of the field winding on two poles, at the flywheel end of the rotor, had taken place. To avoid the risk of a turn to turn short circuit, these coils were not forced back to their original positions but, instead, the copper was carefully cut away (there is no current loading problem) until the affected area was restored as nearly as possible to its original profile. In an attempt to prevent further movement, special bracing bands of glass fibre tape, soaked in Araldite and anchored behind the end V coil support blocks, were fixed on each end of all six poles, covering the top three turns of the field winding.

Further cracking was observed in the top bakelised cloth insulation flange on each pole. The cracks have been injected with Araldite and the flange secured on each side of a crack by drilling holes, half in the bakelised cloth itself and half in the brass spool flange, into which glass fibre pegs were fixed with Araldite.

No.2 rotor was received on site in July, having been re-conditioned using the original poles and field windings. Some of the long taper keys, which hold the poles on to the rotor, were replaced by new ones. The V coil support bolts and blocks have been modified like those on No.1 rotor and all other bolts and studs now have cold rolled threads.

The bakelised cloth spool flanges have been replaced on No.2 rotor by ones made from resin bonded glass cloth, which has superior mechanical and thermal characteristics. No.2 stator was received on site in June, after replacement of some damaged laminations and a complete re-wind.

A rotor of new design was delivered in August. This has the poles forged integrally with the body (see figure 39), and is mechanically superior to the laminated construction in which the poles are keyed in dovetails machined in the rotor body.

In the solid pole rotor, pole caps have to be bolted on to retain the field winding spools and this presents design problems, but these are thought to be less severe than those of the original laminated and keyed assemblies. It is planned to install this rotor in March 1969.

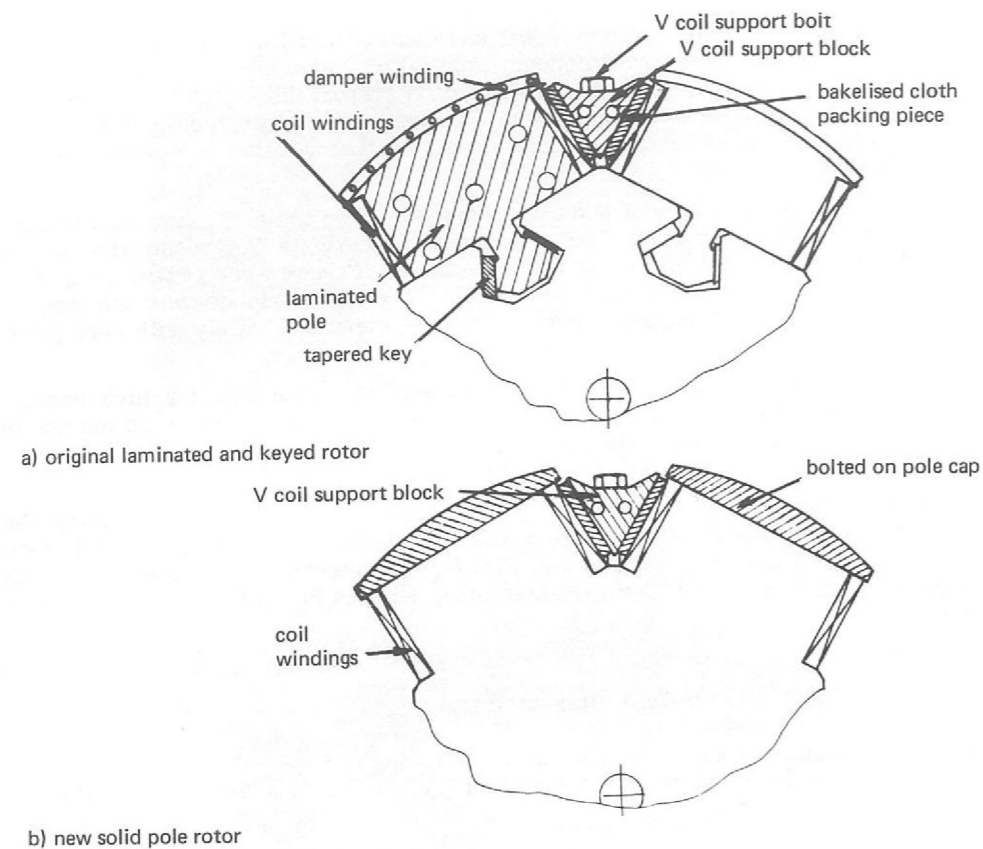
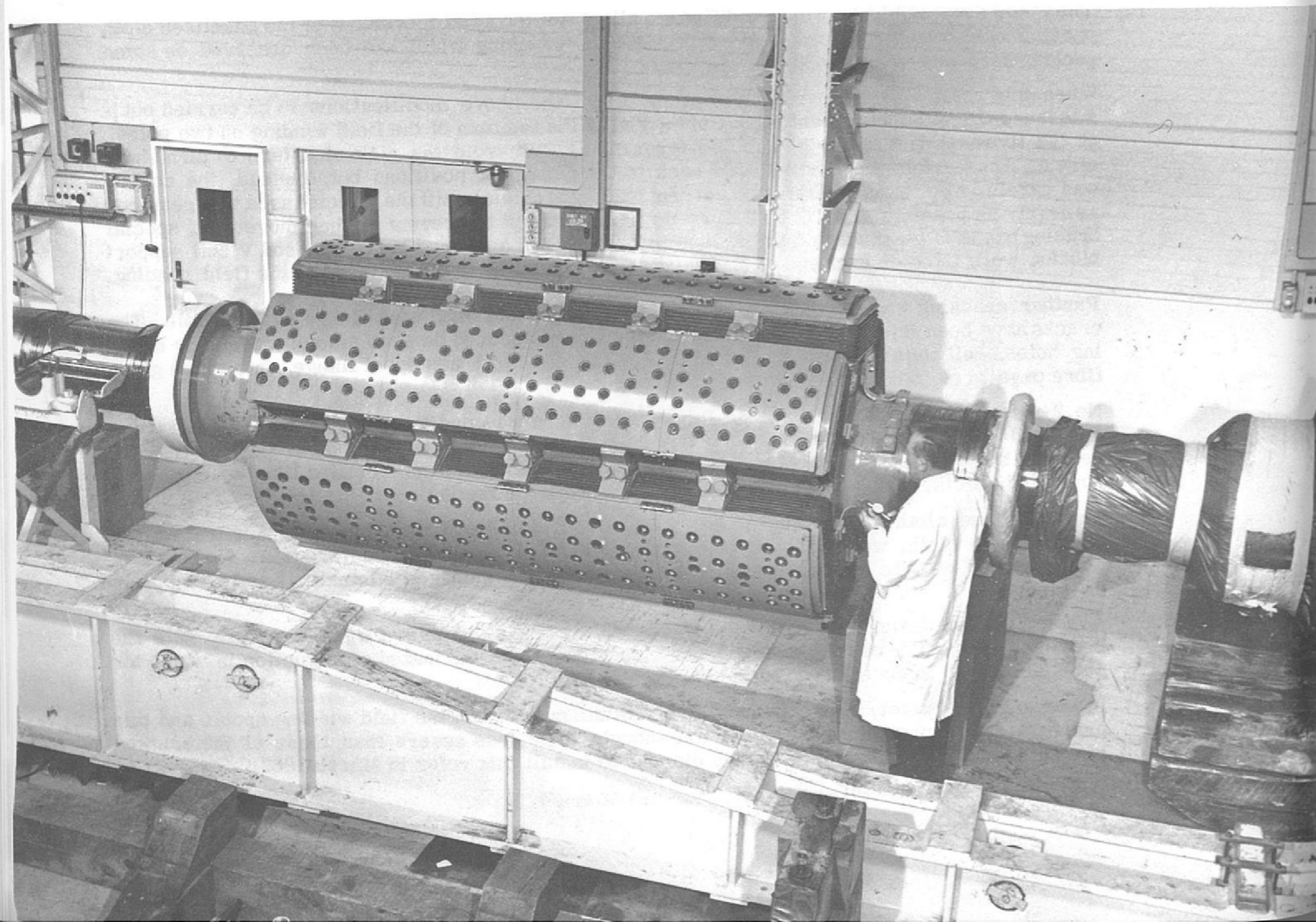


Figure 38. Part cross-sections (diagrammatic only) illustrating construction of original laminated rotor and new solid pole rotor.

Figure 39. New solid pole rotor for Nimrod power supply.



The convertor plant continues to perform very well with an arc-back rate of about one in every 350 hours – even better than the excellent performance in 1967. The whole of the A2 convertor plant has now been fitted with the modified grid control units which permit access to all the grid control circuitry when the plant is operating.

## Synchrotron Development

### *Ion Sources* (69)

Work has continued throughout the year on duoplasmatron ion sources. A source suitable for the PLANIM project has been successfully developed, producing a 1 cm radius, 200 mA beam at 50 kV. Investigation of the emittance of this beam is proceeding and some special features have been built into a laboratory rig for this work. These enable various dimensions of the expansion cup and extraction gap of the source to be changed without breaking the vacuum or disturbing the source in any other way; consistent results can then be obtained.

The current density distribution in the beam has been measured; it is frequently found that a small fraction of the current is concentrated in a sharp peak at the centre of the beam. Experiments are being carried out on a hollow cathode electron emitter for duoplasmatrons, which may prove to be smaller and more robust than the oxide cathodes generally used at present.

### *Injector and Injection*

The present r.f. ion source unit has now been in service for 2 years without fault or deterioration.

A major improvement in the injector has been the successful installation of a debuncher phase ramper. This device enables the energy of the injector beam to be increased, at a controlled rate, during the injection interval which increases the injection and trapping efficiencies. Normally, the intensity of the trapped beam falls from a maximum value just after trapping to about half that value during the first 20ms of acceleration, thereafter remaining constant up to 7 GeV. With the ramper in use, no increase in the maximum beam intensities is observed because these are limited by transverse space charge forces (see PLANIM design study page 64). However, if the rate of ramping is adjusted so as to keep the particle equilibrium orbits at injection fixed and fairly close to the inflector, then all protons can be injected with small amplitudes of radial betatron motion. In these circumstances there is a significant reduction in the beam loss during the first 20 ms and the 7 GeV beam intensity increases by 20-30%. The injector beam energy is controlled by using the debuncher cavity, the phase of which with respect to the linac r.f. is programmed so as to decelerate linac bunches which arrive at the debuncher gap early in the beam pulse and to accelerate those bunches which arrive late. The instantaneous debunching effect on each individual linac bunch is retained. Measurements of the energy spread, at different times during the injector beam pulse, are shown in figure 40 along with the energy spread in the unramped beam. The debunching effect and the increase in the mean energy during the beam pulse can be clearly seen.

Considerable effort was devoted to the study of space charge effects during injection as part of the PLANIM design study and this work is described on page (64).

Some theoretical and experimental work was also done to the vertical match of the injector beam into Nimrod. This is at present poor due to an uncorrected vertical defocussing force in the inflector.

### *Magnet Power Supply*

In order to study the action of two large alternators, electrically in parallel and subjected to a pulsed duty cycle, it is necessary to record continuously and accurately throughout the pulse many quantities such as machine power, load angle, relative shaft displacement of the two machines, etc. Special electronic wattmeters, having a very fast response time have been developed for this work.

This instrumentation has already been used to investigate parallel running conditions when inter polar links are not fitted. The results indicate that such operation is satisfactory.

Although the inter-polar links have never failed, it became clear in 1967 that they were not well designed to withstand certain fault conditions. New, re-designed sets have had to be made available for the two laminated pole rotors and the solid pole rotor, since inter-polar links may still be needed when attempting to operate an alternator with a solid pole rotor in electrical parallel with one having a laminated pole rotor.

A means of fine control of the speed on one of the alternator sets, over a very limited range, has been commissioned. This enables synchronisation of the two machines to be carried out much more rapidly than hitherto.

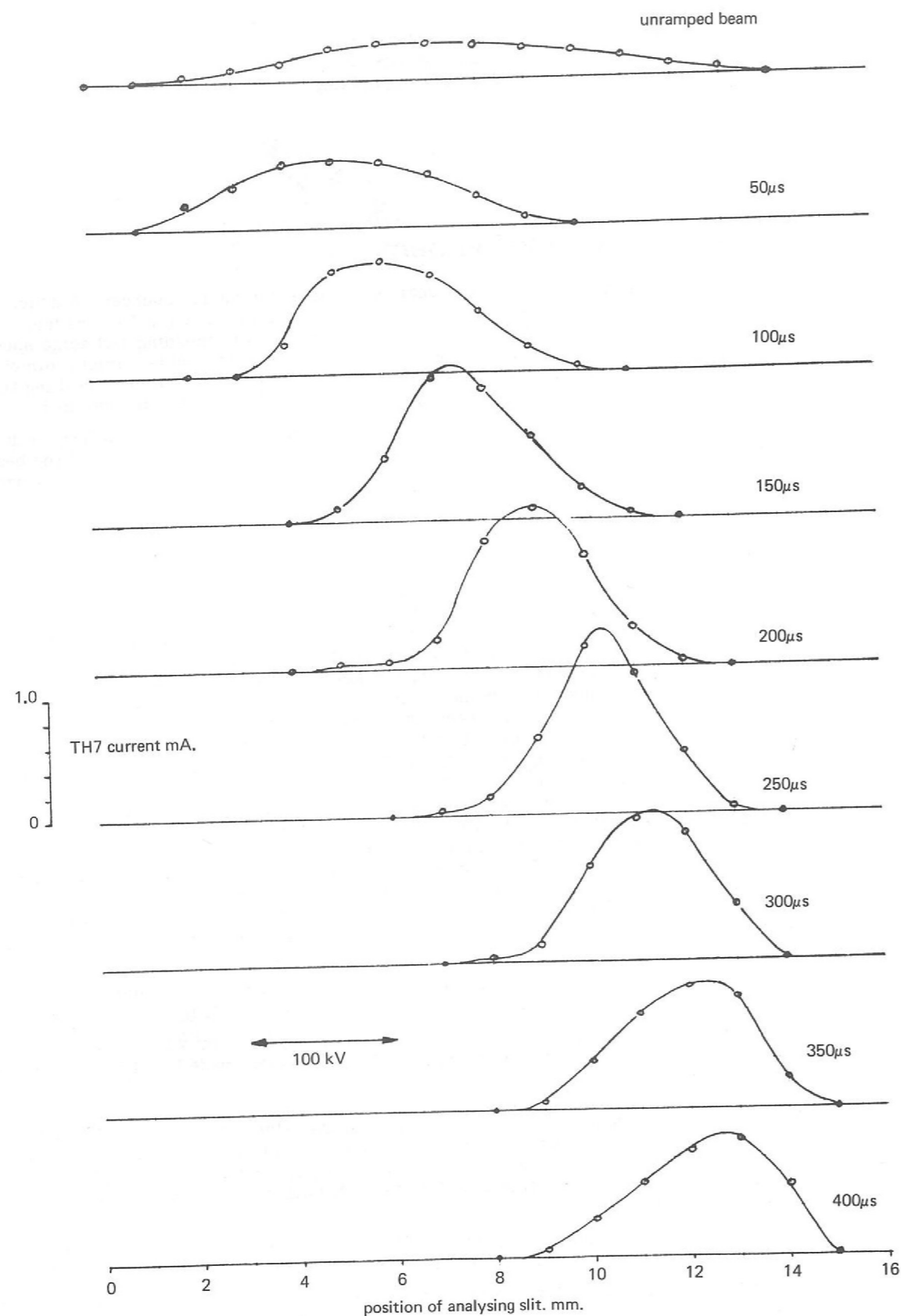


Figure 40. Energy spread of ramped injector beam at various times during beam pulse compared with unramped energy spread.

Following the fatigue failures experienced on this and other proton synchrotron power supplies, Lloyds Register of Shipping have been asked to examine the components of the Nimrod rotating plant and report on those which might fail due to fatigue and/or fretting fatigue. This work is now well advanced and a report has recently been received.

An important series of tests are being carried out with the aid of a specially developed fatigue testing rig to evaluate the improvement in fatigue life expected from the re-designed V coil support bolts.

Stresses on the rotating plant would be reduced if the converter plant could be arranged to change from current rise to flat-top and from flat-top to decay more slowly than at present (6ms), although the duty of the converter vessels would be more onerous. Preliminary control circuitry is being developed to enable this problem to be studied in more detail.

#### Ionisation Systems

A new system was brought into operation during 1968 to measure the beam profile, non-destructively, throughout the acceleration cycle. Similar in principle to the device used on the Argonne ZGS, it makes use of the positive ions created in the background gas of the vacuum system by the beam. These ions are accelerated transversely by an electric field between a pair of large parallel plates, the negative plate being a mesh which allows the ions to pass through and be collected on an array of separate strips. The ion current collected by each strip is measured, amplified and the resulting signals are multiplexed and fed to the main control room for display. The equipment for measurements of radial beam width uses an accelerating potential of 5 kV and has 35 collecting strips 2.5 cm wide spaced across 100 cm of aperture. The vertical system requires an accelerating potential of 15 kV and has 10 collector strips 1.9 cm wide spaced across 20 cm of aperture. Both systems are installed in Straight 6 of the machine. The total ion current collected varies from a few micro-amps to tens of nano-amps through the Nimrod acceleration cycle. The minimum useful signal level is 10 nA, and the multiplexing rate is 10  $\mu$ s/strip. The equipment was used extensively in the PLANIM design study (see page 66). Figure 41 shows a plot of radial beam width against time obtained by photographing the oscilloscope display of the multiplexed output at different times during the machine cycle.

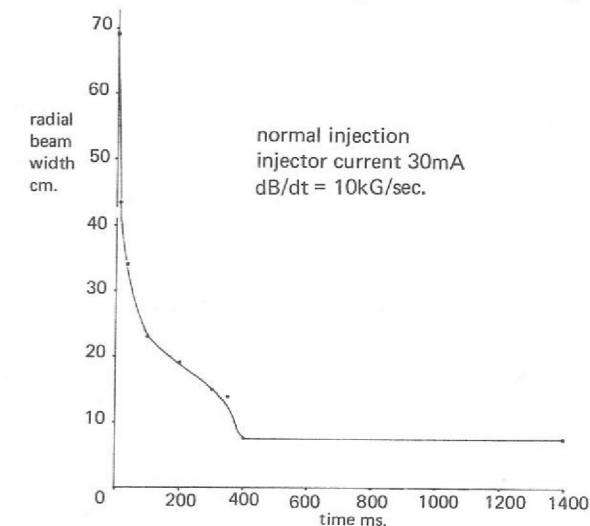


Figure 41. Radial beam width as a function of time.

Recently the equipment has been changed to give a multiplexing rate of 0.5  $\mu$ s/strip and additional equipment gives a display of beam width and position at a sample rate of 20 kHz.

#### Controls

A study has been made of the use of small computers for the control of accelerator equipment. A small PDP8 computer has been used in an exercise to aid the control of a laboratory apparatus for testing the Nimrod r.f. ion source. Much information was gained from this successful exercise which will be useful for the main project now being tackled, which is the computer aided control of the X3 extraction system and beam line. Initially the system will be used to help with the commissioning of the X3 system and beams. Later it will be used for routine operation. The hardware is in an advanced state of manufacture; for example numerically controlled collimators using digital encoders for displacement readings are being developed. The program system is being written ready for commissioning of X3 which is scheduled for the end of March 1969.

New equipment has been installed to stabilise the peak field in the Nimrod magnet. This is most important if consistent results are to be obtained from the extraction systems. The field in the magnet is measured using a pick-up loop and a voltage-frequency converter produces a digital reading of the peak field. This is compared with a reference and any error is corrected for the next magnet pulse by changing the voltage from the magnet power supply. The stabilised value of peak field is typically 14,000  $\pm$  10 gauss. Using the same equipment, other parameters are measured such as the change of field during flat-top, and the value and rate of change of field at injection.

#### Radiation Dosimetry

Radiation dosimetry in the Nimrod vacuum vessels, using dosimeters based on the hydrogen evolution technique, has continued throughout the year. The radial dose pattern shows a maximum at approximately 10 cm from the back wall of the inner vessel. The circumferential pattern of total dose received by the vessel up to August 1968 is shown in figure 42 along with results for the previous year. Table 2 lists the average and peak doses for each octant up to August 1968.

**Table 2**

Average and maximum dose per Octant from first operation to August 1968  
( $21.4 \times 10^{18}$  protons accelerated)

Octant	Maximum Dose Mrad	Average Dose Mrad
1	181	145
2	122	89
3	73	59
4	84	71
5	140	103
6	125	114
7	169	130
8	183	148

This data is further illustrated in figure 43 which gives isodose contours corresponding to the total dose recorded from machine start-up.

### Accelerated Beam Utilisation

Targetting  
(86)

The beam sharing arrangements have been developed so that during high energy physics periods up to seven experiments can receive particles simultaneously. The noise-spill servo (used to produce slow beam spill for counter experiments) has been improved by rebuilding the r.f. amplifiers and detectors, which are now installed in a permanent form. The spectrum of the noise source has been measured and the noise power correlated with the decay rate of the induction electrode signal which serves as a control signal for the servo. Improved methods of measuring effective spill times have been developed. With a magnet flat-top of 500 ms, effective spill times of 300 ms are achieved when all the beam is used on flat-top. If one third of the beam is first used for a fast spill for a bubble chamber, effective slow spill times of 250 ms are achieved. The spill is modulated at the frequency of the Nimrod accelerating voltage and also at the lower frequencies of the magnet power supply ripple. It is important that this structure on the slow beam spill should be reduced to a minimum. The r.f. component is minimised by reducing the accelerating voltage on flat-top and work has continued throughout the year on reducing the magnet ripple.

The lower frequencies in the magnet ripple can be reduced by the existing primary ripple filter, the pre-amplifiers and switching circuits of which have been re-designed, but there are also present higher frequency components due to commutation transients (traced to the interphase reactors). These would be best dealt with by means of a static LC filter. One scheme which has been studied is to use the dynamic ripple filter, with reduced amplifier capacity, on current rise only and switch in a passive circuit during flat-top. In the meantime an earlier system of secondary ripple filtering has been re-connected. This uses some of the Nimrod pole face windings in which self induced ripple currents flow on flat-top only, this giving the best combination of effectiveness and reliability.

To aid in the setting up of different target sharing arrangements, work has continued on a new target monitoring system. As a measure of the intensity of the beam striking an electrically insulated target, the charge lost by it, due to the ejection of secondary electrons, is measured. Tests have been carried out on standard Nimrod copper targets with various methods of insulation. Suitable flexible coupling leads have been developed and a charge sensitive amplifier and gating units have been built. The signal from the target is large, easy to measure, linear and shows good reproducibility. A low energy electron component is present and methods of suppressing this are under investigation.

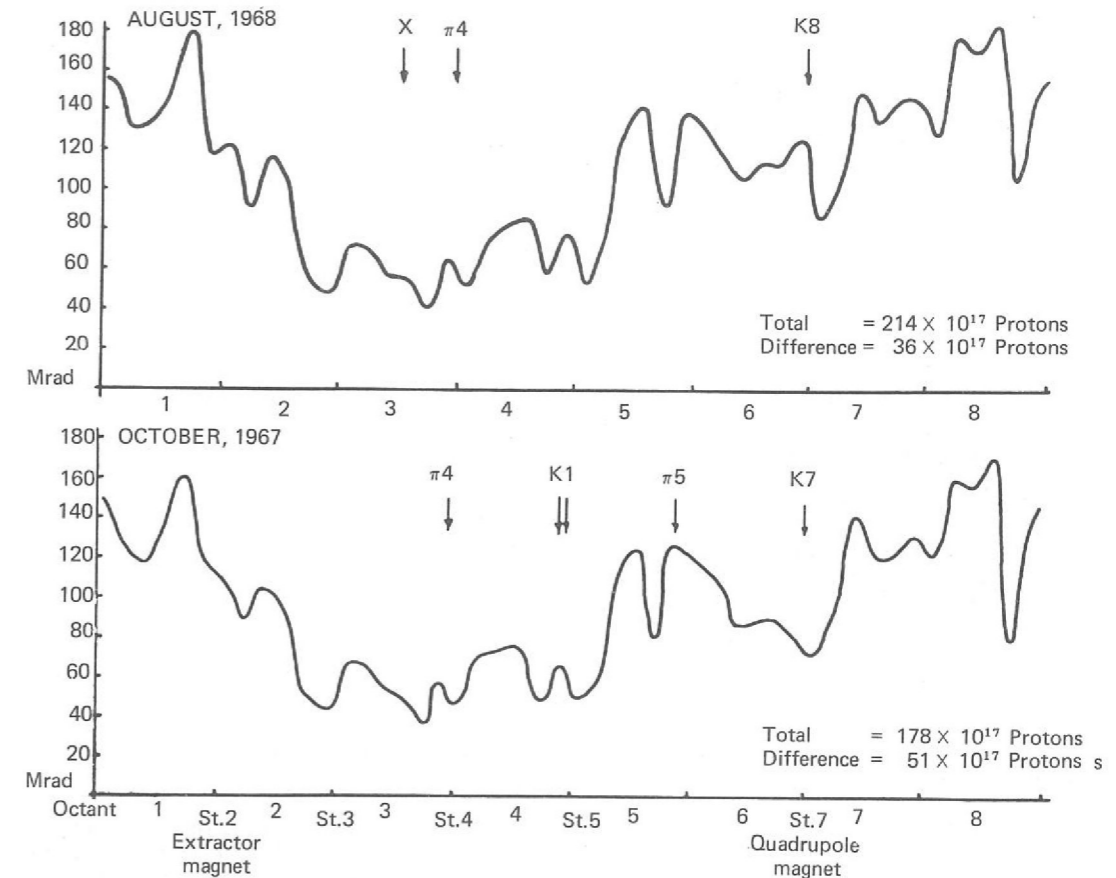


Figure 42. Absorbed radiation dose profiles for the inner vacuum vessel of Nimrod.

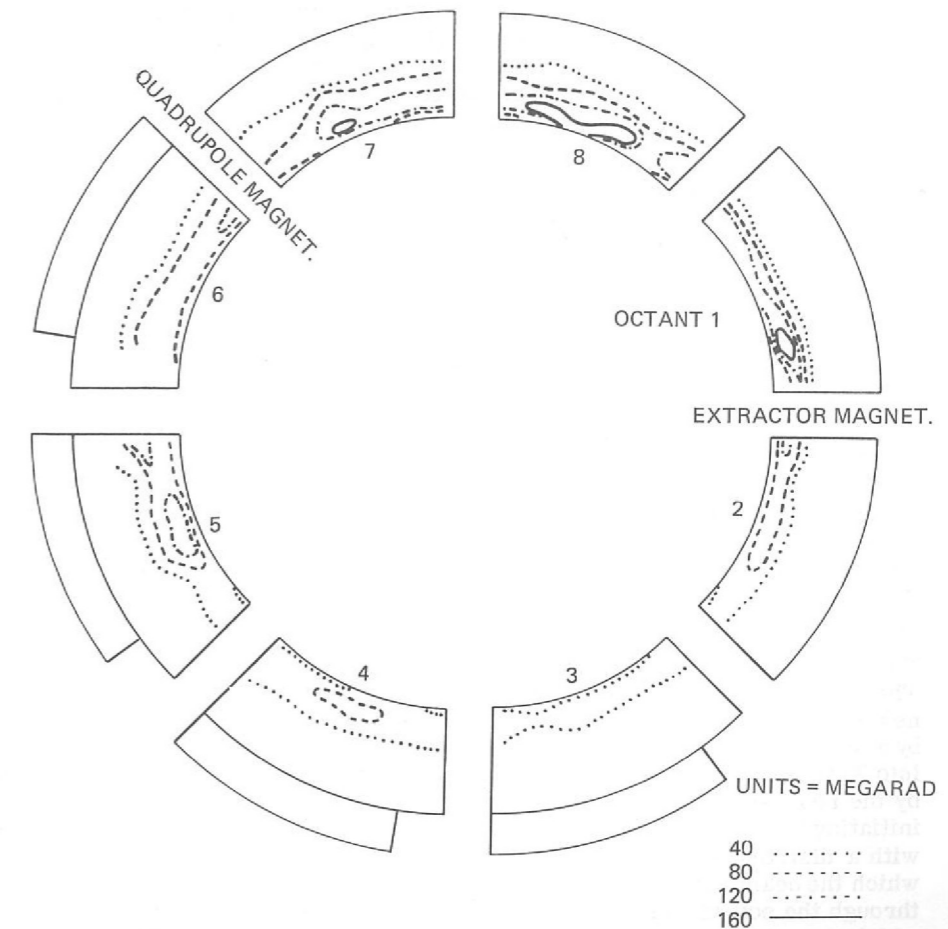


Figure 43. Integrated isodose contours for the inner vacuum vessel of Nimrod.

### External Proton Beams

The two external proton beams X1 and X2, based on the achromatic energy loss (Piccioni) scheme, operated throughout 1968. The proton flux in X2 has been increased to between  $4$  and  $6 \times 10^{11}$  per pulse, depending on the Nimrod circulating flux: intensity in X1 is now about  $2.7 \times 10^{11}$  per pulse.

For part of the HEP programme, the beam was successfully switched from X1 to X2 during the same machine pulse. This was achieved by changing the current level in the extractor magnet using a special transistor controlled power supply. A 1ms burst for the 1.5 m hydrogen bubble chamber was followed by a slow spill for the complex of counter beams served by X2. Good extraction efficiencies were achieved down both lines, although eddy currents in the solid steel yokes of the extractor magnets used can have adverse effects on the field shape. An investigation of these effects has begun and at the same time two new magnets with laminated yokes are being manufactured to overcome them.

Two other methods, mentioned in a previous report, were used to give small amounts of beam to X1, when the extractor magnet was kept at the field level necessary for X2. These methods involved fast spill on to an X1 target during current rise (5 GeV), and spill on to a target placed at an outside radius at full energy.

Pairs of horizontal and vertical collimators placed in the X1 beam line were used in ray tracing experiments (figure 44) which verified that the virtual source was off axis. This was corrected by re-aligning the upstream section of the beam line, with slight improvement in beam intensity and considerable improvement in the angle at which X1 protons strike the external target.

Experimental studies on the excitation of the  $Q_r = 2/3$  resonance were continued using a distributed magnetic field perturbation. The prototype septum magnet and its plunging mechanism were commissioned and installed in Straight 7. An attempt to initiate the resonance was successful, and many of the computed predictions confirmed; a scintillator placed over the magnet's aperture revealed that protons were displaced several centimetres beyond the 3 mm thick septum, an encouraging indication that good efficiency can be expected with this extraction method.

Theoretical and practical work aimed at the reduction of fringe fields at the end of septum magnets has been initiated. A better understanding of how these fields arise has already been obtained, and it is hoped that this knowledge will be usefully applied to the new extractor magnets.

Improvements have been made to the circuitry associated with the secondary emission chambers used for beam intensity measurements. Automatic processing now provides a digital read-out free from errors due to zero offset and temperature drift in the head amplifiers. A 'scaler divider' has been developed to normalise the measurements of extracted beam intensity against circulating protons during multiple target or beam switching operation: it divides the external beam flux by the decrease in circulating beam flux caused by extraction.

### Theoretical Extraction Studies (75, 79, 82)

From the middle of 1969 onwards Hall 3 will be served by the extracted beam X3, a conventional achromatic energy-loss beam, not unlike X1: it will use plunging magnets in Straight 1 and Straight 4. Results of the X1 alignment studies have been incorporated in the X3 design.

In the meantime the design of two new extraction schemes are nearing completion, and it is hoped to incorporate them in X3 at a later stage. The first of these, a modification of the original Piccioni scheme, will use a 1cm septum extractor magnet (XM9), and a magnetic channel in the header vessel. It should reduce the fraction of the beam lost in the septa of the quadrupole and extractor magnets now in use, and in the radially defocussing fringe field of Nimrod. These losses are the main limitation on the extraction efficiencies obtained at present. There is no plunging quadrupole; instead, momentum dispersion is removed by the field gradient in the extractor magnet, and optical dispersion is controlled by the magnetic channel.

The designs for XM9 and the magnetic channel have been carried out computationally, using TRIM. The resulting channel behaves as a quadrupole excited partly by Nimrod's fringing flux and partly by currents in its own windings. Since this flux changes rapidly along the length of the channel the latter will be built in two parts known as XHQ2 and XHQ3, each about 1 metre long and independently powered. A cross section of XHQ2 is shown in Figure 45.

The second extraction scheme is based on slow resonant extraction using the  $Q_r = 2/3$  resonance. The same magnet XM9 will be used but it will be driven to higher field levels by means of a new generator of the homopolar type, supplying peak currents of up to 21,000 A, programmed by a series transistor regulator. A vertically plunged soft kicker magnet in Straight 3 will direct into XM9 those particles whose radial amplitudes of oscillation have been sufficiently increased by the resonance. Extensive computer studies have been made to decide on the best methods of initiating the resonance and of controlling the direction of the emerging beam. The choice rests with a distributed magnetic field perturbation which provides radial regions of instability into which the beam will be drifted by a slight ramp on the peak field. A time variation in the current through the soft kicker magnet will be used to compensate for the slight changes of divergence which occur during the resonant spill.

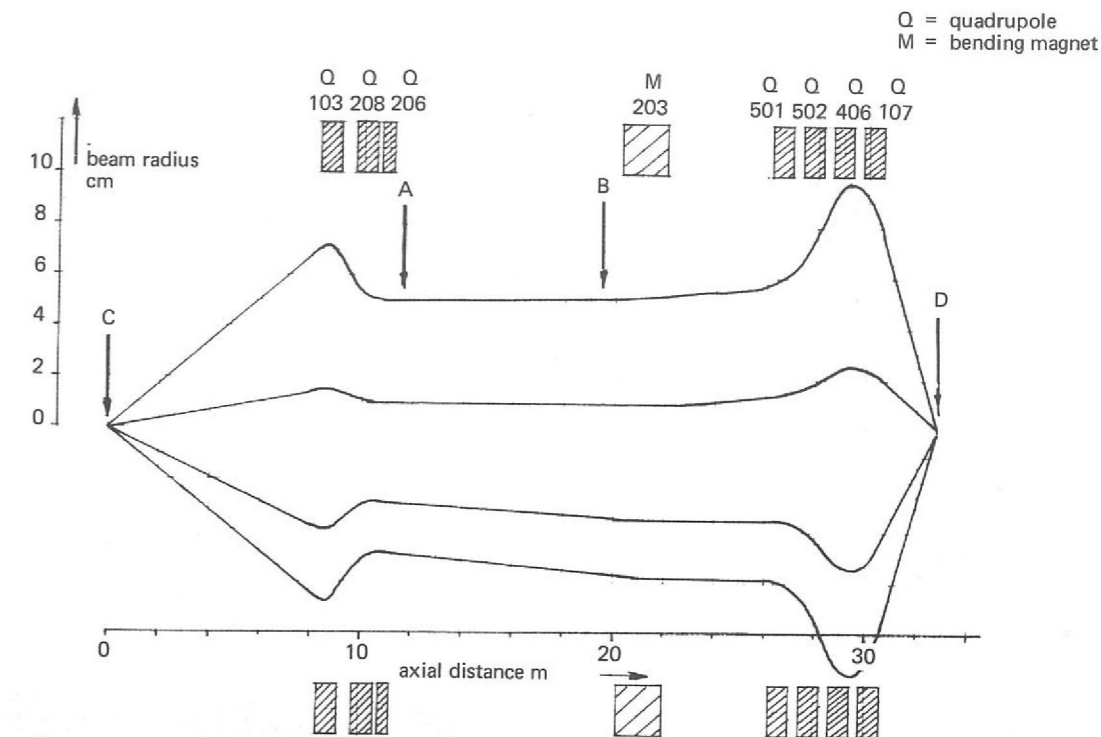


Figure 44. A ray trace in the X1 beam line after optimisation. By using moveable slits at A and B, the rays may be traced to the effective source C and to the target D.

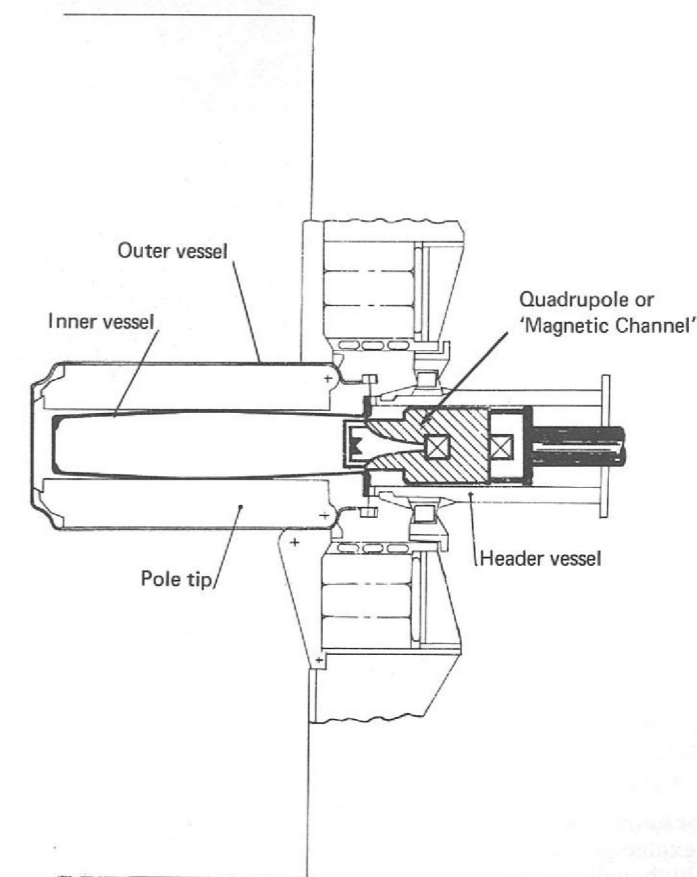


Figure 45. Schematic layout of the header vessel quadrupole XHQ2.

## Beam Transport Components

### Switching and Step Magnets

A stepping magnet has been incorporated into the separated beam K11 to deflect successive entries of particles by a small vertical step across the aperture of the 1.4 m heavy liquid bubble chamber. A particle marking system, similar to that in K9, is also included to label trajectories as they are identified by a Cerenkov counter. Bunching of the wanted particles has been observed in the fast spill beams being produced at present. To enable the stepping magnets to separate these particle bunches better, work is in hand to reduce the rise time of the magnetic field from 10  $\mu$ s to, at most, 3  $\mu$ s.

Two schemes have been considered which would provide switching magnets capable of deflecting high momentum beams into or out of slits and apertures for precise periods of time during short spills. In the first arrangement, a current of 250 A is switched into a multitrans coil, for a time of up to 1 ms, by a large triode valve. By working at 20 kV a rise time of about 10  $\mu$ s is achieved. The second arrangement uses a 1 ohm delay line to drive 5000A for 500  $\mu$ s into a four turn coil. A half-length magnet has been operated successfully.

Basic research has continued on a coiled gas discharge tube acting as a high current magnet with a short pulse length, concentrating on the limitations to the current due to recombination on the walls of the tube.

### High Field Pulsed Magnets

The type IB coil magnet, providing 70 kG over 40 cm, (see figure 46) operated in the enriched  $\Lambda^0$  beam (derived from K9) for 8,000 pulses before ignition occurred in its uranium collimator. Tests on the damaged magnet indicate that the coil design is fundamentally sound, and so several coils are being made for a series of life tests. Future collimators will be made from heavy alloy.

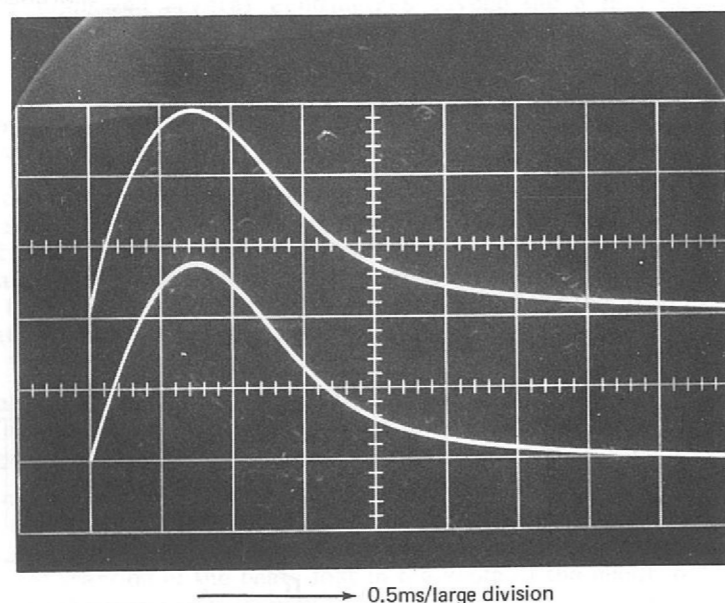


Figure 46. Oscilloscope traces of current and magnetic field in the high field pulsed magnet.  
Upper trace - current, 40,000 A/large division  
Lower trace - magnetic field 26 kG/large division

→ 0.5ms/large division

A Type II magnet to provide a field of 150 kG over 20 cm is being manufactured. The shorter length enables 150 kG to be produced with the same power supply; i.e. a capacitor bank of 0.02  $\mu$ F charged to 4kV and delivering 2 ms pulses of 120,000 A at the Nimrod repetition rate.

### Electrostatic Separators (73)

Effort has been concentrated on resolving the problem of insulator failure when operating at the elevated temperatures required by glass electrodes. A new type of insulator has been designed using alumina loaded porcelain and has been tested with good results. This will permit an immediate increase in the operational performance of separators from 60 kV/cm to 70 kV/cm over a gap of 10cm.

Experiments with megavolt pulses have shown that processes postulated by the unfashionable ion exchange theory probably play a significant part in determining the performance of large gap high voltage devices in vacuum. It has been found that the exchange multiplication factor for this mechanism varies linearly with residual gas pressure. This could provide an explanation for the variation of performance with residual gas pressure that has long been a perplexing effect in electrostatic separator technology.

### Beam Cut-off Units

A new type of beam cut-off unit is in manufacture in which an aperture, through which the beam normally passes, is closed by rotating steel discs, the whole mechanism being in vacuum. Two such units will be installed as part of the X3 blockhouse wall, thus enabling either  $\pi$ 8 or K15 beam line to be isolated (to permit maintenance work for example) without affecting the other line.

### Superconducting RF Separator Research (70)

Build up of laboratory test facilities and measuring equipment has continued throughout 1968, and test cavities operating both in L-band and S-band have been constructed. Recent emphasis has been on lead-plating technique. Currently, unloaded Q-values of about  $5 \times 10^8$  are being achieved at 1.85°K.

## Beam Lines

### Beam Line Design

Considerable use has been made of the existing programs LIMP, TRAMP, IPSO and NIMDYN and a number of important modifications have been made, particularly to LIMP, in order to represent more accurately the effects of Nimrod's radial field distribution. NIMDYN has been changed to incorporate the effects of a magnetic channel in the header vessel region. Some use was made of the SLAC program TRANSPORT where the situation warranted a program more powerful than TRAMP.

Work has continued throughout the year on tuning the K9 separated beam for new experiments and new momenta; development of the diagnostic and control equipment has likewise progressed steadily.

### Beam Line Installation and Commissioning

The layout of beam lines in the experimental halls at the end of the year is shown in figure 1. It will be seen that the layout is basically the same as the end of 1967. 1968 has been mainly a year of consolidation and improvement, the following changes being noteworthy:-

- K10S A liquid hydrogen target and spark chamber array were installed.
- K14A A polarized target was installed.
- K8 A Mk III target mechanism, which permits azimuthal as well as radial movement, was installed in place of a Mk Ic mechanism. This enables the production of particles for K8 to be optimised when K8 is sharing flat top spill with other users. Later in the year, the local control room was re-sited and a Cerenkov counter installed.
- K9 A stepping magnet was installed and modifications carried out to incorporate the high field pulse magnet.
- K11 Two electrostatic separators were installed and commissioned. The final stages of the beam transport were fitted along with a Cerenkov counter.
- $\pi$ 5 -  $\pi$ 7 The  $\pi$ 5 beam line was partially removed and fully re-aligned to become the new  $\pi$ 7.
- $\pi$ 4 - P71 The  $\pi$ 4 beam transport system was re-aligned to become P71, the liquid hydrogen target being refurbished ready for installation in January 1969.
- X2 A flip target mechanism was installed which enables targets in X2 to be changed during each machine burst. A fast spill for K11, using a 2mm  $\times$  2mm  $\times$  100 mm copper target, was followed by a slow spill on to a 4 mm  $\times$  4mm  $\times$  40 mm uranium target for other X2 users.
- X3 Beam transport equipment and the heavily shielded X3 tunnel were installed in the Hall 3 annex.

A liquid hydrogen target was built at the Laboratory and installed at CERN for the Epistle Project (see HEP Division, Experiment 15, page 28).

Four electrostatic separators were fitted during the year with turbomolecular pumps to improve the cleanliness of the vacuum system. These composite pumping systems were built at the Laboratory from standard commercial components.

Sections of 8 inch diameter aluminium beam pipe have been successfully welded together in situ, which, with special couplings, will make the X3 beam line a cleaner vacuum system.

Power supplies of an improved design in both 50 kW and 100 kW ratings, have been put into service. The long term design stability of the 100 kW sets is  $\pm 0.01\%$ . The figure for the 50 kW sets is  $\pm 0.1\%$  and stabilities of  $\pm 0.02\%$  have been observed in practice. Both types have a much

faster response to supply mains variations than of sets installed previously. Typically it requires 150 milli-seconds to correct a 1% step change of the supply mains.

## Targets for High Energy Physics Experiments

### Liquid Hydrogen Targets

The 1967 Annual Report described a target system requiring no external supplies of liquid hydrogen and using a commercially available helium condensing refrigerator (see figure 47). This system has been successfully commissioned except that the emergency vent system has not yet been proved with liquid hydrogen. Three interesting developments have arisen from this work:-

- an accurate liquid hydrogen level gauge has been developed using a silicon diode.
- irradiated polythene sleeves have been heat shrunk onto electrical connections to provide a spark free junction for use in hazardous areas.
- a low mass stop and relief valve, suitable for use with liquid hydrogen has been developed.

Although the hazard present when using this new system is substantially less than with the existing arrangements, the design of igloos is being improved to minimize the effects of an explosion, should one occur on rupture of a target. Forced ventilation across these targets is also being considered, so that igloos can be reduced in size or even dispensed with. This would enable more experimental equipment to be located outside hazardous areas, thus reducing considerably the amount of preparation and maintenance work on it.

Much detailed development work has been done on the design and manufacture of targets made from polyethylene terephthalate film. Methods of cold forming domes in this material have been successfully tried, and re-entrant windows developed.

### Polarized Proton Targets (74, 85)

A target has been provided for a  $\pi^+ p$  scattering experiment (K14A) on Nimrod, which has a number of new features in the cryogenic, microwave and r.f. systems: particularly notable is a new type of nuclear magnetic resonance (NMR) system with which the polarization can be measured with greater accuracy than in previous known systems. Such accuracy is required in the experiments now possible using higher secondary particle fluxes produced by Nimrod external proton beams. In the new system a direct measurement is made of the real part of the admittance of the NMR circuit, from which a rapid calculation of the proton polarization is automatically made for visual display and for feed-out to the local computer.

Good progress is being made on research into target materials, particularly those richer in protons than lanthanum magnesium nitrate (LMN), the present standard target material. In this work, mostly carried out at lower magnetic fields than would be used in a practical target, a wide range of free-radical/solvent combinations has been investigated, and the effects of dissolved oxygen studied. Particularly promising is Fremy's salts in a glycerol/water mixture, a combination not apparently considered elsewhere. Other radicals studied which give enhanced polarization include methyl viologen (Paraquat), tri-tertiary butyl phenoxide and porphyrin. Also, it is planned to synthesize certain inorganic free radicals known to have the properties required for good polarized targets (narrow lines and small g-factor anisotropies). An investigation of LMN (with "1%" neodymium) has shown that the proton relaxation time (at 1°K and 10 kG) increases from 40 minutes to 5 hours when the magnetic field direction is changed from being perpendicular to being parallel to the crystal axis.

This last result, apart from demonstrating the excellent purity of the LMN crystals grown by our chemists, may also find application in a new type of target which is at present the subject of a design study. In this proposal, exceptionally good access for HEP experiments is obtained by freezing-in the polarization for long periods at low temperatures ( $\sim 0.3^\circ\text{K}$ ) and moderate, non-uniform magnetic fields (10 - 20 kG) from superconducting windings. The target, either of LMN or of a material richer in protons, would be initially polarized using the solid effect, as usual, in a secondary magnetic field of appropriate magnitude and uniformity.

Equipment is nearing completion for polarization experiments at 25 kG and later 50 kG, and also for work at temperatures down to  $0.3^\circ\text{K}$ . A 50 kG superconducting magnet for this is already in operation, as is a novel series-resonant broad-band NMR system for work at up to 50 kG. 8 mm ESR equipment has also been set up and preliminary experiments carried out.

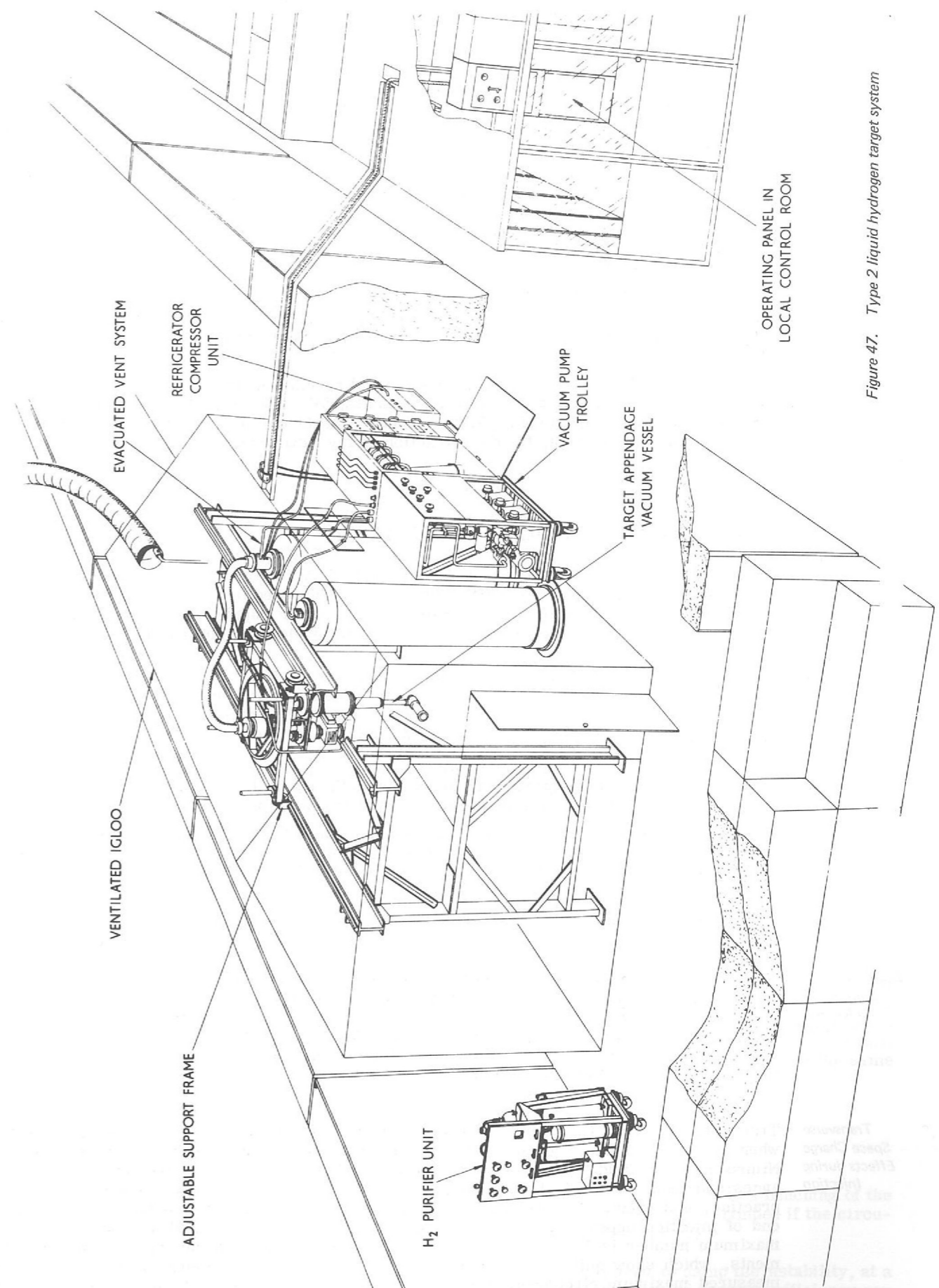


Figure 47. Type 2 liquid hydrogen target system



## New Experimental Hall for Nimrod

Construction of the hall continued during 1968 and by the end of the year all building and civil work, together with much of the mechanical and electrical services has been completed. Limited access to the east half of the hall was obtained during the year to enable a start to be made on installation work associated with the new extracted beam. Outstanding work on building services is due to be finished in January 1969 and the installation and commissioning of the extracted beam is expected to be achieved by the middle of 1969.

The main hall is 300 ft. long, 150 ft. wide and 65 ft. high, while the annexe is 70 ft. long, 90 ft. wide and 40 ft. high. Two parallel tunnels, each measuring 10 ft.  $\times$  10 ft. traverse the whole length of the main hall. Floor trenches with removable covers cross the main hall at 20 ft. intervals and connect with the tunnels. At a height of 25 ft., a 9 ft. wide platform, or gallery, runs along both north and south sides of the main hall and connects with a 14 ft. wide platform which runs across the west end. A passenger lift gives access to the gallery, which is intended to accommodate power supplies.

Two cranes are installed, a 30 ton cab-operated gantry crane with a 34 ft. maximum hook height in the main hall and a 30 ton pendant-operated gantry crane with a 23 ft. maximum hook height in the annexe.

In addition to the normal building services several special services are provided. Four package sub-stations on the gallery provide  $2\frac{1}{2}$  MVA each at 415V. A demineralised cooling water circuit provides a cooling capacity of  $10\frac{1}{2}$  MW. Induced draught ducting is installed at 14 stations, exhausting through the roof, for the extraction of any hazardous gas.

## The European 300 GeV Project

During 1968 a number of study groups have been working under the joint auspices of CERN and ECFA. A few members of the Laboratory have participated in the studies on magnet design, ejection, closed orbit error compensation and the power supply. By the end of the year six member states of CERN had decided to support the project but no final decision has yet been taken to proceed.

## Planim

*Introduction* A design study has been carried out to determine the feasibility of using the PLA as a 50 MeV injector for Nimrod and to estimate the likely increase in beam intensity which would result.

It has been concluded that increasing the injection energy to 50 MeV would lead to an increase in Nimrod beam intensity by a factor of between 3 and 4 and that it is feasible to leave the PLA in its present position and transport the beam about 280m to Nimrod. The project would cost £570,000, including a 15% contingency and would take about 2 years to complete.

A brief review of the main aspects of the design study is given below.

*Beam Intensity Limitations in Nimrod (71)* The basis for the PLANIM project is that the beam intensity in Nimrod is at present close to the transverse, incoherent, space charge limit at injection and r.f. trapping. Simple space charge theory predicts that this limit increases as  $\beta^2 \gamma^3$  with increasing injection energy. By changing the injection energy from 15 to 50 MeV the charge injected into Nimrod can thus be increased by a factor 3.5 before a new, higher space charge limit is reached. Considerable theoretical and experimental work has been done to verify these ideas.

*Transverse Space Charge Effects during Injection* Transverse behaviour has been examined in detail by computing the motion of individual protons when injected in a beam occupying a finite area in phase space and when subjected to the real Nimrod magnetic fields with space charge effects included. The protons are subjected to resonances and many are lost, both vertically and horizontally; more protons are injected as in practice, and eventually a dynamic equilibrium state is reached. The number surviving at the end of injection depends on the details of the field shape; for normal Nimrod conditions the maximum number is  $1.6 \times 10^{13}$ . This is in good agreement with the experimental measurements, which show quite conclusively that the circulating beam is space charge limited. The measured maximum circulating charge is in the range  $1.4 - 1.6 \times 10^{13}$  protons and shows the same saturation characteristic as that predicted.

*Trapping Efficiency* The trapped charge, measured 1 ms after r.f. on time, is shown as a function of injected charge in figure 48.

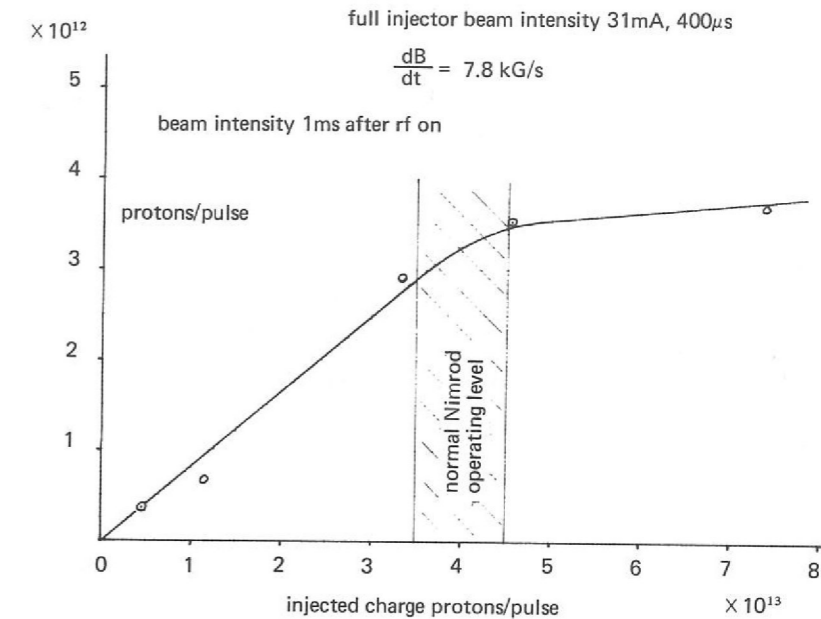


Figure 48. Diluter measurements of trapped charge as a function of injected charge.

For injection at 50 MeV, the same computations give a limiting circulating beam intensity of  $6 \times 10^{13}$  protons for the field shapes expected at injection. In the study it has been assumed that those characteristics (such as number of injected turns) which affect injection efficiency would be kept as nearly as possible the same as with 15 MeV injection.

Nimrod is normally operated at an intensity of  $1 \times 10^{13}$  protons at the end of injection and this is just before serious space charge effects set in. Thus an increase in this value, at 50 MeV, to  $3-4 \times 10^{13}$  protons is realistic and it should be an operating level at which space charge effects are not too serious.

There is a marked saturation at  $3.5 \times 10^{12}$  protons, the normal operating level for Nimrod being at the point where saturation sets in, as shown. For all lower intensities a linear relationship is found between trapped and injected charge, corresponding to a trapping efficiency of about 33%. Theoretical calculations of trapping efficiency, ignoring space charge and using a simplified distribution of energy and betatron amplitudes, give a value of 29% - satisfactory agreement bearing in mind the limitations of the theoretical model. With the debuncher ramp in use, set up so as to inject protons with small betatron amplitudes, a trapping efficiency of 56% is measured, in good agreement with the theoretical value of 59%. Similar calculations for the case of 50 MeV injection, with enough energy spread to damp longitudinal instabilities (see below), give a trapping efficiency of 38%. It is concluded that the trapping efficiency will not be lower at 50 MeV than at present and that the trapped charge will increase by the same factor as the circulating charge.

*Longitudinal Space Charge Effects during Injection and Trapping* Longitudinal space charge effects during the injection process can lead to a bunching of the beam before the accelerating voltage is turned on. The instability can be damped if the circulating beam has sufficient energy spread, as is the case in Nimrod now.

It has been shown theoretically that the energy spread required to damp the instability, at a beam intensity of  $3-4 \times 10^{13}$  protons, is about  $\pm 300$  keV and that good trapping efficiency can be obtained in the normal r.f. bucket.

*Definition of  
50 MeV Beam  
Parameters*

The necessary phase space characteristics of the 50 MeV beam have been defined from the detailed studies described above. Comparison of these requirements with the present properties of the PLA and the 50 MeV CERN PS injector, to which the modified PLA would be very similar, show that they could be provided by the latter together with suitable matching arrangements for the radial and axial motion. To achieve the necessary circulating charge, a beam current of 75 mA with a pulse length of up to 500  $\mu$ s would be required.

*Beam Losses  
after Trapping*

Nimrod exhibits an unexplained beam loss, by a factor of about two, in the first 20 ms of the acceleration cycle. Similar attenuation is observed in other constant gradient synchrotrons. Measurements have been made of the attenuation as a function of beam intensity, using diluters and these show that the effect is independent of intensity. It is assumed that this beam loss will not be higher at 50 MeV.

*Coherent  
Resistive Wall  
Instability*

This is an intensity-dependent effect in which beam-induced charges on the synchrotron vacuum vessel walls react destructively on the beam. This effect is a problem with some accelerators and by appropriate beam steering can be induced in Nimrod now. The beam blow-up is controllable using a servo feed-back system; such a system is installed in Nimrod but is not required for operation at present intensities.

*Beam  
Size Effects*

Starting with a radial aperture full of 50 MeV protons the beam width would be greater than it is now at all energies during acceleration. Sufficient good field must be provided for this new condition.

The vertical and horizontal beam sizes in Nimrod have been measured non-destructively during injection and throughout acceleration using the ionisation systems (see page 55). The variation of beam width with time is shown in figure 41. The dimensions during injection are consistent with the theory of injection described on page 64, but the variations during acceleration are not those expected from simple damping theory. Initially the beam size decreases more rapidly than expected, thereafter it remains approximately constant or fluctuates with little or no overall damping. Experiments have shown that the latter effect may well be due to the  $Q_x = 2/3$  resonance and if this is so it can be removed using the pole face windings. It is planned to arrange these corrections for normal operation at present intensities. The useful aperture will then be sufficiently large to contain the beam resulting from 50 MeV injection.

The effect of the increased beam size on extraction efficiency using the present energy-loss target method has been studied using a computer model, the effect is negligible.

*Changes  
Required  
in the PLA*

The main changes in the performance of the PLA itself are the greatly increased beam current and greatly reduced duty cycle. A system to transport and match the PLA output beam to Nimrod will also be required. Some details of these changes are given below.

**Pre-injector.** To obtain the required current of 75mA at 50 MeV, the pre-injector would have to deliver a beam current of about 200mA in pulses up to 500  $\mu$ s long. This assumes a transmission efficiency of 40%, based on practical experience on the CERN linac. It is also assumed that the proton percentage in the beam will be at least as high as at CERN. Design figures of 250mA and pre-injector energy of 500 keV have been assumed; the estimated emittance valve at this energy is 2 cm-mrad (area of emittance diagram/ $\pi$ )

A prototype pre-injector has been constructed and is being tested. It consists of a duoplasmatron ion source mounted on a 28 cm long section of Van de Graaff accelerator tube operating at a potential gradient of 18kV/cm. External insulation is achieved by mounting the Van de Graaff tube between re-entrant conical flanges inside a 50 cm diameter, 100 cm long insulating tube as shown in figure 72. (Please see Engineering Division section, page 108). The space between the two tubes is filled with sulphur hexafluoride at a pressure of 2 atmospheres and the correct potential gradient is maintained by a spiral of carbon resistors wound round the outer tube. Computations show that if a 200 mA beam of radius 1cm can be extracted directly from the ion source with a waist at the top of the extraction electrode, then it will pass through the accelerating tube without much expansion due to space charge. It is expected that the 'emittance blow-up' effect which occurs in conventional pre-injectors will be absent in this device.

Preliminary tests with a high voltage power supply limited to 400kV have been very promising. With the accelerating tube shortened to maintain the correct potential gradient, 160  $\mu$ s beam pulses of 150 mA have been accelerated. The device is easy to condition and the sparking rate does not increase when the beam is present, provided the latter is efficiently collected and secondary electron emission suppressed.

Preliminary design of the low energy drift space has been carried out. Quadrupole focussing lenses of larger aperture than those used at present on the PLA will be required, though the total length of the drift space should not change much.

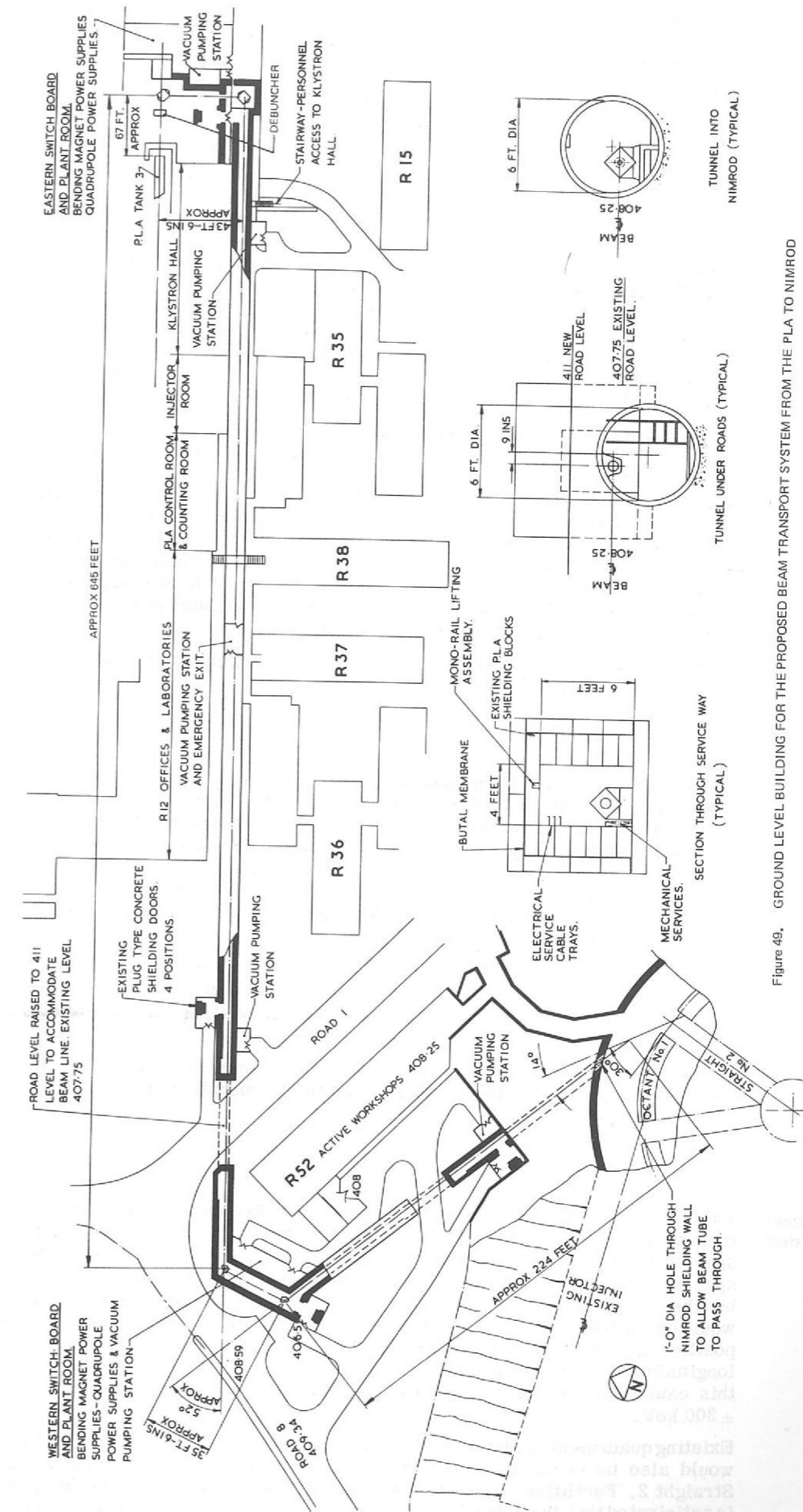


Figure 49. GROUND LEVEL BUILDING FOR THE PROPOSED BEAM TRANSPORT SYSTEM FROM THE PLA TO NIMROD

**PLA tanks.** The existing PLA tank 1 is grid focused and therefore exhibits a low beam transmission. Quadrupoles would be needed inside the drift tubes to achieve the intensities required for PLANIM. A design already existed for a new tank 1. This permitted much more control of the characteristics of the PLA beam than would be required for PLANIM. The alternative adopted for PLANIM is to copy, electro-magnetically, the first tank of the CERN-PS injector. Most of the existing tank 1 vacuum tank could then be used and the tools for shaping the drift tubes and quadrupoles are available for use. No changes are required to the structure of tanks 2 and 3.

It should be noted that the CERN-PS injector, which is virtually the same structure as that proposed here, operates at about 100 mA but with a shorter pulse length of 10  $\mu$ s.

**RF power.** The PLA runs now using five grounded-grid triode valves (GGT's) as final amplifiers to supply r.f. power to the tanks. For PLANIM the beam loading power would be about the same as that dissipated in the copper resonator, so the required peak r.f. output would be double the present operating level. However, because Nimrod pulses only once every two seconds the duty cycle required for PLANIM is less by a factor of about 100 than that obtaining now for the PLA at 50 Hz. Advantage has therefore been taken of this reduced mean power requirement to increase peak output through a modification of the GGT design.

A GGT r.f. power amplifier valve with an anode cavity manufactured to new dimensions has operated satisfactorily under test conditions for 1,000 hours at a power output level of 1.8 MW for 600 microseconds (the specified performance for PLANIM) pulse duration at 5 Hz. Two other valves having standard anode cavities modified to the new dimensions did not quite meet the above specification. This is attributed to mechanical details of the modification rather than a physical limitation of the valve and is a problem which can be solved. Six modified GGT's would provide the peak power required at the Nimrod repetition rate; 6 would be required as spares. The cost would be about one-third that of a new system based on commercially available valves. The lower level r.f. system and high power feeds to the tanks have been studied and solutions to the problems obtained.

A prototype modulator for driving the GGT's at the higher peak power and lower duty cycle has been tested and shown to be feasible in principle.

#### Location of PLA

Two possibilities have been considered: (a) leave the PLA in its present position and transport the beam some 280 m to Nimrod; or (b) move the PLA to a position alongside the present injector. The great attraction of (a) is that this scheme would cost about £100,000 less than (b) and would take only about 2 years to execute compared with 3 years for (b). Also, if the PLA were to be moved, the amount of refurbishing arising from the disturbance is very uncertain. Scheme (a) requires a novel beam transport system, but, as explained below, the beam could be transported without degradation of its properties. It is proposed therefore to leave the PLA where it is.

The tunnel for the beam transport system is shown in figure 49. After an initial drop in the level of the beam pipe at the output of the PLA, the tunnel level is at one height right through to Nimrod. The tunnel would be made mainly from existing concrete blocks to provide sufficient radiation shielding.

By injecting into Straight 2 of Nimrod, beam commissioning of the PLA and the transport system could proceed without interference to the operation of Nimrod with the 15 MeV injector which injects at Straight 1.

#### Beam Transport System

This has been studied in some detail and the problems resolved. The effects of aberrations in the various bending and focussing magnets have been shown to be small as have the effects of space charge on the transverse properties of the beam. A further problem of longitudinal space charge effects has also been resolved. In this latter case the space charge forces in the bunches of particles give rise to additional energy spread in the beam which, if uncorrected, would be unacceptably large for injection into Nimrod. The addition of a debuncher in a suitable position allows the energy spread to be decreased when the bunches have already spread out longitudinally. The space charge forces are then less and the increase in energy spread from this cause can be reduced so that the total energy spread is at the acceptable level of about  $\pm 300$  keV.

Existing quadrupoles, as used in the PLA experimental area, and two existing bending magnets would also be used. A three-element achromatic inflection system would be used to inject at Straight 2. Facilities would be provided for beam monitoring and for steering corrections. It is anticipated that there would be some computer-assisted control for setting-up and operation.

#### Nimrod Components

Before the detailed study started it had been shown that the Nimrod vacuum vessels would have a life of at least ten years for a four-fold increase in intensity. Residual activity levels had also been shown to be manageable. Further work has been done on other components prone to radiation damage, particularly the main magnet coil insulation and the pressure bags which support them. It is concluded that none of Nimrod's components would limit the useful lifetime of Nimrod after a four-fold intensity increase. The present installed accelerator building shielding would be sufficient for such intensities.

The main Nimrod r.f. system would have to supply additional power to the accelerated beam. Tests on the system show that the valves of the output stage would provide adequate power if a higher anode voltage supply were installed, but the driver stages would have to be replaced by higher power ones.

Preliminary calculations show that the graphite beam trimmers, at present installed on the outside of the vacuum vessel, would have to be made thicker. The graphite curtain on the inside wall of the vacuum vessel would probably still provide adequate protection with a 50 MeV injected beam, though it may have to be extended into Octant 4. Otherwise, little or no change would be required to Nimrod itself.

#### Controls

Controls have been arranged such that, after an initial shake-down period, the PLA and the injection system would be operated from the Nimrod main control room.

ON LINEAR  
R DIVISION



PROTON LINEAR  
ACCELERATOR DIVISION

# Proton Linear Accelerator Division

Division Head: W. D. Allen

Use of the PLA for nuclear physics experiments continued at a very high level in 1968. The machine was scheduled for over 7,500 hours of operation which is 1,000 hours more than in any previous year and is 87% of the total available time. The number of hours available for use was also a record 6836 hours giving an availability of 91% to be compared with 90% for the previous year. (See Table 1). The majority of faults on the machine were of a minor nature. A graph showing the availability of the PLA to experimenters since its commissioning in 1960 is shown in figure 50. Table 2 shows the distribution of hours between the nuclear physics teams using the machine.

In view of the impending closure of the machine in October 1969 there was no annual shutdown for major machine improvements during 1968 and this is reflected in the running time figures given above. The machine performance continued at a very high level however and the installation of a re-designed low energy drift space and of the debuncher which was completed towards the end of 1967 has been reflected in beams of high intensity and low energy spread throughout the year. Beams of mean intensity  $5 \mu\text{A}$  with energy spreads of 70 keV (f.w.h.h.) have been regularly available. The polarised proton source was used for about 4 months during the year and produced an average beam of  $1.2 \times 10^9$  protons/second with 50% polarization, giving an improvement in the  $\text{IP}^2$  "figure of merit" of about 25% on the previous years performance.

One major piece of nuclear physics equipment which has been commissioned during the year is a universal cryogenic scattering chamber. Apart from allowing the usual remote control of the target and of the angles of several detectors it also allows the detectors to be operated at any temperature between ambient and the boiling point of liquid nitrogen ( $-196^\circ\text{C}$ ). Operation at the lowest temperatures is required if the best energy resolution is to be obtained from semiconductor type detectors.

The programme of nuclear physics experiments has continued along the lines established in previous years with the emphasis on using the major facilities available on the PLA; the polarized proton source, the  $n=2$  double focussing spectrometer and the neutron time of flight apparatus.

The study of proton-deuteron scattering has been extended to measurements of the D and R parameters for 7 angles at 50 MeV. Measurements of the scattering and polarization of protons from  $\text{He}^3$  at 30 and 50 MeV and of protons from  $\text{He}^4$  at energies in 2 MeV steps from 40 to 50 MeV have been made. Reactions induced by protons in  $\text{He}^3$  and  $\text{He}^4$  which leave two nucleons in the final state have been studied to obtain more information about final state interactions. The neutron spectra from reactions on  $\text{He}^3$ ,  $\text{H}^3$  and  $\text{He}^4$  have been measured using the time of flight technique.

Measurements of the elastic and inelastic scattering of protons by heavier nuclei have been extended both to other targets and to wider angles and a great deal of information is now available. Further measurements have also been made of one and two nucleon pick-up reactions and the study of these reactions using polarized proton beams has continued. The work on (p, n) reactions has been extended to a range of p-shell nuclei.

All this work, together with the associated experimental techniques and theoretical studies are very fully described in the 1968 PLA Annual Progress Report (RHEL/R 170) which is freely available. To minimise duplication two experiments of particular interest will be described where visitors from overseas came to the laboratory for several months to use facilities available on the PLA which are not readily available elsewhere. Brief summaries of the remaining experiments then follow.

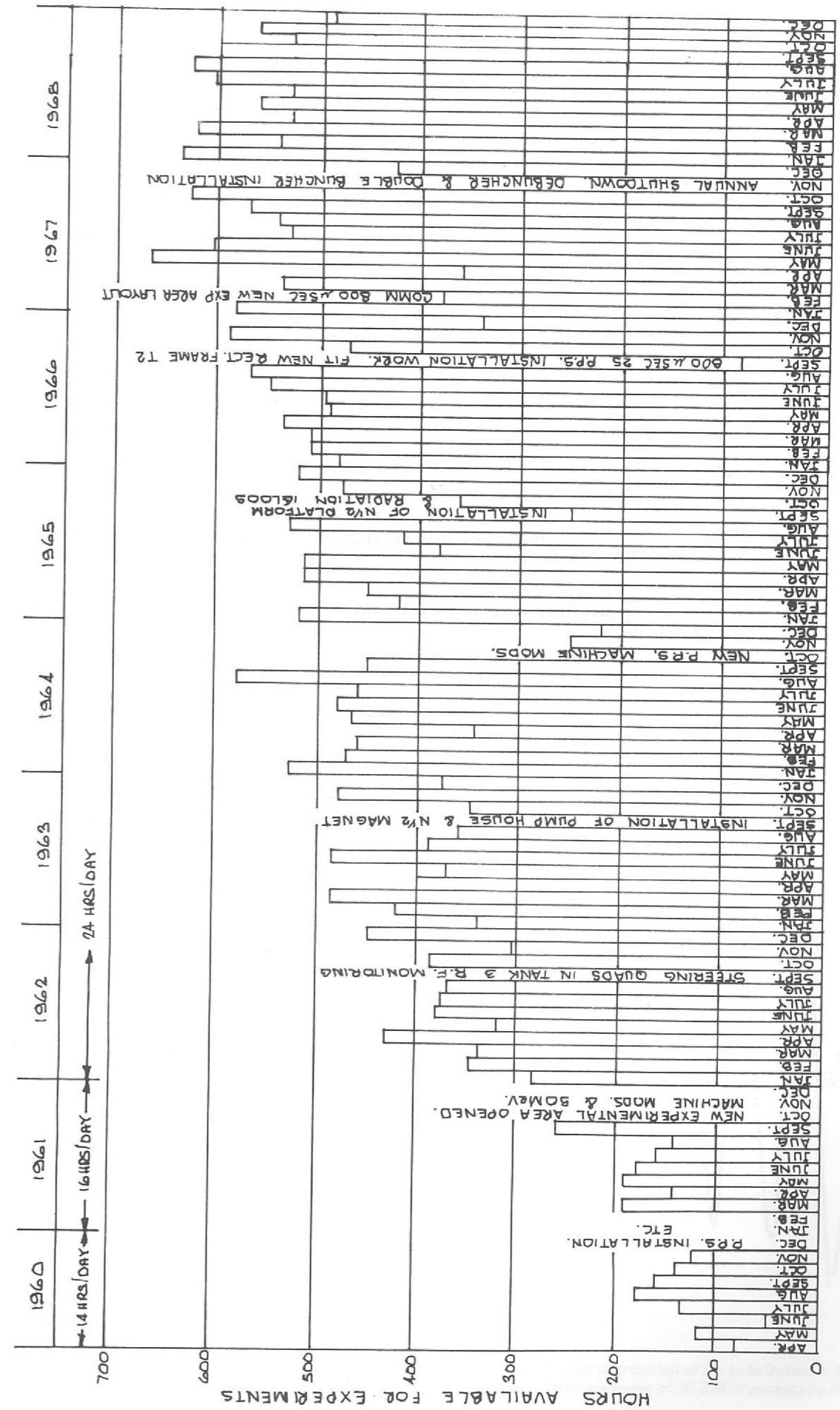


Figure 50. Availability of the PLA to experimenters since 1960.

## Experiments at the Proton Linear Accelerator

Number	Experiment	Group
1†	Precision Measurements of the Polarization in Elastic Scattering.	University of Minnesota, USA University of Birmingham
2	Stripping of H <sup>-</sup> Ions in a Magnetic Field.	TRIUMF project (Canada)
3†	Polarization in Elastic and Inelastic Scattering.	University of Birmingham
4†	Triple Scattering Parameters for Proton-Deuteron Elastic Scattering.	Queen Mary College, London Westfield College, London Queen's University, Belfast
5†*	Cross-Sections and Polarization for Elastic and Inelastic Scattering.	King's College, London West Ham College of Technology
6†*	Elastic and Inelastic Scattering of Protons.	University of Manchester
7†	Elastic Scattering of Protons from He <sup>4</sup> .	Rutherford Laboratory
8†	Elastic Scattering of Protons from He <sup>3</sup> .	Westfield College, London Queen's University, Belfast
9	Study of (p, n) Reactions using the Time-of-Flight Technique.	Rutherford Laboratory Queen Mary College, London
10	The Interaction of Protons with He <sup>3</sup> and He <sup>4</sup> .	Westfield College, London Queen's University, Belfast
11†	Asymmetries in Two Nucleon Pick-up Reactions.	University of Oxford Rutherford Laboratory
12 *	Pick-up Reactions.	University of Oxford Rutherford Laboratory
13 *	Investigation of the Levels of C <sup>12</sup> .	University of Oxford Rutherford Laboratory

† Experiments using polarized proton beam

\* Experiments using double focussing magnetic spectrometer

## Experiment 1

UNIVERSITY OF MINNESOTA, USA  
UNIVERSITY OF BIRMINGHAM

*Precision measurements of the polarization in elastic scattering*

For many years it has been usual to analyse data on the elastic scattering of nucleons by nuclei in terms of the optical model. Soon after the PLA came into operation it was realised that much more definitive analyses could be made if several experimental terms collaborated in measuring the cross-sections, polarization and reaction cross-sections for a range of selected nuclei. As a result of this work a very complete set of experimental data for these nuclei has been made available and several different analyses of these results have been made in terms of the optical model.

More recently a group under the direction of Professor G.W. Greenlees at the University of Minnesota, who had participated in the original polarization measurements at the PLA whilst at the University of Birmingham, proposed a reformulation of the optical model. In this model the real parts of the interaction potential are derived from the nuclear matter density distribution and the various components of the nucleon-nucleon force. This model was very successfully applied to the PLA data but it was found that improved polarization data was required to give a more stringent test of the model and to place further constraints on the model parameters. With the increased beams now available from the polarized proton source, measurements to an accuracy of 1% are possible. Professor Greenlees spent 5 months at the Rutherford Laboratory during 1968 collaborating with a group from the University of Birmingham in a precision measurement of the polarization in the elastic scattering of 30 MeV protons by Ni<sup>58</sup>, Sn<sup>120</sup> and Pb<sup>208</sup>.

The experimental arrangement was conventional with four detectors in use simultaneously. See figure 51. Two completely separate polarimeters were used to monitor the polarization of the incident beam. An example of the final results obtained is shown in figure 52. Over the majority of the angular range (20° to 120°) the results have an accuracy of better than 1% except at the backward angles (120° to 165°) where the accuracy is less than 2%.

Analyses of these results are now in progress using the new model. It is hoped that the new data will make it possible to specify more closely the relative contributions of the nuclear matter size and the range of the nucleon-nucleon force used.

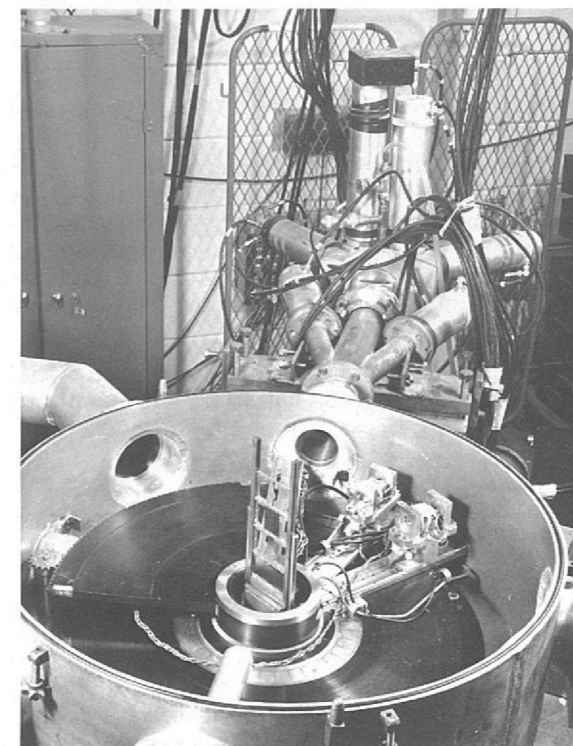


Figure 51. Scattering chamber used for the polarization measurements of Experiment 1.

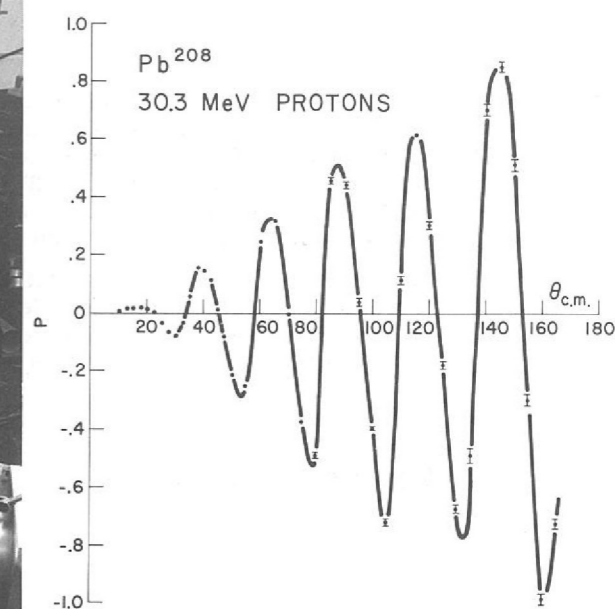


Figure 52. Angular distribution of the polarization in the elastic scattering of 30.3 MeV protons by Pb<sup>208</sup>.

## Experiment 2

TRIUMF PROJECT, CANADA

Stripping of  $H^-$  ions in a magnetic field

Four universities located in Western Canada have recently received approval for the construction of a 500 MeV variable energy cyclotron to be built at a site close to the University of British Columbia in Vancouver. For reasons which are now largely historical the project was named TRIUMF. The accelerator design utilizes negative hydrogen ions to achieve the variable energy feature and a 100% extraction efficiency.

Of critical importance in the design of the cyclotron magnet is the lifetime of  $H^-$  ions in a magnetic field. As the binding energy of the second electron in the ion is only 0.76 eV, the bond can be easily broken by the electric field which results from the motion of the ion in a magnetic field. However the predictions of various theoretical calculations are in some disagreement whilst experimental measurements, which do not entirely cover the region of interest, are rather inaccurate. As the successful extraction of the beam at optimum cost requires a better knowledge of the lifetime of  $H^-$  ions in a magnetic field, an experiment to measure this was carried out at the PLA by a group of Canadian visitors.

The beam of  $H^-$  ions was produced by gas exchange in a water vapour canal located in the injection column of the PLA. In this way an  $H^-$  beam of approximately  $10^5$  ions/sec was produced which was adequate for this experiment. It is believed that this is the first time  $H^-$  ions have been accelerated in a linear accelerator. The  $H^-$  ions were separated from the protons, which were also accelerated, by a bending magnet.

The stripping fields were provided by a Nimrod Type I bending magnet, loaned for the purpose, which with special pole tips gave magnetic fields of up to 23 kilogauss. The chamber inside the magnet was evacuated to about  $10^{-8}$  torr by means of 2 getter ion pumps to minimise stripping of the  $H^-$  ions by gas molecules. The general arrangement of the beam line and experimental apparatus is shown in figures 53 and 54.

The electrically stripped  $H^0$  particles were detected by an acoustic spark chamber system. The unstripped  $H^-$  ions were detected by fast scintillation counter telescopes. From the number of  $H^0$  particles detected the lifetime of the  $H^-$  ions in the magnetic field could be calculated and the results are given in figure 55. The results indicate that the  $H^-$  ion lifetime is down by a factor of 3 from that predicted by the theoretical curves. As a result the TRIUMF magnet needs to be somewhat larger than originally expected and the design has now been changed slightly in view of these measurements.

## Experiment 3

UNIVERSITY OF BIRMINGHAM

Polarization in Elastic and Inelastic Scattering

The work on the elastic scattering of protons by  $O^{18}$  to obtain information about resonant states in  $F^{17}$  has been extended. Excitation functions for six backward angles at 34 energies between 18.0 and 30.7 MeV have been measured and give evidence for resonances at 20.3 and 27 MeV and indications of structure at 21.6 and 23.4 MeV. The energy dependence of the polarization at  $160^\circ$  has been measured at 11 energies between 19.7 and 21.2 MeV and angular distributions measured for 5 energies between 19.7 and 21.9 MeV. Analysis of the data is in progress.

The measurements of the polarization in inelastic scattering of 30 MeV protons have been extended to larger angles for  $Fe^{56}$ ,  $Ni^{58}$  and  $Fe^{54}$ . The measurements on p-shell nuclei have also been continued. Theoretical analyses are in progress but so far the quantitative agreement between experiment and theory is poor.

## Experiment 4

QUEEN MARY COLLEGE, LONDON  
WESTFIELD COLLEGE, LONDON  
QUEEN'S UNIVERSITY, BELFAST

Triple Scattering Parameters for Proton-Deuteron Elastic Scattering (131)

Measurements of the triple scattering parameters for proton-deuteron scattering at 50 MeV have continued. The D and R parameters have been measured at seven angles between  $40^\circ$  and  $70^\circ$  to an accuracy of approximately  $\pm 0.15$  at each angle. An experiment to measure the A parameter is in preparation.

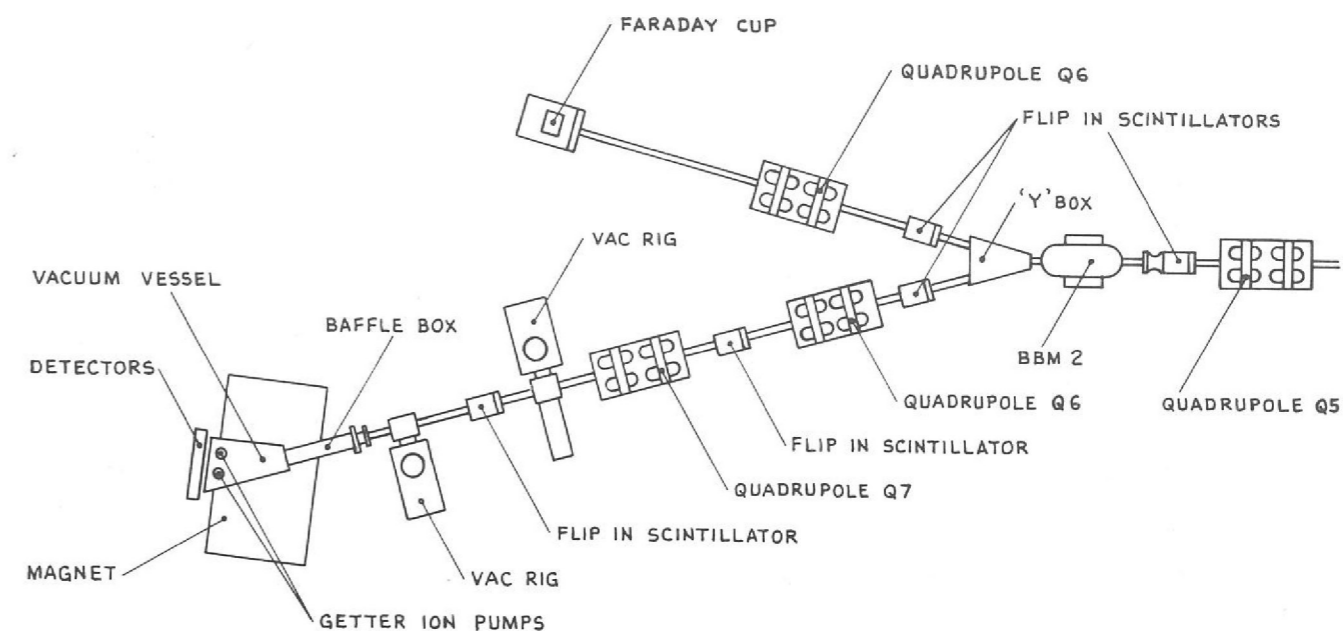


Figure 53. General arrangement of beam lines and apparatus for the TRIUMF experiment.

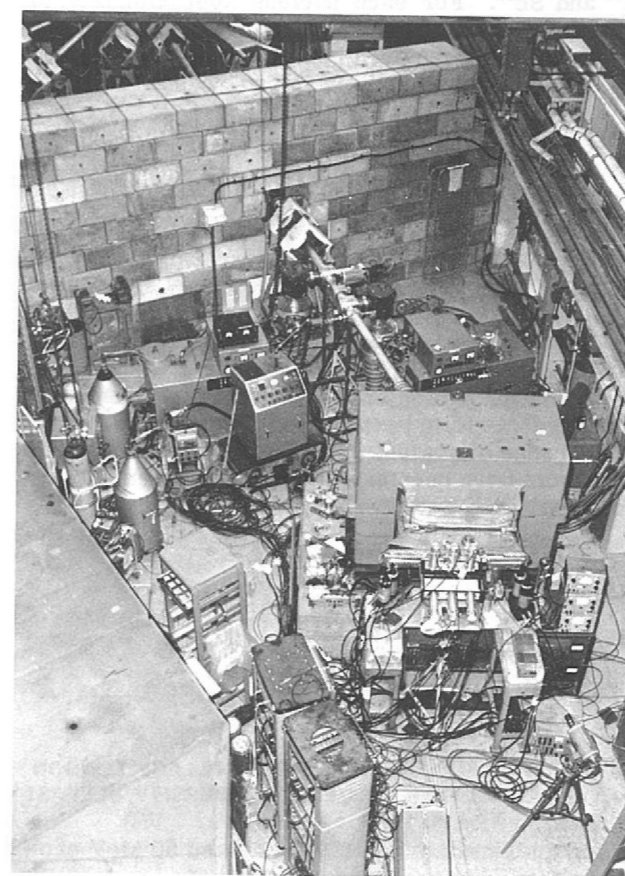


Figure 54. TRIUMF experiment. The  $H^-$  beam line enters through the shield wall and leads to the magnet, in front of which is located the detector array.

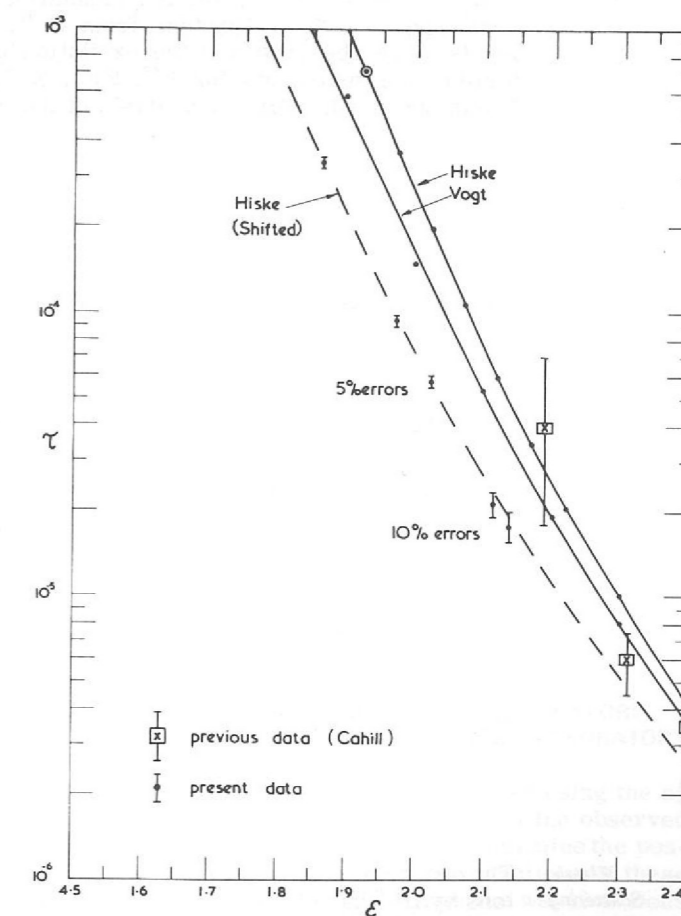


Figure 55. The lifetime of  $H^-$  ions as a function of the electric field.

## Experiment 5

KINGS COLLEGE, LONDON  
WEST HAM COLLEGE OF TECHNOLOGY

*Cross-Sections  
and Polarization  
for Elastic  
and Inelastic  
Scattering  
(108, 111, 132,  
143, 146)*

The work on polarization and cross-section measurements for pairs of isotopes has continued. Measurements have been made over a wide angular range for  $\text{Cu}^{63,65}$  at 30 and 50 MeV and for  $\text{Zn}^{64,66,68}$  at 30 MeV. Asymmetry data for elastic and inelastic scattering at 50 MeV from  $\text{Sm}^{148}$  has also been obtained.

Using a gas target the cross sections and polarization for elastic and inelastic scattering of 30 and 50 MeV protons from  $\text{Ar}^{40}$  has been measured. Optical model analyses of the elastic scattering data encounter similar difficulties to those found for  $\text{Ca}^{40}$  in this energy region. Satisfactory fits to the inelastic scattering results have been obtained using the strong coupling approximation.

The experiments to measure the large angle ( $124^\circ - 176^\circ$ ) scattering of protons have been continued using the technique described in last years Annual Report. Measurement for 50 MeV protons scattered by  $\text{C}^{12}$  and  $\text{O}^{16}$  show unexpected violent fluctuations in the polarization at backward angles. Cross-sections have been measured for Si,  $\text{Ca}^{40}$  and  $\text{Pb}^{208}$ .

## Experiment 6

UNIVERSITY OF MANCHESTER

*Elastic and  
Inelastic  
Scattering  
of Protons  
(117)*

Measurements of the polarization and cross-sections for elastic and inelastic scattering of 50 MeV protons from  $\text{Be}^9$  have been completed and microscopic analyses of this and other p-shell nuclei are in progress.

Polarization and cross section measurements have also been made for elastic and inelastic scattering of 50 MeV protons from  $\text{Ca}^{42}$ ,  $\text{Ca}^{44}$  and  $\text{Sc}^{45}$ . For each nucleus approximately 20 levels were observed and the excitation energies compared with those found in other work. Similar measurements for  $\text{Y}^{89}$ ,  $\text{Zr}^{91}$ ,  $\text{Zr}^{92}$ ,  $\text{Zr}^{94}$  and  $\text{Zr}^{96}$  have been completed and again many levels observed. Further analysis of this very large amount of data is in progress.

## Experiment 7

RUTHERFORD LABORATORY

*Elastic  
Scattering  
of Protons  
from  $\text{He}^4$   
(114, 128)*

To complete the programme of measurements of the polarization and differential cross-section of protons elastically scattered from  $\text{He}^4$ , measurements have been made in the range 30 to 40 MeV in approximately 2 MeV steps over a wide range of angles. The phase-shift analyses of elastic scattering data discussed in last years report have been extended to data taken earlier at this laboratory in the 25 to 29 MeV energy region.

## Experiment 8

WESTFIELD COLLEGE, LONDON  
QUEEN'S UNIVERSITY, BELFAST

*Elastic  
Scattering  
of Protons  
from  $\text{He}^3$   
(99)*

The differential cross-section and polarization for the elastic scattering of 30 and 50 MeV protons by  $\text{He}^3$  have been measured. Analysis of this data is in progress.

## Experiment 9

RUTHERFORD LABORATORY  
QUEEN MARY COLLEGE, LONDON

*Study of (p,n)  
Reactions  
using the  
Time-of-Flight  
Technique  
(90, 91, 92, 93,  
95, 139)*

The study of (p,n) reactions on p-shell nuclei has been extended and neutron spectra were measured from  $\text{Be}^9$ ,  $\text{B}^{10}$ ,  $\text{B}^{11}$  and  $\text{C}^{12}$  bombarded by 30 and 50 MeV protons. The data have been analysed in terms of a microscopic model and values for the effective isospin-dependent two body potentials obtained.

Neutron spectra have also been measured from  $\text{He}^3$  and  $\text{H}^3$  at 30 and 50 MeV and from  $\text{He}^4$  at 50 MeV. Broad resonances were observed and these have been compared with two and three body photo-reaction data. Further analysis and interpretation is in progress.

The results obtained previously at this laboratory on quasi-elastic (p,n) reactions have been shown to be in good agreement with the predictions of the reformulated optical model discussed earlier.

## Experiment 10

WESTFIELD COLLEGE, LONDON  
QUEEN'S UNIVERSITY, BELFAST

*The Interaction  
of Protons with  
 $\text{He}^3$  and  $\text{He}^4$*

The interaction of protons with  $\text{He}^3$  and  $\text{He}^4$  has been studied with particular reference to those reactions where there is a strong interaction between two particles in the final state. Energy spectra have been measured for the reactions  $\text{He}^3(p,d)2p$ ,  $\text{He}^4(p,t)2p$  and  $\text{He}^4(p,\text{He}^3)pn$  at 50 MeV and for  $\text{He}^3(p,d)2p$  at 30 MeV. The results have been compared with predictions of the usual Watson-Migdal type of theory and a modified version in which an attempt is made to include the interaction of the detected particle with the residual two-nucleon system.

## Experiment 11

UNIVERSITY OF OXFORD  
RUTHERFORD LABORATORY

*Asymmetries in  
Two Nucleon  
Pick-up  
Reactions  
(94, 145)*

The measurement of asymmetries produced by polarized protons in two nucleon transfer reactions to study spin-orbit effects has continued. The reaction  $\text{Si}^{28}(p,t)\text{Si}^{26}$  has been used to investigate the possibility that the predictions of the asymmetry from DWBA calculations are sensitive to the signs of the components of the nuclear wave functions. Measurements have also been made for the  $\text{N}^{14}(p,\text{He}^3)\text{C}^{12}$  reaction and analysis of the data is in progress.

## Experiment 12

UNIVERSITY OF OXFORD  
RUTHERFORD LABORATORY

*Pick-up  
Reactions  
(96)*

A large amount of information on (p,t) reactions on  $\text{Ni}^{58,60,62,64}$  has been obtained using the  $\frac{1}{2}$  spectrometer magnet. DWBA fits have been used to obtain the spins and parities of the observed levels. The (p,t) reactions on  $\text{Sr}^{88}$ ,  $\text{Sr}^{86}$  and  $\text{Y}^{89}$  have been investigated to determine the possible configuration mixing in a shell model description of the ground state wavefunctions of these nuclei. The  $\text{Ne}^{20}(p,t)\text{Ne}^{16}$  reaction has been studied to obtain information on the wavefunctions of the ground and low lying states in  $\text{Ne}^{18}$  and their analogues in  $\text{O}^{18}$ . In conjunction with these experiments the  $\text{Ne}^{20}(p,d)\text{Ne}^{19}$  reaction was also investigated to obtain further information about the excited states of mass 19 nuclei.



## Experiment 13

UNIVERSITY OF OXFORD  
RUTHERFORD LABORATORY

Investigation  
of the Levels  
of  $C^{12}$   
(130)

A previous experiment from this laboratory suggested that the 14.08 MeV level had spin  $2+$  although other work had suggested a spin of  $4+$ . The level has been investigated using the  $N^{14}(p, He^3)C^{12}$  reaction which was found to strongly excite the state and confirmed a spin  $4+$ . Experiments using the  $C^{13}(p, d)C^{12}$  reaction, which can only excite states of spin  $\leq 2+$ , showed that the 14.08 MeV level is not excited in this reaction. Further work is in progress to continue the study of high lying collective states in  $C^{12}$ .

## Engineering on the Proton Linear Accelerator

The period from 5 December 1967 to 5 December 1968 was the first full twelve months during which the PLA had run without any planned shutdown. The reliability of the machine was of the order of 91 per cent and the availability of the machine over the twelve months (except for four days at Christmas) was 86 per cent. Output currents of 5 microamperes of unpolarized protons with an energy spread of 40 keV were regularly available. The conspicuous feature of the year's running has been the steady reliability of the whole system and improved optimisation of machine performance. There were no major faults during this period. The grounded grid triode valves supplying r.f. to the tanks have run exceptionally well with some valves having run for 30,000 hours without faults. Two trial grounded grid triode valves with new thin anodes were manufactured to establish the maximum power output that could be achieved pulses per second; 2.3 MW was reliably obtained. The deuterium thyratrons switching the modulator power to the grounded grid triode valves also have been extremely reliable. These valves, (VX3336), have in certain instances run up to 20,000 hours without faults, switching nearly 1.3 MW of power at 50 Hz.

A considerable amount of effort in the past year has gone into the engineering side of the design study for the PLANIM project - that is, the proposal to make the PLA an injector for Nimrod. This work, together with accounts of the development of specialised items of nuclear physics apparatus is described in the section of this Report devoted to the Engineering work of the Laboratory. Due to the planned closure of the machine in October 1969, all the engineering effort on design and development has been redeployed on to high energy physics apparatus work, and the staff remaining on operations and maintenance is now at a minimum.

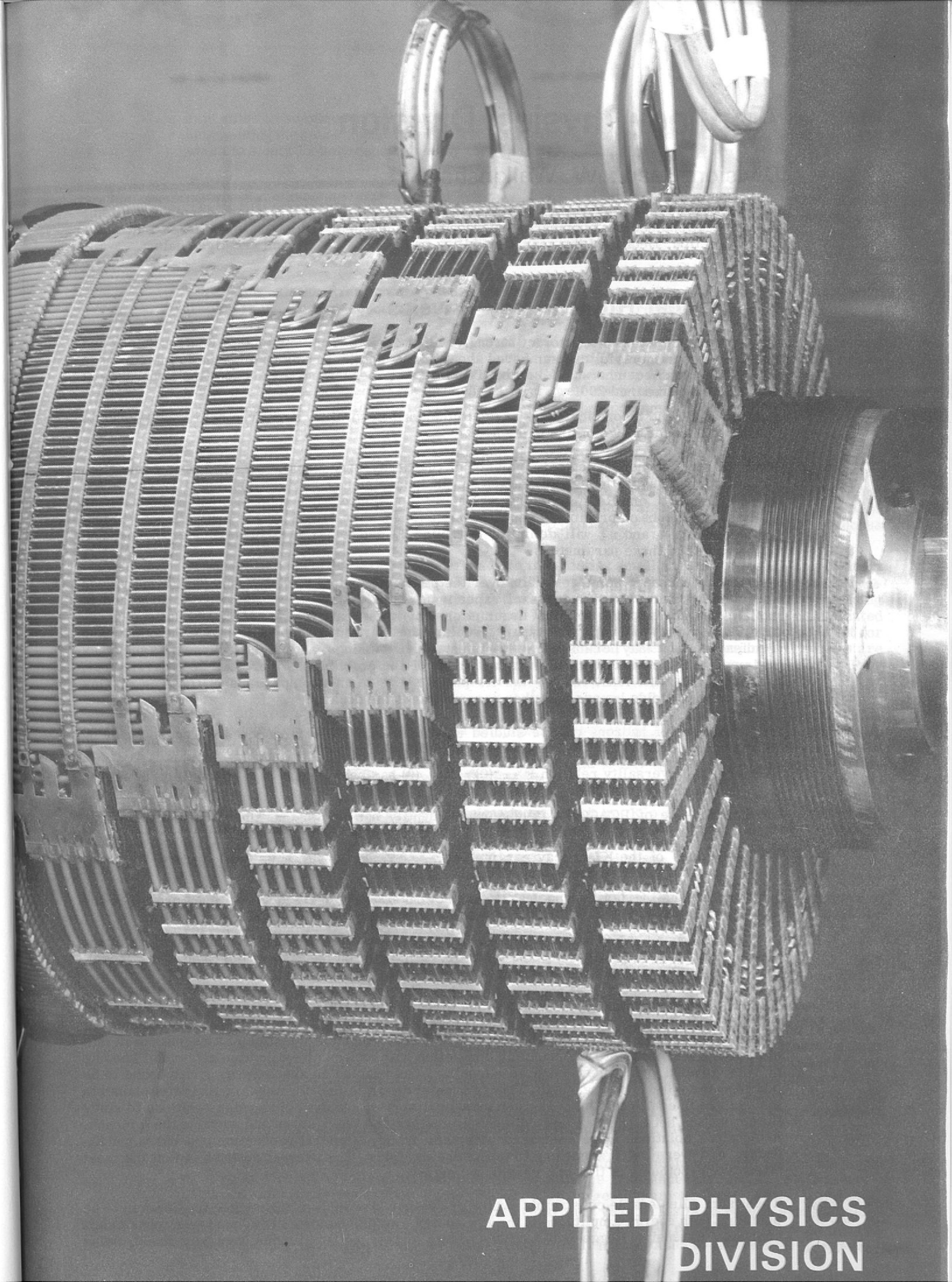
Table 1 - Running Time 1960-1968

	Hours scheduled	Hours available for use	Availability (%)
1960	1,420	980	69
1961	3,660	2,149	59
1962	5,544	3,971	72
1963	5,453	4,405	81
1964	5,573	4,664	84
1965	6,128	5,260	86
1966	6,303	5,605	89
1967	6,521	5,847 $\frac{1}{2}$	90
1968	7,553 $\frac{1}{4}$	6,836 $\frac{1}{2}$	91
	48,155 $\frac{1}{4}$	39,718	

Table 2 - Running Time 1968

Experimental Teams	Hours scheduled	Hours available for use
University of Birmingham	631	601 $\frac{3}{4}$
King's College, London	1,471 $\frac{1}{2}$	1,311
University of Manchester	1,321 $\frac{1}{2}$	1,165 $\frac{1}{2}$
University of Minnesota (USA) and University of Birmingham	674 $\frac{1}{2}$	610 $\frac{1}{2}$
University of Oxford	538 $\frac{1}{2}$	498
Queen's University, Belfast Westfield College, London, and Queen Mary College, London	1,086 $\frac{1}{2}$	1,033 $\frac{1}{4}$
Rutherford Laboratory and Queen Mary College, London (I)	694	589 $\frac{1}{4}$
Rutherford Laboratory and Queen Mary College, London (II)	456 $\frac{1}{2}$	436
Rutherford Laboratory (Nuclear Physics Tests)	86 $\frac{1}{2}$	75 $\frac{3}{4}$
Rutherford Laboratory (Accelerator Physics)	145 $\frac{1}{4}$	129 $\frac{3}{4}$
TRIUMF Project, Canada	216	187 $\frac{3}{4}$
Others	231 $\frac{1}{2}$	198
	7,553 $\frac{1}{4}$	6,836 $\frac{1}{2}$

PHYSICS  
DIVISION



APPLIED PHYSICS  
DIVISION

# Applied Physics Division

Division Head : W. Walkinshaw

The work of this Division covers the fields of theoretical high energy physics, computer systems and applications, bubble chambers, superconducting magnets, cyclotron ion sources and radiation protection. Details of the year's activities on each of these topics are given below.

## Theoretical High Energy Physics

The group has continued to interact strongly with theorists from many other centres. Long and short term summer visitors numbered about thirty, and there was once again an informal two and a half day December conference. Ten invited papers were given, and the attendance at some sessions reached 200.

Details of recent theoretical work at the Rutherford Laboratory are given below, and serve to illustrate the wide range of topics studied.

CP Violation  
(155, 156)

An extensive phenomenological analysis of the decay process  $K^0 \rightarrow 2\pi$  has been completed. Among other things, this study showed up an inconsistency between published values of the parameters  $|\eta_{00}|$  and  $\text{Re } \epsilon$ , a finding which was confirmed when more recent measurements of  $|\eta_{00}|$  cast doubt on previously reported values. Another result of the analysis showed that knowledge of  $\eta_{+-}$  and  $\eta_{00}$  will definitely establish T- and/or TCP- noninvariance, independent of the values of these parameters.

Semileptonic  
K decays  
(162)

There is at present some confusion over the parameter  $\xi$  in  $K_L^0$  decay, since different values are obtained from various types of experiment. Several hypotheses have been advanced to explain the discrepancy on the assumption that it is real. These include violations of T-invariance or of  $\mu$ -e universality, or a scalar admixture in the interaction. On the other hand the disagreement may be caused by experimental shortcomings, and might disappear as accuracy is improved. A dispersion relation treatment of the problem has therefore been carried out, using various trial functions for the  $K\pi$  phase shifts in an attempt to place limits on  $\xi$ . This approach also yields bounds for other parameters of the decay.

Form Factors  
(165, 166, 167)

The structure of hadrons can be studied either through the various decay processes, or by means of the form factors  $F(q^2)$ . The latter technique has yielded the following results

- (i) The universality relation  $F_{\pi\pi}^0(0) = F_{\pi\pi}^+(0)$  has been generalised to small  $q^2$  by means of field-current identity and a universality model.
- (ii) The use of PCAC and field-current identity has shown that the  $q^2$  dependence of the pion weak form factor is related to that of the pion charge form factor.
- (iii) Values of the  $K_L^0$  decay parameters  $\lambda_+$ ,  $\lambda_-$ , and  $\xi(0)$  have been derived from two models, and are consistent with existing data.
- (iv) The scaling law for nuclear form factors ( $G_p^N(q^2) \propto G_n^N(q^2)$ ) has been proved on the assumption that the Chou-Yang model for pp and pn elastic scattering is valid.
- (v) The  $\pi$ , K,  $\rho$  and  $\omega$  form factors have been calculated numerically, as functions of  $q^2$ , from  $\pi p \rightarrow \pi p$ ,  $Kp \rightarrow Kp$  and  $\gamma p \rightarrow (\rho, \omega) p$ , again on the basis of the Chou-Yang model. It has been shown that the process  $\gamma p \rightarrow \phi p$  is a crucial test for this model.

$\pi$ - $\pi$  Scattering  
(194, 203)

The  $\pi\pi$  S-wave  $I=0$  interaction, which is not directly accessible experimentally, is a subject of wide interest. It plays a role in several weak and electromagnetic decay processes, the current algebra predictions concerning the scattering length, and the question of a resonance in this state (the  $\sigma$  meson) is of importance in connection with hadron classification schemes. The use of very general principles, such as causality, has enabled an approximate lower bound to be placed on the  $I=0$  scattering length. This is a useful result in that a number of otherwise plausible models are in conflict with it. Another investigation used forward dispersion relations to study the connection between low energy dipion parameters and the position and width of the  $\sigma$  meson. Alternative solutions were compared with data from peripheral production processes and  $K_{e4}$  decay, and were rated according to theoretical criteria. The present position is that the most attractive hypothesis is that of a very broad sigma.

Finite Energy  
Sum Rules and  
 $\pi$ N Scattering  
(150, 151, 173, 188)

These sum rules enable constraints (which are rather simple in a Regge-pole framework) to be placed on high energy amplitudes if the low energy amplitudes have been found from phase shift analysis. Extensive Regge-pole analysis of high energy  $\pi N$  amplitudes have been made, using

Kaon-Nucleon  
Sum Rules and  
Regge Poles  
(153, 154, 193)

sum rules to supplement the scattering data. The sum rules have proved particularly helpful in determining the spin-dependence of P and P' exchanges, and the parameters of the  $\rho'$  singularity, which are only loosely constrained by the high energy data alone.

Finite energy sum rules were used to relate the following three regions of  $K^+p$  and  $K^-p$  scattering (i) the unphysical region, with  $\Lambda$  and  $\Sigma$  poles, (ii) the intermediate phase-shift-analysed region and (iii) the high energy Regge-pole-analysed region. The ensuing constraints indicated a preference for the larger (Kim) values of the  $\Lambda$  and  $\Sigma$  coupling constants, the non-resonant  $K^+p$  phase-shift solution and certain specific signs and magnitudes for Regge-pole spin-flip terms.

These sum rule constraints were used in making new Regge-pole fits to kaon-nucleon scattering, leading to predictions concerning  $K^\pm p$  polarization and of  $K^0$  regeneration in hydrogen.

Regge  
Absorption  
Model for  
 $\pi$ N Charge  
Exchange  
(199)

In this approach, absorptive corrections are added to pure Regge exchanges, thus combining desirable features of the two models. It may be regarded as specifying the Regge branch cuts, without new parameters, and was tested against the scattering data and finite energy sum rules for  $\pi^-p$  charge exchange. This process is fairly well described by a single  $\rho$  Regge pole, but the absorptive corrections give better agreement with experiment. In particular, the correct non-zero polarization is obtained and the fit to the sum rules is better.

Regge-pole  
Analysis of  
Vector Meson  
Production:  
 $\pi N \rightarrow \rho N$  and  
 $KN \rightarrow K^*N$   
(191, 192)

It is important to establish whether Regge poles can give a consistent representation of all high energy processes. Vector meson production, though one of the simpler reactions, contains a great deal of structure in its dependence on spin, isospin, s and t and forms a significant test for the Regge model. Analysis of this type of reaction may also shed more light on questions such as the possible conspiracy of the pion pole in  $\rho$  production, and the role of the Pomanchuk pole in  $K^*$  production.

Generally good detailed fits have been made to the existing small angle data, consisting of about 900 data points in the region 2-16 GeV/c. The decay density matrix elements favour "conspiratorial" solutions which are, however, inconsistent with factorisation and the corresponding Regge fits to  $\gamma + p \rightarrow \pi^+ + n$  and  $n + p \rightarrow p + n$ . This suggests the presence of more complicated Regge pole or cut contributions associated with the pion. The energy dependence of  $d\sigma/dt$  for  $K^\pm + p \rightarrow K^{*\pm} + p$  is a problem for the Regge-pole model, since the experimental results are not compatible with dominant contributions from the appropriate higher-lying trajectories P or P'; for a good fit, a trajectory with a low intercept,  $\alpha(0)$ , of about 0.2 is required.

Pion-Deuteron  
Scattering at  
High Energies  
(200)

Pion-deuteron scattering above 1 or 2 GeV/c is a sensitive test of the Glauber theory of the double scattering contribution. In the simplest approximation, the theory predicts a dip in  $d\sigma/dt$  near  $t = -0.4$  (GeV/c)<sup>2</sup> which is in conflict with experimental data. The inclusion of a real part plus spin-flip in the  $\pi N$  amplitude does not lead to full agreement. There is, however, excellent agreement when the D-state component of the deuteron wave function is included.

Recurring Dips  
in Differential  
Cross-Sections  
(149)

It has been suggested that recurring minima in  $d\sigma/dt$  for  $\pi p$ ,  $K^-p$  and  $\bar{p}p$  scattering contrasting with the virtual absence of minima in pp scattering may be due to an approximately cyclic residue structure of the P' and  $\omega$  Regge exchanges. This somewhat bizarre explanation fits the data quite well out to  $t = -4$  (GeV/c)<sup>2</sup>, at least in the  $\pi N$  case.

Electron Mass

A recent unpublished calculation of the effect of the cosmic background radiation on the mass of the electron modifies the result published by Power. The changes in energy level splittings are very much smaller than Power's estimates.

## Central Computer Systems

During the year 1968-69 the computers (the IBM System /360-75I and the Honeywell DDP-224) have operated for three shifts on weekdays, plus occasional, but increasingly frequent, single shifts at weekends. The number of jobs passing through the 360 per week has increased from 1800 to 2500, and the number of magnetic tapes held now exceeds 1000. Computer operators regularly run the HPD and CYCLOPS film-measuring machines, which are attached to the 360 via the DDP. The year has seen many changes and additions to the hardware of both machines, and to the system software. Figure 56 shows the system in block diagram form.

Hardware

The 360 now has a second card-reader, to act as a spare for the main one and to allow the input of special jobs at any time without interfering with the main input stream. A fourth 9-track magnetic tape drive has arrived, which should ease congestion among 2-tape jobs. A magnetic drum has been ordered, and will be installed early next year. This is to reduce system overheads during transitions from one job-step to another, but will pay off only when a selector sub-channel for the magnetic tapes is also fitted, permitting the tapes to be taken off the channel

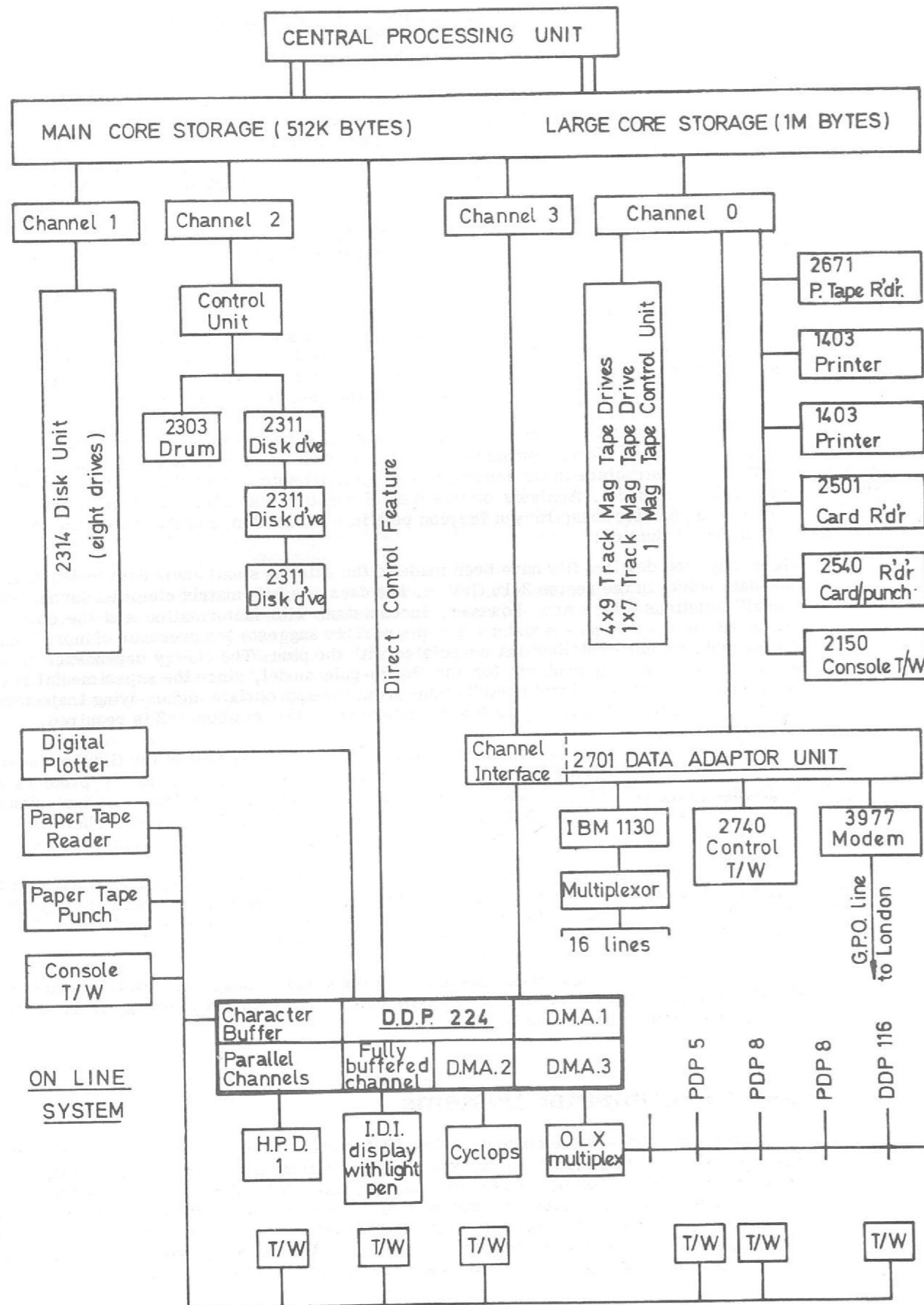


Figure 56. The Rutherford Laboratory Central Computer, IBM 360/75.

which is due to be shared by the drum and the IBM-2311 magnetic disc. Telecommunication hardware has also been installed to serve the link between the 360 and the INDRA project at the London Institute of Computer Science. A terminal adaptor now connects the 360 with the IBM-1130 computer which will control the activities of several rough-digitising machines.

On the DDP-224, the magnetic tape equipment has been removed and replaced by a third Direct Memory Access channel to give more efficient service to on-line experiments. A Fully Buffered Channel facilitates output to the Visual Display equipment which is now beginning to be used for the inspection of photographs which have already been scanned and stored. The facilities for the associated light-pen have also been improved. Changes to the several on-line typewriters have greatly increased the convenience of these both as input and output devices. The high-address 4096 words of core store are now of the same type as the remainder.

*Software* In the field of system software, the first half of the year was a period of consolidation during which users were disturbed as little as possible by reforms. User-routines continued to be developed for the DDP side of the on-line data-collection system DAEDALUS, and Fortran-usable routines were written to enable Rutherford programmers to use the Stromberg-Carlson graphic output equipment at the Atlas Laboratory.

During the second half of the year plans were made for exploiting the new IBM operating system MFT2. This was designed to give the possibility of running more than one stream of off-line jobs as well as the long-lasting on-line jobs which MFT1 allowed, although these too would benefit by improved scheduling methods. The DAEDALUS sub-system was reformed so as to be as nearly independent as possible of later changes to the operating system, and the overhaul has proved beneficial to all on-line applications. After testing, the MFT2 system was brought into use in October. Intensive use revealed many software faults, the diagnosis of which was made difficult by the fact that some of the new software employed hardware features not previously used. Much effort was devoted to overcoming problems, but at the same time thought was given to the best usage of the improved job-accounting information which was now available.

A software package which will give fast displays on the cathode-ray tube output device, and accept light pen input therefrom, is currently being checked out.

Planning is in progress to ensure the optimum use of the space that will become available when the 4-bay extension to Building R1 is completed.

## Computer Applications

*CRT Film Scanner (CYCLOPS)*

A fully operational routine system is now working with CYCLOPS (a device where the film is raster scanned by a flying spot from a CRT); Figure 57 is a general view of this device. The machine is currently measuring 35 mm film from a Nimrod experiment on the leptonic decays of neutral kaons (see Experiment 7, p. 19) and a Daresbury experiment (e-p scattering). So far some 150,000 events have been measured on the Nimrod experiment and 5,000 on the Daresbury one. The machine is on-line to the IBM 360/75 for upwards of 12 hours per day and measures at the rate of 400-600 events per hour.

*Spark Chamber Programs (211)*

A general program has been developed for finding tracks directly from CYCLOPS digitising. This program is now in a production state for the K13 experiment and is in the process of analysing the 150,000 measured events.

No prescanning information is required for this program but development is underway on a 'patch up' system to rescue good events which have failed in the analysis program. Using an interactive visual display an operator can give the program some help in identifying and associating tracks.

*HPD*

The rebuilt HPD1 machine shown in figure 58, is now fully operational and has been in production for much of the year. Measurements for the first experiment ( $K^+p$  interactions in the 80 cm Saclay chamber) have been completed. This involved over 30,000 two-prong events, and the results had the high accuracy expected of an HPD (2-4 microns on film). Measurements for the next experiment ( $p\bar{p}$  in the CERN 2-metre chamber) have started.

The HPD machine is also capable of measuring the bubble density of tracks. This measurement is, however, dependent on the quality of the film and the consistency of the operating conditions of the bubble chamber. Bubble density measurements were used in the first experiment but with only limited success, and work is in progress to produce more reliable results. A display under computer control is being developed, so that some failed tracks can be corrected with a light pen. Modifications to the filtering program, and tests of the "minimum guidance" system and of "track matching" which correlates stereoscopic views, are in progress.

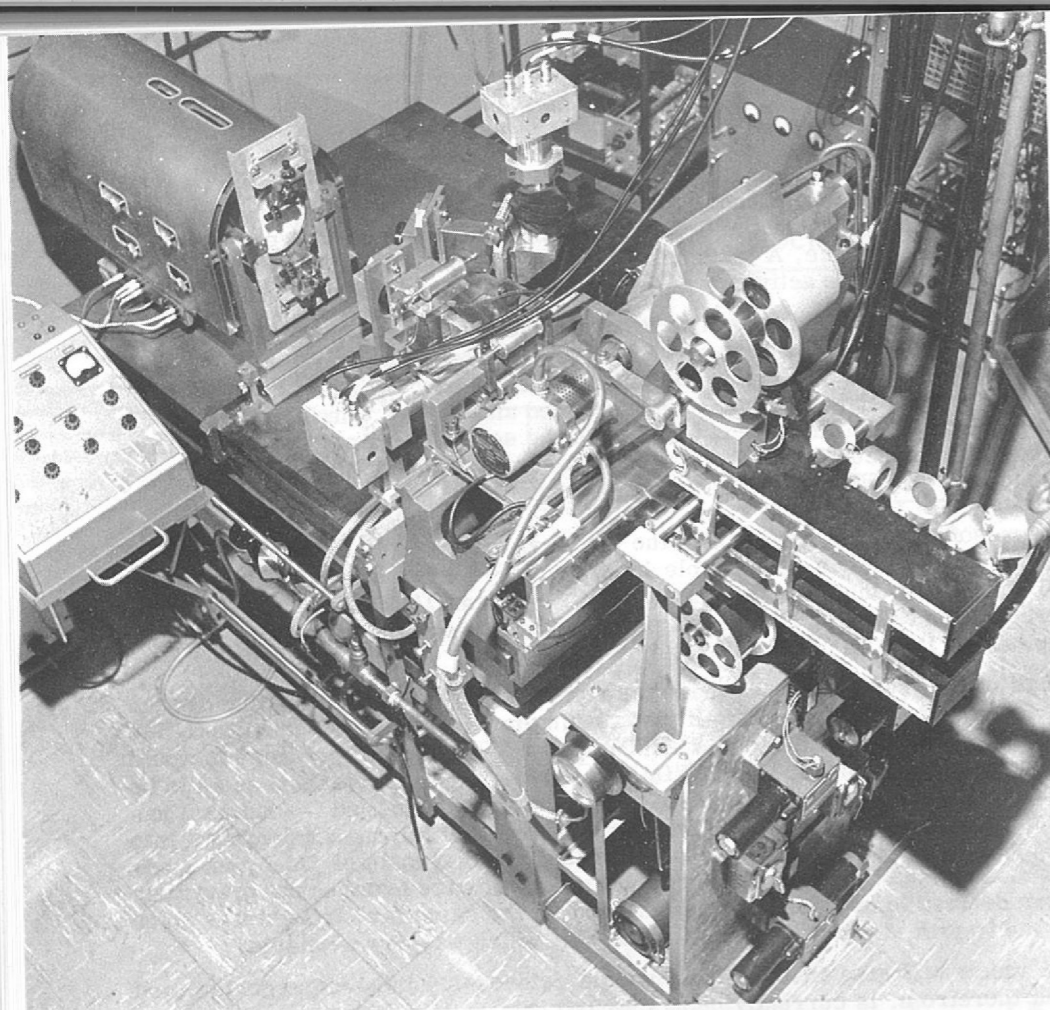


Figure 57.  
CRT Film Scanner (CYCLOPS)

*On-Line Rough  
Digitiser  
System*

The rough digitiser system is used to provide guidance measurements for the HPD film scanner. The measurements (accurate to 0.001 inch) which are obtained by scanners using co-ordinate measuring tables need to be checked for consistency before being stored on the disc store, of the IBM 360/75, and this is most conveniently done by working directly on-line with the computer.

An IBM 1130 computer with a 16K core store and disc storage was delivered to the Laboratory in April 1968. It is now connected to the IBM 360/75 via the 2701 data adaptor and a hardware interface built at the Rutherford Laboratory. A fifteen way input/output multiplexor has also been designed and commissioned in the Laboratory; six rough digitisers with their typewriters will be connected initially to this interface.

Programs for the system are in an advanced state and a preliminary evaluation of the system will be made using one of the rough digitisers.

## Bubble Chambers

*Helium  
Bubble Chamber  
(170)*

Following the completion of the first experiment of 750,000 pictures, no further runs were scheduled for this chamber during the year. A magnetic field survey to an overall accuracy of 0.1% required for the final analysis of results of this experiment has been carried out.

The camera modifications for double pulse operation with an interval between exposures of 400 milliseconds have been successfully tested on one camera and are now being applied to the others. The telecentric lenses were assembled in the lens plate of the chamber for photographic tests, after measurements on them had been carried out at Imperial College, London.

*Heavy Liquid  
Bubble Chamber*

The modifications to the building and bubble chamber to satisfy safety requirements for operation with propane were completed; the buildings are shown in figure 59, and figure 60 depicts the camera side of this chamber. In the first technical run, the whole system was tested using a filling of heavy freon  $\text{CF}_3\text{Br}$  operating at a temperature of  $30^\circ\text{C}$ , satisfactory operation being achieved. The filling was then changed to 57% freon  $\text{CF}_3\text{Br}$  and 43% propane for technical tests in preparation for the main experimental run, and good quality pictures were obtained at an operating temperature of  $40^\circ\text{C}$ . While the chamber was being cooled down to enable preparations for the data taking run to be completed, failures of the flash tube glass envelopes occurred. Despite these difficulties 340,000 pictures out of the required total of 600,000 had been taken by the end of the year.

The test programme on Grove expansion and recompression valves, started last year, has paid dividends in the reliable operation and long life obtained during the experimental run, while the modifications to the camera cassettes introduced to reduce the effort involved in changing films have improved the operational efficiency. The picture quality and operational efficiency are now very satisfactory and no problems should arise in completing this experiment when further data taking time becomes available.

*Hydrogen  
Bubble Chamber  
(214, 219)*

Data taking runs commenced at the beginning of the year but the alternator failure on Nimrod limited operation to a low repetition rate. By the start of the summer shut down over 500,000 pictures of acceptable quality had, however, been taken.

During the shut-down the chamber was prepared for the Cambridge hyperon experiment, involving the use of uranium collimation in the vacuum tank in addition to the assembly of the pulsed magnet in the steel yoke of the chamber magnet. At the same time a liquid dump system was installed to allow rapid emptying of the chamber into a cooled reservoir. Difficulties were experienced in commissioning this system and its use had to be postponed to a later date. The failure of a compressor motor and breakdown of the pulsed magnet made it necessary to delay the start of this experiment.

The chamber has now been prepared for data taking experiments and the new set of condenser lenses has been coated, assembled and fitted in the hydrogen shield. Modifications to the cooling system for the liquid dump reservoir have been made which have resulted in better refrigeration control than with the earlier circuit. The chamber is now data taking at the full Nimrod repetition rate with a hydrogen filling and preparations are complete for continuing with a technical run using deuterium in the bubble chamber early in 1969. Excellent picture quality is now being obtained and the chamber is operating with good reliability.

Future experiments require the use of a hydrogen or deuterium target operating within the chamber which will contain a mixture of neon and hydrogen. This programme is being carried out in collaboration with CERN who will be responsible for the target design and manufacture. Additional fittings and controls are being made to allow the system to be tried out in a technical run in the spring of 1969.

The identification of particles by recording on the film is now available for experiments requiring this facility. It has also been established that satisfactory quality is obtained using reversal

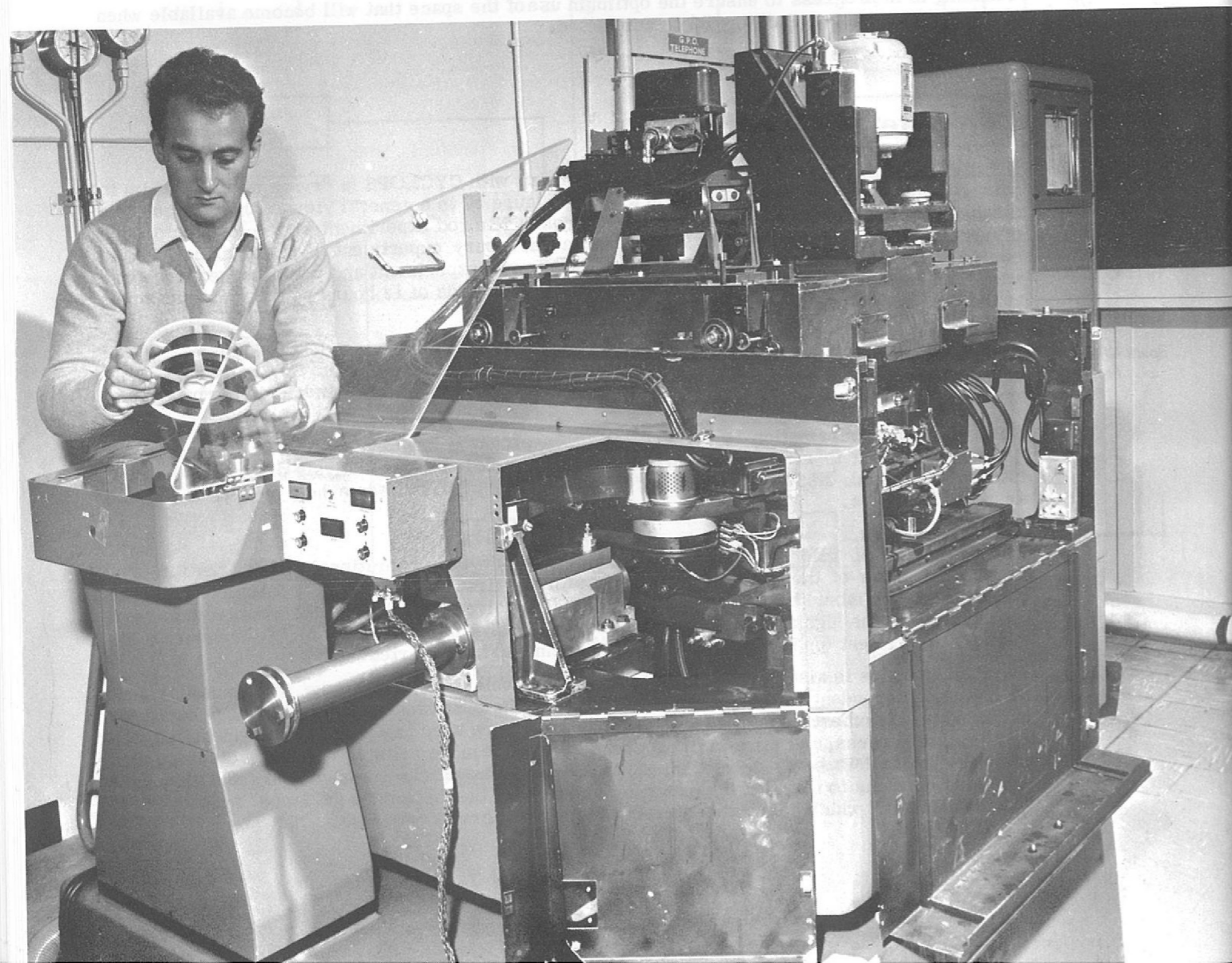


Figure 58.  
Automatic film measuring machine HPDI.



Figure 59. Heavy Liquid Bubble Chamber Building modified for use with propane — showing separate control room, expanded polystyrene frangible walls and extract ventilation plant.

*High Field  
Bubble Chamber  
(184, 217)*

development of the standard Ilford track chamber film, so as to give the white tracks on black background preferred by the track analysis machines. The improvement in the optical alignment in the chamber produced pictures with better contrast than previously.

Work on the design of the liquid phase expansion system using four pistons is being finalised and a proposal has been prepared giving costs and effort involved. The conversion is estimated to take six months and would result in faster, more reliable and more flexible operation of the chamber.

Future bubble chambers will employ some form of computer for data logging and control and a pilot scheme has been prepared based on the hydrogen chamber. It would be used initially for data logging, following which control problems of progressive complexity could be investigated.

A detailed account of the work carried out on the Research and Development programme for the High Field Bubble Chamber during 1967 was published in January. This year effort has been concentrated mainly on the three parts of the chamber which are of prime importance for the achievement of the specified operational characteristics; the magnet, the expansion system and the optics. A general arrangement of the proposed High Field Bubble Chamber is shown in figure 61.

The trial winding tests on a full size magnet coil started in collaboration with H9 workshop, AERE, have been satisfactorily completed using copper conductor  $50 \times 3\text{mm}$  and stainless steel support strips of the same total cross section. It is not envisaged that any serious problems will arise in winding superconducting coils using this technique.

Samples of stabilised superconductor have been manufactured by IMI through our research contract and tested here. In addition, measurements at highfields have been made using the RRE Malvern test facility. Conductor of selected design has now been supplied in sufficient quantity to allow one section of a small coil to be wound for tests relevant to the design and operation of the full size coils. Six sections will be required for the complete test assembly (called RACOON) and the overall dimensions will be length 655mm, bore 135mm and outside diameter 305mm. The conductor is designed to carry 7500A in a cross section of  $50 \times 3\text{mm}$  at a field of 80 kilogauss (8 Tesla). Initial tests at 2.6 Tesla will be made here and further tests in BRARACOURCIX, the CERN test facility, should enable 8.0 Tesla to be reached.

During the tests with flat strip conductors on the variation of the current carrying capacity with the direction of the magnetic field, it was found that the degree of anisotropy depended upon the manufacturing processes used in producing the strip. As expected, it was highest for rectangular cross sections having large ratios of width to thickness, but it also increased with field, usually reaching a maximum in a field of about 5 Tesla.

Some interesting results have been obtained by measuring the magnetisation set up in the flat strip superconductor used in the RACOON coil. One section of the coil was placed in a cryostat inside a conventional bubble chamber magnet. The decay of the magnetisation field within the conductor was measured for different orientations and magnitudes of the applied field. Theoretical estimates of the time constants involved agree well with the measured values and indicate the importance of twisting the superconducting filaments within the strip.

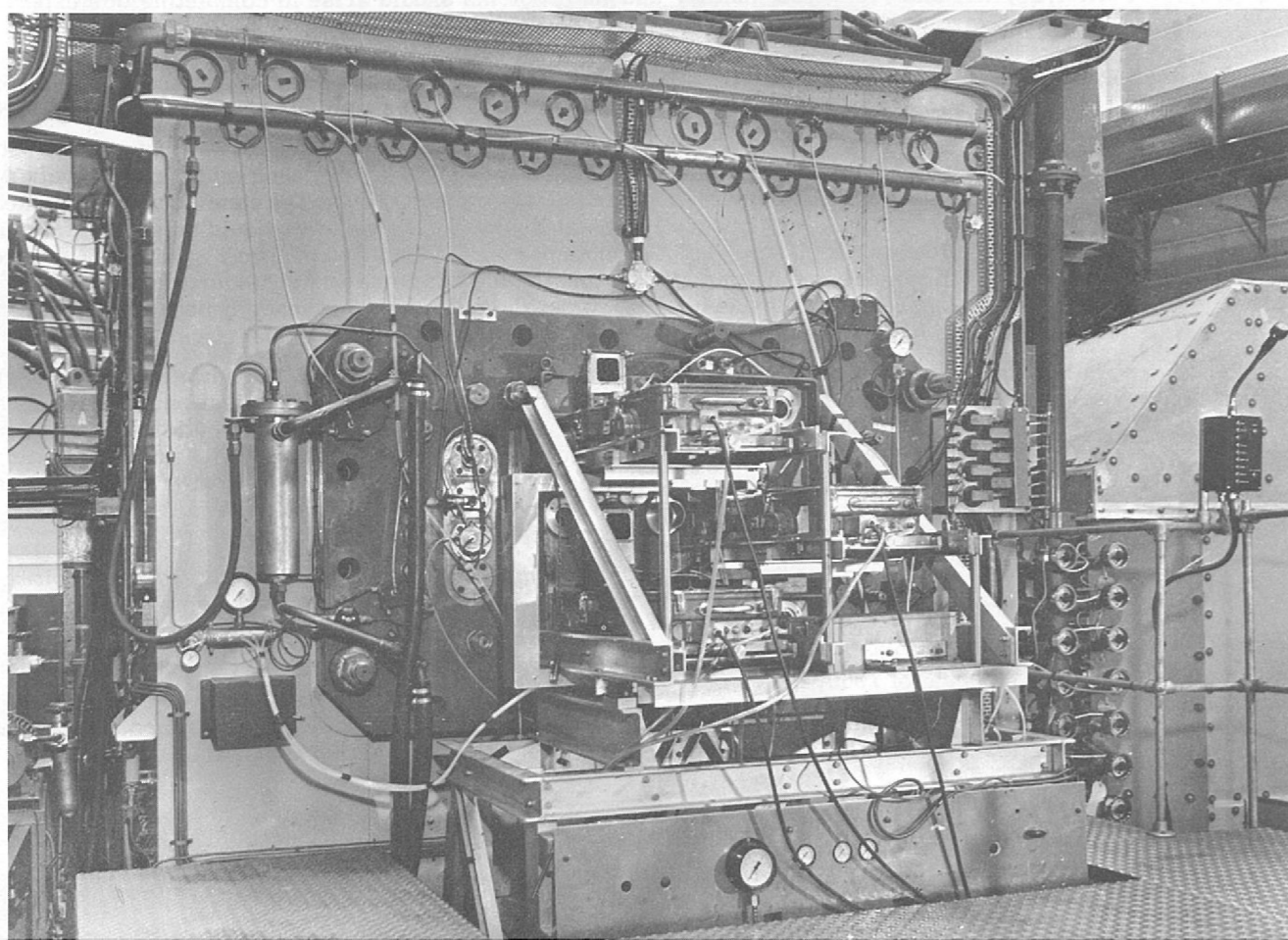
Because of the very high magnetic field used with this chamber, eddy current heating induced in any moving parts in contact with the chamber liquid must be reduced to a minimum. The use of epoxy resin bonded fibre glass as a material for such components has therefore been studied. So far, the effort has been concentrated on the component used to seal the expansion piston to the body of the chamber, which takes the form of a single omega bellows. Very encouraging results have been obtained in the life tests on one-fifth scale models of such bellows using the rig depicted in figure 62. Over 10 million expansions were completed at room temperature with full pressure cycling conditions and further tests at constant pressure and at liquid nitrogen temperature are currently in progress. Fatigue tests on small samples of the material used have already indicated that a substantial improvement in fatigue properties should occur at the lower temperature.

To meet the requirement for fast cycling a resonant expansion system in which the pressure cycle is sinusoidal and initiated by releasing a latching mechanism has been studied. A system using a friction clutch has been manufactured and has now operated for a long period in a test rig with very promising results, fuller details of which are given in the Engineering Report, page 103. On the basis of these tests a full size assembly allowing single or multiple expansion cycles in a resonant system seems feasible.

Most bubble chambers now under construction employ a bright field optical system based on the use of Scotchlite as a retrodirector. It would be advantageous in this chamber to use a dark field system as this should require a smaller bubble size. Experiments on Scotchlite have therefore been made in the 10 inch bubble chamber test facility to determine the scattering function.

Results show however that a dark field system is unlikely to be acceptable with the Scotchlite at present used in the bright field chambers. Alternatives to Scotchlite for a dark field system are now being investigated.

Figure 60. Camera side of the Heavy Liquid Bubble Chamber installation.



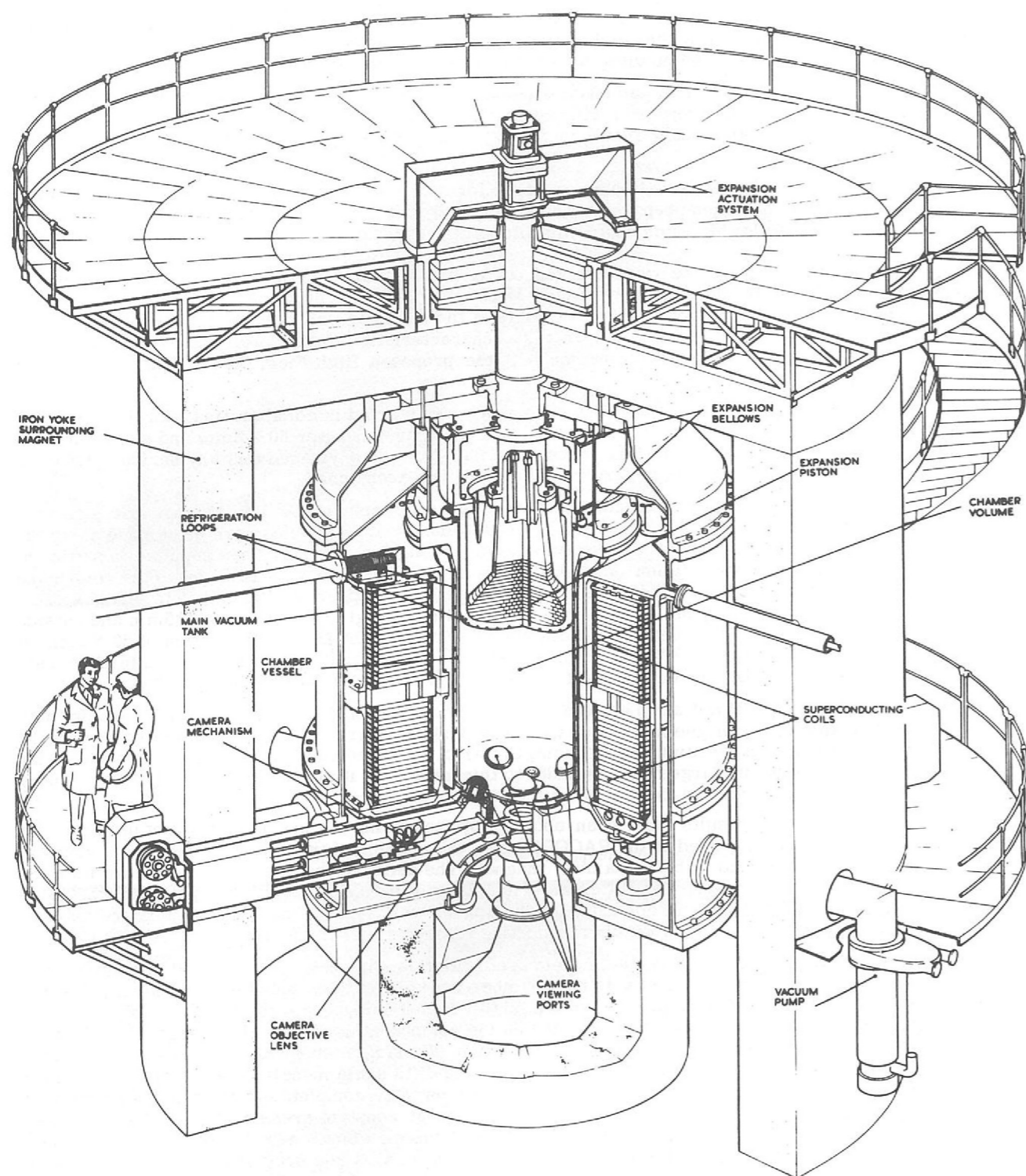


Figure 61. General arrangement of proposed High Field Bubble Chamber.

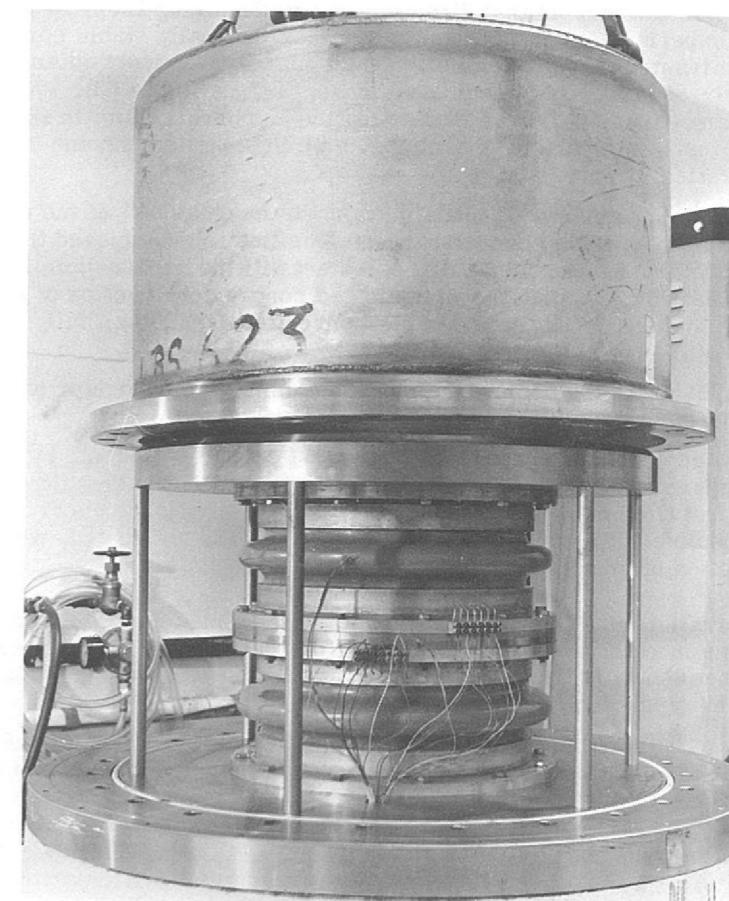


Figure 62. Test rig for omega bellows intended for use in the expansion system of the HFBC.

Large bubble chambers are driven to the use of fish-eye optics using wide angle lenses since large windows are impracticable for these dimensions. This chamber at 1.5m diameter would require about the largest window that could be manufactured to the required optical tolerances. Work has so far been concentrated on the problems associated with fish-eye optics, and the components for a trial fish-eye window assembly have now been manufactured. The system is now being assembled for test in the 10 inch bubble chamber. In conjunction with the Optics Department at Imperial College the manufacturing and assembly tolerances for the windows of the bubble chamber have been assessed.

With the emphasis now being on the use of the bubble chamber at CERN or on the 300 GeV accelerator, alternative schemes for housing the chamber for technical runs at the Rutherford Laboratory have been prepared. By utilising the present experimental areas as much as possible the amount of building work required has been considerably reduced. In addition, the installation is being arranged to allow the transportation to another site of items such as cranes and the ventilation and cooling equipment.

## Superconducting Magnets

**Objectives** Superconducting magnets provide high magnetic fields with negligible power consumption. They offer both economic and practical advantages over conventional magnets, and are likely to be used extensively in high energy physics in the future. The use of such magnets in bubble chambers is already assured. Economic and reliable designs for large scale use in beam handling systems have yet to be demonstrated, though the way seems clear to realizing them; more speculative is the application to synchrotrons, though a promising start has been made in the development of a conductor suitable for pulsed applications.

The work in this group is based on the recognition that, in order to achieve the full economic and practical gains, it is necessary to develop designs which have a simplicity and reliability comparable to those of conventional magnets.

*Filamentary  
Conductors  
(182)*

A major advance in this direction was made during 1968, by the development (in collaboration with Imperial Metal Industries) of a new intrinsically stable composite conductor. This consists of a twisted array of fine superconducting filaments (diameter 0.003 inch) embedded in a matrix of supporting metal, usually copper (see figure 63). This is theoretically free from flux jumping (the prime cause of degradation and unreliability in superconducting alloys) and extensive tests on a variety of samples, both in short lengths and in small coils, amply confirm the theoretical predictions.

Such a conductor can be made in which as much as 50% of the cross-section is superconductor, allowing much higher overall current densities to be achieved than with conventionally stabilised composites. Furthermore, direct contact with the liquid helium is no longer necessary to achieve stabilisation, so that the complicated porous construction of stabilised coils can be dispensed with, and replaced by a simple conventional winding, fully insulated, and impregnated for strength.

The design of the prototype quadrupole using this conductor has been initiated, and will incorporate many simplified engineering techniques.

*Pulsed Magnets*

A second important property of this type of conductor is that, by incorporating a matrix material of higher resistivity (such as cupro-nickel), and increasing the twist rate, the a.c. loss can for the first time be reduced sufficiently for use in pulsed synchrotron magnets. Sample quantities of possible a.c. conductors are now being made and tested, with a view to the subsequent construction of prototype pulsed magnets.

*Stabilised  
Magnets  
(183, 185, 218)*

In parallel with the preceding studies, a number of stabilised magnets have been constructed for engineering and operational experience. The largest of these is the 40 kG, 2m long bending magnet shown in figure 64. The winding has now been completed and first tests on the whole assembly are expected in April, 1969.

A 40 kG 10 inch bore solenoid shown in figure 65 was also completed and was used in conjunction with a 20 inch cryostat for energy extraction experiments and for simulation of several other emergency situations.

*Other Work  
(180, 181, 210)*

The Group has collaborated with the High Field Bubble Chamber Group on several aspects of the design of the proposed 70 kG 2m bore magnet, in particular the study of the adverse effects of magnetisation currents induced in the wide strip conductor.

Theoretical studies have continued on the economic and practical aspects of superconducting proton synchrotrons, and optimised separated function lattices have been computed for a number of typical high energy machines, including possible schemes for the future conversion or extension of Nimrod.

In addition, the design study was completed for a spark chamber magnet employing a Helmholtz pair of superconducting coils to provide a large volume 2m dia. by 2m high of roughly uniform 20kG field with good experimental access. The design is based on conventionally stabilised Nb-Ti composite conductor of roughly square section (1 cm<sup>2</sup>) wound in concentric layers. As in all two coil magnets of this type special care has to be given to the problem of holding the coils apart against the large attractive forces without incurring too large a heat inleak.

## Variable Energy Cyclotron

Although this machine is now operated by AERE, the Rutherford Laboratory has contributed to the continuing development of the ion source, and has designed an axial injector system for installation early in 1969.

*Ion Source  
Development*

The cyclotron operated steadily throughout the year; over 50 settings, covering a wide range of ions and energies have now been used. With the high power source in operation 2  $\mu$ A of 150 MeV N<sup>5+</sup> ions have been extracted; carbon and oxygen ions are also in regular use. The acceleration and extraction of 0.08  $\mu$ A of 175 MeV C<sup>5+</sup> was particularly encouraging. Some development work on the ion source is still continuing in the Laboratory and a duoplasmatron source is being investigated for multiply charged heavy ion production.

*Axial Injector*

The design of the injector has been completed and most of the components are manufactured ready for installation on the cyclotron in April 1969.

Orbit studies on the computer agreed fairly well with experiments on the model cyclotron for acceleration at the fundamental of the r.f. frequency, but orbits for high harmonics were difficult to calculate with any accuracy. However the work on the model cyclotron shows that good acceleration is possible on high harmonics, and beam has been detected up to the 13th harmonic. Experiments on axial injection in the model cyclotron have been simulated using a positively

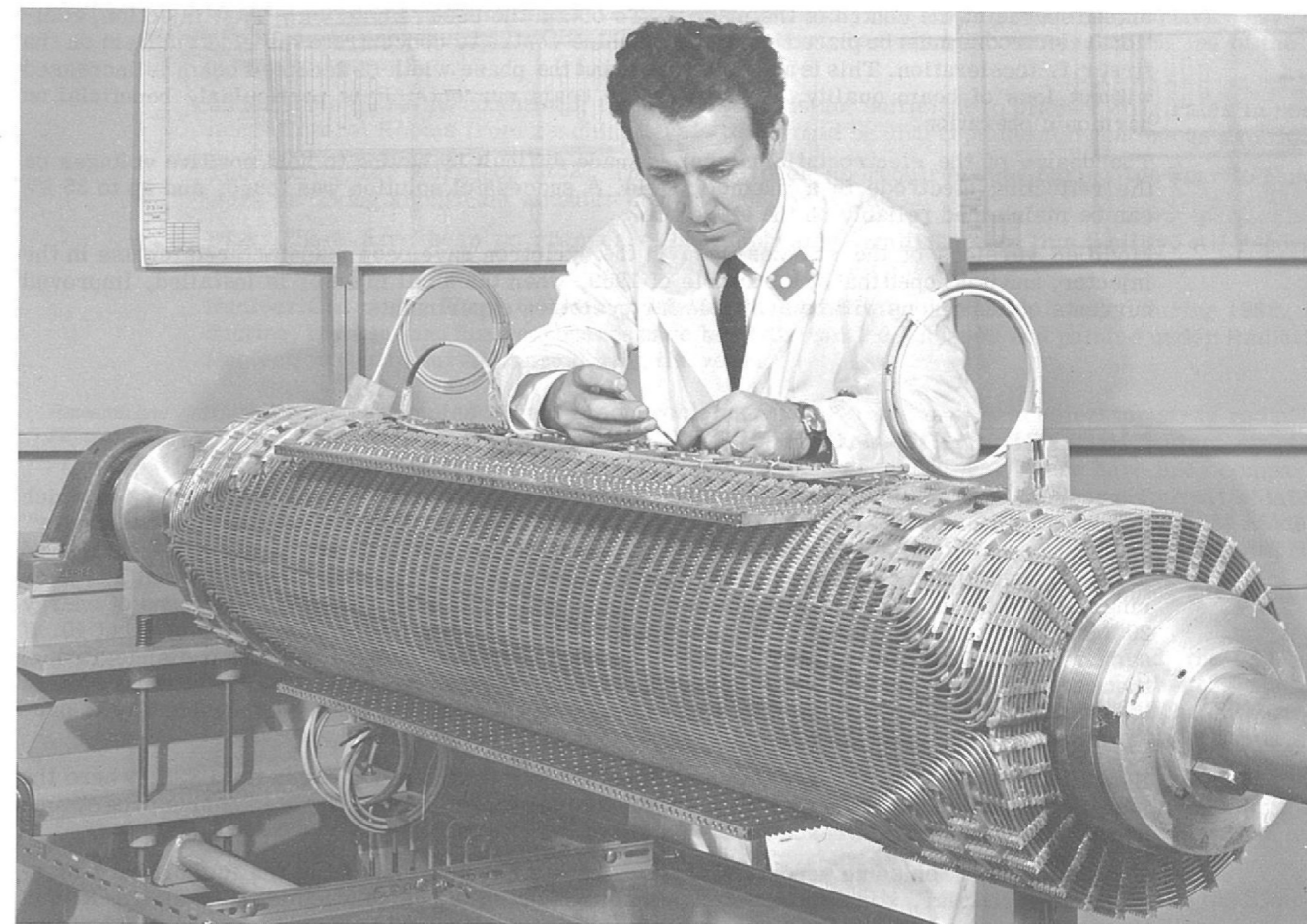


Figure 64. Assembling the Superconducting Magnet Coil.

Figure 65. A 40 kG 10 inch bore solenoid.

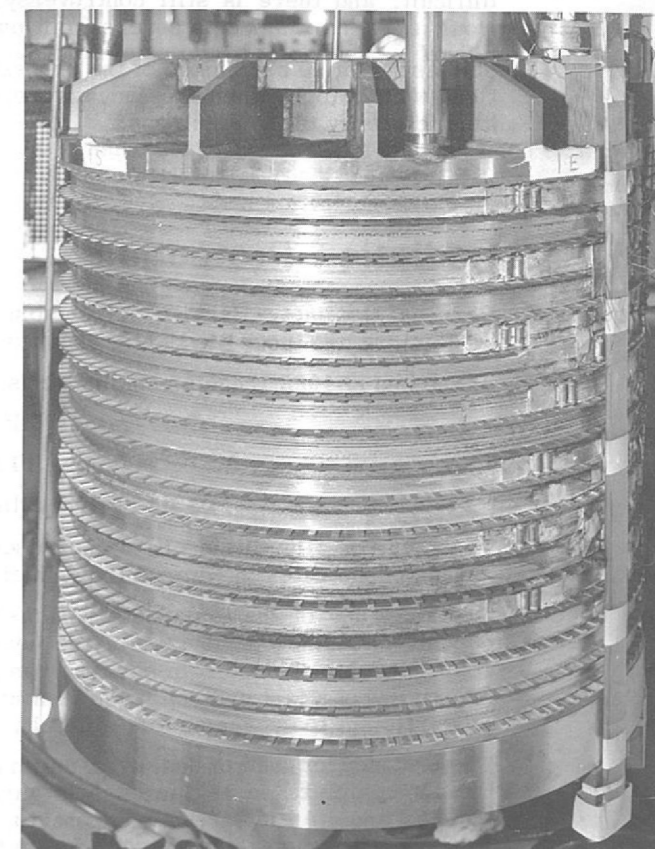
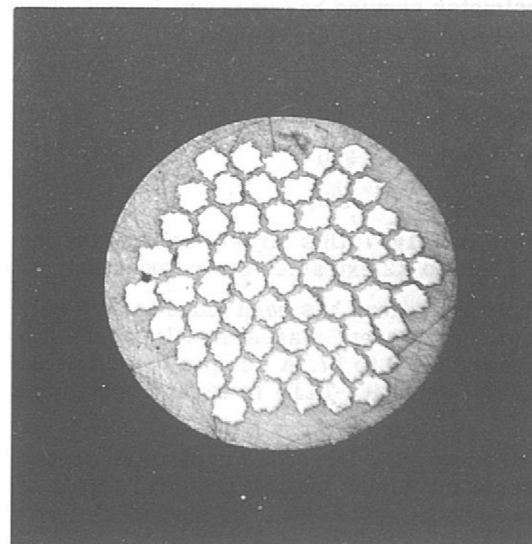


Figure 63. Cross section of filamentary conductor.





biased source at the centre of the magnet. To obtain the best results with axial injection, additional electrodes must be placed near the machine centre to concentrate the electric field on the first r.f. acceleration. This is a complication, but the phase width of accepted beam is increased without loss of beam quality, giving greater beam currents; it is particularly beneficial on harmonic operation.

The design of the electrostatic mirror is made difficult by having to hold positive voltages on the reflecting electrode in a magnetic field. A successful solution was found, and up to 35 kV can be maintained reliably on the electrode.

Modified versions of the sources used in the cyclotron have been manufactured for use in the injector, and it is hoped that by the middle of 1969, when the axial injector is installed, improved currents of heavy ions will be available for cyclotron experiments.

## Electron Ring Accelerator

(163, 174, 175,  
176, 177, 178,  
179, 208, 209)

Three members of the Laboratory attended the study group at Berkeley in February in which the potentialities of this device (alternatively known as the "Collective Linear Ion Accelerator" or "Smokatron") were explored. The proposal is to form small relativistic self-constricted partially neutralized electron rings in which the ratio of protons to electrons is about 1%. Such rings, typically of a few centimetres diameter and containing  $10^{13}$  -  $10^{14}$  electrons of energy 20 MeV would have a charge to mass ratio less than that of a proton by a factor of about 40. If such rings can then be accelerated as a whole in a linear accelerator without disintegrating, then one might hope to obtain a reduction factor of up to 40 in the length of accelerator required to accelerate the protons to a given energy, giving (hopefully) a not too expensive way of producing protons of very high energy.

Experimental work on the formation of the rings was first carried out in the USSR, where the idea for such an accelerator first took shape; this has been followed by an intensive programme now under way at the Lawrence Radiation Laboratory in Berkeley.

Theoretical work on some aspects of this device has been carried out at the Rutherford Laboratory. In particular, some inconsistencies were found in the calculation of the radiative loss of the ring in passing through the accelerating cavities (at frequencies higher than the accelerating frequency). Further order of magnitude calculations by a different method suggested that these would be more severe than at first believed. Accurate calculations appear to be exceedingly difficult, and there is still controversy about the validity of these results, which, if correct, would appear to impose a severe limit on the maximum energy which can be reached.

Studies have also been made of the properties of ring beams, especially the fundamental limitations which apply when the inductive energy associated with the ring current approaches the kinetic energy of the electrons.

## Radiation Protection

Operational  
Health  
Physics

**Personal Dosimetry Service** A thermoluminescent dosimeter service has been introduced. The dosimeters are issued to lightly exposed persons and are read every six months.

At the end of 1968, regular dosimeter issues were as follows:

Beta-gamma films (monthly issue)	800
Beta-gamma TLD (6-monthly issue)	300
Fast neutron films (monthly issue)	500

Fast neutron film issues have increased by 75% since mid-1967; this largely reflects the increased dose rates in Nimrod Experimental Hall No. 1 due to X2 extracted beam operation.

The response of the fast neutron films to Nimrod stray radiations has been found to be highly dependent on the "hardness" of the neutron spectrum. In different places the films exhibit a response, in reported rem per true rem, which varies from 0.6 to 17. A composite dosimeter (consisting of a fast neutron track film and a slow-neutron-sensitive TLD) is being investigated in an attempt to overcome this difficulty.

The tendency for neutron dose over-estimation discussed above, the increased dose rates around the X2 complex and an increase in gamma doses received during maintenance and repair of Nimrod and its radioactive components, are expected to cause some reported personnel doses to approach, or possibly exceed, 5 rem for the year.

**Nimrod Environmental Surveys** General levels of dose rate from induced radioactivity have not significantly increased, but the distribution pattern has changed because of the use of the X2 extracted beam.

Under some operating conditions, the X2 shielding is not sufficient to prevent dose rates in some Local Control Rooms from reaching levels that would be unacceptable for continuous exposure.

**The Radioactive Workshop (R52)** There have been no requirements during the year to handle work involving significant amounts of loose contamination.

**PLA** There have been no changes of health physics significance on this facility. All reported personnel doses are expected to be less than 1.5 rem for the year.

**Nuclear Chemistry Wing** Only very low levels of activity have been handled during 1968. All ducting, trunking and fume cupboards have been dismantled, cleaned and painted under Radiation Protection Group surveillance during the year.

Research and  
Development  
(171, 205, 206,  
207, 215)

**Radiation Field Studies** The study of problems related to high energy accelerator stray radiation fields has continued. Dose equivalents have been calculated for various broad neutron spectra, including examples of those observed around proton accelerators. These have been compared with dose estimates which would be produced using routine methods of measurement. This has led to the development of a simple two detector system (using the activation of carbon and moderated indium) which will give good estimates of neutron dose equivalent in widely differing spectra.

Neutron spectrum unfolding programmes have been further developed and are being successfully used on data from Bonner spheres and threshold detectors.

Experimental work has included investigations of radiation fields around Nimrod, the PLA and Nina, studies of beam loss patterns around extracted beams and their targets, depth-dose studies and detector calibrations and intercomparisons. The latter have been carried out at the Rutherford Laboratory and in collaboration with the Daresbury Laboratory, Princeton-Pennsylvania and Stanford.

The electro-magnetic cascade and the stray radiation fields of high energy electron accelerators have been investigated in collaboration with Daresbury Health Physics Section. The results will provide design information for present accelerators and for studies of future machines.

The Royal Post Graduate Medical School (Hammersmith Hospital) contributed to the Nimrod field studies by determining an LET spectrum.

A plant mutation experiment, performed in co-operation with AERE Health Physics, made an interesting contribution to the stray field studies on Nimrod. The results were not inconsistent with physical measurements of the same fields.

**Threshold Detectors** Three additional threshold detectors have undergone development: bismuth fission tracks in dielectrics (threshold about 50 MeV),  $\text{Be}^7$  polythene (32 MeV) and  $\text{F}^{18}$  in aluminium (30-40 MeV).

**Equipment** The counting equipment has been moved to a larger room and has been extensively modernised. All counter systems now have automatic print-out. The new SCIPP 1600 channel analyser has greatly facilitated gamma spectrum analyses and activation detector measurements.



ENGINEERING  
DIVISION

# Engineering Division

Division Head and Chief Engineer: P. Bowles

Engineering at the Laboratory is concerned with the design, manufacture and installation of the wide range of experimental apparatus used to realize the full potential of Nimrod and the PLA as fundamental research tools as well as in their operation and continuing improvement and development. Whilst experimental apparatus includes major projects such as bubble chambers and superconducting magnets, steady progress is being made on the optimisation of the design and development of the vast array of smaller but no less essential electronic, electrical and mechanical equipment.

Included in this work is the provision of new buildings and the maintenance of existing ones together with many laboratory services such as the provision of electricity, water, air, gas and liquefied gases.

## Static Power Supplies

*Pulse Loading  
Tests on  
Power Systems  
(222, 223)*

The Static Power Supply study programme was continued throughout the year, to examine the possibility of powering large accelerator type pulsed loads direct from the public electricity network. The emphasis shifted from the reactive compensator device itself to a more detailed theoretical and practical study of power system dynamic behaviour when subjected to an accelerator type pulse load.

In order that system tests should be as representative as possible of the immediate interests in Static Power Supply applications (i.e. Nimrod and the proposed 300 GeV accelerator) it was desirable to utilise pulse powers in the region of 160 MW. Practical tests on power systems involving cyclic pulse load applications of this magnitude are difficult to arrange. Such loads do not normally exist (in the Western Hemisphere only Nimrod qualifies) but unfortunately existing plant connections make a temporary direct hook-up for full power tests impracticable.

However, the presence of the d.c. Channel link which interconnects the British and French power systems, via submarine cable, offered unique possibilities and arrangements were made between the CEGB and Electricité de France (EdF) to conduct a series of pulse loading tests during mid-day and mid-night periods on 20th/21st June.

Cyclic power pulsations were applied by repetitive blocking and de-blocking of the Lydd converter groups (British terminal) to produce a train of square pulses having amplitudes of 80-160 MW and repetition rates of 15 to 30 pulses per minute. The power flow was from CEGB to EdF so that the British power system was repetitively pulse loaded and the French system repetitively unloaded.

Measurements were made at selected generating stations and sub-stations in the vicinity of Lydd to obtain load transfer variations, response characteristics of turbo-generating plant and associated AVR and governor systems, and pulse-induced disturbances at load groups. System frequency measurements were made at four locations - three in Britain and one at CERN (Geneva) on the EdF Genissiat lines.

The SRC and CERN frequency measurements were analysed immediately after the tests at the Atlas Computing Laboratory using the BOMM suite of programs for time series analysis.

The results were very encouraging. No dynamic magnification was observed and the maximum pulse-induced frequency disturbance on the CEGB system was 0.053% occurring at night (minimum system energy) at maximum pulse amplitude (160 MW) and minimum pulse frequency (0.25 Hz). The CERN measurements showed a considerably lower disturbance amplitude on the EdF system (about 0.03%) due in part to the beneficial effect of the a.c. inter-tie between the various European power systems (UCPTE).

Although the pulse induced frequency disturbances are satisfyingly low, the part played by the various power system elements in the dynamic response of the system - particularly the damping effect of system load - its inertia, power/voltage and power/frequency dependence are not fully understood. These considerations have special importance in the case of generating groups or dynamic load groups in close electrical proximity to the pulse load. Collaborative studies with CEGB are therefore continuing in order to give final clearance to these questions.

The CEGB study is based on a multi-element representation of the British power system, while the Rutherford Laboratory study in association with the Atlas Computing Laboratory is related to the investigation of turbine governor response (turbo-generators with and without reheat, hydro-machine characteristics etc.) and more limited machine group representation.

Later in the year, the Rutherford and Atlas laboratories collaborated with CERN in the direct pulse tests on the Swiss power system (SIG) in connection with a Static Power Supply application to the CERN PS-Booster. Advantage has been taken of the continuing development of reactive compensation devices to modify certain of the computer programs to give more accurate compensation characteristics, as well as providing an opportunity to tidy up the theory.

## Safety Group

The Group's task is

- to promote an active interest in accident prevention throughout the Laboratory and to advise on safety matters.
- to examine proposals for new activities or modifications to existing activities from the safety viewpoint.
- to maintain an active liaison between safety officers, and fire services in AERE and similar establishments, and with industry.

Improved communication has been one of the year's themes: instruction information and advice is being constantly supplied to all Laboratory personnel in the form of Safety Notices and Safety News Sheets. Many existing Codes are being revised and reissued to enable staff to understand and appreciate their responsibilities for safety more easily and to ensure the practical nature of safety precautions. The Safety Committee's terms of reference have been revised; the Committee advocated a comprehensive safety training scheme which has reached the stage at which a programme will be issued early in 1969.

Safety Group staff inspect, watch and advise in the more potentially hazardous situations such as those involving high voltage electricity, flammable gas, pressure vessels and mechanical handling equipment.

Regular tours under the direction of the Safety Committee, and safety displays in the various show cases distributed around the site, in addition to the distribution of "Safety News" sheets constantly draw attention to hazards.

Exchange of information with industry and other government establishments, especially those having an interest in flammable gases, has continued during the year. The Safety Officer has lectured to outside bodies on the subject of electrical equipment for use in flammable gas areas.

Some 52 Emergency First Aid Classes were held and about 370 staff attended instructions or refresher classes. Training was also given in manual lifting and handling.

The number of items requiring regular safety inspection is now 3442, a 5% rise on the 1967 figures, and includes 2053 items of lifting tackle, 352 lifting machines, 640 pressure vessels, 238 installations of high voltage apparatus and 124 items of safety equipment.

During the year a total of 123 injuries were reported, the average lost time being 11.3 days; these figures represent approximately a 10% reduction on those for 1967. The All Injury Frequency Rate fell from 5.06 to 4.51 and the Lost Time Frequency Rate fell from 0.59 to 0.55.

## Engineering Design & Development Department

Three groups in this Department (Applied Physics Apparatus, Nuclear Physics Apparatus, Nimrod Design Group) devote their efforts to the design, research and development problems involved in the supply of the wide range of equipment used by scientific groups in the use and optimisation of the Laboratory's accelerators. The following examples are typical of the Department's work. The work of the fourth group in this department, the PLA Engineers Group, is shown in the report of the PLA Division. (See page 80).

## Applied Physics Apparatus Group

Low Temperature  
Testing of  
Materials  
(220)

Much of the current research in the Laboratory involves apparatus working at very low temperatures. Although considerable information on the behaviour of materials in these conditions, particularly in the temperature range 20-300° K, has become available from the international space programmes, little is known of the properties of materials conforming to British Specifications operating at liquid helium temperatures (i.e. in the region of 4° K.)

A cryogenic test apparatus for obtaining such data has been constructed; it is housed in a cryostat holding the specimen within a helium bath. A quick change working section permitting tension, compression and bending tests to be arranged contributes to the simplicity and versatility of the rig which can also measure thermal contractions (see figure 66). Setting up and cool down times are such that two tests per day can be completed.

The equipment has been in use for about 2 years and recently a machine of higher capacity has been modified to enable a larger number of routine tests to be made with greater convenience. Two examples indicate the scope of the apparatus. In the first a flexible electrical insulating material was required for the Superconducting Bending Magnet. The material was to be injection moulded but comparable to stainless steel and copper in compressive strength and thermal contraction. Available data indicated that unfilled plastics contract much more than metals during cooldown to 4° K but tests on certain glass loaded nylons showed suitable characteristics. In the second example, data was required on the change in electrical resistivity with temperature, hardness and mechanical strain, for copper and aluminium of various purities, these being likely materials for use in stabilizing superconductors.

Tensile tests on specimens carrying an electric current were carried out, the change of resistance being measured potentiometrically. Some of the problems encountered with differential thermal contractions in low temperature apparatus which the rig has helped to solve are mentioned on page (105) of this Report under 'Fish Eye Optical Windows'.

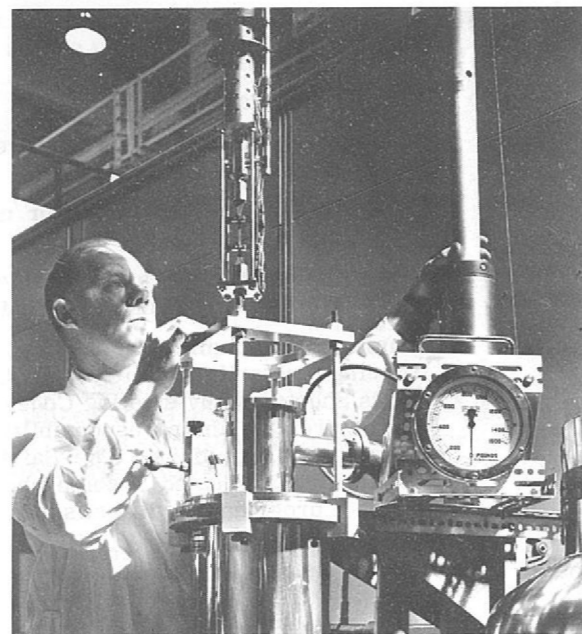


Figure 66. Low temperature testing.

Superconducting  
Bending Magnet

The stainless steel spool was assembled in mid 1968 and winding of the superconductor coil is now completed. Winding involved building up 19 layers (a total wire length of 15000 feet) such that each layer had a specified number of turns so that the overall profile of the completed coil took on the required elliptical cross section. Layers are separated by a series of slotted strips moulded from 40% glass loaded nylon providing inter-turn insulation and cooling channels. Further details of the coil winding process are given on page (120) under 'Superconducting Magnets'.

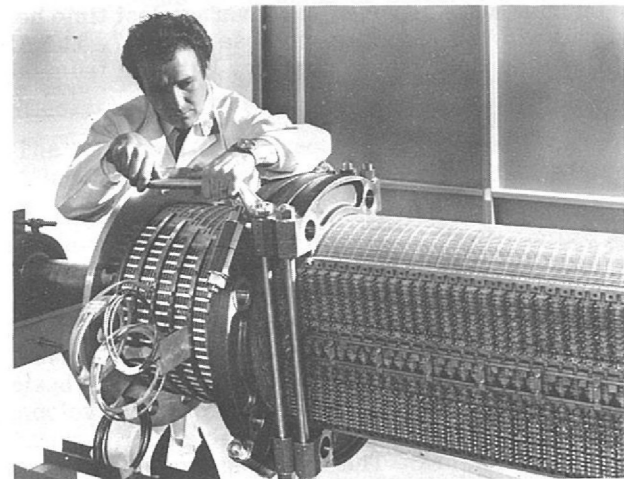


Figure 67. Fitting supports to the Superconducting Magnet.

The next stage will be the fitting of the support structure massive 'I' section clamps of stainless steel which are required to support the coil against electromagnetic bursting forces totalling 300 tons (see figure 67). End thrust will be restrained by a series of flanges slotted into the spool tube together with longitudinal tie rods.

In order to minimise liquid helium requirements, the design of the cryostat demanded particular attention to the reduction of heat flow into the magnet vessel, and includes a helium vapour cooled shield between the magnet and liquid nitrogen vessels and also retractable current leads.

When the coil is shut down or discharged suddenly eddy-currents are induced pro-

hibiting the use of a high conductivity material such as copper for the vapour cooled shield. The solution chosen is an annular vessel formed from stainless steel sheet rolled to form channels with an  $\frac{1}{8}$  inch interspace through which the helium vapour is passed. Similar methods enable a liquid nitrogen cooled sleeve to pass through the centre bore of the magnet.

Final assembly of the cryostat is due to start in March 1969 and consists of 3 vessels concentrically assembled within the outer vacuum vessel and interconnected by tie rods, arranged to minimise the effect of differential contraction on alignment. A trial assembly of the cryostat without the magnet is envisaged.

The RACOON  
Coil

This coil is being designed to test full size superconducting material for the High Field Bubble Chamber (HFBC) Magnet, at the full magnetic field of 7 Tesla (70 kG) and current of 7500 A. To meet these requirements while still maintaining reasonable size and cost, the coil will be suspended within an existing magnet to achieve the required field strength; use of the CERN superconducting coil BRARACOURCIX has been offered for this purpose.

To suit the BRARACOURCIX coil parameters of 35 cm bore and 5.2 Tesla field, a coil having 6 double pancakes of 32 turns (total 192) has been designed. When powered at 7500 A this will give a magnetic field of 8.4 Tesla with the BRARACOURCIX backing field and 2.6 Tesla without.

Industry in collaboration with the Laboratory is producing the superconducting material, which consists of Nb-Ti filaments in a stabilising matrix of fully annealed copper.

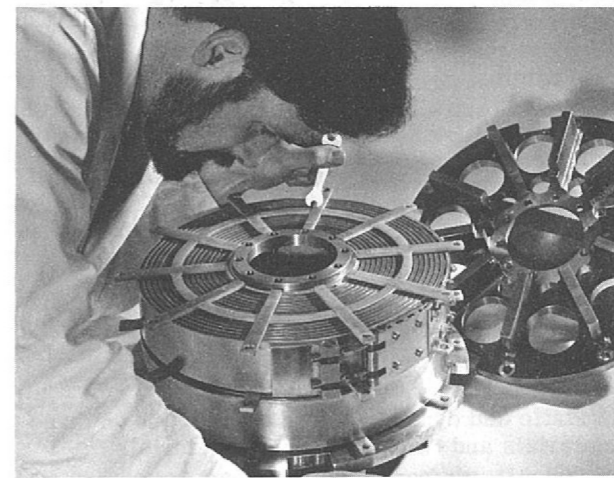


Figure 68. RACOON Coil Pancake

During operation the coil will be immersed in liquid helium at 4° K, and it is essential that a high proportion of the conductor surface area be exposed to the helium. In addition the coil is subjected to large hoop forces which the conductor alone could not withstand, and it is therefore necessary to provide some reinforcement. To meet both these requirements a stainless steel strip with buttons welded to it is wound into the coil. Inter-turn insulation is provided by 0.2 mm Termex tape and lateral insulation between layers by epoxy glass laminate spiders, as may be seen in figure 68.

In order to gain experience in the problems of winding multi-element coils, it was decided to wind the coil at RHEL and special winding equipment was designed and built for this purpose.

Each double pancake is wound from a continuous length of conductor, which is joggled at the centre to provide a cross-over from one layer to the other. The material is wound on an insulated centre boss one layer at a time, the material for the second layer being stored on reels attached to the winding table. To ensure a tight coil, the tapes are tensioned during winding and on completion the ends are strapped together to lock in the winding tension.

To date one pancake has been wound (see figure 68), and it was found to have zero winding error radially and to be flat within 0.1 mm. Further coils will be wound as material is delivered; on completion the six pancakes will be stacked and clamped between stainless steel end plates, and the electrical connections will be made by soldering and clamping to form a complete coil. The coil will be tested in its own magnetic field at the Rutherford Laboratory before operating at CERN.

Development of  
Fast Acting  
Brakes for  
the Expansion  
System of  
the HFBC

A mass-spring system is proposed for rapidly expanding and re-compressing the liquid in the bubble chamber. The spring function is obtained from the compressibility of the liquid and the mass is the piston which acts upon the liquid. The periodic time for the mass-spring system becomes the cycle time for the expansion-recompression process and is adjusted by changing the mass. Three separate mechanisms are required when considering the practicalities of the system: (1) a slow acting precompression unit to force the piston down to the compressed position, (2) a fast acting unit which will hold this position, release and then halt the piston again at the compressed position, and (3) a make-up energy unit.

A fast acting multiple brake system has been proposed for item (2) and the development of a prototype unit is described below. The main parameters for the High Field Bubble Chamber are:

- (i) Amplitude or vertical displacement of the piston - 0.5 inch
- (ii) Cycle time, mass of  $3\frac{1}{2}$  tons - 50 milliseconds

- (iii) Cycle time, mass of 14 tons – 100 milliseconds
- (iv) Static force to hold compressed position – 100,000 lbf
- (v) Time for brake release and re-application – 5 to 7 milliseconds
- (vi) Operating pressure for brake material and piston – 2000 lbf/in<sup>2</sup>

Manufacturers of commercial brake mechanisms and pad materials were consulted but this application was outside their experience. However they offered useful suggestions and samples of various types of materials.

The Laboratory's development programme for 1968 set out to investigate brake pad and brake tongue materials, brake piston and cylinder construction, the response time of the system, and to develop hydraulic circuitry, fast acting valves and instrumentation.

The objective was to develop a unit using commercially available materials to a stage where it could be accepted as the prototype for the multiple braking system. The work was carried out on one pair of brakes with a total holding force of approximately 10,000 lbf, this parameter being set by the available driving force of the hydraulic vibrator.

The brake rig, shown diagrammatically in figure 69, consists of two identical hydraulic piston-cylinder assemblies mounted on a bridge, with each piston driving a brake pad; the two cylinders are also clamped together as a mating pair with sufficient gap between them to admit the brake tongue which in turn is attached to the double acting hydraulic oscillator. The pistons are 3 inches in diameter operating at 2000 lbf/in<sup>2</sup> and the pads were made from a variety of commercial materials. One electro-hydraulic servo valve controls the oil supply to the cylinders and the electronic control circuits are arranged to apply the brakes so that the hydraulic oscillator is halted and held at the bottom of the stroke.

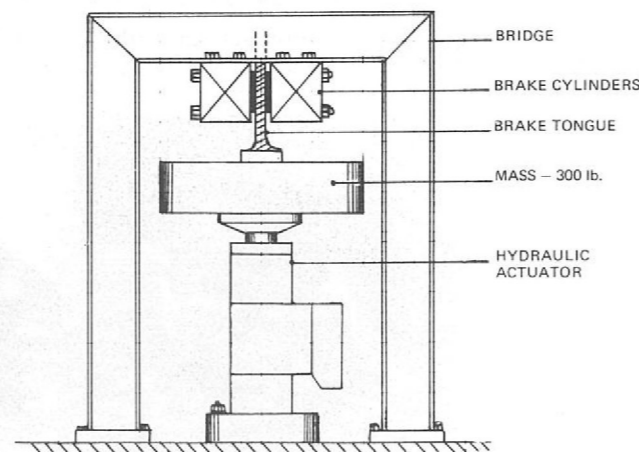


Figure 69. Brake Test Rig

A large number of test runs, both static and dynamic, were carried out on three types of brake pistons and cylinders, five pad materials and two brake tongue materials.

An acceptable design of brake system for the HFBC has now been established using a lapped piston-cylinder assembly, Capex 310 pads Araldited to  $\frac{1}{4}$  inch thick steel backing plates, and a cast iron brake member. The results are summarised in the Tables below.

Brake Material	
(i) Type	Capex 310 ( $3\frac{1}{2}'' \times 2\frac{1}{2}'' \times \frac{3}{8}''$ )
(ii) $\mu$ (static)	0.29
(iii) $\mu$ (dynamic)	0.35 initially 0.45 after $10^5$ operations 0.45 after $10^6$ operations
(iv) Wear rate	0.1% after $10^5$ operations 0.3% after $10^6$ operations
Piston-Cylinder	
(i) Specification	mild steel cylinder (3" diameter bore) with lapped brass piston
(ii) Oil leakage rate	400 cc per hour after $10^6$ operations at 10 per second

*Mechanical Aspects of the Proposed 'Fish Eye' Optical System for the HFBC*

The size of the chamber is such that a conventional optical system would require large heavy glass windows presenting great difficulties in manufacture and handling. An alternative system using 'fish eye' windows, that is three individual glass windows one close to each camera lens, is being considered. The hemispherical form of these windows avoids light being reflected into the camera lens and they will be made from borosilicate glass to reduce thermal shock. They have to be concentric to better than 0.002 inch and remain within this tolerance during cooldown from 300° to 26° K to ensure accurate reconstruction of the particle tracks.

In order to keep the stress level in the glass below 1000 lbf/in<sup>2</sup> the mount must be of a material with a similar coefficient of contraction to that of the glass and a series of tests has shown that a nickel iron alloy (42% Ni 58% Fe) is suitable.

The mount takes the form of a 0.020 inch thick spinning optimised in shape to maintain the concentricity requirements but sufficiently flexible to allow for the differential contraction between the mount and the stainless steel chamber body. The joint between the glass and the mount is an aluminium loaded Araldite giving an interspace film of 0.005 inch.

To minimise the heat input from the window nearest the camera lens (which is at ambient temperature) to the window in contact with liquid hydrogen at 26° K, the interspaces are evacuated to less than  $10^{-7}$  torr, and the centre window edge is cooled with liquid hydrogen.

Computer calculations indicate that the thermal stresses and gradients are within the requirements stated and a set of windows has been manufactured to enable testing of a complete assembly to be carried out.

*Investigation of Low Level Surface Water Disposal System at RHEL*

Nimrod and its experimental areas are sited at such a level that conventional gravity drainage is not practicable; a specially designed low level surface water disposal system was installed during the original construction of Nimrod, and was intended to prevent flooding during the most intense storms known to this country.

The construction of the new experimental Hall 3 and extension of the Bubble Chamber area has subsequently increased the catchment area and a study was carried out to determine the return period of a critical storm, i.e. to predict the frequency of occurrence of severe storms which would cause flood damage to equipment sited at low level.

This necessitated an assessment of the inter-related behaviour of a number of simultaneous events which were grouped under the three heads of catch, arisings and dissipation. Catch is dependant on the area and the predicted intensity and duration of the storm; the quantity and rate of the arisings at the drain are dependant on the evaporation rate, surface permeabilities and delayed run off. Dissipation is dependent on storage, soakaway and overflow capacities of the system.

The catchment area is approximately 410,000 ft<sup>2</sup> of which about half is covered by buildings, roads, etc, the remainder being grassed over. Predicted storm parameters are shown in figure 70. Evaporation and delayed run-off are negligible under the influence of very intense rainfall and only small proportions will permeate into the grassed areas.

Up to 60,000 ft<sup>3</sup> of water can accumulate in two deep sumps (12 ft diameter  $\times$  50 ft deep) and the upper and lower tunnels (each 6 ft 3 inch diameter  $\times$  900 ft long). Unlined portions of the tunnels provide 6700 ft<sup>2</sup> of soakaway surface, which will dissipate up to 110 ft<sup>3</sup>/min. A 27 inch diameter overflow drain 2600 ft long will discharge up to 980 ft<sup>3</sup>/min from the upper tunnel to Chilton Pond.

It has been deduced that (a) the danger period occurs between 20 and 30 minutes after the commencement of an intense storm, (b) overflow to the Chilton Pond may occur once in 20 years, and (c) the disposal system will afford protection against storms having a predicted return period of 800 years, a 400 year storm falling on snow, and continuous rainfall of 1.9 inches per hour. These results are illustrated in figure 70.

## Nuclear Physics Apparatus Group

*Foil Stretching Techniques for Spark Chambers*

An increased demand for large foiled spark chambers arose early in 1968. Previous foil stretching methods relied on mechanical stretching tables which proved cumbersome, time consuming and often unreliable. A simple and efficient solution has been developed which is now tending to supersede other methods. Small scale experiments suggested that sufficient foil movement could be obtained by inflating a rubber tube lying in a deep recess beneath a foil sheet clamped over a simply constructed wooden frame; the effectiveness of the method can be seen in figure 71. 'G' clamps are used to clamp the foil between the loose top frame and the base frame. It is important to straighten out major wrinkles in the foil before clamping and also to ensure that

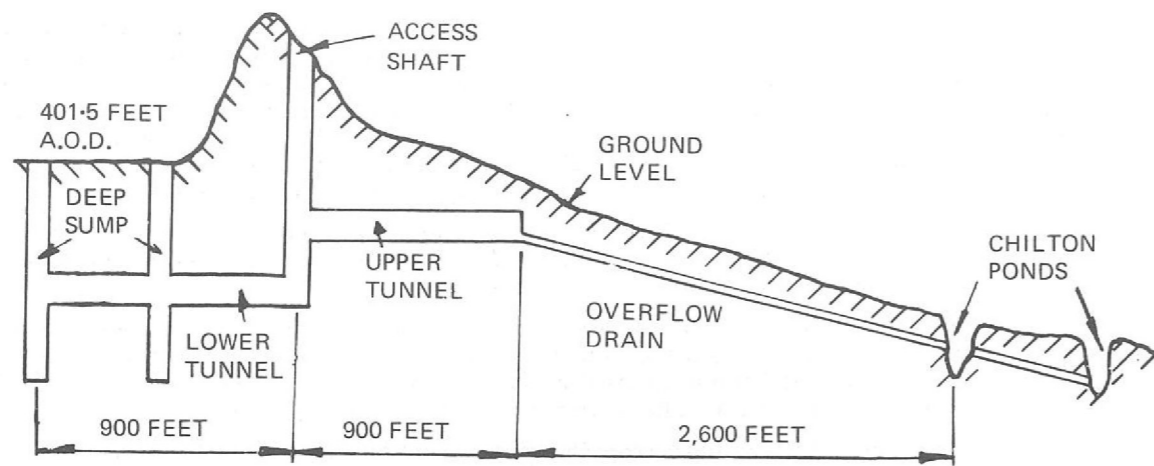


Figure 70 (i) Diagrammatic section of drainage system

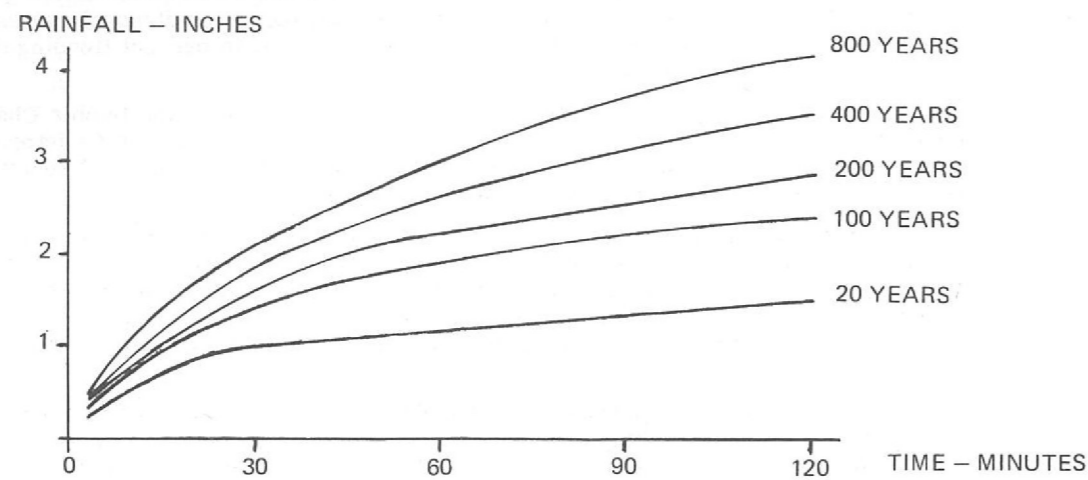


Figure 70 (ii) Rainfall - Intensity/Frequency/Duration

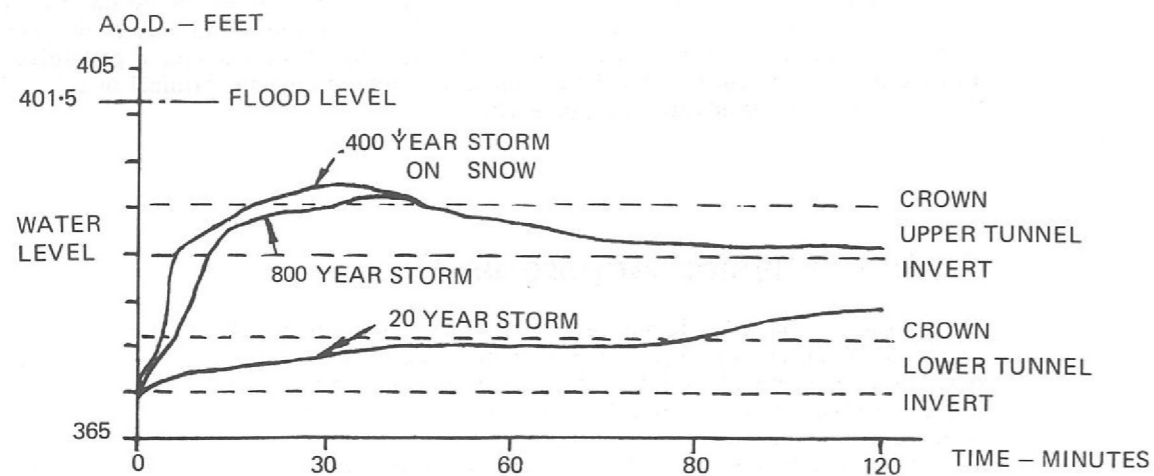


Figure 70 (iii) Water level vs. time for various storm conditions.

in the deflated condition the rubber tube lies totally within its recess, especially at the corners of the frame. Stretching frames of this type are reliable in use, quick and cheap to manufacture, and easy to store. The largest made so far can accommodate spark chamber frames 9 ft x 4½ ft.

A stretched foil obtained by this device is smooth and unwrinkled, and although not necessarily flat and co-planar, is sufficiently robust to allow transfer to a spark chamber frame using Eastman's 910 adhesive. The flatness, surface finish and stability of the spark chamber frame therefore determines the final flatness and position of the stretched foil. Successful results using plain foils were followed by similar success using composite Melinex/aluminium membranes. Previous methods of producing composite foils relied on shrinking the Melinex surround by means of hot air blowers, thus tightening the central aluminium foil. This shrinking proved difficult to control and resulted in many failures.

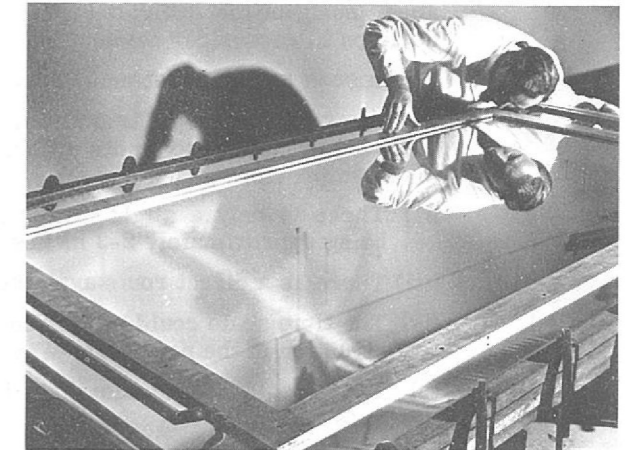


Figure 71. Stretching foil for spark chambers

The inflatable tube method of stretching composite foils produces uniformity of tension such that shrinking methods are unnecessary except in extreme cases of complex foil shapes; it has also been used to stretch wired cloth with good results. The cold box and warm table method of foil stretching whilst still applicable in some cases is tending to be superseded by the inflatable tube. However both techniques are fully established.

Portable Modular Control Rooms

The concept of modular control rooms was first introduced for the Rutherford Laboratory team currently running the S70 experiment on the CERN synchrotron at Geneva. The main objective was to provide a fully screened control room complete with electronics equipment and electrical and mechanical services, so that on site labour and commissioning time could be minimised. An added advantage was their usefulness as large packing cases for the shipment of all the spark chambers and other delicate experimental equipment from the United Kingdom. The success of this system was such that it has now been adopted as a Rutherford Laboratory standard and other Laboratories have shown great interest.

The control room system comprises a basic module measuring 20 ft x 8 ft in plan and 9 ft 6 in high which is a readily transportable size. Side and end panels are easily removed making it possible to assemble many units together to form a large control room suite; door assemblies, cable bulkheads, window assemblies, etc. are all based on the cladding module and may therefore be positioned to suit site and control room conditions. Normally three or four of these units are sufficient to house enough electronics equipment and a small computer for the average experiment. Illustrations of a portable control room are shown in figures (18) and (19).

Each control room suite is complete with a separate electrical-mechanical plant room which houses the electrical switchgear and distribution systems and also the air conditioning equipment required to maintain suitable working environments for both electronics equipment and personnel. The plant room may be positioned on any convenient side of the control room suite; both mechanical and electrical connections are easily made to the plant room, and from the plant room to the control rooms. The air required for cooling the control rooms and the electronics racks is distributed via an underfloor duct which is part of each control room module.

Both the plant room and the control room module design are based on commercially available mass produced freight containers which are built to stringent BSI and ISO specifications. A composite steel asbestos material (Durasteel) was selected for the side and end panels on the control rooms because of its excellent fire resisting properties.

Because the potential total load, as estimated by the user, for any control room module could be in the region of 180 A, single phase, the sub-circuit distribution is arranged over three phases. Attenuation of mains borne interference is provided by taking the supply to each control room unit via an externally mounted three phase and neutral r.f. filter. All final sub-circuits are protected by miniature circuit breakers. Each control room module has electrical services as follows:- (i) Electronic Rack Supplies - 11 off 20 A outlets, (ii) General Purpose Sockets - 24 off 5 A outlets, arranged in groups of four, (iii) General Lighting with associated, battery maintained, emergency lights. Personnel protection comprises Emergency Off push stations and fire detectors sited in each control room module.

Planim Design Study

"Planim" is a proposal to use the existing proton linear accelerator as an injector for Nimrod, making it possible to increase the beam output of Nimrod considerably. The underlying physics is discussed on page (64).

When Planim was first considered the proposal was to resite the whole PLA in a new building between the Active Workshop and the existing Nimrod injector, this being the most convenient site for injecting a beam into Nimrod's Straight 2. Preliminary building layouts showed the difficulty of siting a suitable size of building in this area. Other considerations of equal importance, such as the difficult task of dismantling the PLA and all its services, influenced the decision to reconsider transporting the beam to Nimrod from the present position of the PLA.

It was soon realised that many advantages would accrue from this approach, namely:

- (i) Nimrod beam height is approximately at road and ground level so that existing site services would not have to be disturbed. This makes a ground level building feasible at lower cost than previous schemes.
- (ii) There is only a slight difference in Nimrod and PLA beam heights, the PLA beam height being approximately 2-3 inches higher than that of Nimrod.
- (iii) There is a direct route available which means minimum disturbance to existing buildings.
- (iv) The time scale could be reduced as the PLA would remain in its existing position and construction of the new Beam-Way could commence before the PLA closed down.
- (v) There would be minimum disturbance of the existing PLA equipment and minimum disturbance of Nimrod.
- (vi) The cost would be considerably less, as would the demands on Laboratory design and scientific staff.

The proposed building is a small cross-sectional area shielded tunnel (Beam-Way) constructed mainly from existing PLA shielding blocks weatherproofed by a butyl rubber membrane buried in the concrete construction. The Beam-Way allows limited but sufficient access for maintenance and replacement of faulty equipment. Vacuum pumps, bending magnet and quadrupoles power supplies are housed in prefabricated buildings situated at points along the Beam-Way, access to which is via four plug type concrete doors. The tunnel through the Nimrod mound would be constructed in concrete tube and positioned by a thrust boring technique; the overall scheme is shown in figure (49).

The beam line is divided into six approximately equal sections; each section is considered as a self-contained vacuum system, being pumped by a turbo-molecular pump backed by a rotary pump. Each section of beam line is defined by a 4 in. valve which will close automatically and hence isolate a particular section of beam tube if there is a vacuum leak. Indication of vacuum pressure and the state of all valves is relayed back to the existing PLA control room which is the control centre for the Beam-Way and all its equipment.

The quadrupole lenses will be built up from existing PLA units mounted in triplet formation on accurately machined bedplates. Each quadrupole assembly will incorporate steering facilities. Particular attention will be given to all equipment which is required to be accurately aligned in the beam line and it is envisaged that this will be pre-aligned on a master alignment stand away from the Beam-Way so that quick changes of spare beam line equipment can be made in the event of a fault situation occurring.

Some engineering modifications would be required to the PLA itself. A new short accelerating column d.c. gun will replace the existing unit. Most of the Low Energy Drift Space will remain, with the possible addition of a single large aperture buncher instead of the two bunchers that exist at the moment. Tank 1 will be modified and will incorporate new drift tubes with quadrupoles based on the CERN design, using their blanking tools for production of the magnet laminations. Since the drift tubes would be suspended from the top of the liner, a modified vacuum header vessel will be required to accommodate this structure. New modulators will be required and the layout of the r.f. system will need alteration.

*Design of a  
Medium Gradient  
Ion Column*

Due to the growing need for higher outputs from proton accelerator pre-injectors, their size and complexity is tending to increase, making the manufacture and in some cases operation and maintenance a difficult and more costly process. To meet the requirements of Planim a pre-injector has been designed to allow the testing of a 28 cm long (12 section) length of standard Van de Graaff accelerating column. It is required to run with 500 kV across the ends and to be safe and reliable in operation, easy to produce and maintain, and of low initial cost.

The pre-injector is shown diagrammatically in figure 72. It consists of a length of conventional Van de Graaff accelerating column, supported and located by two re-entrant metal cones. Four spark gaps are provided at each of the accelerating column electrodes, set for H.V. breakdown at 60 kV and with one per set of four used as one end of the connection to the grading resistor which is wound on the outside of the 18 inch internal diameter SRBP outer tube.

The volume bounded by the outer tube, the accelerating column and the two metal cones is filled with sulphur hexafluoride ( $SF_6$ ) gas for H.V. insulating purposes at a normal working pressure of 15 lbf/in<sup>2</sup> gauge.

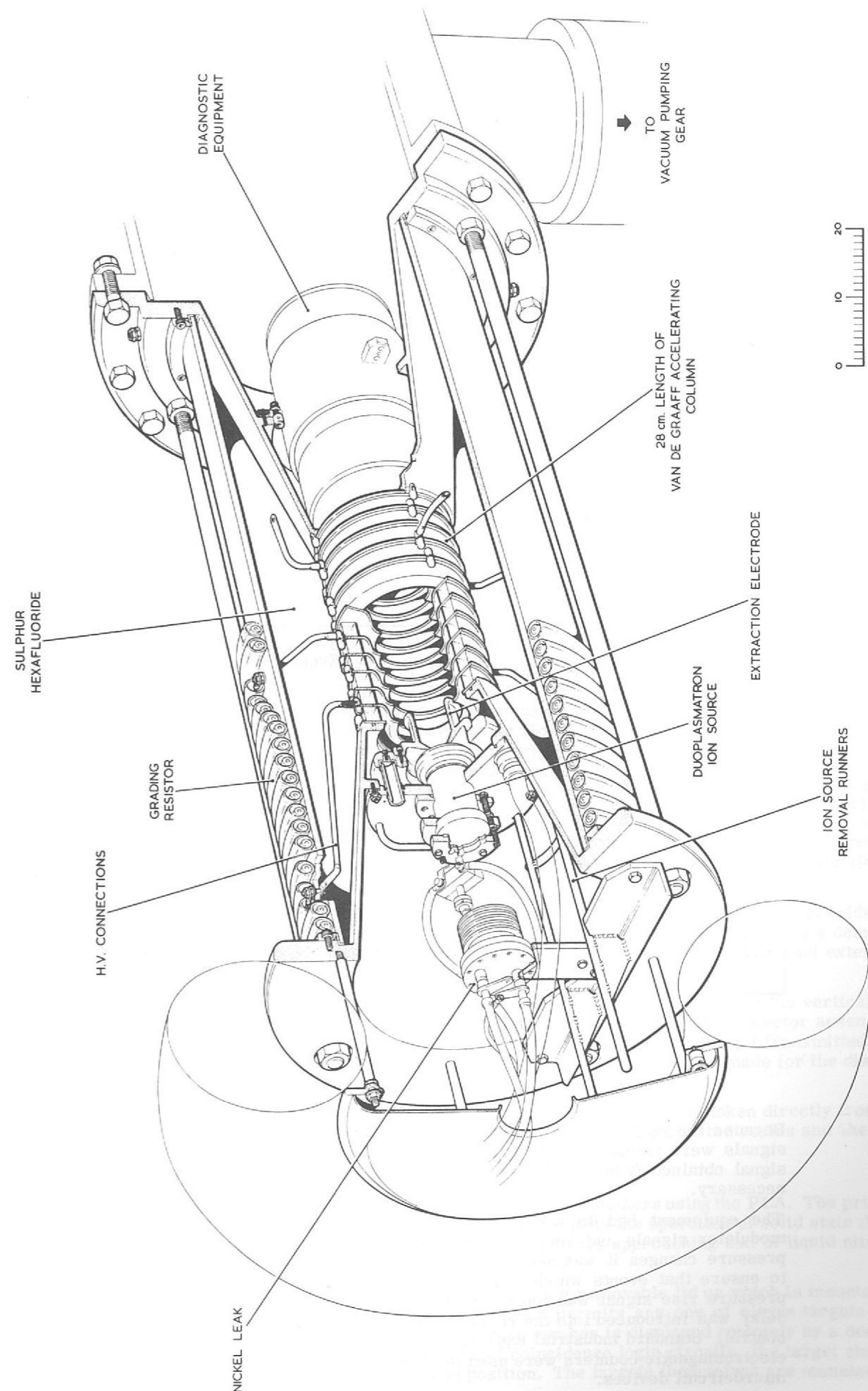


Figure 72. Medium gradient ion column.

The whole unit is held together by four tie rods and cantilevered from a 23 inch diameter vacuum vessel which houses the majority of the beam diagnostic equipment and carries the vacuum pumping gear which consists of a 12 inch oil diffusion pump with cold trap giving pressures of less than  $1 \times 10^{-6}$  torr.

At the other end of the pre-injector, the ion source is mounted in such a manner as to facilitate its removal or precise positional replacement.

*Fault Testing  
on High Power  
Radio Frequency  
Triodes*

In order to utilise the PLA grounded grid triode valves for the Planim (see Planim design study above) duty cycle, it was necessary to modify the anode structure to cope with the considerably higher peak powers involved (1.8 MW at 0.5 Hz for Planim, 0.8 MW at 50 Hz for PLA). As under these conditions the peak power was limited by voltage breakdown, it was necessary to register the number of electrode to ground faults occurring within the valve during the testing periods. These faults were to be counted independently of other faults external to the valve.

The valves are continuously pumped, and a flashover occurring within the vacuum envelope, causes a slight pressure rise in the system. This characteristic was used to classify valve and external circuit faults. Tests showed that a single electrode to ground flashover caused a signal voltage of some 10-20 mV with a rise time of 75 ms at the "Vacion" pump control unit. The rate of rise of pressure on fault was sensed, and a threshold value of 0.13 volts per second was found to be suitable.

To differentiate between the various possible faults, it was necessary to set up a logic circuit which would identify the different faults on the grounds of coincidence of two or more events. Figure 73 shows the logic circuitry employed, and the logic requirements for each fault are given below.

Fault	Event Coincidence
Anode to ground	Vacuum pressure rise AND anode current > normal (175% F.L.) AND r.f. drive failure.
Cathode to ground	R.f. drive forward power normal AND r.f. drive reverse power > normal AND vacuum pressure rise.
R.f. drive	R.f. drive forward power normal AND r.f. drive reverse power > normal AND NOT a vacuum pressure rise.
Modulator failure	Modulator trigger normal AND NOT anode volts normal (less than 30%).
R.f. output	R.f. output forward power normal AND r.f. output reverse power > normal.

Because the equipment had to operate in a high ambient r.f. noise level all transducer pulse signals were transmitted at high level (> 20 volts) and attenuated at the level detectors. The signal obtained from the "Vacion" pump control unit was too small and local amplification was necessary.

The equipment had to accept signals of varying pulse lengths - 600 to 2  $\mu$ s for r.f. and modulator signals and several milliseconds for the vacuum pressure rise. Because of the slow pressure changes it was necessary to hold all signals for 50 ms by means of monostable units to ensure that events which were coincidental were correctly recorded. Where the vacuum pressure rise signal was used to inhibit a gate (e.g. r.f. drive fault, see figure 73), a 30 ms delay was introduced into the remaining inputs to that gate to ensure that the inhibit signal had control. Standard industrial logic elements with an operating speed of 10 kHz and conventional electromagnetic counters were used in conjunction with a high speed input section consisting of microcircuit devices.

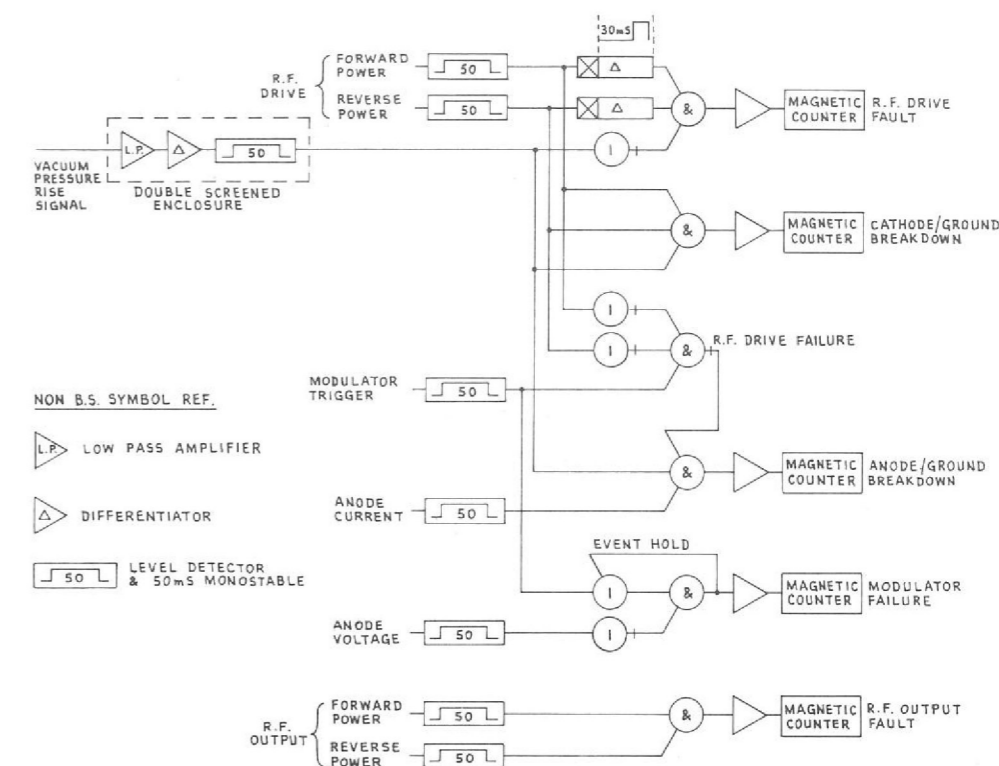


Figure 73. Fault testing on high power radio frequency triodes, diagram of logic circuit.

*Detector  
Movement in  
Three Planes*

One of the functions of the Nuclear Physics Apparatus Group is to give engineering support to former users of the PLA who will in future be using AERE Accelerators.

A detector system has recently been designed and manufactured for use by experimenters from King's College, London and Queen's University, Belfast, to be used in conjunction with the AERE Variable Energy Cyclotron. It was specified that the apparatus should have the necessary facilities to enable "In Plane" and "Out of the Plane" scattering experiments to be conducted.

The apparatus, shown in figure 74, consists of a centrally positioned target assembly with two detector assemblies mounted on independent, movable arms that can rotate about the target axis. The angular position of each detector may be set between  $10^\circ$  and  $80^\circ$  for the "In Plane" movement and between  $0^\circ$  and  $60^\circ$  for the "Out of Plane" movement. The precision of movement, which is carried out manually, is  $0.2^\circ$ , and all four detectors can be moved from outside the scattering chamber.

The Target Assembly, which may be rotated "In Plane" with respect to the beam, provides for each of six targets to be precisely indexed into the beam, the targets being attached to a demountable frame which may be interchanged. Target rotation and indexing is also carried out externally to the scattering chamber.

The "In Plane" movements are achieved by rotating the arms radially about the vertical axis of the target, while the "Out of Plane" movement is derived by moving the detector assemblies around a curved track via the motion of a worm and worm wheel arrangement transmitted from the external driving boss through a bevel gear drive. Provision is also made for the distance of detectors from the target to be varied.

Positive positional indication of the detector and target movements is taken directly from the driving bosses, the "In Plane" movements being indicated against graduated scales and the "Out of Plane" movement on a mechanical counter.

*Universal  
Cryogenic  
Scattering  
Chamber*

During the past year this facility has been provided for experimenters using the PLA. The primary difference from the chambers already in use is that it permits the operation of solid state detector systems between ambient temperature and temperatures approaching that of liquid nitrogen ( $77^\circ$  K).

The cylindrical mild steel chamber (see figure 75), has a removable lid on which is mounted the remotely operated target changer mechanism which permits any one of eleven targets to be introduced into the path of the beam. The target number is displayed remotely by a decimal digitizer shaft encoder system, and, by the use of coincidence logic circuits, the target changer will drive until the preselected target is in position. The targets themselves are mounted in a



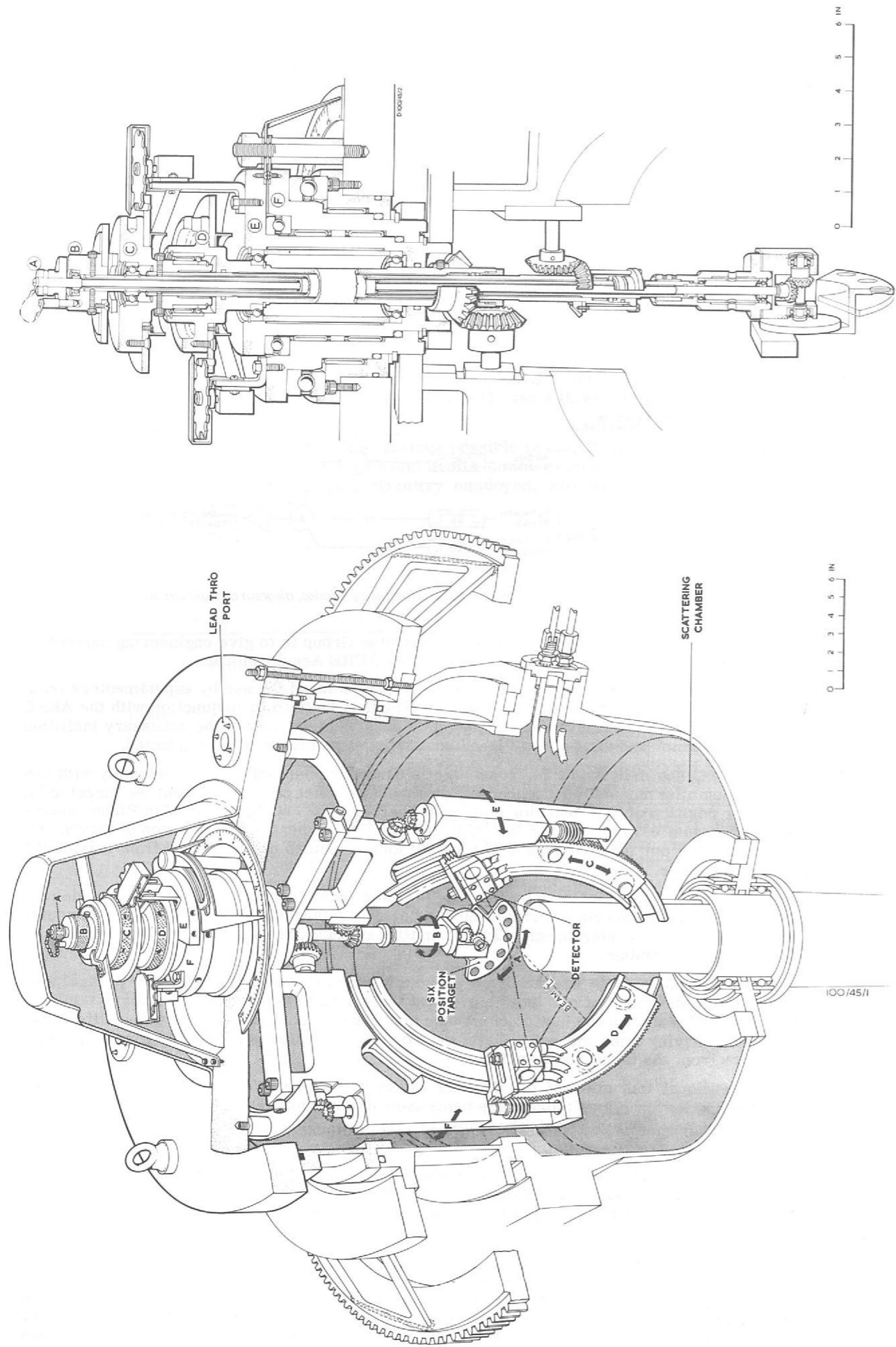


Figure 74. Detector system in three planes.

- 1 VACUUM VESSEL
- 2 ROTATING LID
- 3 TARGET CASSETTE
- 4 TARGET MOUNTING PLATE
- 5 TARGET INDEXING AND DRIVE MECHANISM
- 6 TARGET HORIZONTAL DRIVE MECHANISM
- 7 TV MONITOR FOR TARGET ANGULAR POSITION
- 8 COOLED PLATFORM FOR DETECTOR MOUNTING
- 9 TYPICAL DETECTOR ASSEMBLY
- 10 THERMOCOUPLE
- 11 RADIATION SHIELD
- 12 DETECTOR PLATFORM HEATER
- 13 DETECTOR LEADS CONNECTOR JUNCTIONS
- 14 DETECTOR PLATFORM DRIVE RING
- 15 COOLANT DISTRIBUTION MANIFOLD
- 16 INDIUM SEAL
- 17 BELLOWS TO COMPENSATE THERMAL MOVEMENT
- 18 ROTARY JOINT - SEE DETAIL
- 19 ROTATING SEAL FACE
- 20 SEAL FACE LOADING SPRING
- 21 BELLOWS TO COMPENSATE THERMAL MOVEMENT
- 22 COOLANT TRANSFER LINE ROUGHING OUTLET
- 23 DEMOUNTABLE JOINT
- 24 TRANSFER LINE
- 25 LIQUID NITROGEN DISPENSING ASSEMBLY
- 26 HEAT EXCHANGER
- 27 SOLENOID VENT VALVE
- 28 BURSTING DISC
- 29 PRESSURE RELIEF VALVE
- 30 HEATER
- 31 DEWAR FLASK
- 32 SCINTILLATOR BOXES
- 33 GATE VALVES
- 34 PORT FOR INTERNAL VIEWING
- 35 VACUUM GAUGE HEADS
- 36 WHITE SPOT FILLING LINE

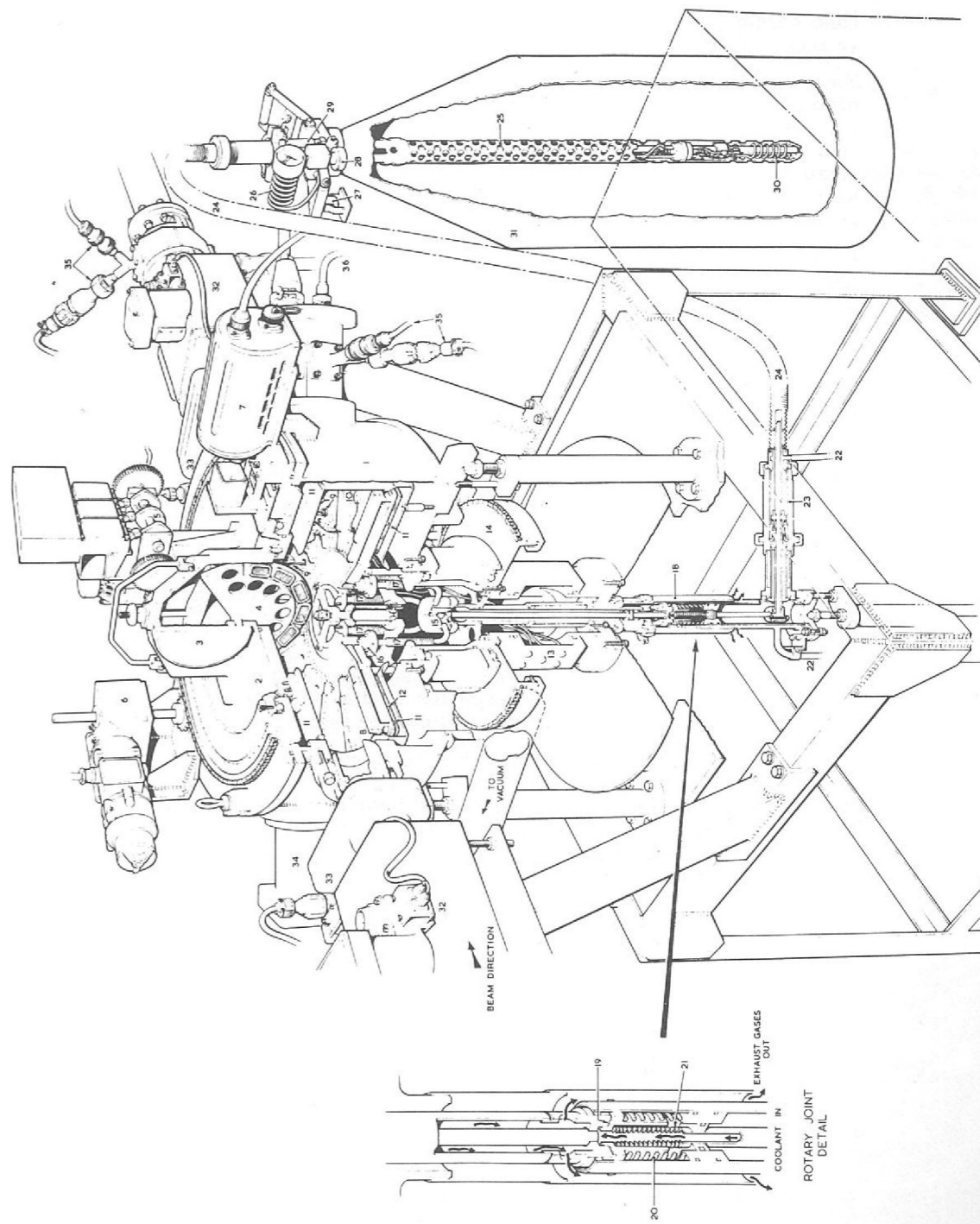


Figure 75. Universal Cryogenic Scattering Chamber.

case assembly designed so that targets may be prepared and transported to the chamber under vacuum, thus preventing contamination of the targets.

Housed in the bottom of the chamber is a circular detector platform on which the detector assemblies may be mounted in ten radial positions. The platform, which is fabricated from aluminium, contains passageways through which the coolant is passed to maintain the detectors at the required operating temperature. A specially designed joint fitted to the underside of the chamber permits rotation of the detector platform even when coolant is being fed into it, at the same time preserving a high vacuum in the chamber. Icing up of the joint is avoided by discharging the exhaust coolant gases over the outside of the joint.

Both the detector platform and the target changer assembly may be rotated in a horizontal plane from a remote control panel. The angular positions of the targets and detectors are at present monitored by closed circuit television but a remote indication system using decimal digitizers has been designed and partially installed.

Liquid nitrogen is dispensed from a standard dewar to the detector platform via a transfer line having a specially designed vacuum jacket. A small heater causes the pressure in the dewar to rise and liquid nitrogen to be expelled through the transfer line. The temperature of the cooled plate is controlled by a commercial potentiometric controller which supplies current to the dewar heater proportional (over a small range) to the temperature error. The required operating temperature may be set at any point between room temperature and  $77^{\circ}\text{K}$ , and servo controlled to  $\pm 2^{\circ}\text{K}$ .

*Hall Plate  
Magnetometers  
for Nimrod  
Experiments*

A Hall plate magnetometer system has been in use on the PLA for some 18 months for precise measurement of magnetic fields. It has proved to be both reliable and accurate, having a long term accuracy of 0.01%. This equipment is now being used with a number of modifications for experiments on Nimrod.

The system consists of a control unit, a constant current source, and a number of probe heads. Normally a digital voltmeter is used for display of Hall voltage, and conversion data from voltage to flux density is obtained by calibration against a nuclear magnetic resonance device.

The original current source which was variable over a range 20-200 mA has been altered to give one fixed value of output current. This simplified the arrangement since the reference voltage is now developed across a two resistor divider chain instead of using a Kelvin-Varley slide. The two resistors are located in the change of state oven used for the current measuring resistors, the Zener reference diode and the error amplifier, thus improving the stability against ambient temperature changes.

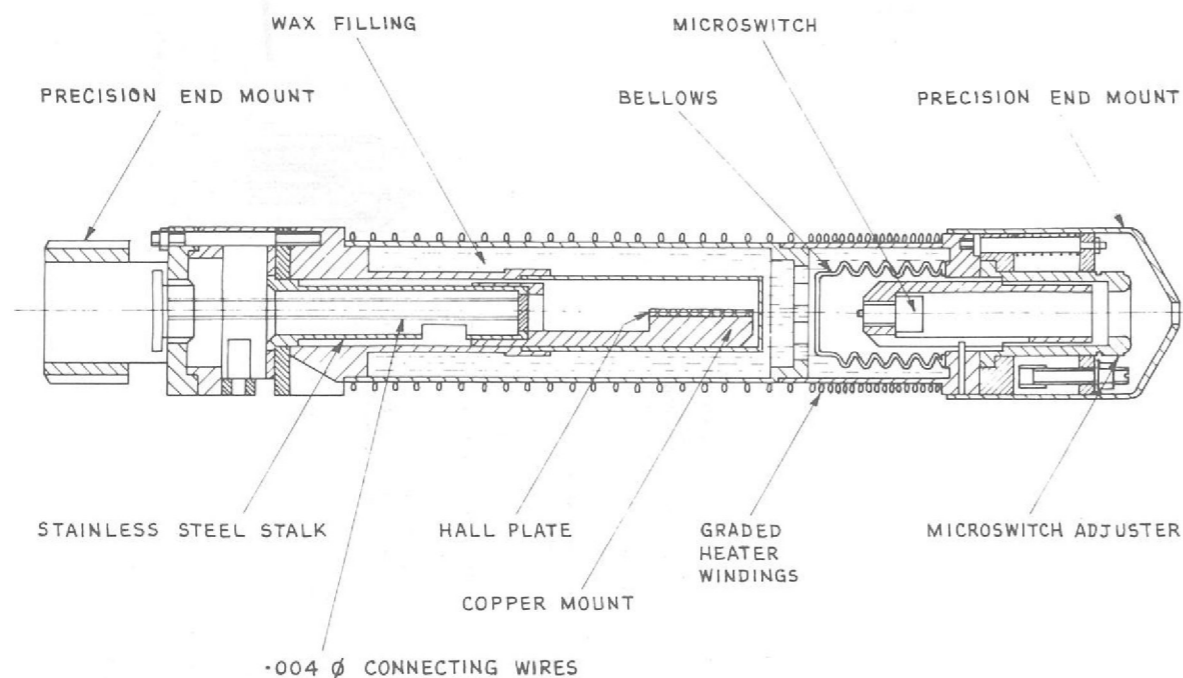


Figure 76. Cross-section of the Probe.

The control unit is for use with a three Hall probe system and is built in a single width '2000' series chassis. A selector switch enables any of the three Hall voltages to be monitored, and also the value of the Hall current. For optimum stability it is important to keep the probe head heater cycling at a rate determined by initial tests; this means that the voltage across the oven winding must be kept at  $24\text{ volts} \pm 1\text{ volt}$ . The heater supplies therefore have switched compensation for cable lengths of 50-250 yards between probe heads and control unit.

The Hall probe units shown in figure 76 are being made to the original design with only one or two modifications. Each unit comprises a Hall plate mounted inside a change of state oven whose temperature is maintained constant at about  $54^{\circ}\text{C}$ . An annular space in the oven is wax filled and the expansion on partially changing from solid to liquid operates a microswitch to control the current in the heating element. Modifications from the original design consist of (i) the use of a standard T05 glass to metal seal to enable more leads to be brought out from the oven cavity, (ii) a Hall voltage dividing resistor, located in the oven, to enable fields in excess of 16 kG to be measured with the same sensitivity on the same range of the digital voltmeter and (iii) an improved method of plug location making each head interchangeable.

## Nimrod Design Group

In addition to the work described below, accounts of many activities of this Group are incorporated in the section on Nimrod (pages 48 to 69).

*Proton Beam  
Extraction  
Systems*

Two Plunging Mechanisms were initially installed in Nimrod's magnet to provide part of the Piccioni extraction system for the extracted proton beams X1 and X2. A significant part of the down time of Nimrod has been due to failure of the swash plate oil pumps that form a major part of these mechanisms. These pumps are the prototype versions of those now commercially available. The cause of failure was traced to fatigue of the forged silicon bronze swash plates, due largely to the very high duty demanded of this pump. Since improvement can only be made by major modification, the running hours are limited to a maximum of 4000. It is planned to change these pumps after approximately 2000 hours which is compatible with the planned machine shut down times. The problems posed by the very demanding performance that is required of these pumps have been pointed out to the manufacturer, and improvements are anticipated.

A number of modifications are in hand to improve the reliability of this mechanism (now known as the Mk I Plunging Mechanism) since it is expected that both of these units will still be used and not changed to the Mk II system described below, and illustrated in figure 77.

The new Experimental Hall 3, will have a primary beam line known as X3, which is designed only for an extracted proton beam; a MkII system will be used. It is essential that a high degree of reliability is obtained from the plunging mechanisms that form part of this extraction system. Experience of the Mk I system showed many areas where the design could be changed to improve reliability and to assist maintenance.

The mechanism has been re-arranged to facilitate maintenance and the new design treats the plunging mechanism, plunged magnet and the straight section box as one system, with equipment arranged to allow for simple replacement with the least disturbance to adjacent parts.

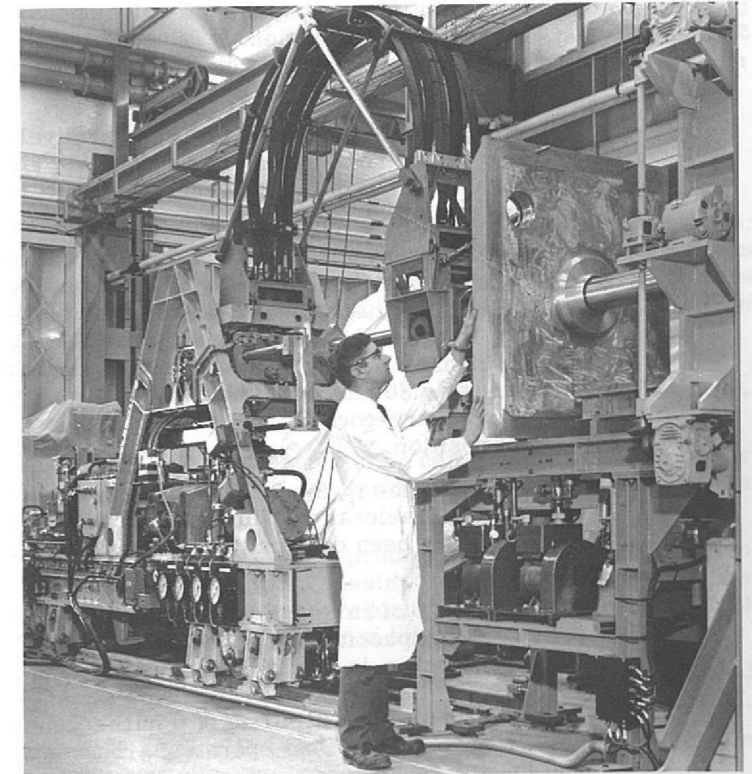


Figure 77. The Mk II Plunging Mechanism.

The performance has been limited to a minimum stroke time of 0.35 seconds, thus allowing the installation of an improved design swash pump and a smaller drive motor. The existing bed shift system (the top part of the mechanism slides on the bottom part) that provides the basic position control of the plunged magnet relative to the mean radial orbit, has been discarded. The whole mechanism is now mounted on rails, and clamped to them by spring loaded clamps, which, when movement of the mechanism is required, are hydraulically off-loaded. This system provides an accurate magnet position control and allows the magnet to be withdrawn from the machine with the minimum of physical contact and in much shorter time. Tests have shown that it is possible to withdraw a magnet and decouple it from the mechanism in 15 minutes. Remote operation is possible with little adaptation.

Commissioning trials on these mechanisms is almost complete. An effort is being made to display in the Nimrod Main Control Room either a trace showing a differentiated angular velocity/time display of the movement of the swash plate of the pump, or a direct display of acceleration.

The latter necessitates fitting to the swash plate an angular accelerometer. This is most desirable but will involve development work. In either case a limit is necessary to the accelerations and decelerations imposed on the swash plate, and a visual or audible register of excessive operation is desirable.

One problem that has arisen on the Mk I mechanism is that of high rate of wear of ball bearings supporting the magnets in the machine. This is not yet resolved, but the design of undercarriage supporting the extractor magnets is being changed to ensure that skidding of bearings in the high vacuum environment is eliminated. A theoretical investigation is in hand to study the mechanism of ball bearing wear in vacuum, and equipment is being assembled to provide realistic test conditions.

#### External Targets

A target known as Oscillating Target Type III was installed in the X2 beam line to provide a facility whereby two experiments can share beam during one pulse from the machine, but from different external targets. Two targets are mounted on a single frame and each is alternately presented to the extracted proton beam during the pulse, by pneumatically oscillating the frame. The system is capable of a movement time of 20 milliseconds, but due to vibration of the supporting structure this time is limited to 50 milliseconds. A stiffer structure will be made to exploit the potentially better performance of the system.

A new design is being manufactured, with eight stations, each carrying a target or diagnostic equipment, that can be remotely indexed into position in the beam. Provision is made for the whole indexing head to be within vacuum if so required. Stations are accurately located to each other, and the indexing head can be moved in three planes with remote actuation and a position 'readout' suitable for computer control. Indexing is effected by a stepping motor driving through a Geneva mechanism modified to provide controlled lost motion at the beginning and end of the motor drive.

#### Fast Vacuum Shut Off Valve

A new type of fast acting shut off valve designed and constructed for use in the Nimrod vacuum system is now in operation. It is used to protect the main ring vacuum vessel against a rise in pressure in the Injector, and is illustrated in figure 78.

The valve is fast acting and uses a comparatively low air pressure (80 lbf/in<sup>2</sup> gauge) for its operation, thus enabling the general site utility air line system to be used.

The operation, damping and re-cocking functions are all carried out pneumatically. The pressure load is held by a mechanical latch which is electrically triggered, control being exercised by any one of three sensing heads which are located not less than 20 feet from the valve itself. The valve may be re-cocked from a remote or local control position.

The closure time is about 16 milliseconds, and its smooth deceleration with complete absence of bounce has been demonstrated by means of a high speed film.

An adaptation of an 8 inch version of this valve provides a compact fast acting electrical contact breaker closing in 8 milliseconds with a gap setting of  $\frac{1}{4}$  inch when operating with air at 80 lbf/in<sup>2</sup> gauge. A closure time of 6 milliseconds can be achieved with an operating pressure of 150 lbf/in<sup>2</sup> gauge.

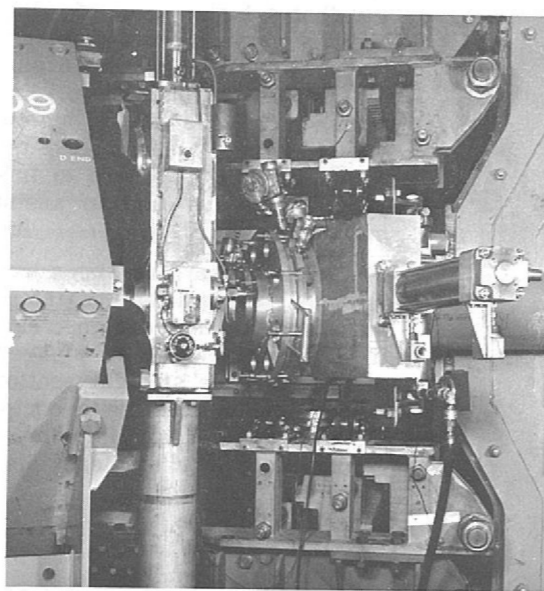
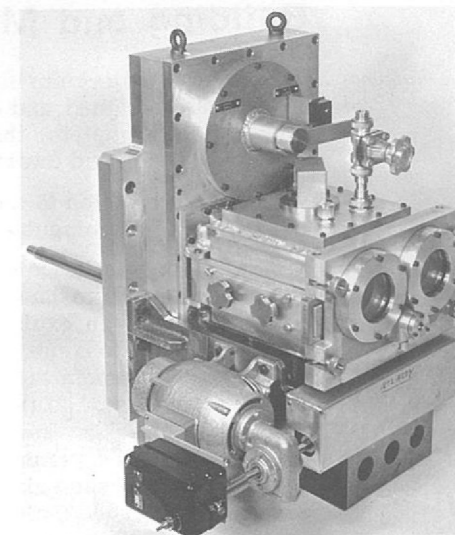


Figure 78. 8 inch fast shut-off valve in beam line.

Figure 79.  
Internal target mechanism.



#### Internal Target Operating Mechanisms

These mechanisms (see figure 79) have been in use over the last year and have proved to be useful and reliable. Although  $4 \times 10^6$  operations have been achieved with these mechanisms, the probable life is limited by the composite bearings and some bearing development work has been initiated. This investigation uses a parallel motion mechanism to investigate dry running with high lead content bearings.

#### Extraction System Magnets

A general purpose septum magnet known as XM9 is to be used in Nimrod Straight Section 4 for a modified Piccioni extraction system and for a resonant extraction system. This magnet is now being built, the yoke consisting of 105 plates each 6mm thick separated by 0.005 inch thick Melinex film bolted together with four 1 inch diameter high tensile steel bolts. The yoke is 310 mm  $\times$  310 mm  $\times$  700 mm long, weighing approximately 1500 lbs. The yoke profile (approximately hyperbolic) was machined to within  $\pm 0.0025$  inches. The 1 cm septum is made up from 4 copper sheets each 2.5 mm thick with twenty 0.75 mm  $\times$  2 mm water cooled channels formed in the copper by the lost indium process. The septum is designed for a heat dissipation of 45 kW.

A header vessel quadrupole magnet (XHQ2) is being designed for a modified Piccioni extraction system. The magnet has 6 mm laminations, with an overall length of 1 metre. It will weigh approximately 1 ton. It is being designed in two halves to facilitate assembly of the windings made up of 120 hollow copper conductors carrying 133 A.

A solid yoke magnet 700 mm long (RX1), with a through aperture of 4 cm and a water cooled copper septum 3 mm thick, was built and installed in Straight Section 7. The septum was made from a copper sheet with twenty 1 mm  $\times$  1.5 mm water cooled channels formed in the copper by the lost indium process. Its total weight is about 105 lbs. This magnet was plunged vertically in 0.5 seconds with a down stroke of 6 inches and withdrawn in about 1 second, and was operated by a hydraulically driven rotary actuator. The magnet septum was adjusted radially by tilting the ram tube. Through this tube was carried the excitation current (up to 7000 A peak) and the cooling water. Another magnet has been designed for use in Straight Section 3 resonant extraction experiment. This is a laminated magnet with a through aperture of 6 cm with a 2.5 mm thick septum.

## Engineering Services Department

This Department of Engineering Division includes among its functions the following activities; arranging for the design and construction of new buildings and the maintenance and modifications of existing buildings, the operation and maintenance of all site installations and services (except the accelerators and beam lines), electrical and electronic design, procurement of equipment, materials technology and technical records.

#### Technical Services

The Section provides a Laboratory service for estimating, drawing reproduction and storage, and a catalogue library as well as maintaining centralised records for the Department.

Estimates are prepared to enable alternative design schemes to be compared financially or for budgeting purposes and to control expenditure on running contracts with industry who work on a time and material cost basis.

Some 125,000 drawing reproductions or "blue prints" were produced in the year mainly from the Laboratory's own dye line printing machines. An increasing use is made of microfilms enabling 60,000 drawings to be stored thereby very greatly reducing storage space whilst still providing ease in examining stored drawings when it is required to do so.

Several thousand proprietary catalogues, price lists and technical brochures are accommodated in the library provided for that purpose and a reference and loan service is available to all staff.

During the year the Section provided information and statistics and collaborated with private consultants engaged on industrial staff productivity research.

## Building and Mechanical Services Group

### Buildings (225)

The major project during the past year has been the construction of the Experimental Hall 3, which was designed and constructed in conjunction with the UKAEA Engineering Group, and is now almost complete; the main building, shown in figures 80 and 81, is 300 ft long, 150 ft wide, 65 ft high and dwarfs all the surrounding buildings.

A four bay extension to the main Laboratory office building (R1) to house ancillary services for the IBM 360/75 computer is due to be completed by June 1969.

Minor building works completed during the year include the adaption of the Heavy Liquid Bubble Chamber annexe to have two frangible and two explosive resistant walls (see Figure 59); the construction of an explosive resistant, demountable, control room; permanent offices for the Safety Group; extensions to the Film Processing building to provide bubble chamber film archive store and dark room facilities; a display and exhibition corridor leading to the Nimrod Control Room; an extension to the Electrical Groups workshops; and new car parks and access roads.

### Mechanical Services

In addition to the planned maintenance of the existing raw, demineralised and cooling water, heating, compressed air, gas and drainage services for the whole site new work has also been completed in 1968. Included in this is the design and installation of the air conditioning system for the IBM 1130 computer, and another stage of the helium recovery system with an additional 1000 ft<sup>3</sup>/hour compressor and additional collection points. The Chemistry Group's new location was provided with air conditioning, fume extraction and cooling water.

The Heavy Liquid Bubble Chamber area's heating and ventilating system was remodelled in conjunction with an emergency system with high level gas discharge, the vent chimney being fitted with explosion relief panels. Other new work included specialised services to the Film Process Laboratory, the Electrical Workshop and a motorised damper installation to safeguard the bubble chamber cooling system.

### Manufacturing Services

The main workshop completed over 650 jobs, at costs of up to £2000 each; included are the assembly and machining of laminated magnet yokes and trolleys for the main extraction magnets of Nimrod.

About 60 industrial firms have assisted in the production of a further 1800 jobs, the value of the work in hand at any one time having risen from £27,000 in 1967 to £32,000 in 1968.

## Electrical Design and Services Group

### Magnets for Beam Extraction and Beam Transport

As has been pointed out elsewhere in this Report, an improved beam extraction system is essential if the new Experimental Hall 3 is to be fully exploited. To permit two pulses to be extracted in one accelerator cycle a further redesign of the extractor magnet has been undertaken. This magnet must now be switched rapidly from one field level to another and requires a laminated yoke instead of the solid yoke used previously. Consequently it is no longer practicable to cool

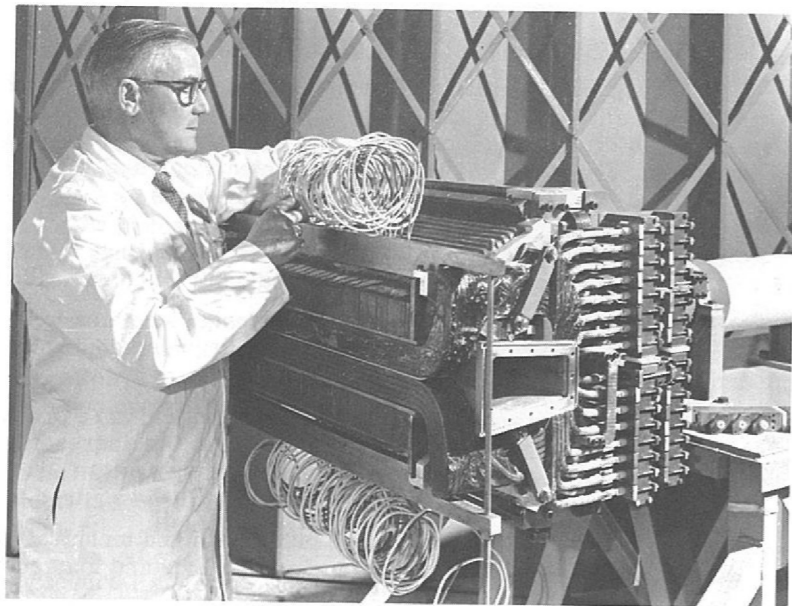


Figure 82. Assembling an Extraction Magnet.

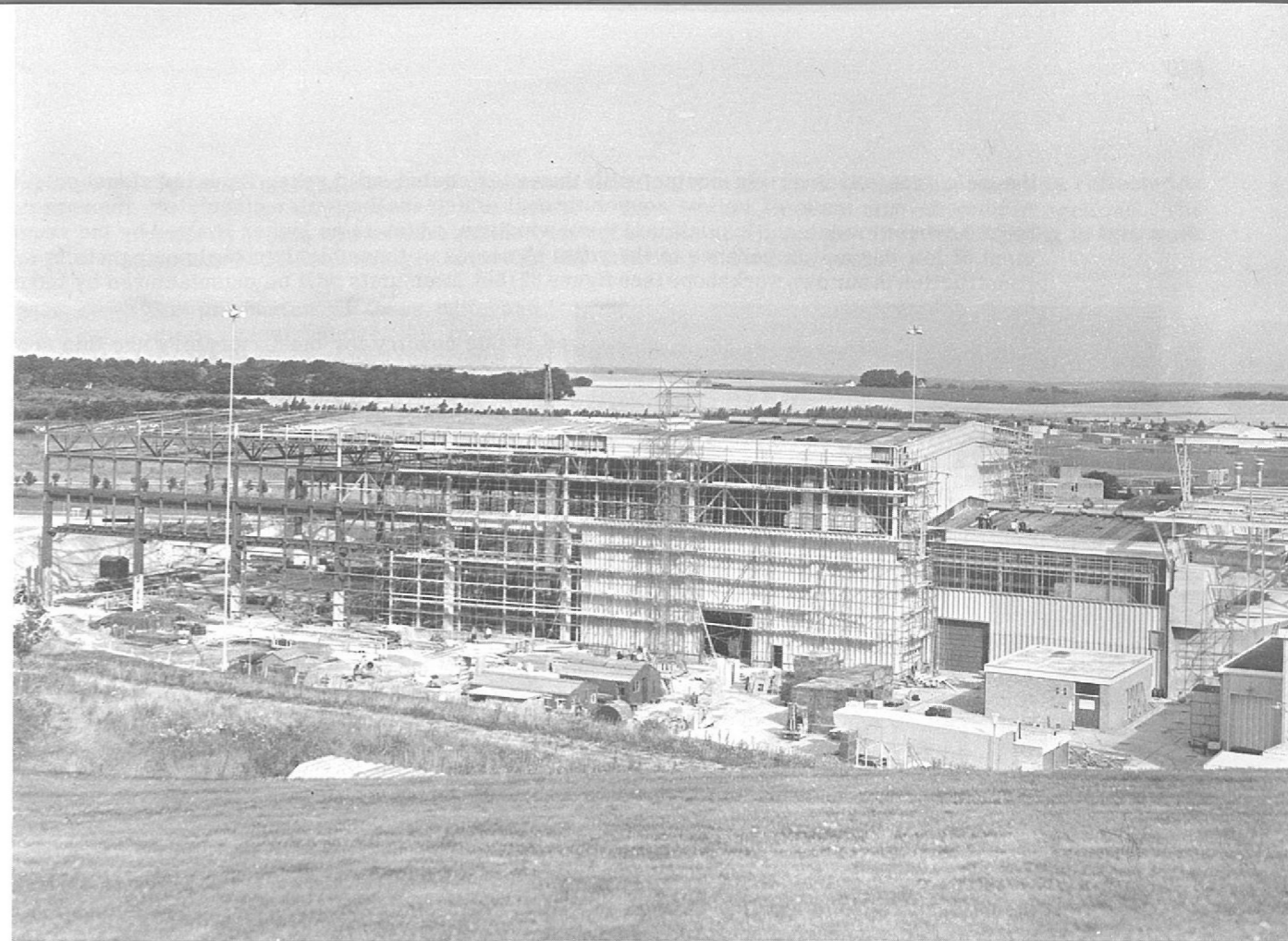


Figure 80. Construction of the new Experimental Hall. August 1968.

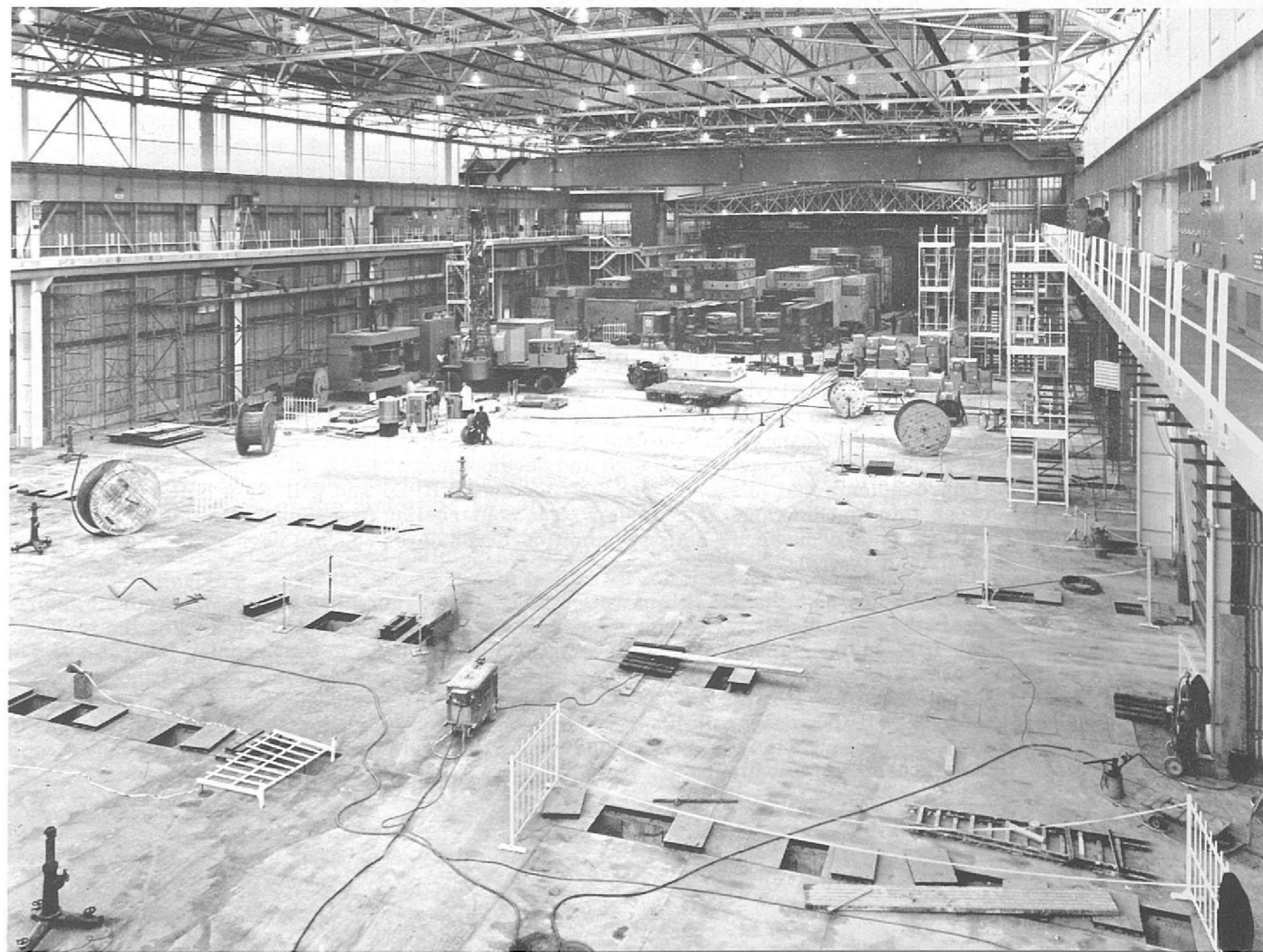


Figure 81. Inside the new Experimental Hall 3. December 1968.

the pole face windings via contact with the water cooled solid yoke. Each individual pole-face winding is now made of hollow copper through which cooling water circulates. Improvements have also been made to the insulation of these windings, which is no longer limited by the requirement of low thermal impedance to the yoke. A series of these highly complex magnets is under construction in our own workshops (see figure 82) but later units will be manufactured by industry under guidance.

The most difficult magnets yet manufactured in this country for the Laboratory are thin septum bending magnets required for the target blockhouses of the X3 extracted proton beam for Hall 3. The requirement of the thin septum involved a reduced copper section for this part of every turn; two sizes of hollow copper were therefore used and two joints made per turn. The current density in the septum is 75,000 A/in<sup>2</sup> at full power. Two such magnets have been delivered and have been successfully tested.

The 1967 Report referred to the K9 beam line stepping magnet system. A similar system incorporating further improvements and refinements was designed, built, installed and successfully used in the K11 beam line during the past year.

#### Superconducting Magnets

The construction of the 40 kG superconducting bending magnet is nearly complete after six months of sustained effort in the electrical workshop. A considerable amount of development work was necessary in order to overcome problems in the fabrication and insulation of the windings and in providing them with adequate support against the very high electromechanical forces which will exist in service. Tribute must be paid to the skill and the patience of the craftsmen who wound these coils with each of the many hundreds of turns positioned to an accuracy of a few thousandths of an inch. The windings can be seen in Figure 64, and the cryogenic aspects of this magnet are described on page 102.

Development has included a pulsed bridge method for testing this magnet for inter-turn short circuits and a complex flux readout and control system. This flux control system uses a Hall probe as the sensing element and maintains the magnetic field at its preset level when the supply leads from the external power unit are disconnected so reducing the consumption of liquid helium. The output stage of this system is yet to be completed. It comprises a superconducting air-cored transformer with mechanical contacts operating as a flux pump and mounted in the cryostat. This design was adopted because of the difficulty of magnetically shielding the rotary type of flux pump available commercially.

The power supply for this magnet has been designed and constructed. It consists of 2000 A transformer-rectifier set used initially to bring the magnet up to the working current level. The protective system is being developed so that in the event of the magnet going normal it will rapidly discharge the stored energy into an external dump resistor. Design and development work is complete on a range of instrumentation used for monitoring auxiliary aspects of this magnet system. This includes liquid helium level, controlling liquid nitrogen level, strain measurement and temperature measurement.

Other activities include support work for the power supply and protection system for the testing of the RACOON coil now being manufactured for the HFBC (see page 91), evaluation of requirements for a high current power supply for superconductivity work and the specification of a 15000 A supply for this purpose, and development of a helium control system for the polarized target.

#### Film Analysis Machines

The early part of the year was spent on the final detailed improvement of the automatic film measuring machine HPD1, to increase its reliability and efficiency and to allow it to be controlled by computer operators (see figure 58). It is now classed as a production machine with daily and longer term maintenance under the control of the specialist maintenance section. The engineering team is now engaged upon the design and development of HPD2 which will take a stage further the improvements that followed from the speed up of HPD1 and will allow better communication between this machine and the computer. The construction programme for this work will follow a critical path deduced by using a modified CAPSTAN program developed by AERE for such analysis and control.

The main efforts of the Track Analysis Maintenance section has been to incorporate improvements in the rough digitizers as they are prepared for on-line operation following the installation of the IBM 1130 computer and its associated machine links in the scanning laboratory. These improvements are intended to allow even longer intervals between routine maintenance procedures without losing the steady increase in machine reliability already achieved. Besides the work taken over on HPD1, responsibility has also been assumed for another automatic film measuring device, the CRT machine CYCLOPS (see figure 57); in this case electronic performance, operational checks and fault finding are included.

#### Electronic Services

The ever increasing use of electronic techniques in the work of the Laboratory is reflected in the growing work load in the electric manufacture, repair and calibration sections. The majority of jobs now involve printed wiring and the small design office specialising in this work produced 125 card designs involving 800 drawings during the year.

The production of these units and others under contract by industry has an annual value in excess of £100,000, and varies from single items to small batch production on very short time scales. This work load reached its peak in August, in order to meet the requirements of the two experiments now being carried out at CERN. These services are also made available to other SRC establishments with similar requirements. Data acquisition equipment for computer control of the X3 beam line is being built following a design similar to that used at CERN.

The electronic development work has continued to concentrate on stabilised power supplies, protection, field measurement and direct current transformers. The solid state replacement for the 5kW amp-lidyne generators used in large numbers around the Laboratory is complete and is awaiting acceptance tests. The model shop has developed a line of small regulated power units with a separate overvoltage/overcurrent protection card which will be standardised by the Laboratory and will be stocked by the Stores together with a low cost 19 inch chassis system.

Much of the instrumentation in use is of recent design and liaison with the manufacturers enables the best performance to be obtained from the instruments; in return the manufacturer benefits from the knowledge of performance in the field particularly as this often covers abnormal environmental and operational cycles. Where time scales allow, full use is made of specialist industrial concerns for the repair and calibration of commercial high quality instruments and data processing equipment.

The standards and calibration room facilities and equipment are in great demand and particularly in the field of voltage standards, calibration and measurement together with accurate resistance measurement. In this connection assistance has been provided to one of the Laboratory's contractors, who are making power units with digital/analogue converters of high precision for the CERN ISR project.

#### Electrical Services

The new substation supplying power to Hall 3 is in use and the last of the four packaged sub stations (each providing 2.5 MW at 415 volts) is being installed in the Hall (see figure 84). This increases the installed transformer capacity within the Laboratory to 38.5 MVA. Other site installation work in hand in Hall 3 concerns the a.c. and d.c. cabling to and from the rectifier gallery where extensive use is made of solid aluminium conductor cables.

The installation work in the Laboratory is performed by contractors, working under the supervision and guidance of the Laboratory staff who also do the initial design work and advance order most of the materials and plan the work. The total value of this work is over £100,000 for this year being enhanced by the peak load of the Hall 3 installation work. Installations completed during 1968 for building services and plant include the extension to R20 and R2, the refurbishing of R34, and M-G sets in R5, R6 and R25. There was also a wide variety of equipment associated with Nimrod and the bubble chambers including a new arrangement of supplies for the Heavy Liquid Bubble Chamber with controls and ventilation adequate for use with propane.

The use of contractors for the planned maintenance is increasing wherever possible thus allowing more efforts to be devoted to specialised manufacture such as the superconducting and extractor magnets referred to earlier. Other manufacturing work completed during the year includes a vacuum control cubicle for the AERE Variable Energy Cytotron ion source, and a 20,000 A transistorised regulator shown in figure 85 is nearing completion.

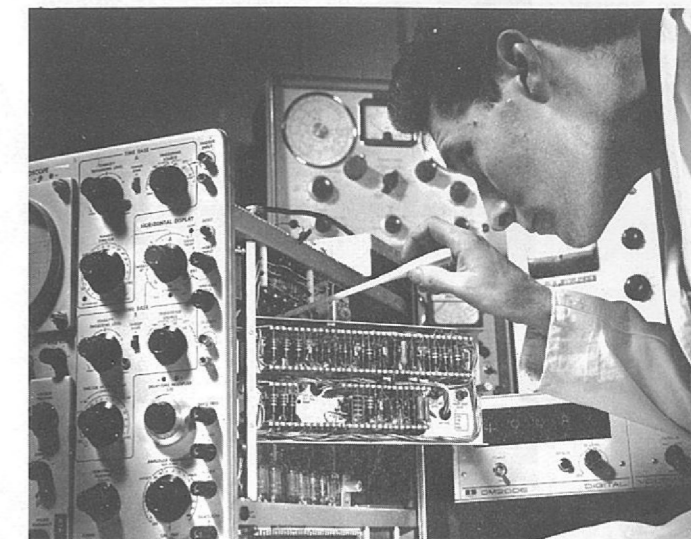


Figure 83. Servicing electronic equipment.



Figure 84. One of the 2.5 MW packaged substations in Hall 3.

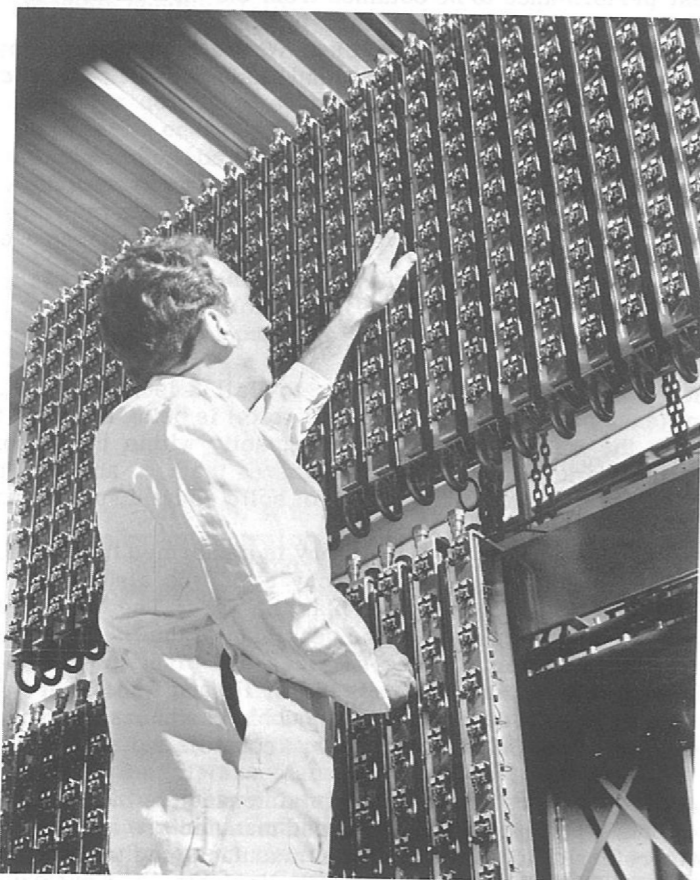


Figure 85. Assembling the 20,000A transistorised regulator.

## Chemical Technology and Radio Chemistry Group

(220, 221, 224) The larger cryogenic test apparatus mentioned briefly on page (102) under "Low Temperature Testing of Materials" is in regular use and some 250 tests have already been completed. The items investigated include such diverse subjects as magnet sub-assemblies, soldered and adhesive bonded joints and materials, composite reinforced plastics and thermoplastic materials, some of this work being undertaken in response to industrial requests. Further development of the test apparatus will include a multi specimen test rig which is designed to minimise down time for specimen changing and to effect economies in the consumption of liquid helium. The low temperature testing facility is shown in figure 86.

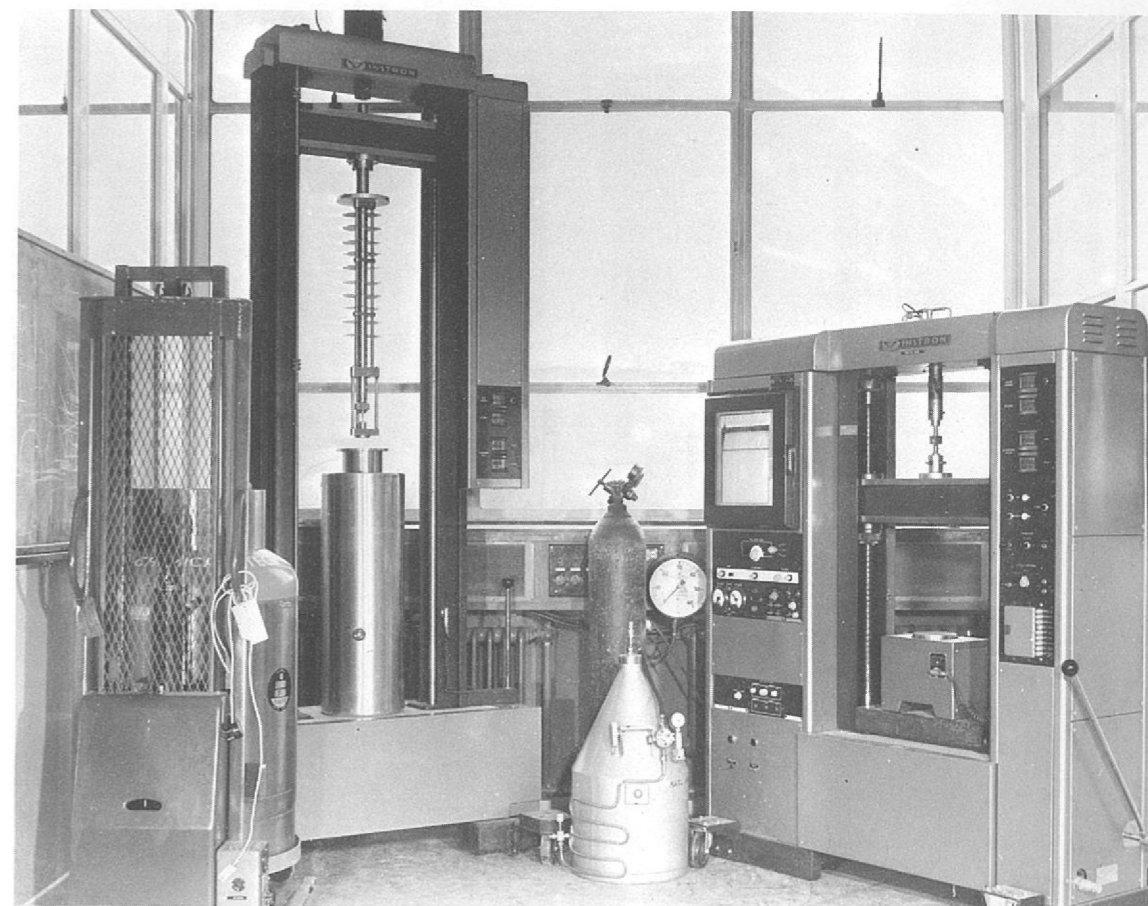


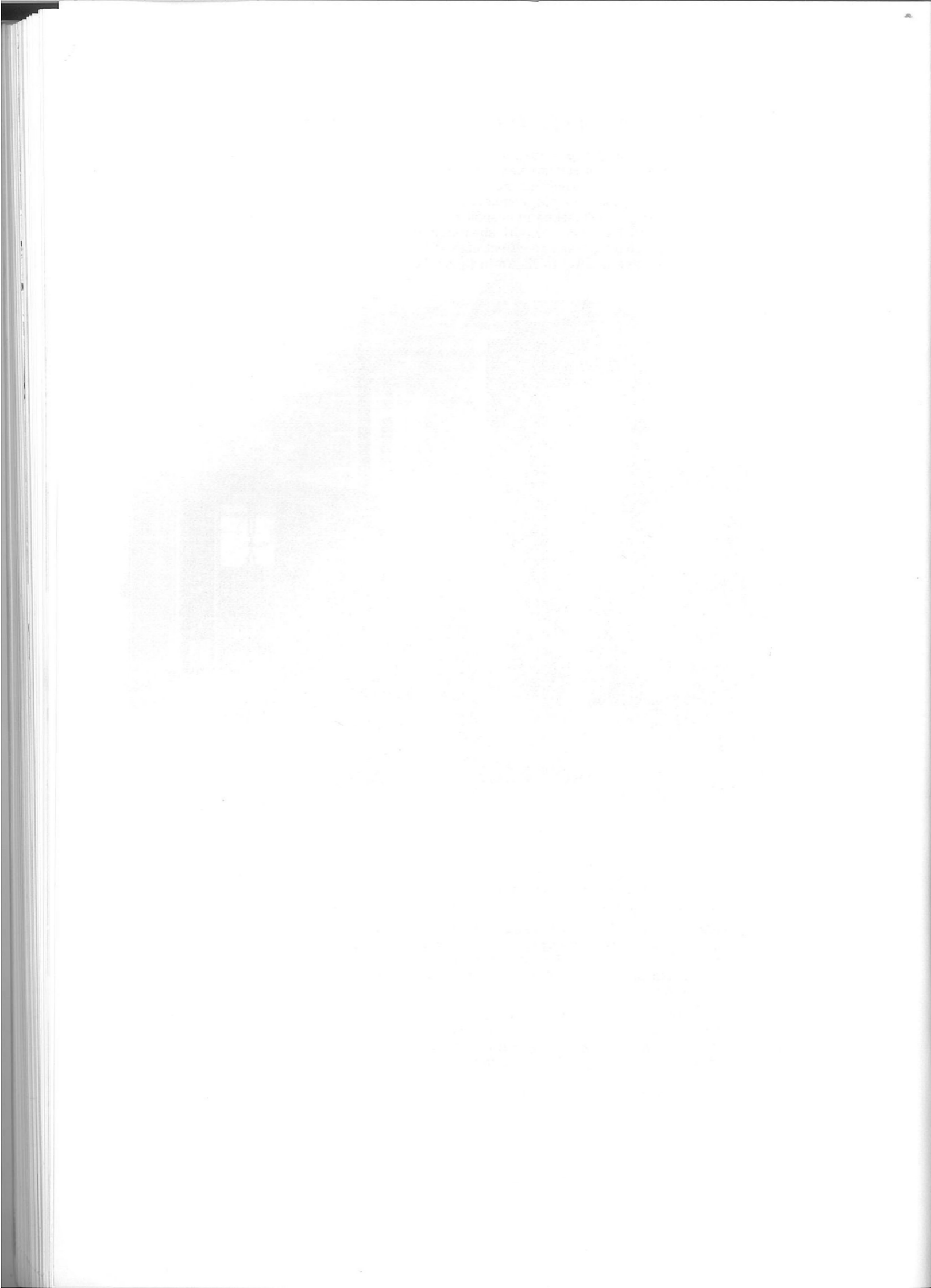
Figure 86. Low temperature testing facility.

The programme of evaluating the mechanical properties of insulators under conditions of severe ionising radiation has continued and a number of insulating systems that had been shown to be satisfactory have been successfully applied by industry in contracts for commercial magnets.

Improved data on the radiation levels around the Nimrod vacuum vessels, beam lines and other components has been obtained using the hydrogen pressure dosimeter. This has enabled greater resolution of the dose pattern to be obtained which can thus more easily be related to the various operational modes of Nimrod. The device is now in use in a number of accelerator centres throughout the world.

A recent innovation, now covered by a provisional patent application, is a technique for constructing magnets using a cementaceous aggregate. The process is now being developed and commercially exploited, its advantage being that it permits the construction of magnet coils which will not suffer damage from the high levels of radiation to be found in the large accelerators planned for the future.

ADMINISTRATION  
DIVISION



ADMINISTRATION  
DIVISION

# Administration Division

## Division Head and Laboratory Secretary: J.M. Valentine

This section of the Report covers the work of the General Administration, Personnel, Finance and Accounts, and Scientific Administration Groups, together with details of the training courses pursued by Laboratory employees. The financial data refers to the financial year 1968-69, the training report covers the academic year 1967-68, while other parts of this section, like the rest of the Report, deal with the calendar year 1968. Though there are few innovations to report, the year has been a busy one; comparison of the statistical data with that for 1967 shows a general all-round increase of the order of 5%.

### Experiments at CERN

Two of the experiments in the Laboratory's High Energy Physics programme are being run at CERN, one on the Proton Synchrotron and the other on the Synchrocyclotron. (These are experiments 14 and 15, described on pages 27 and 28). Several sections of the Administration Division have been involved particularly those concerned with the transportation of equipment and the accommodation of the experimental teams and their families. The CERN administration has co-operated to the full at every stage and the exercise has afforded further opportunities to compare administrative practices at the two Laboratories.

The Stores section has been responsible for despatching over 100 consignments during the year, the total weight of equipment being 55 tons. This has involved a great deal of work in connection with customs clearance and documentation, as well as with packing and arranging transport. The difficulties have been eased by the adoption of modular control rooms built from international package freight containers, which are described in detail on page 107.

The Laboratory now have leases on 19 apartments and one villa in Geneva, all this accommodation being fully furnished. The CERN Housing Officer has sub-leased 10 apartments to the Rutherford Laboratory and has assisted in the arrangements for leasing the remaining property from private landlords.

### Travel and Subsistence

In connection with the installation of these experiments, a number of short visits to CERN have been made by engineers, technicians and craftsmen. This, and the long-term arrangements mentioned earlier, have been in large measure responsible for the substantial increase in the number of travel bookings made during the year. Short-term overseas visits totalled 366, long-term postings 62, and over 8,500 individual travel and subsistence claims were paid.

### Computer Processing of Administrative Records

During the year the application of computer techniques has been extended to a wider range of activities. All the programs are written in COBOL and special precautions are taken to ensure the privacy and permanence of the record files. The advent of decimal currency has been catered for and the disruption at change-over date should therefore be minimal.

It was mentioned in last year's Annual Report that programs has been written to monitor stock levels and to initiate re-ordering in respect of certain stores items. This work has now been extended to provide analyses of costing stores withdrawals to projects; the programs are expected to be fully operational by early 1969. ADP techniques have also been applied to personnel records. Basic data on every employee is now held on a magnetic tape file, from which lists, sorted for instance by grade, can be printed as required.

With the completion of this work, it has become possible to devote more effort to computerising the records and procedures of the Finance and Accounts Group. Records of cash flow are already maintained and updated by computer methods, and the next stage will be the development of programs for the recording of commitments against project budgets. The automation of other financial operations is under consideration; decisions on future development will be taken in the light of experience gained with the cash flow and commitment programs.

### Finance

The Laboratory's expenditure for the financial year 1968/69 totalled approximately £7.5 million, of which £1.4 million was for capital items and £6.1 million was recurrent. Apart from staff expenditure, the remaining sum of £5.21 million resulted from 23,800 invoices. The items making up the £7.5 million total expenditure are shown below, together with a diagrammatic breakdown of the R & D expenditure. A direct comparison with the corresponding diagram for last year is not possible because of organisational changes; there have, however, been no major changes in the distribution.

	£ million
Staff Expenditure	2.29
Research & Development	3.81
Plant and Equipment	0.67
Building Works	0.73
	<u>7.50</u>

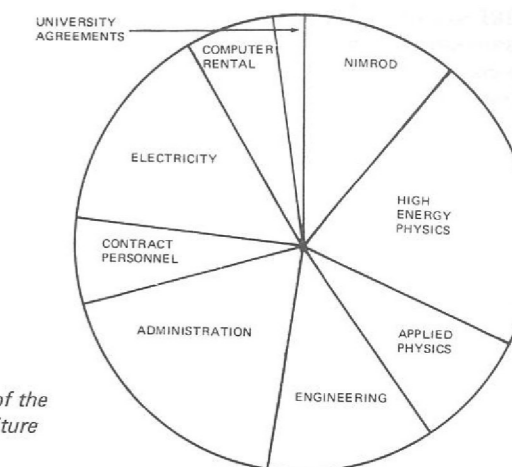


Figure 87. Breakdown of the £3.81 M R & D expenditure

Staff Numbers The Table below shows the staff position at the beginning and end of the year.

### Staff Numbers for 1968

	Opening Strength 1.1.68	Changes during 1968		Closing Strength 31.12.68
		Gains	Losses	
<b>PROFESSIONAL</b>				
Senior and Banded Staff	18	6	1	23
SO class	63	11	12	62
Fixed Term	39	16	23	32
Research Associates	0	15	0	15
Exp. O. class	123.5	17	14.5	126
Engineers I, II, III	95	7	2	100
ADE	9	0	4	5
<b>Total Professional</b>	<b>347.5</b>	<b>72</b>	<b>56.5</b>	<b>363</b>
<b>ANCILLARY</b>				
SA and SSA	67	15	24.5	57.5
Draughtsmen	33.5	17	8.5	42
Technical class	203.5	17	12	208.5
Non-Techs. and Stores	36	3	3	36
Executive	30	5	3	32
Clerical	46	13.5	11	48.5
Secretarial and Typing	28	9	9	28
Photographers	5	1	2	4
Photoprinters	5	0	0	5
Machine Operators	9	7	3	13
Asst. Hostel Manageress	1	0	0	1
Telephone Operators	0	2	0	2
Scanners	27	18	6	39
<b>Total Ancillary</b>	<b>491</b>	<b>107.5</b>	<b>82</b>	<b>516.5</b>
<b>INDUSTRIAL</b>				
Craft	174	44	30	188
Non-craft	157	30.5	39.5	148
Apprentices	34	6	6	34
<b>Total Industrial</b>	<b>365</b>	<b>80.5</b>	<b>75.5</b>	<b>370</b>
<b>GRAND TOTALS</b>	<b>1,203.5</b>	<b>260</b>	<b>214</b>	<b>1,249.5</b>

The figures listed under "changes" include new entrants, resignations and promotions. Staff on sandwich courses, and those working part-time are counted as half.



The figures on the previous page relate to the staff of the Laboratory; in addition some 97 students have spent periods of up to 6 months at the Laboratory during university vacations or as part of their industrial training.

The new entry in the Table of "Research Associates" reflects a recent change in the method of employing research physicists on short-term appointments. The former systems of Fixed Term Appointments in the Scientific Officer class has been replaced by one analogous to the Civil Service Research Fellowship scheme. In future, SRC Research Associates will be appointed, normally for a period of three years, at a fixed salary arrived at by reference to Civil Service SO, SSO and PSO salary scales.

**Staff Relations** The local Whitley Committee and Joint Consultative Committee (for non-industrial and industrial staff respectively) have continued to meet regularly and have successfully fulfilled their functions as forums for discussions and negotiations concerning a wide range of staff matters. Among the most important agreements reached at the Joint Consultative Committee was the abolition of time-clocking for industrial employees.

Members of both committees have participated fully in SRC-wide negotiations which have led to the agreement of further chapters in the appropriate Conditions of Employment Manuals. In January 1968 it was agreed at the SRC Joint Negotiating Committee that industrial employees of the Council (two-thirds of whom work at the Rutherford Laboratory) would adopt Civil Service rates of pay and general conditions of service. For the Rutherford Laboratory industrial staff this involved the severance of the links with the UKAEA staff structure and a transfer of super-annuation rights from the UKAEA scheme to that of the SRC.

**Training** The Laboratory's policy of encouraging its staff, by means of training concessions, to pursue suitable courses of further education and training was described in detail in last year's Report, and has continued to operate. The detailed figures which are tabulated below are remarkably similar to those for the academic year 1966-67, the only difference worthy of note being an increase in day class attendances at the expense of evening classes. The courses attended covered the entire spectrum from GCE O-level to M. Sc.

	Short Courses	Evening Classes	Day Courses	Full-time Courses	Examinations	
					Entrants	Passes
Scientific Staff	64	6	42	11	50	43
Engineering Staff	185	19	155	1	147	108
Administrative Staff	19	6	3	0	3	3
	268	31	200	12	200	154

Three of the evening students attended courses leading to University of London M.Sc. degrees in Physical Electronics (1) and Radiological Physics (2). One full time student gained an M.Sc. while holding a college Research Assistantship. The other eleven full-time students were engaged on first degree courses, one with an SRC award and the remainder with Local Authority awards. One other student graduated during the year, with an Honours degree in Applied Physics.

The Laboratory provided industrial training for 1 M.Sc. and 46 first degree sandwich course students in Applied Physics, Applied Chemistry, Applied Mathematics and Electronics. 4 Scientific Assistants, 7 Student Apprentices and 22 Craft Apprentices received training at the specialist schools run at AERE.

**University Research Agreements** During the year agreements were in force with the Universities of Birmingham; Bristol; Cambridge; Exeter; Glasgow; Liverpool; London (Imperial College, Kings' College, Queen Mary College, University College, Westfield College); Manchester; Oxford; the Queen's University of Belfast; Salford; Southampton; Surrey. The following list shows the number of these agreements at the beginning and end of 1968, classified according to type of research.

Classification	1.1.68.	31.12.68.
Experiments with Nimrod	15	11
Experiments with PLA	7	7
Extra-mural Research	3	3
University use of AEA Accelerators	3	8
Major Film Analysis Projects	3	2
	<u>31</u>	<u>31</u>

**Exhibitions** The Laboratory contributed an exhibit on the hydrogen evolution radiation dosimeter to the 1968 Physics exhibition. This device, which was described in last year's Annual Report, measures integrated doses in the megarad range; it is now being manufactured commercially under licence. A joint exhibit with the Daresbury Nuclear Physics Laboratory at the Manchester International Vacuum Congress illustrated the exacting demands made on vacuum technology by modern particle accelerators.

A display centred on the Helium Bubble Chamber was mounted in connection with a Royal Society soirée. A model of the chamber originally built for this occasion is now on loan to the Ministry of Technology who are using it as part of a mobile display unit which is touring schools in the United Kingdom in order to stimulate interest in professional engineering as a career.

During the year facilities were provided for eleven firms to exhibit and demonstrate their products at the Laboratory. In several such cases seminars were arranged on topics closely connected with the equipment being shown, examples being computers and high vacuum technology.

**Conference Organisation (135)** Two symposia were held during the year. The first lasted for two and a half days in March, the subject being the use of Nimrod for nuclear structure studies. There was an attendance of about 180 and the proceedings have been published as a Rutherford Laboratory Report. A less formal one-day meeting in October discussed the future development of automatic bubble chamber film measuring; the proceedings are in preparation.

**Visits** Conducted tours of the Laboratory were arranged for parties totalling 1050 persons, mainly from professional institutions, scientific societies, universities, technical colleges and schools. Nimrod is seldom accessible to such visitors; a display area has therefore been provided in which slide projectors and pictorial panels can be used to describe the Laboratory's research programme. The revised Nimrod brochure and the two films "Rutherford Laboratory" and "Nimrod" are also used during visits; the films have been loaned to outside organisations on frequent occasions.

During the summer 15 students in the 15-16 age group spent a fortnight at the Laboratory under a scheme devised in conjunction with the Technical Education Unit of Reading University. They worked on small but nevertheless genuine tasks in various parts of the Laboratory in order to gain an insight into the realities of science and technology. During April about 50 members of the IPPS Low Temperature Group visited the Laboratory and participated in informal talks and discussions relating to the Laboratory's work in the cryogenic field. Visits have also been made by managerial representatives from a number of British industrial firms and organisations, including the British Nuclear Forum and the Electrical Research Association; tours and discussions on suitably selected topics were arranged to illustrate the ways in which collaboration could be beneficial.

**Library and Documentation** Total loans have once again exceeded those of the previous year, as shown in the adjacent graph. All but 9% of the 6143 items borrowed were supplied from the Library's own holdings, which during the year were increased by 940 books (520 new titles), 3200 reports and preprints and 200 pamphlets. The total stock is now:

Books	6840 volumes
Reports & Preprints	14700 titles
Pamphlets	880 titles

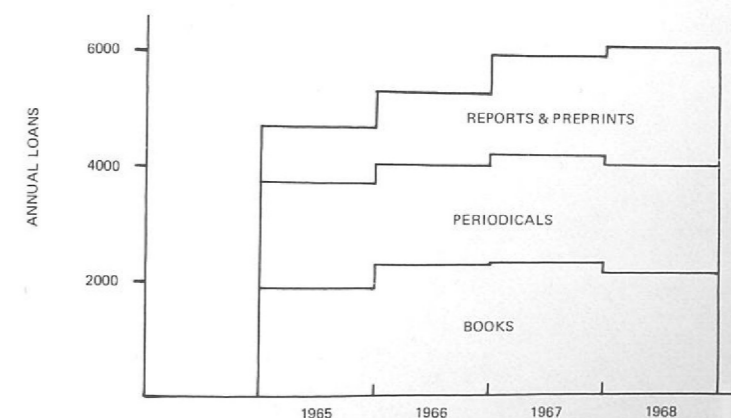
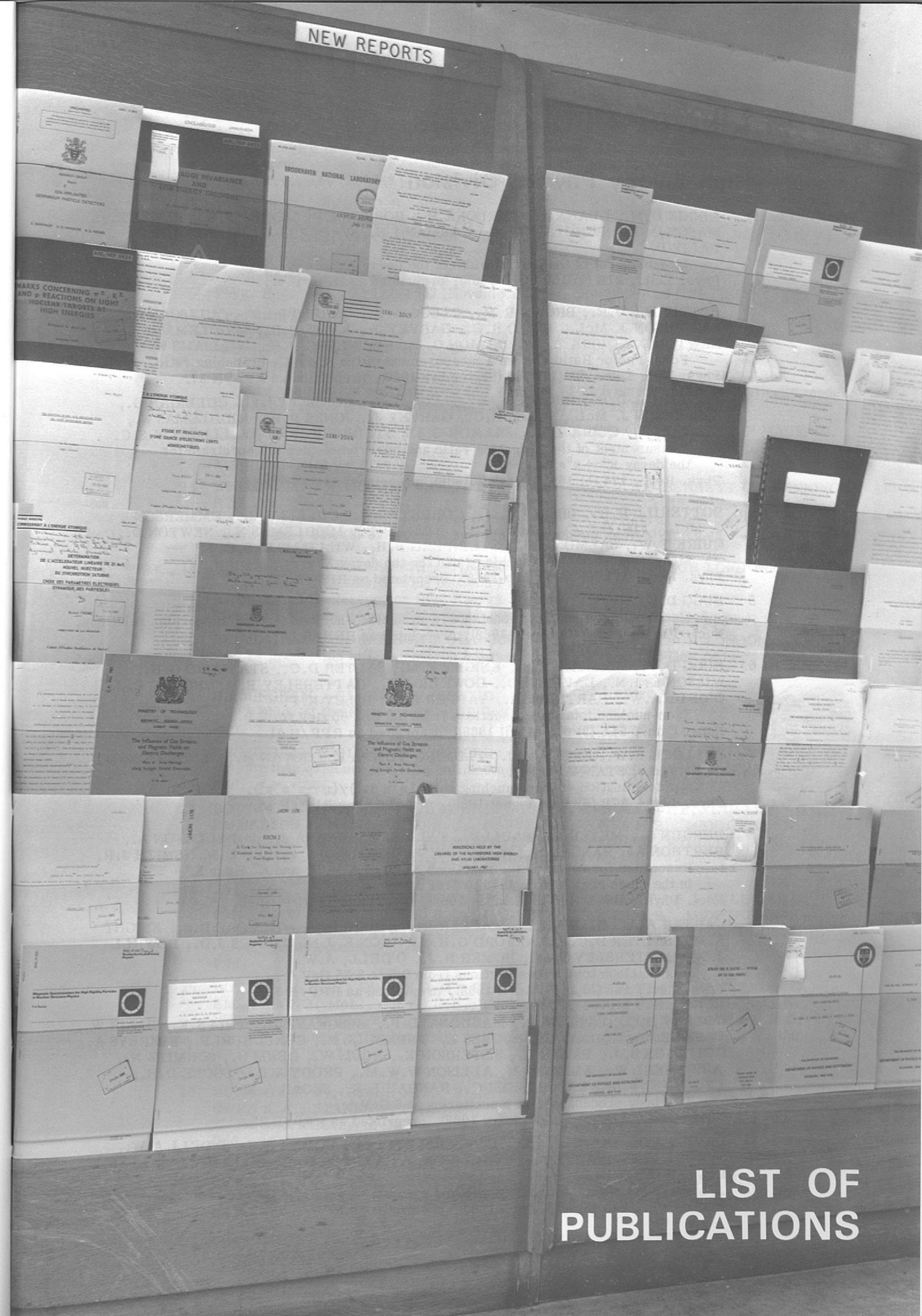


Figure 88 - Annual growth of Library loans.

The number of periodical titles taken remains at about 400. The publications subscribed to are kept under constant review, and some journals have been discontinued as being no longer of interest (due, for instance, to changes in their subject coverage). 20 of the journals are new to the Library this year, some being new publications and others established journals which are now relevant to the Laboratory's work.

16 reports in the RHEL/R series and 53 preprints in the RPP series were issued during the year. Copies were sent to the Libraries with whom the Laboratory has exchange agreements. These now number 267, in 46 different countries.

*Annual Report* The editors are again indebted to the many people throughout the Laboratory who have provided material for this Report. Thanks are particularly due to the following, who have acted as co-ordinators for their respective Divisions:  
T.G. Walker, D.C. Salter, P.B. Nichols (HEP), H. Wroe (Nimrod), C.J. Batty (PLA) J.H. Coupland, A.P.F. Watterson (Applied Physics), J.B. Marsh, E.G. Higgins (Engineering).



LIST OF  
PUBLICATIONS

# List of Publications

## High Energy Physics Division

Journal Articles

- 1 BINNIE D.M., DUANA A., FARUQI A.R., HORSEY J.P., JONES W.G., KAY M.E., MASON D.C., NICHOLSON P.J., RAHMAN I.U., WALTERS J., WILSON J.G., PALIT P.  
Measurement of the partial width of the decay  $\phi \rightarrow e^+e^-$ .  
Phys. Lett., **27B** (2) 106 (June 1968), preprinted as RPP/H 41.
- 2 BOTTERILL D.R., BROWN R.M., CLEGG A.B., CORBETT I.F., CULLIGAN G., EMMERSON J. McL., FIELD R.C., GARVEY J., JONES P.B., MIDDLEMAS N., NEWTON D., QUIRK T.W., SALMON G.L., STEINBERG P.H., WILLIAMS W.S.C.  
Form Factor Ratio  $\xi$  from a measurement of the  $K_{e3}^+ / K_{e3}^-$  branching ratio.  
Phys. Rev. Lett., **21** (11) 766 (September 1968), preprinted as RPP/H 37.
- 3 BOTTERILL D.R., BROWN R.M., CLEGG A.B., CORBETT I.F., CULLIGAN G., EMMERSON J. McL., FIELD R.C., GARVEY J., JONES P.B., MIDDLEMAS N., NEWTON D., QUIRK T.W., SALMON G.L., STEINBERG P.H., WILLIAMS W.S.C.  
Measurement of the branching ratio and positron momentum spectrum for the decay  $K^+ \rightarrow \pi^0 e^+ \nu$ .  
Phys. Rev., **174** (5) 1661 (October 1968), preprinted as RPP/H 34.
- 4 BOTTERILL D.R., BROWN R.M., CORBETT I.F., CULLIGAN G., EMMERSON J. McL., FIELD R.C., GARVEY J., JONES P.B., MIDDLEMAS N., NEWTON D., QUIRK T.W., SALMON G.L., STEINBERG P.H., WILLIAMS W.S.C.  
Measurement of the branching ratio for the decay  $K^+ \rightarrow e^+ \nu_e$ .  
Phys. Rev., **171** (5) 1402 (July 1968), preprinted as RPP/H 27.
- 5 BUGG D.V.  
Meson-nucleon coupling constants from nucleon-nucleon forward dispersion relations.  
Nucl. Phys., **B5** (1) 29 (April 1968), preprinted as RPP/H 14.
- 6 BUGG D.V., GILMORE R.S., KNIGHT K.M., SALTER D.C., STAFFORD G.H., WILSON E.J.N., DAVIES J.D., DOWELL J.D., HATTERSLEY P.M., HOMER R.J., O'DELL A.W., CARTER A.A., TAPPER R.J., RILEY K.F.  
Kaon-nucleon total cross sections from 0.6 to 2.65 GeV/c.  
Nuovo Cim., **54A** (3) 608 (April 1968), preprinted as RPP/H 31.
- 7 BULLOCK F.W., ESTEN M.J., FLEMING-TOMPA E., GOVAN M., HENDERSON C., OWEN A.A., STANNARD F.R.  
A determination of the branching ratio  $(\eta \rightarrow 3\pi^0) / (\eta \rightarrow \pi^+ \pi^- \pi^0)$ .  
Phys. Lett., **27B** (6) 402 (August 1968), preprinted as RPP/H 40.
- 8 BURGUN G., MEYER J., PAULI E., TALLINI B., VRANA J., de BELLEFON A., BERTHON A., RANGAN K.L., BEANEY J., DEEN S.M., FISHER C.M., SMITH J.R.  
Resonance formation in the reactions  $K^+ p \rightarrow K^+ + \Xi^-$  and  $K^- p \rightarrow K^0 + \Xi^0$  in the mass region from 1915 to 2168 MeV.  
Nucl. Phys., **B8** (2) 447 (December 1968), preprinted as RPP/H 50.
- 9 CARTER A.A., RILEY K.F., TAPPER R.J., BUGG D.V., GILMORE R.S., KNIGHT K.M., SALTER D.C., STAFFORD G.H., WILSON E.J.N., DAVIES J.D., DOWELL J.D., HATTERSLEY P.M., HOMER R.J., O'DELL, A.W.  
Pion-nucleon total cross sections from 0.5 to 2.65 GeV/c.  
Phys. Rev., **168** (5) 1457 (April 1968), preprinted as RPP/H 32.
- 10 COLLEY D.C., DODD W.P., MACDONALD F., MUSGRAVE B., TULI S.K., BLAIR W., ERSKINE R., GORDAN J., HUGHES I., TURNBULL R., CHAUDHURI P., ESKREYS A., GOLDSACK S.J., PALER K., SISTERTON K., BLUM W., DEHM G., SCHMITZ N., SCHRANKEL W., ALLISON J., ALLISON W.W.M., BRODY A.D., LOCKE D.H., LYONS L., FINNEY P., FISHER C., RANGAN L.K., SEGAR A.M.  
Two body processes in  $K^+ p$  scattering at 6 GeV/c.  
Nuovo Cim., **53A** (2) 522 (January 1968), preprinted as RPP/H 25.
- 11 DAVIES J.D., DOWELL J.D., HATTERSLEY P.M., HOMER R.J., O'DELL A.W., SPROUL M.E., CARTER A.A., RILEY K.F., TAPPER R.J., BUGG D.V., SALTER D.C., WILSON E.J.N.  
Particle production from copper and uranium targets by 8 GeV/c protons.  
Nuovo Cim., **54A** (3) 608 (April 1968), preprinted as RPP/H 28.

- 12 DUKE P.J., JONES D.P., KEMP M.A.R., MURPHY P.G., THRESHER J.J., ATKINSON H.H., COX C.R., HEARD K.S.  
Scattering of  $\pi^-$  mesons in the momentum range 875-1579 MeV/c from a polarized target.  
Phys. Rev., **166** (5) 1448 (February 1968).
  - 13 FIELD R.C., JONES P.B.  
S-wave  $K\pi$  interaction in the  $K_{e3}$  decay mode.  
Phys. Rev. Lett., **21** (5) 327 (July 1968), preprinted as RPP/H 38.
  - 14 JONES P.B.  
Renormalisation of the  $K_{e3}$  form factor.  
Phys. Rev. Lett., **21** (22) 1553 (November 1968), preprinted as RPP/H 42.
  - 15 LITCHFIELD P.J.  
The decay  $\eta \rightarrow \pi^+ \pi^- \pi^0$  and the S-wave  $\pi\pi$  phase shift.  
Nuovo Cim., **58A** (2) 468 (November 1968), preprinted as RPP/H 36.
  - 16 RANFT G.  
The annihilation reaction  $p + \bar{p} \rightarrow 2\pi^+ + 2\pi^-$  at high energy and a multi-Regge model.  
Nuovo Cim., **58A** (2) 425 (November 1968), preprinted as RPP/H 39.
  - 17 UNIVERSITY COLLEGE, LONDON / LRL, BERKELEY / UNIVERSITY OF MADISON.  
A study of  $K_{e4}$  decays.  
Phys. Rev., (in the press).
  - 18 WHITEHEAD C., McEWEN J.G., OTT R.J., AITKEN D.K., BENNETT G., JENNINGS R.E.  
Observation of an enhancement in the  $I = 0 \pi^+ \pi^-$  system at 1085 MeV.  
Nuovo Cim., **53A** (3) 817 (February 1968), preprinted as RPP/H 33.
- Conference Papers
- 19 BIRMINGHAM / EDINBURGH / GLASGOW / IMPERIAL COLLEGE LONDON.  
A study of  $K\pi$  interactions between 1.8 and 2.2 GeV/c.  
International Conference on High Energy Physics, Vienna, 1968.  
(Items 19-34 were contributed papers, not reproduced in the Proceedings.)
  - 20 BIRMINGHAM / EDINBURGH / GLASGOW / IMPERIAL COLLEGE LONDON.  
 $Y^*$  production in  $K^-$  - neutron interactions at 1.45 and 1.65 GeV/c.  
Ibid.
  - 21 BIRMINGHAM / GLASGOW / OXFORD.  
A study of the  $K\pi\pi$  system at 10 GeV/c.  
Ibid.
  - 22 BIRMINGHAM / GLASGOW / OXFORD.  
Further evidence for a  $\Lambda n$  enhancement in  $K^+ p$  interactions at 10 GeV/c.  
Ibid.
  - 23 BOTTERILL D.R., BROWN R.M., CLEGG A.B., CORBETT I.F., CULLIGAN G., EMMERSON J. McL., FIELD R.C., GARVEY J., JONES P.B., MIDDLEMAS N., NEWTON D., QUIRK T.W., SALMON G.L., STEINBERG P., WILLIAMS W.S.C.  
The form factor ratio  $\xi$  from a measurement of  $K_{e3}^+ : K_{e3}^-$  branching ratios.  
Ibid.
  - 24 BOTTERILL D.R., BROWN R.M., CLEGG A.B., CORBETT I.F., CULLIGAN G., EMMERSON J. McL., FIELD R.C., GARVEY J., JONES P.B., MIDDLEMAS N., NEWTON D., QUIRK T.W., SALMON G.L., STEINBERG P., WILLIAMS W.S.C.  
 $K^+$  semi-leptonic decays.  
Ibid.
  - 25 BOTTERILL D.R., BROWN R.M., CLEGG A.B., CORBETT I.F., CULLIGAN G., EMMERSON J. McL., FIELD R.C., GARVEY J., JONES P.B., MIDDLEMAS N., NEWTON D., QUIRK T.W., SALMON G.L., STEINBERG P., WILLIAMS W.S.C.  
Measurement of the branching ratio and positron momentum spectrum for the decay  $K^+ \rightarrow \pi^0 e^+ \nu$ .  
Ibid.
  - 26 BULLOCK F.W., ESTEN M.J., FLEMING-TOMPA E., GOVAN M., HENDERSON C., OWEN A.A., STANNARD F.R.  
A determination of the branching ratio  $(\eta \rightarrow 3\pi^0) / (\eta \rightarrow \pi^+ \pi^- \pi^0)$ .  
Ibid.
  - 27 EDGINGTON J.A., HOWARD V.J., MILLER M.C., OTT R.J., SLEEMAN J.C., DUKE P.J., HILL R.E., HOLLEY W.R., JONES D.P., THRESHER J.J.  
Polarization effects in the reaction  $\pi^- + p \rightarrow \Sigma^- + K^+$  at 1130 MeV/c.  
Ibid.

- 28 GAILLARD J.M., GALBRAITH W., HUSSRI A., JANE M.R., LIPMAN N.H., MANNING G., RATCLIFFE T.J., FAISSNER H., REITHLER H.  
The decay of long lived neutral kaons into two neutral pions.  
Ibid.
- 29 LITCHFIELD P.J., SMITH P.R.,  
The reaction  $\pi^+ + n \rightarrow p + \eta$  near threshold.  
Ibid.
- 30 RANFT G.  
The annihilation reaction  $p + \bar{p} \rightarrow 2\pi^+ + 2\pi^-$  at high energy, and a multi-Regge model.  
Ibid.
- 31 RANFT G.  
The double Regge model and an "anti-cornering" effect in three particle production processes.  
Ibid.
- 32 RHEL / SACLAY  
The reaction  $\pi^+ + n \rightarrow \eta + p$  near threshold.  
Ibid.
- 33 SACLAY / COLLEGE de FRANCE / RHEL  
Cross-section determination for the reactions  $K^- + p \rightarrow \Lambda + \pi^0$ ,  $K^0 + n$ ,  $\Sigma + \pi$  and  $\Xi + K$  in the momentum region 1.2 - 1.85 GeV/c.  
Ibid.
- 34 SACLAY / COLLEGE de FRANCE / RHEL  
Partial wave analysis in a  $K^-p$  formation experiment in the c.m.s. energy region 1.9 - 2.2 GeV/c.  
Ibid.
- 35 BAIRSTOW R., CAWTHRAW M.J.  
Data handing system for sonic and/or magnetostrictive readout. Nucleonic Instrumentation Conference, Reading, September 1968. Proceedings (IEE Publication No. 47) p. 166.
- 36 HERBST L.J.  
New fast analogue modules for nuclear instrumentation.  
Ibid, p. 174.
- 37 CRAWFORD J.F., OSMAN P.E., STRONG J.A.  
A Vidicon system for spark chamber read-out. International Symposium on Nuclear Electronics, Versailles, September, 1968.
- 38 CRAWFORD J.F., OSMAN P.E., STRONG J.A.  
Monitors for a Vidicon system.  
Ibid.
- 39 CRESSWELL J.V., MILBORROW R.S., WILDE P.  
A new system for counter instrumentation.  
Ibid.
- Unpublished Preprints
- 40 BUSZA W., DUFF B.G., GARBUTT D.A., HEYMANN F.F., NIMMON C.C., POTTER K.M., SWETMAN T.P., BELLAMY E.H., BUCKLEY T.F., DOBINSON R.W., MARCH P.V., STRONG J.A., WALKER R.N.F.  
 $\pi^\pm p$  elastic scattering in the 2GeV region.  
RPP/H 49, submitted to Phys. Rev. Lett.
- 41 COX C.R., DUKE P.J., HEARD K.S., HILL R.E., HOLLEY W.R., JONES D.P., SHOEMAKER F.C., THRESHER J.J., WARREN J.B., SLEEMAN J.C.  
Scattering of  $K^-$  mesons in the momentum range 1.08 - 1.37 GeV/c from a polarized proton target.  
RPP/H 45, submitted to Phys. Rev.
- 42 COX C.R., DUKE P.J., HEARD K.S., HILL R.E., HOLLEY W.R., JONES D.P., SHOEMAKER F.C., THRESHER J.J., WARREN J.B., SLEEMAN J.C.  
Scattering of  $\pi^-$  mesons in the momentum range 0.643 - 2.14 GeV/c from a polarized proton target.  
RPP/H 46, submitted to Phys. Rev.
- 43 EDGINGTON J.A., HOWARD V.J., MILLER M.C., OTT R.J., DUKE P.J., HILL R.E., HOLLEY W.R., JONES D.P., THRESHER J.J., SLEEMAN J.C.  
Polarization of  $\Sigma^-$  in the reaction  $\pi^- + p \rightarrow \Sigma^- + K^+$  at 1130 MeV/c.  
RPP/H 47, submitted to Phys. Rev.

- 44 GAILLARD J.M., GALBRAITH W., HUSSRI A., JANE M.R., LIPMAN N.H., MANNING G., RATCLIFFE T.J., FAISSNER H., REITHLER H.  
The decay of long-lived neutral kaons into two neutral pions.  
RPP/H 35, submitted to Nuovo Cim.
- 45 RANFT G.  
The double Regge model and an "anti-cornering" effect in three particle production processes.  
RPP/H 43, submitted to Nuovo Cim.
- 46 RANFT G., TURNBULL W.  
A double Regge analysis of the reaction  $K^- + p \rightarrow K^- + \omega + p$ .  
RPP/H 48, submitted to Nuovo Cim.
- Reports and Memoranda
- 47 BAIRSTOW R., CAWTHRAW M.J.  
A modular electronic data acquisition system for magnetostrictive readout of wire spark chambers.  
RHEL / R 157.
- 48 MILBORROW R.S.  
The miniature logic system.  
RHEL / M 141.
- 49 PITTS P.R.  
Automatic scan card punching.  
RHEL / M 138.
- 50 OXFORD UNIVERSITY / RHEL.  
The results of asymmetry measurements in  $\pi^-p$  elastic scattering from a polarized target in the momentum range 0.643 - 2.146 GeV/c.  
RHEL / M 137.
- Doctoral Theses
- 51 BENNETT G. (University College, University of London)  
An investigation of final states involving a neutron from  $\pi^-p$  interactions.
- 52 CLAYTON M.J. (University of Cambridge)  
Collisions of fast protons with deuterons.
- 53 COX C.R. (University of Oxford)  
The measurement of polarization effects in the elastic scattering of  $K^-$  mesons by protons.
- 54 DOBINSON R. (Westfield College, University of London)  
A study of the  $N_{3/2}^*(2420)$  and a design study for measuring the  $\Sigma$  decay parameters.
- 55 FIELD R.C. (University of Oxford)  
Studies in elementary particle physics by electronic techniques.
- 56 HEARD K.S. (University of Oxford)  
A study of polarization effects in  $\pi^-p$  elastic scattering.
- 57 HORSEY J. (Imperial College, University of London)  
The electron - positron decay mode of the phi meson.
- 58 LITCHFIELD P.J. (University of Oxford)  
A study of  $\eta$  mesons produced in  $\pi^+$  interactions with deuterium.
- 59 MASON D.C. (Imperial College, University of London)  
Spark chamber analysis of di-kaon production near threshold.
- 60 MILLER M.C. (Queen Mary College, University of London)  
A study of polarization effects in the reaction  $\pi^- + p \rightarrow \Sigma^- + K^+$  at 1 GeV.
- 61 OWEN A.A. (University College, University of London)  
Eta meson decays.
- 62 RATCLIFFE T.J. (University of Oxford)  
Studies of  $K_2^0$  decay.
- 63 SMITH V.J. (University of Bristol)  
Pion-proton elastic scattering.
- 64 STRONG J.A. (Westfield College, University of London)  
The elastic scattering of pions by protons in the region of 2 GeV/c.

- 65 TREUTLER O. (University College, University of London)  
A study of stopped K mesons in a heavy liquid bubble chamber.
- 66 UR RAHMAN I. (Imperial College, University of London)  
Time of flight study of the reaction  $\pi^- + p \rightarrow n + K^+ + K^-$  near threshold.

## Nimrod Division

- Journal Articles*
- 67 HAGEDORN R., RANFT J.  
Statistical thermodynamics of strong interactions at high energies (II) Momentum spectra of particles produced in p-p collisions.  
Nuovo Cim. Suppl., **6** (2) 169 (1968).
- 68 RANFT J.  
Determination of shielding requirements around present and future proton synchrotrons by Monte Carlo nucleon-meson cascade calculations.  
Trans. Amer. Nucl. Soc., **11** 391 (June 1968).
- 69 WROE H.  
Emittance measurements with a single gap accelerator, and the production of very low emittance proton beams.  
Nucl. Instrum. Meth., **58** (2) 213 (January 1968).
- Conference Papers*
- 70 CARNE A., BRADY B.G., NEWMAN M.J.  
Superconducting r.f. separator research at the Rutherford Laboratory.  
International Summer Study on Superconducting Devices and Accelerators, Brookhaven, July 1968.
- 71 GARDNER I.S.K., GRAY D.A., RANFT J., REES G.H., WROE H.  
Intensity limitations in Nimrod.  
Conference on Particle Accelerators, Moscow, October 1968.
- 72 REDGRAVE R.  
Diagnostic equipment in high energy beam lines.  
Symposium on Beam Intensity Measurements. Daresbury, April 1968. Proceedings (Hatton V.W. & Lowndes S.A. (eds.) DNPL/R1), p.49.
- 73 SMITH W.A., MASON T.R., CHILDS T.L.K.  
Impulse breakdown and the pressure effect.  
3rd International Symposium on Discharges and Electrical Insulation in Vacuum, Paris, September 1968. Proceedings (Goldman M. & Goldman A. (eds.)), p.203.
- Reports and Memoranda*
- 74 ATKINSON H.H.  
Some ideas for a polarized target with good access for high energy experiments.  
RHEL / M 154.
- 75 CONTE M.  
Resonant extraction from a weak focussing synchrotron with straight sections.  
RHEL / M 158.
- 76 GRAY D.E. (ed.)  
Nimrod operation and development - quarterly report, 1st October to 31st December, 1967.  
RHEL / R 162.
- 77 GRAY D.E. (ed.)  
Nimrod operation and development - quarterly report, 1st January to 31st March, 1968.  
RHEL / R 167.
- 78 GRAY D.E. (ed.)  
Nimrod operation and development - quarterly report 1st April to 30th June 1968.  
RHEL / R 172.
- 79 HAROLD M.R.  
A resonant extraction system for Nimrod.  
RHEL / R 173.
- 80 PLANNER C.W., WALSH T.R.  
The possibility of a linac booster for Nimrod.  
RHEL / M 156.

- 81 RANFT J.  
Particle yields at Nimrod.  
RHEL / M 162.
- 82 RANFT J.  
Calculation of perturbed orbits for resonant extraction from Nimrod.  
RHEL / R 163.
- 83 RANFT J.  
An improved description of particle production by the thermodynamic model.  
RHEL / R 165.
- 84 REES G.H.  
Control of the r.f. in a proton synchrotron with beam loading.  
RHEL / R 158.
- 85 RUSSELL F.M.  
Proposal for a new polarized target with good access.  
RHEL / M 155.
- 86 SANDELS E.G.  
The measurement of effective spill-time and duty factor in slow-spill targeting in Nimrod.  
RHEL / M 159.
- 87 SETHI V.K.  
The effects of radiation on the electrical characteristics of transistors.  
RHEL / M 153.
- 88 WALSH T.R.  
Basic geometry of a separated orbit cyclotron.  
RHEL / M 145.
- M.Sc. Dissertation*
- 89 PLANNER C.W. (Chelsea College of Science & Technology, University of London)  
High frequency electrical discharges by secondary electron resonance.

## Proton Linear Accelerator Division

- Journal Articles*
- 90 BATTY C.J., BONNER B.E., FRIEDMAN E., TSCHALÄR C., WILLIAMS L.E., CLOUGH A.S., HUNT J.B.  
The  $\text{Li}^6(p, n)\text{Be}^6$  and  $\text{Li}^7(p, n)\text{Be}^7$  reaction at intermediate proton energies.  
Nucl. Phys., **A120** (2) 297 (November 1968), preprinted as RPP/P15.
- 91 BATTY C.J., BONNER B.E., FRIEDMAN E., TSCHALÄR C., WILLIAMS L.E., CLOUGH A.S., HUNT J.B.  
Excitation of isobaric analogue states in (p,n) reactions at 30 and 50 MeV and the isospin dependence of the optical model.  
Nucl. Phys., **A116** (3) 643 (August 1968), preprinted as RPP/P 14.
- 92 BATTY C.J., BONNER B.E., KILVINGTON A.I., TSCHALÄR C., WILLIAMS L.E., CLOUGH A.S.  
Intermediate energy neutron sources.  
Nucl. Instrum. Meth., (in the press), preprinted as RPP/P 19.
- 93 BATTY C.J., FRIEDMAN E., GREENLEES G.W.  
An analysis of quasi-elastic (p,n) reactions using a reformulated optical model.  
Nucl. Phys. (in the press), preprinted as RPP/P 20.
- 94 CHANT N.S., NELSON J.M.  
A DWBA analysis of polarization analysing powers and differential cross-sections for the (p, d) reaction on  $\text{Si}^{28}$  and  $\text{Ca}^{40}$ .  
Nucl. Phys., **A117** (2) 385 (September 1968).
- 95 CLOUGH A.S., BATTY C.J., BONNER B.E., TSCHALÄR C., WILLIAMS L.E.,  
Neutron spectra from the  $\text{D}(p, n) 2p$  reaction at 30 and 50 MeV.  
Nucl. Phys., **A121** (3) 689 (December 1968), preprinted as RPP/P 18.
- 96 DAVIES W.G., KITCHING J.E., McLATCHIE W., MONTAGUE D.G., RAMAVATARAM K., CHANT N.S.  
Levels excited in the reaction  $\text{Ni}^{58}(p, t)\text{Ni}^{56}$ .  
Phys. Lett., **27B** (6) 363 (August 1968).

- 97 ELTON L.R.B.  
The distributions of neutrons in nuclei.  
Phys. Lett., **26B** (12) 689 (May 1968).
- 98 ELTON L.R.B., JACKSON D.F.  
Nuclear models.  
Phys. Education, **3** 131 (May 1968).
- 99 HARBISON S.A., KINGSTON F.G., GRIFFITHS R.J., JOHNSTON A.R., MEGAW J.H.P.C.  
Polarization in the elastic scattering of 30 MeV protons by He<sup>3</sup>.  
Nucl. Phys., **A112** (1) 137 (May 1968).
- 100 JACKSON D.F.  
Nuclear reactions.  
Phys. Education, (in the press).
- 101 JACKSON D.F.  
Nuclear structure studies at medium energies.  
Advanc. Phys., **17** (68) 481 (July 1968).
- 102 JACKSON D.F.  
Localisation of nuclear reactions and the investigation of the nuclear surface.  
Nucl. Phys., **A123** (2) 273 (January 1969).
- 103 JACKSON D.F., JAIN B.K.  
Study of the (p,2p) reaction in the energy region 160 MeV to 1 GeV.  
Phys. Lett., **27B** (3) 147 (June 1968).
- 104 JACKSON D.F., MORGAN C.G.  
Scattering of medium energy alpha particles (I) Phenomenological analysis of elastic scattering.  
Phys. Rev., **175** (4) 1402 (November 1968).
- 105 JAIN B.K.  
Spectroscopic analysis of the (p,2p) reaction on the nuclei Si<sup>28</sup>, Mg<sup>24</sup> and Na<sup>23</sup>.  
Nucl. Phys., **A116** (2) 256 (August 1968).
- 106 JOHNSON R.C., SANTOS F.D.  
J-dependence in (p,d) reactions and the effects of the deuteron D-state.  
J. Phys. Soc. Japan, **24** 283 (1968).
- 107 JOHNSON R.R., GRIFFITHS R.J.  
The Ar<sup>40</sup> (p,d) Ar<sup>39</sup> and Ar<sup>36</sup> (p,d) Ar<sup>35</sup> reactions at 27.5 MeV.  
Nucl. Phys., **A108** (1) 113 (January 1968).
- 108 JOHNSON R.R., GRIFFITHS R.J.  
Proton elastic and inelastic scattering from argon at 25 MeV.  
Nucl. Phys., **A117** (2) 273 (September 1968).
- 109 KINGSTON F.G., GRIFFITHS R.J., JOHNSTON A.R., GIBSON W.R., McCLATCHIE E.A., MEGAW J.H.P.C.  
A study of the Mg<sup>26</sup> (p,t) Mg<sup>24</sup> and Mg<sup>26</sup> (p,He<sup>3</sup>) Na<sup>24</sup> reactions at 50 MeV.  
Nucl. Phys., **A124** (1) 225 (February 1969).
- 110 LEWIS V.E.  
An alpha-particle thickness gauge.  
Nucl. Instrum. Meth., **64** (3) 293 (October 1968).
- 111 LEWIS V.E., CALDERBANK M., GANGULY N.K., FRICKE M.P.  
Analysis of the inelastic scattering of 50 MeV protons,  
Nucl. Phys., **A117** (3) 673 (September 1968).
- 112 MANI G.S., DIX A.D.B.  
Energy levels in Li<sup>6</sup> and Li<sup>7</sup> from inelastic proton scattering.  
Nucl. Phys., **A106** (2) 251 (January 1968).
- 113 MEGAW J.H.P.C., JOHNSTON A.R., GIBSON W.R., KINGSTON F.G.  
Polarization in elastic scattering of 9.5 MeV and 21.6 MeV protons by deuterons.  
Nucl. Phys., **A122** (3) 689 (December 1968).
- 114 PLUMMER D.J., HODGES T.A., RAMAVATARAM K., MONTAGUE D.G., CHANT N.S.  
A unique set of phase shifts for the scattering of protons by helium.  
Nucl. Phys., **A115** (2) 253 (July 1968).
- 115 REEVE P.A.  
The design of beam lines with high resolving power.  
Nucl. Instrum. Meth., **67** (1) 13 (January 1969).

- 116 RUSH A.A., GANGULY N.K.  
Collective-model analysis of the inelastic scattering of 49.5 MeV protons by Mg<sup>24</sup>.  
Nucl. Phys., **A117** (1) 101 (September 1968), preprinted as RPP/P 16.
- 117 TSCHALÄR C.  
Straggling distributions of extremely large energy losses.  
Nucl. Instrum. Meth., **64** (3) 237 (October 1968).
- 118 TSCHALÄR C., BICHSEL H.  
Mean multiple scattering correction to the energy loss of heavy particles.  
Nucl. Instrum. Meth., **62** (2) 208 (June 1968).
- 119 TSCHALÄR C., BICHSEL H.  
Mean excitation potential of light compounds.  
Phys. Rev., **175** (2) 476 (November 1968).
- Conference  
Papers
- 120 CARNE A., DICKSON J.M., NORCLIFFE S., WEBB J.S., BATCHELOR K.  
Reduction of energy spread on the Rutherford Laboratory PLA.  
Linac Conference, Brookhaven, (1968), preprinted as RPP/P 17.
- 121 ELTON L.R.B.  
Nuclear physics at high energies.  
Symposium on the use of Nimrod for nuclear structure studies, RHEL, March 1968  
Proceedings (Batty C.J. (ed.) RHEL/R166) p.7.
- 122 ELTON L.R.B., JACKSON D.F.  
Investigation of the nuclear surface.  
Ibid, p.33.
- 123 JACKSON D.F., JAIN B.K.  
Survey of the (p,2p) reaction in the energy region 160 MeV to 1 GeV.  
Ibid, p.80.
- 124 GRYPEOS M.E.  
A possible determination of the  $\Lambda$  - nucleon correlation function.  
IPPS Conference on Nuclear Physics, AERE, Harwell, March 1968.
- 125 JACKSON D.F., KEMBHAVI V.K.  
The relation between the optical potential for alpha-particles and the nuclear matter distribution.  
Ibid.
- 126 JOHNSTON A.R., MEGAW J.H.P.C., SQUIER G.T.A., GIBSON W.R., KINGSTON F.G., HARBISON S.A., STEWART N.M.  
Polarization in the elastic scattering of 10 MeV and 22 MeV protons by deuterons.  
Ibid.
- 127 NELSON J.M., CHANT N.S., FISHER P.S.  
Triton asymmetries in the two nucleon transfer reactions C<sup>12</sup> (p,t) C<sup>10</sup> and O<sup>16</sup> (p,t) O<sup>14</sup>.  
Ibid.
- 128 PLUMMER D.J., RAMAVATARAM K., MONTAGUE D.G., HODGES T.A., GANGULY N.K., ZUCKER A.  
Polarization and cross-section measurements for p-He<sup>4</sup> scattering.  
Ibid.
- 129 RUSH A.A., GANGULY N.K.  
Analysis of the inelastic scattering of 49.5 MeV protons by Mg<sup>24</sup>.  
Ibid.
- 130 SCOTT D.K., CHANT N.S., NELSON J.M., FISHER P.S., SHOTTER A.C.  
The 4+ level of C<sup>12</sup>.  
Ibid.
- 131 STEWART N.M., KINGSTON F.G., GIBSON W.R., JOHNSTON A.R., MEGAW J.H.P.C.  
Measurement of the depolarization parameter for 50 MeV proton-deuteron elastic scattering.  
Ibid.
- 132 THOMAS G.L., BURGE E.J., SMITH D.A.  
Polarization measurements on the elastic scattering of 30 MeV protons from Cu<sup>63</sup> and Cu<sup>65</sup>.  
Ibid.

- 133 TSCHALÄR C.  
Straggling effects and multiple scattering corrections in precise energy loss measurements.  
Ibid.
- 134 ZUCKER A., MONTAGUE D.G., HODGES T.A., GANGULY N.K., RAMAVATARAM K., PLUMMER D.J.  
The triple scattering R-parameter measurement on Ca<sup>40</sup>.  
Ibid.

*Reports and Memoranda*

- 135 BATTY C.J. (ed.)  
Proceedings of the symposium on the use of Nimrod for nuclear structure physics.  
RHEL / R 166.
- 136 BATTY C.J. (ed.)  
PLA progress report 1968.  
RHEL / R 170.
- 137 REEVE P.A.  
Magnetic spectrometers for high rigidity particles in nuclear structure physics.  
RHEL / R 169.
- 138 TSCHALÄR C.  
Straggling distributions of extremely large energy losses by heavy particles.  
RHEL / R 164.

*Doctoral Theses*

- 139 CLOUGH A.S. (Queen Mary College, University of London)  
Direct reactions of 30 and 50 MeV nucleons with light nuclei.
- 140 DWIGHT J.R. (Battersea College of Advanced Technology, University of London, now the University of Surrey).  
Exchange effects in (p,pd) and similar reactions.
- 141 JAIN B.K. (University of Surrey)  
A study of the single particle states in 1p and 2s - 1d shell nuclei with the (p,2p) reaction.
- 142 LAW J. (Battersea College of Advanced Technology, University of London, now the University of Surrey).  
Extended shell model studies in selected nuclei and hypernuclei.
- 143 LEWIS V.E. (Kings College, University of London)  
Polarization in the scattering of 50 MeV protons.
- 144 MEGAW J.H.P.C. (Queen's University, Belfast)  
A study of proton-deuteron elastic scattering.
- 145 NELSON J.M. (University of Oxford)  
Asymmetries in nucleon transfer reactions induced by polarized protons.
- 146 RUSH A.A. (King's College, University of London)  
Interactions of 30 and 50 MeV protons with Mg<sup>24</sup> and Ar<sup>40</sup>.
- 147 SANTOS F.D. (Battersea College of Advanced Technology, University of London, now the University of Surrey).  
The effect of the D-state of the deuteron in (d,p) reactions.

*M. Sc. Dissertation*

- 148 REEVE P.A. (Chelsea College of Science & Technology, University of London)  
Magnetic spectrometers.

## Applied Physics Division

*Journal Articles*

- 149 BARGER V., PHILLIPS R.J.N.  
Interpretation of recurring minima in elastic scattering at large momentum transfers.  
Phys. Rev. Lett., **20** (11) 564 (March 1968).
- 150 BARGER V., PHILLIPS R.J.N.  
Vacuum exchange amplitudes from a family of sum rules.  
Phys. Lett., **26B** (12) 730 (May 1968).

- 151 BARGER V., PHILLIPS R.J.N.  
Location of a secondary  $\rho$  Regge pole in the reaction  $\pi^- + p \rightarrow \pi^0 + n$ .  
Phys. Rev. Lett., **21** (12) 865 (September 1968).
- 152 BERENDS F.A., DONNACHIE A., OADES G.C.  
Theoretical study of  $K_{L4}$  decay.  
Phys. Rev., **171** (5) 1457 (July 1968).
- 153 DASS G.V., MICHAEL C.  
Factorisation,  $\omega$  crossover, polarization and finite energy sum rules, for kaon-nucleon scattering.  
Phys. Rev. Lett., **20** (19) 1066 (May 1968), preprinted as RPP/A37.
- 154 DASS G.V., MICHAEL C.  
Regge poles and finite energy sum rules for kaon-nucleon scattering.  
Phys. Rev., **175** (5) 1774 (November 1968).
- 155 KABIR P.K.  
Unitarity and TCP-invariance in  $K^0 \rightarrow 2\pi$  decay.  
Phys. Rev. Lett., **21** (5) 314 (July 1968).
- 156 KABIR P.K.  
Tests of T and TCP - invariance.  
Nature, **220** (5174) 1310 (December 1968).
- 157 KABIR P.K.  
 $\eta$  asymmetry without C - nonconfiguration.  
Phys. Rev., (in the press).
- 158 KAMAL A.N.  
Crossing symmetry, current algebra and KSRF relation.  
Phys. Rev., (in the press).
- 159 KAMAL A.N., SHYMKO R.M.  
Pion form factors and phase shifts.  
Nucl. Phys., (in the press).
- 160 KENNY B.G.  
Phase space factors in  $\eta K \rightarrow 3\pi$  decay.  
Phys. Rev., **175** (5) 2054 (November 1968), preprinted as RPP/A 40.
- 161 KENNY B.G.  
Structure in  $\eta K \rightarrow 3\pi$  decay.  
Phys. Rev., **176** (5) 1735 (December 1968), preprinted as RPP/A 39.
- 162 KENNY B.G.  
Parameters in  $K_{L3}$  decay.  
Phys. Rev. Lett., **20** (21) 1217 (May 1968).
- 163 LAWSON J.D.  
Electron ring accelerators : a cheap path to very high energy protons?  
Nature, **218** (5140) 430 (May 1968).
- 164 LAWSON J.D.  
Space charge and vertical motion near the centre of the cyclotron.  
Nucl. Instrum. Meth., **64** (2) 214 (September 1968).
- 165 LO S.Y.  
The neutron form factor.  
Phys. Lett., **27B** (5) 308 (August 1968), preprinted as RPP/A 41.
- 166 LO S.Y.  
The shape of mesons.  
Nucl. Phys., **B9** (1) 10 (January 1969), preprinted as RPP/A 52.
- 167 LO S.Y.  
Field - current identity, universality and  $K_{L3}$  decay.  
Nucl. Phys., **B7** (1) 68 (September 1968).
- 168 MICHAEL C.  
S-Matrix theory.  
Methods in Subnuclear Physics Vol. II (Nikolic M., ed.) (Gordon & Breach, 1968).
- 169 PHILLIPS R.J.N., RINGLAND G.A.  
U - channel Regge poles and total cross-sections.  
Phys. Rev., (in the press).

- 170 ROAF D., BAILEY C.A., DAVEY G., HANDS B.A., MCKENZIE J., MILLER A.B., MOFFATT J., PEEL T.D., SHAW D.F., TURNER W., WEEKS G.C., HADLEY H., SNOWDEN M., TALLIS W.J., WALKER R.N., WELFORD W.T.  
An 80 cm. liquid helium bubble chamber.  
Nucl. Instrum. Meth., **64** (3) 301 (October 1968).
- 171 SHAW K.B., STEVENSON G.R., THOMAS R.H.  
Evaluation of dose equivalent from neutron energy spectra.  
Health Phys., (in the press), preprinted as RPP/R 5.
- 172 WILSON M.N.  
The optimisation of magnet winding to produce uniform transverse fields.  
J. Sci. Instrum., (J. Phys. E), **1** (5) 575 (May 1968).
- Conference Papers 173 BARGER V., PHILLIPS R.J.N.  
Evidence for a flat Pomeranchuk trajectory and location of a secondary  $\rho$  pole.  
International Conference on High Energy Physics, Vienna, 1968.  
(Contributed paper, not reproduced in Proceedings).
- 174 LAWSON J.D.  
Some useful parameters.  
Symposium on Electron Ring Accelerators, Berkeley, February 1968. Proceedings (UCRL 18103) p.184.
- 175 LAWSON J.D.  
Notes on relativistic dynamics.  
Ibid., p.224.
- 176 LAWSON J.D.  
The effect of trapped ions on the Q values at injection.  
Ibid., p.298.
- 177 LAWSON J.D.  
Build-up of electron oscillation amplitude in the ring if the  $Q_r = 1$  resonance is crossed.  
Ibid., p.301.
- 178 LAWSON J.D.  
What is the axial extent of the ring and the field available to accelerate the ions.  
Ibid., p.376.
- 179 LAWSON J.D.  
Criterion for electrons to pull away from ions when crossing the r.f. gap.  
Ibid., p.379.
- 180 SMITH P.F.  
Superconducting proton synchrotrons - a review.  
International Summer Study on Superconducting Devices and Accelerators, Brookhaven, July 1968.
- 181 SMITH P.F.  
Synchrotron power supplies using superconducting energy storage.  
Ibid.
- 182 SMITH P.F., WILSON M.N., WALTERS C.R., LEWIN J.D.  
Intrinsically stable conductors.  
Ibid., preprinted as RPP/A 43.
- 183 SMITH P.F., WILSON M.N., LEWIN J.D.  
A possible source of instability in fully stabilised coils.  
Ibid.
- 184 TROWBRIDGE C.W., CLEE P.T.M., THOMAS D.B.  
A 70 kilogauss magnet for the proposed Rutherford Laboratory 1.5 metre diameter hydrogen bubble chamber.  
Ibid.
- 185 WILSON M.N., STOVOLD R.V., LAWSON J.D.  
The Rutherford Laboratory bending magnet.  
Ibid.
- Unpublished Preprints 186 ATKINSON D.  
A proof of the existence of functions that satisfy exactly both crossing and unitarity (II) Charged pions, no subtractions.  
RPP/A 51.

- 187 ATKINSON D., DIETZ K.  
Infinitely rising Regge trajectories and crossing symmetry.  
RPP/A 42.
- 188 BARGER V., PHILLIPS R.J.N.  
Exploratory deductions at large  $t$  from new  $\pi N$  data.  
COO - 201 (University of Madison).
- 189 COSTA G., SHAW G.  
Soft pions and finite energy sum rules: application to pion -  $\frac{1}{2}^+$  baryon scattering.  
RPP/A 36.
- 190 DANCE D.R., SHAW G.  
The Harari model, and the forward pion nucleon scattering amplitude.  
RPP/A 48.
- 191 DASS G.V., FROGGATT C.D.  
Regge pole model for vector meson production. (I): the reaction  $\pi N \rightarrow \rho N$   
RPP/A 46.
- 192 DASS G.V., FROGGATT C.D.  
Regge pole model for vector meson production. (II): the reaction  $KN \rightarrow K^* N$ .  
RPP/A 47.
- 193 DASS G.V., MICHAEL C., PHILLIPS R.J.N.  
Regge pole models for kaon-nucleon scattering.  
RPP/A 56, (submitted to Nucl. Phys.)
- 194 GOEBEL C.J., SHAW G.  
Phenomenological bounds on  $\pi-\pi$  scattering lengths.  
RPP/A 38.
- 195 KABIR P.K.  
 $\pi-\pi$  phase shifts in  $K^0 \rightarrow 2\pi$  decay.  
RL/KIB.
- 196 LICHTENBERG D.B.  
Baryon supermultiplets of  $SU(6) \times O(3)$  in a quark - diquark model.  
RPP/A 53.
- 197 LO S.Y.  
A model for diffractive excitation processes.  
RPP/A 55.
- 198 LO S.Y.  
A model for diffractive excitation processes.  
RPP/A 57.
- 199 MICHAEL C.  
Regge pole absorption model for  $\pi N$  charge exchange and crossover.  
RPP/A 45.
- 200 MICHAEL C., WILKIN C.  
Diffraction minima in hadron-deuteron cross-sections.  
RPP/A 54.
- 201 MITRA A.N.  
Form factors for hadronic decays in broken  $SU(6) \times O(3)$ .  
RPP/A 44.
- 202 MITRA A.N.  
The nuclear three-body problem.  
RPP/A 50.
- 203 MORGAN D., SHAW G.  
Low energy pion-pion parameters from forward dispersion relations.  
RPP/A 58, submitted to Nucl. Phys.
- 204 SHAW G.  
Phenomenological bounds on the  $\pi-\pi$  coupling constant.  
RPP/A 49.
- Reports and Memoranda 205 BURRELLS W.  
A low background counting room and ancillary apparatus.  
RHEL/R 161.



- 206 HARGREAVES D.M., STEVENSON G.R.  
Unfolding neutron energy spectra using the "ALFIE" routine.  
RHEL/M 147.
- 207 HARGREAVES D.M., STEVENSON G.R.  
A user guide to the "DECOR" programme.  
RHEL/M 150.
- 208 LAWSON J.D.  
Radiation from a ring charge passing through a resonator.  
RHEL/M 144.
- 209 LAWSON J.D.  
Orbits and Q values in partially neutralised electron ring beams.  
RHEL/M 152.
- 210 LEWIN J.D., SMITH P.F.  
Recent work on superconducting synchrotrons and a new Nimrod conversion scheme.  
RHEL/M 161.
- 211 NORRIS S.  
The CYCLOPS on-line diagnostic program LBOW.  
RHEL/M 143.
- 212 NUTHAKKI P.R., OXLEY A.J.  
Calibration of measuring machines.  
RHEL/M 142.
- 213 PERRY D.R.  
The feasibility of a Nimrod low energy pion irradiation facility for radiobiological research.  
RHEL/M 160.
- 214 SEAGER P. (ed.)  
Film user guide to 1.5 metre hydrogen bubble chamber.  
RHEL/M 146.
- 215 SHAW K.B., STEVENSON G.R., THOMAS R.H.  
Depth dose and depth dose equivalent data as functions of neutron energy.  
RHEL/M 149.
- 216 STENNING P.J., TROWBRIDGE C.W.  
The Pathfinder programme and its application to ion optics.  
RU/RL - 1 (University of Reading).
- 217 THOMAS D.B. (ed.)  
Progress report for 1967 on the research and development programme for the high field bubble chamber.  
AP/DS/HFC/10.
- 218 WILSON M.N.  
Computer simulation of the quenching of a superconducting magnet.  
RHEL/M 151.
- M. Sc. Dissertation* 219 DALY I.K. (University of Southampton)  
Liquid phase expansion system for the 1.5m hydrogen bubble chamber.

## Engineering Division

- Conference Papers* 220 EVANS D., MICKLEWRIGHT C.E., SHELDON R., STAPLETON G.B.  
Mechanical testing at 4.2°K.  
2nd International Cryogenic Engineering Conference, Brighton, May 1968. Proceedings (Iliffe, London 1968) p.236, preprinted as RPP/E 10.
- 221 EVANS D., MORGAN J.T., SHELDON R., STAPLETON G.B.  
Mechanical properties of glass reinforced epoxy resins at 4.2°K.  
6th International Reinforced Plastics Conference, London, November 1968. Preprinted as RPP/E 11.

- Reports and Memoranda* 222 FOX J.A., KENT P.  
Cross-channel pulse power tests between UK and France - 20th/21st June 1968.  
Analysis of power system frequency disturbance.  
E/PS - DS/300 GeV/JAF - 4.
- 223 FOX J.A., TROWBRIDGE C.W.  
The mathematical representations used in the static power supply computer programmes.  
E/PS-DS/300 GeV/JAF-5.
- 224 SHELDON R., STAPLETON G.B.  
The effect of high energy radiation on the mechanical properties of epoxy resin systems used for particle accelerator construction.  
RHEL/R 152.
- 225 SIMMONDS G.E., HARRISON D.A.  
A method of explosion venting a building.  
RHEL/R 168.

## Administration Division

- 226 BANFORD A.P., TELLING F.M. (eds.)  
The work of the Rutherford Laboratory in 1967.  
RHEL/R 160.

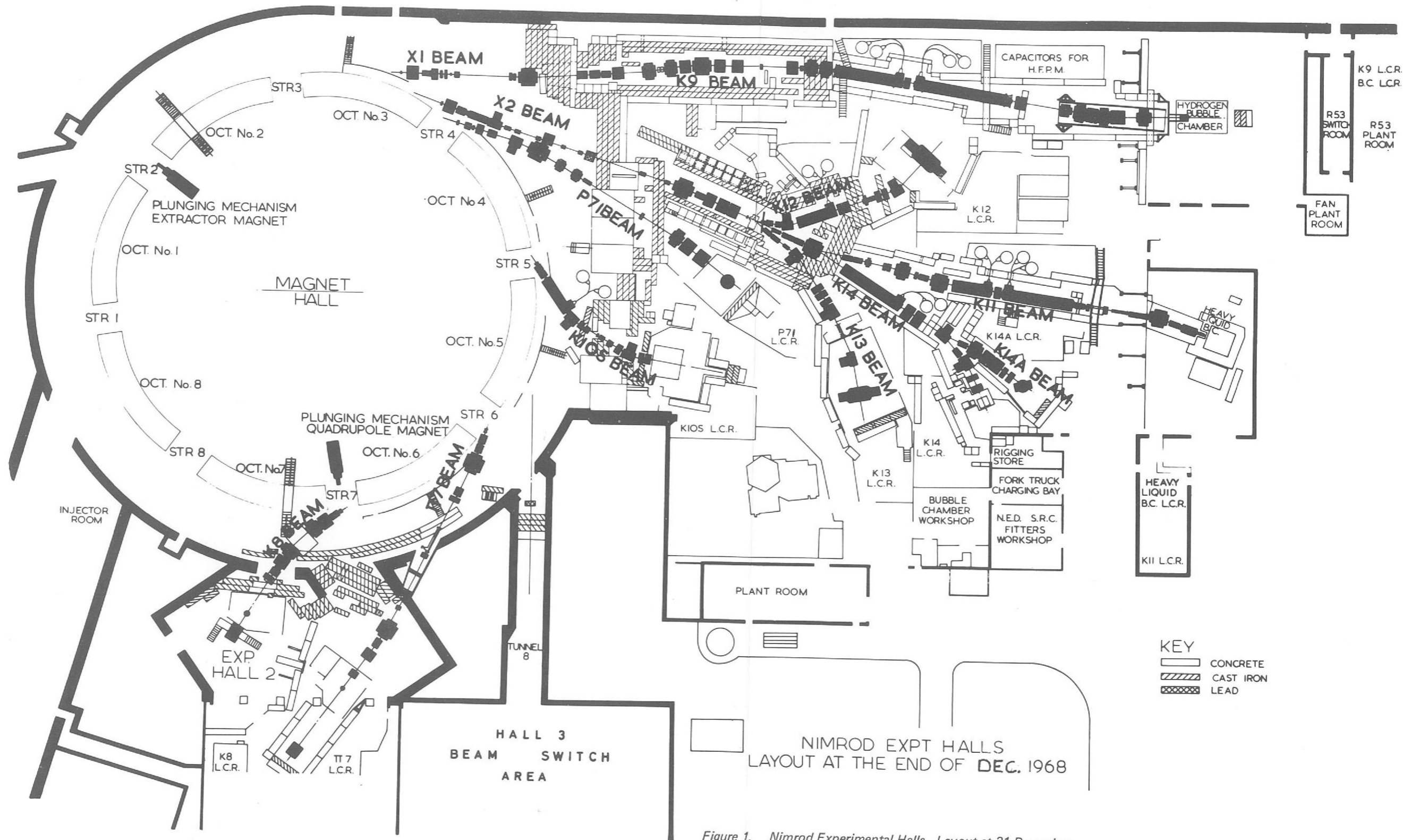


Figure 1. Nimrod Experimental Halls. Layout at 31 December.